Imperial College London

The Reproductive Tract Microbiota in IVF

A thesis submitted in partial fulfilment of the degree of Doctor of Philosophy to Imperial College London

Shahriar Mowla

Institute of Reproductive and Developmental Biology (IRDB)

Department of Metabolism, Digestion and Reproduction

Hammersmith Campus, Imperial College London

London, UK

June 2023

Supervisors:

Professor David A. MacIntyre

Professor Phillip R. Bennett

Abstract

Reproductive tract microbiota play an important role in health and disease. In pregnancy, loss of commensal vaginal bacteria and increased bacterial diversity associate with poor reproductive outcomes. Several studies have implicated the microbiota in success of fertility treatments with inconsistent results. The impact of hormonal manipulation during *in vitro* fertilisation (IVF) on the vaginal microbiota and host immune response is poorly defined. To address this, women undergoing fresh/frozen IVF cycles were recruited. Interactions between sex hormones, immune analytes and bacterial composition in fresh IVF cycles were examined and several relationships were observed. E2 had an anti-inflammatory effect during IVF cycles with inverse relationships with immune mediators. IL-1β and IL-8 were found to be significantly higher in cervico-vaginal samples of patients with successful treatment outcomes during embryo transfer. Furthermore, enrichment for *L. crispatus* was associated with unsuccessful frozen IVF cycles. Regardless, the vaginal microbiota was not a strong predictor of IVF outcome in the cohorts investigated. However, a pilot study examining the cervicovaginal metabolome in these women highlighted the potential of metabolic profiling to both discriminate vaginal microbiota composition and predict success of IVF treatment outcome.

The investigations described in this thesis provide a new insight into the vaginal and seminal microbiota and their role in shaping fertility outcomes. Modulation of sex hormones during IVF treatment shapes clinically relevant microbiota-host interactions despite the data indicating that the vaginal microbiota is not a strong predictor of IVF success. However, the assessment of the vaginal metabolome by DESI-MS provides potential to predict bacterial composition and treatment outcome during IVF. Finally, results confirming that semen harbours a microbiome that modulates parameters of sperm quality and function highlights the importance of examining male and female partners in futures studies investigating the role of the microbiome in reproductive outcomes.

Copyright Declaration

The copyright of this thesis rests with the author. Unless otherwise indicated, its content are licensed under a Creative Commons Attribution Non-Commercial 4.0 International License (CC BY-NC).

Under this licence, you may copy and redistribute the material in any medium or format. You may also create and distribute modified versions of the work. This is on the condition that: you credit the author and do not use it, or any derivative work, for a commercial purpose.

When reusing or sharing this work, ensure you make the licence terms clear to others by naming the licence and linking to the licence text. Where a work has been adapted, you should indicate that the work has been changed and describe those changes.

Please seek permission from the copyright holder for uses of this work that are not included in this licence or permitted under UK copyright Law.

Statement of Originality

I certify that the research conducted in this the product of my own work. Quotations from the literature and contribution of collaborators are fully acknowledged with respect to standard referencing practices.

S. Mowla

List of Publications and Conference Presentations

List of Publications:

1. **Mowla, S**,. Bennett P.R,. and MacIntyre, D.A. The Vaginal Microbiome, in The Handbook of Genetic Diagnostic Technologies in Reproductive Medicine: Improving Patient Success Rates and Infant Health. Edited By Carlos Simón and Carmen Rubio, Taylor and Francis Publishing. 2021 (1).

Publications in preparation:

2. **Mowla S,**. Tharakan, T,. Farahani, L,. Lee, Y,. Correia G,. Kundu, S,. Khanjani, K,. Sindi, E,. Rai, R,. Regan, L,. Ramsay, J.W.A,. Bennett, P.R,. Dhillo, W.S,. Minhas, S,. Jayasena, C.N,. MacIntyre, D.A. The relationship between semen microbiota and functional parameters in fertile and infertile men. (In preparation).
3. **Mowla S,.** Lee, Y,. Correia G,. Kundu, S,. Khanjani, S,. Bennett, P.R,. MacIntyre, D.A. The cervicovaginal microbiota and host response in women undergoing fresh IVF cycle treatment. (In preparation).
4. **Mowla S,.** Pruski P,. Lee, Y,. Correia G,. Kundu, S,. Khanjani, S,. Bennett, P.R,. MacIntyre, D.A. Rapid assessment of vaginal microbiota composition and IVF outcome by direct on-swab metabolic profiling (In preparation).

List of Conference presentations:

1. **Mowla, S**., Xie, Y,. Lee, Y. Kundu, S,. Bennett P.R,. MacIntyre D.A,. Khanjani S,. Cytokines of cervico-vaginal fluid and IVF outcomes. Fertility2019 conference, Maternal factors session. Oral presentation 04/01/2019.

2. **Mowla, S**., Xie, Y,. Lee, Y. Kundu, S,. Bennett P.R,. MacIntyre D.A,. Khanjani S,. Characterisation of vaginal cytokine expression during ART: A cohort study. SRI 66th annual scientific meeting. Poster presentation 15/03/2019.

3. **Mowla, S**., Xie, Y,. Lee, Y. Ben-Nagi J,. Bennett P.R,. MacIntyre D.A,. Khanjani S, Characterisation of vaginal microbiome and host-immune response in ART cycles and its association with treatment outcome. Fertility2020 conference. Assisted conception topics. Poster presentation 09/01/2020.

4. **Mowla S,**. Tharakan, T,. Farahani, L,. Lee, Y, Correia G,. Kundu, S,. Khanjani, K,. Sindi, E,. Rai, R,. Regan, L,. Ramsay, J.W.A,. Bennett, P.R,. Dhillo, W.S,. Minhas, S,. Jayasena, C.N,. MacIntyre, D.A. Associations between seminal microbiota compositions and ROS in men with fertility disorders. Oral presentation, 38th Annual EAU Congress, EAU 2022.

5. Farahani, L,. **Mowla S,**. Tharakan, T,. Lee, Y,. Kundu, Correia G,. S,. Khanjani, K,. Sindi, E,. Rai, R,. Regan, L,. Ramsay, J.W.A,. Bennett, P.R,. Dhillo, W.S,. Minhas, S,. Jayasena, C.N,. MacIntyre,. D.A. Next generation sequencing analysis of the seminal

microbiome in male partners of women with idiopathic recurrent pregnancy loss: results of a prospective cohort study. Oral presentation, 38th Annual meeting, ESHRE 2022.

6. **Mowla S,**. Tharakan, T,. Farahani, L,. Lee, Y,. Correia G,. Kundu, S,. Khanjani, S,. Sindi, E,. Rai, R,. Regan, L,. Ramsay, J.W.A,. Bennett, P.R,. Dhillo, W.S,. Minhas, S,. Jayasena, C.N,. MacIntyre, D.A. Seminal microbiota and fertility parameters in fertile and infertile patients. Oral presentation, Annual Scientific meeting BAUS 2023 (June 2023).

List of Awards:

1. SRF Travel Grant Award: Fertility 2018, 2019, and 2020
2. SRF Travel Grant Award: SRI 2019
3. SRF Travel Grant Award: EAU 2022

Scientific Society memberships:

- Society for Reproduction and Fertility (SRF)
- British Fertility Society (BFS)
- Society for Reproductive Investigation (SRI)
- European Society of Human Reproduction and Embryology (ESHRE)

Contents

1 CHAPTER I 1
1.0 INTRODUCTION 1
1.0 Human fertility 1
1.1 Reproductive endocrinology 2
1.1.1 Estradiol 3
1.1.2 Progesterone 5
1.2 Assisted Reproductive Technologies (ART) 6
1.2.1 IVF Treatment protocols 6
1.2.2 Intracytoplasmic Sperm Injection (ICSI) 7
1.2.3 Preimplantation genetic diagnosis and screening 7
1.2 The Microbiome 11
1.2.1 Human Microbiome 11
1.2.2 Antenatal to Adult Microbiome 11
1.2.2.1 Menopause 12
1.2.2 Characterisation of Microbiota: From Culture-Based Methods to Metataxonomic Profiling 13
1.2.3.1 Conventional approaches for bacterial detection in the reproductive tract 14
1.3 Reproductive tract microbiome 15
1.3.1 Female reproductive tract microbiome 15
1.3.1.1 Factors influencing the composition of the vaginal microbiome 18
1.3.1.2 Vaginal microbiota, pathogen colonisation and host response 20
1.3.1.3 Vaginal microbiome and pregnancy outcomes 22
1.3.1.4 Upper reproductive tract microbiome 28
1.3.2 Semen and male reproductive tract microbiome 34
1.3.2.1 Sperm 34
1.3.2.2 Seminal fluid 34
1.3.2.3 Sperm DNA fragmentation and ROS in semen 35
1.3.2.4 Overview of male reproductive tract bacteria and origins of semen bacteria 38
1.3.2.4.1 Bacteria and male fertility 39
1.3.2.4.1 Bacteria detection in semen: culture-based and metataxonomic studies 41
1.4 Reproductive tract mucosa: key modulators between host immunity and environment 45
1.4.1 Reproductive tract immune regulation and embryo implantation 47
4.2 Immune regulation of pregnancy 49
1.4.2.1 Activation of inflammation 51
1.5 Metabolome of the cervicovaginal mucosa 54
1.6 Hypothesis, aims and objectives 56

1.6.1 Hypothesis 56
1.6.2 Aims and objectives 56
2 CHAPTER II 57
2.0 METHODS AND MATERIALS 57
2.1 Participants and study design 57
2.2 Role of the PhD candidate 59
2.4 Sample collection 60
2.4.1 Collection method for microbiome swabs 60
2.4.2 Materials for microbiome sample collection and storage 61
2.4.3 Collection methods for semen samples 62
2.4.4 Materials for semen sample collection and storage 62
2.5 Materials for DNA extraction 62
2.6 DNA extraction laboratory procedures 63
2.7 Polymerase Chain Reaction (PCR) Amplification 65
2.8 Materials required for immune analyte profiling 67
2.9 Sample preparation for immune analyte analysis 68
2.9.1 Sample preparation for immune analyte analysis: additional notes 68
2.10 Reagent and standards preparation for immune analyte profiling 68
2.11 Immune analyte profiling: laboratory procedure 69
2.12 Quantitative bacteriology 70
2.12.1 Materials 70
2.12.2 Quantitative bacteriology laboratory procedure 71
2.14 Assessment of semen quality and function 73
2.14.1 Routine semen analysis 73
2.14.2 ROS analysis 73
2.14.3 Sperm DNA fragmentation assessment 74
2.14.3.1 TUNEL assay 74
2.14.3.2 Comet assay 75
2.15 Materials required for metabolome analysis 75
2.16 Metabolome analysis using DESI-MS 76
2.17 Metabolome analysis laboratory procedure 76
2.17.1 Mass spectral data pre-processing 77
2.18 16S rRNA data processing 77
2.19 Statistical analysis 78
3 CHAPTER III The cervicovaginal microbiota and host response in women undergoing fresh IVF cycle treatments 80
3.0 INTRODUCTION 80
3.1 Results: Patient recruitment and sample collection 82

3.2 Assessment and comparison of E2 and P4 levels throughout fresh and frozen IVF cycles 82
3.3 Patient demographics for fresh IVF cycles 88
3.4 Assessment of cervicovaginal (CVF) immune analytes across fresh IVF cycles 90
3.5 Relationships between immune analytes and hormones across fresh IVF cycles 93
3.5.1 Cross sectional analysis of immune analyte and hormone relationships at different clinical stages 94
3.5.1.1. Coordination appointment 94
3.5.1.2. Pituitary suppression 95
3.5.1.3. Ovarian stimulation 95
3.5.1.4. Egg collection 96
3.5.1.5. Embryo transfer 96
3.5.2 Paired analyses of hormone and immune analyte relationships at different clinical stages of IVF treatment 97
3.5.2.1 Coordination appointment to pituitary suppression 97
3.5.2.2 Pituitary suppression to ovarian stimulation 99
3.5.2.3 Ovarian stimulation to egg collection 102
3.5.2.4 Egg collection to embryo transfer 103
3.6 The relationship between immune analytes and clinical outcomes 105
3.7 Metataxonomic characterisation of vaginal bacteria during IVF 109
3.7.1 Microbiota characterisation and data exploration 112
3.7.2 Vaginal microbiome composition 112
3.7.2.1 Co-occurrence relationships of the most abundant vaginal taxa 114
3.7.2.2 Assignment of vaginal microbiota community state types (CSTs) 115
3.8 Characterisation and comparison of vaginal microbiota in fresh IVF cycles 116
3.8.1 Stability of vaginal microbiome throughout fresh IVF cycles 122
3.8.2 Assessment of bacterial load for samples collected on the day of embryo transfer for fresh IVF cycles 123
3.8.3 The relationship between highly abundant taxa and hormones 125
3.8.3.1 Cross-sectional analysis of highly abundant taxa and hormones 126
3.9.3.1.1. Coordination appointment 129
3.9.3.1.2. Pituitary suppression 130
3.9.3.1.3. Ovarian suppression 130
3.9.3.1.4 Egg collection 130
3.9.3.1.5 Embryo transfer 131
3.8.4 Relationship between vaginal taxa with hormones and immune analytes 132
3.8.4.1 Coordination appointment 139
3.8.4.2 Pituitary suppression 143

3.8.4.3 Ovarian stimulation 146
3.8.4.4 Egg collection 149
3.8.4.5 Embryo transfer 152
3.8.5 Within patient changes in vaginal microbiota across clinical sampling timepoints . 155
3.8.5.1 Coordination appt to pituitary suppression 155
3.8.5.2 Pituitary suppression to ovarian stimulation 156
3.8.5.3 Ovarian stimulation to egg collection 156
3.8.5.4 Egg collection to embryo transfer 156
3.9 Vaginal bacteria random forest modelling for predicting IVF success rates 157
3.9.1 Prediction of IVF success using ReceptIVFity™-type vaginal microbiome parameters 159
3.10 Discussion 160
3.10.1 Limitations 167
3.10.2 Summary of main findings 167
4 CHAPTER IV: The cervicovaginal microbiota in women undergoing frozen IVF cycle treatment 168
4.0 INTRODUCTION 168
4.1 Results: Patient recruitment and sample collection 170
4.2 Patient demographics for frozen IVF cycles 170
4.3 Characterisation and comparison of vaginal microbiota in frozen IVF cycles 172
4.3.1 CST classification of cervico-vaginal bacteria in frozen IVF cycles 172
4.4 Stability of vaginal microbiome throughout frozen IVF cycles 180
4.5 Vaginal bacterial load at embryo transfer for frozen IVF cycles 182
4.6 The relationship between highly abundant vaginal taxa and clinical treatment outcomes 185
4.7 Longitudinal assessment of vaginal taxa 188
4.7.1 Coordination appointment to pituitary suppression 188
4.7.2 Pituitary suppression to embryo transfer 190
4.8 Vaginal bacteria of IVF cycles with preimplantation genetic testing and diagnosis (PGT-A and PGD) 191
4.9 Vaginal bacteria random forest modelling for predicting IVF success rates 192
4.9.1 Prediction of IVF success using vaginal microbiome parameters akin to the ReceptIVFity™ study 193
4.10 Discussion 194
4.10.2 Summary of main findings 198
5 CHAPTER V. Rapid metabolic profiling of the cervico-vaginal niche for prediction of microbiota composition and IVF success 199
5.0 INTRODUCTION 199
5.1 Results 201

5.1.1 Prediction of vaginal microbiota composition using DESI-MS profiles 201
5.1.2 Prediction of microbiota composition under differing hormonal conditions 205
5.1.3 Putative identification of discriminatory metabolites 214
5.2 Discussion 216
6. CHAPTER VI: Assessment of seminal microbiota and their relationships with seminal quality and function parameters 219
6.0 INTRODUCTION 219
6.1 Study population characteristics and demographics at study entry 220
6.2 Semen quality and functional parameters of the study population 220
6.3 Genera level classification of semen microbiota profiles 223
6.4 Assessment of semen microbiota at species level resolution 227
6.5 Relationship between semen microbiota genera clusters and semen function and quality parameters 231
6.6 Non-parametric differential abundance analysis of semen microbiota 233
6.7 Comparison of semen quality and function parameters in controls and cohorts of men undergoing fertility investigations 236
6.8 Assessment of seminal function and quality parameters within controls and study subjects and their relationships with seminal microbiota 237
6.9 Discussion 242
7 CHAPTER VII 246
7.0 Overall conclusions 246
References 250
Appendix 283

List of Figures

Figure 1.1: Hypothalamic, pituitary, and gonadal axis of the female 3
Figure 1.2: E2 biosynthesis in the ovaries 4
Figure 1.3: Enzymatic regulation of steroidogenesis 5
Figure 1.4: Diagrammatic representation of IVF protocols 7
Figure 1.5: Vaginal microbiome of non-pregnant women of reproductive age 18
Figure 1.6: Overview of factors influencing vaginal microbiota composition and stability and its relationship with health and disease states 20
Figure 1.7: Microbiota-host interactions at epithelial mucosal interface throughout the reproductive tract 21
Figure 1.8: Schematic representation of free radical formation 37
Figure 2.1: Flow diagram of the study design and included cohorts in this thesis 58
Figure 2.2: Demonstration of successful DNA amplification 67
Figure 2.3: PCR cycle conditions 71
Figure 2.4: BactQuant Standard curve 72
Figure 2.5: BactQuant Amplification plot 72
Figure 3.1: Summary of patients recruited and sampled in the ART1 study 82
Figure 3.2: Concentrations of serum E2 and P4 for fresh and frozen IVF cycles. 83
Figure 3.3: Comparison of E2 concentrations between fresh and frozen IVF cycles at comparable stages of sample collection 85
Figure 3.4: Comparison of P4 concentrations between fresh and frozen IVF cycles at comparable stages of sample collection 86
Figure 3.5: Longitudinal E2 and P4 concentrations throughout fresh IVF cycles 87
Figure 3.6: Longitudinal concentration of immune analytes across stages of sample collection 92
Figure 3.7: Linear regression between immune analytes and E2 93
Figure 3.8: CVF immune analytes significantly correlated with serum E2 at the time of coordination appointment 94
Figure 3.9: Linear regression between immune analytes and E2 throughout ovarian stimulation 95
Figure 3.10: Within patient hormone level changes from coordination appointment to pituitary suppression 98
Figure 3.11: Within patient IL-1ra concentration changes from coordination appointment to pituitary suppression 99
Figure 3.12: Within patient E2 and P4 changes from pituitary suppression to ovarian stimulation 100
Figure 3.13: Within patient Immune analyte concentration changes from pituitary suppression to ovarian stimulation 101
Figure 3.14: Within patient E2 and P4 changes from ovarian stimulation to egg collection 102
Figure 3.15: Within patient E2 and P4 changes from egg collection to embryo transfer 103

Figure 3.16: Within patient Immune analyte concentration changes from egg collection to embryo transfer 104

Figure 3.17: Comparison of immune analyte concentrations from samples collected on the day of embryo transfer with respect to clinical outcomes 106

Figure 3.18: Comparison of regression slopes between successful and unsuccessful outcomes for IL-1β and E2 at the coordination appointment timepoint 107

Figure 3.19: Assessment of run-to-run sequencing variation in vaginal microbiota profiles. 110

Figure 3.20: Venn diagram describing the number of species detected in each run 111

Figure 3.21: Vaginal microbiome compositions 113

Figure 3.22: Correlation plot for highly abundant species with 25% prevalence inclusion threshold 115

Figure 3.23: Ecological parameters of vaginal bacteria based on CST classifications in fresh IVF cycles 117

Figure 3.24: CST representations at various stages of sample collection for fresh IVF cycles 118

Figure 3.25: Longitudinal relative abundance changes of taxa 120

Figure 3.26: Within patient sample collection timeline for fresh IVF cycles 123

Figure 3.27: CSTs and bacterial load for samples collected on the day of embryo transfer124

Figure 3.28: Clinical outcomes and bacterial load for samples collected on the day of embryo transfer 125

Figure 3.29: Cross-sectional linear regression R2 values of CLR transformed abundance of highly abundant taxa with E2 levels 127

Figure 3.30: Cross-sectional linear regression R2 values of CLR transformed abundance of highly abundant taxa with P4 levels 128

Figure 3.31: Linear regression between CLR transformed abundance of *L. iners* with E2 for samples collected at coordination appointment 129

Figure 3.32: Linear regression between CLR transformed abundance of *L. jensenii* with P4 for samples collected throughout pituitary suppression 130

Figure 3.33: Linear regression between CLR transformed abundance of *P. bivia* with serum hormone concentrations for samples collected on the day of egg collection 131

Figure 3.34: Linear regression of *L. jensenii* with E2 for samples collected on the day of egg collection 131

Figure 3.35: CCA variance plot across all stages of sample collection 133

Figure 3.36: Linear regression R2 values for highly abundant taxa and immune analytes across the whole dataset 135

Figure 3.37: Linear regression of *L. crispatus* and immune analytes across the whole dataset 136

Figure 3.38: Linear regression of *L. iners* and IL-8 across the whole dataset 136

Figure 3.39: Linear regression of *L. vaginalis* and IL-1β across the whole dataset 137

Figure 3.40: Linear regression of *G. vaginalis* and IL-1β across the whole dataset 137

Figure 3.41: Linear regression of *S. anginosus* and immune analytes across the whole dataset 138
Figure 3.42: Linear regression of *D. micraerophilus* and IL-18 across the whole dataset .. 139
Figure 3.43: CCA variance plot for samples collected at coordination appointment..... 140
Figure 3.44: Linear regression R2 values for highly abundant taxa and immune analytes for samples collected at coordination appointment 141
Figure 3.45: Linear regression of *L. crispatus* and IL-1β for samples collected at coordination appointment 142
Figure 3.46: Linear regression of *P. indolicus* and IL-1ra for samples collected at coordination appointment 142
Figure 3.47: Linear regression of *P. bivia* and immune analytes for samples collected at coordination appointment 143
Figure 3.48: CCA variance plot for samples collected throughout pituitary suppression 144
Figure 3.49: Linear regression R2 values for highly abundant taxa and immune analytes for samples collected throughout pituitary suppression 145
Figure 3.50: CCA variance plot for samples collected throughout ovarian stimulation 146
Figure 3.51: Linear regression R2 values for highly abundant taxa and immune analytes for samples collected throughout ovarian stimulation 148
Figure 3.52: Linear regression of *S. anginosus* and immune analytes for samples collected throughout ovarian stimulation 149
Figure 3.53: Linear regression of *D. micraerophilus* and immune analytes for samples collected throughout ovarian stimulation 149
Figure 3.54: CCA variance plot for samples collected on the day of egg collection 150
Figure 3.55: Linear regression R2 values for highly abundant taxa and immune analytes for samples collected on the day of egg collection..... 151
Figure 3.56: Linear regression of *L. crispatus* and IL-1β for samples collected on the day of egg collection 152
Figure 3.57: CCA variance plot for samples collected on the day of embryo transfer 153
Figure 3.58: Linear regression R2 for highly prevalent taxa and immune analytes for samples collected on the day of embryo transfer 154
Figure 3.59: Within patient abundance change of *P. timonensis* for samples collected at coordination appointment and throughout pituitary suppression 155
Figure 3.60: Within patient relative abundance changes of vaginal taxa throughout pituitary suppression to ovarian stimulation 156
Figure 3.61: Within patient relative abundance changes of vaginal taxa from egg collection to embryo transfer 157
Figure 3.62: Capacity of vaginal microbiota, immune analytes and hormones to predict IVF clinical success rates tested using random forest classifiers 158
Figure 3.63: Clinical success predictability model based on the ReceptIVFity study 159
Figure 4.1: Summary of frozen cycles recruited and sampled in ART1 and ART2 studies 170
Figure 4.2: Comparison of mean richness and diversity of vaginal CST groups identified in frozen IVF cycles 173

Figure 4.3: CST representations at various stages of sample collection for frozen IVF cycles 174
Figure 4.4: Comparison of CSTs at equivalent stages of sample collection between fresh and frozen IVF cycles 175
Figure 4.5: Longitudinal abundance changes of bacterial species during frozen IVF treatment cycles..... 177
Figure 4.6: Microbiota stability across frozen IVF cycles 181
Figure 4.7: CSTs and bacterial load for samples collected on the day of embryo transfer. 182
Figure 4.8: Clinical outcomes and bacterial load for samples collected on the day of embryo transfer 183
Figure 4.9: Fresh and frozen bacterial load for samples collected on the day of embryo transfer 184
Figure 4.10: Comparison of relative abundance of *L. crispatus* based on clinical outcomes. 185
Figure 4.11: Comparison of species diversity for CST I based on clinical outcomes 186
Figure 4.12: Comparison of relative abundance of *P. indolicus* based on clinical outcomes for samples collected on the day of embryo transfer 187
Figure 4.13: Within patient relative abundance changes of vaginal taxa for samples collected on coordination appointment and throughout pituitary suppression 189
Figure 4.14: Within patient relative abundance changes of vaginal taxa throughout pituitary suppression to embryo transfer 190
Figure 4.15: Comparison of relative abundance of *L. crispatus* for cycles with PGT based on clinical outcomes..... 191
Figure 4.16: Random Forest modelling ROC curves 192
Figure 4.17: Clinical success predictability model based on the ReceptIVFity study 193
Figure 5.1: PCA analysis for metabolites..... 201
Figure 5.2: Random Forest models for prediction of vaginal microbiota composition using DESI-MS metabolic profiles 202
Figure 5.3: Metabolite feature importance for discriminating between *Lactobacillus* dominance and depletion 203
Figure 5.4: Representative features discriminating vaginal *Lactobacillus* dominance and depletion 204
Figure 5.5: Random Forest modelling for microbiota composition prediction at different stages of sample collection 206
Figure 5.6: Top 15 important features discriminating between *Lactobacillus* dominant and depleted samples at different stages of sample collection 207
Figure 5.7: Feature *m/z* 148.9893034 discriminating between vaginal compositions at different stages of sample collection. Random Forest modelling for bacterial composition prediction at different stages of sample 208
Figure 5.8: Features *m/z* 786.5277438 and *m/z* 789.5469565 discriminating between vaginal compositions at different stages of sample collection. Random Forest modelling for bacterial composition prediction at different stages of sample collection 209

Figure 5.9: Random Forest modelling for treatment outcome prediction at different stages of sample collection 210

Figure 5.10: Top 15 important features discriminating between treatment outcomes at different stages of sample collection 211

Figure 5.11: Feature *m/z* 747.5169172 discriminating between successful and unsuccessful pregnancy at different stages of sample collection 212

Figure 5.12: Feature *m/z* 266.1511397 discriminating between successful and unsuccessful pregnancy at different stages of sample collection 213

Figure 5.13: Feature *m/z* 637.6708501 discriminating between successful and unsuccessful pregnancy at different stages of sample collection 213

Figure 6.1: Heatmap of Log10 transformed read counts of top 25 most abundant genera identified in semen samples 224

Figure 6.2: Genera level categorisation of seminal microbiota identified three major clusters 225

Figure 6.3: Ecological parameters of seminal microbiota clusters at genera level 226

Figure 6.4: Bacterial load of seminal microbiota clusters at genera level 227

Figure 6.5: Heatmap of Log10 transformed read counts of top 25 most abundant species identified in semen samples 228

Figure 6.6: Relative abundance of the top 6 most abundant species in the identified in semen microbial clusters at species-level taxonomy 229

Figure 6.7: Species level categorisation of seminal microbiota 230

Figure 6.8: Bacterial load of seminal microbiota based on age 233

Figure 6.9: Relative abundance and prevalence matrices of *Flavobacterium* in relation to semen quality 236

Figure 6.10: Seminal quality and function parameters according to recruited cohorts 237

Figure 6.11: Ecological parameters of seminal microbiota for the recruited study cohorts 238

Figure 6.12: Bacterial load of seminal microbiota in recruited study cohorts 239

List of Tables

Table 1.1: Comparison of complete chromosomal screening methods 9

Table 1.2: Comparison of biopsy techniques for preimplantation genetic testing. 10

Table 1.3: A summary of studies investigating the relationship between the vaginal microbiota and IVF success 24

Table 1.4: A summary of studies investigating the relationship between the endometrial microbiota 29

Table 1.5: A summary of studies investigating mechanisms by which bacteria negatively impact sperm cells 40

Table 1.6: A summary of studies investigating relationship between seminal microbiota and their relationship with health 42

Table 1.7: Cytokines, PGs and growth factors involved during the embryo-epithelial interaction 49

Table 1.8: NF-κB target genes involved in inflammation activation and progression 52

Table 2.1: Contents and volumes of the enzymatic master mix 64

Table 2.2: Contents and volumes of the PCR mix 66

Table 2.3: Standard cocktails and reconstitution volumes for immune analyte analysis 69

Table 2.4: Reagents and volumes used for TUNEL assay 75

Table 2.5: Source Parameters and DESI-MS Instrumental Settings 76

Table 3.1: Summary of E2 and P4 fold change during hormonal manipulations of fresh IVF cycles 88

Table 3.2: Patient demographics and clinical outcomes for women undergoing fresh IVF cycles 89

Table 3.3: Longitudinal changes across stage for immune analytes. p-values for changes for immune analytes 90

Table 3.4: Overview of the relationship between immune analytes and E2 96

Table 3.5: Cross-sectional immune analyte concentration changes according to treatment outcomes 105

Table 3.6: The relationship between immune analytes and E2 with respect to clinical outcomes 107

Table 3.7: The relationship between immune analytes and P4 with respect to clinical outcomes 108

Table 3.8: Longitudinal abundance changes for highly abundant taxa 119

Table 3.9: Cross-sectional CST representations according to outcome for fresh IVF cycles: CST I vs other CSTs 121

Table 3.10: Cross-sectional CST representation according to outcome for fresh IVF cycles: CST Lacto-dominant vs CST IV 122

Table 3.11: Linear regression R2 values for the highly abundant taxa and serum hormones for all available samples 126

Table 3.12: Performance metrics for the random forest predictions models 158

Table 4.1: Patient demographics and clinical outcomes for women undergoing frozen IVF cycles 171

Table 4.2: Longitudinal changes across stage for highly abundant taxa. p-values for changes for taxa 176

Table 4.3: Cross-sectional CST representations according to outcome for frozen IVF cycles: CST I vs other CSTs 178

Table 4.4: Cross-sectional CSTs representations according to outcome for frozen IVF cycles: CST Lacto-dominant vs CST IV 179

Table 4.5: Notable metrics for random forest modelling. 193

Table 5.1: Important metabolites identified by random forest modelling 215

Table 6.1: Comparison of mean age and prevalence of ethnicities in study recruitment cohorts 220

Table 6.2: WHO defined lower limits of seminal parameters 221

Table 6.3: Patient demographics and notable parameters of seminal quality and function for controls and study subjects 222

Table 6.4: Distribution of clinical factors, microscopic seminal parameters, confounding factors, and recruitment cohorts according to genera clusters 231

Table 6.5: Richness and diversity of seminal bacterial based on seminal quality and function parameters 232

Table 6.6: Non-parametric differential abundance analysis for specific taxa at genera level 234

Table 6.7: Non-parametric differential abundance analysis for specific taxa at species level 235

Table 6.8: Non-parametric differential abundance analysis for specific taxa at genera level for controls and MFIs only 240

Table 6.9: Non-parametric differential abundance analysis for specific taxa at species for controls and MFIs only 241

Acknowledgements

First, I would like to thank Prof. Phillip R. Bennett for giving me the opportunity to undertake my PhD at Imperial College London and providing me with expert advice and support. Prof. Bennett's scientific expertise and kind nature has nurtured a dynamic research group of enthusiastic scientists thriving for success and I am very privileged to have been a part of it.

I would also like to sincerely thank my project manager Dr. Yun S. Lee for helping me with many technical aspects of my project. You patiently explained the protocols, helped me in the laboratory, supported me with consumables and most importantly you always cared. You even allowed me to use your pipettes on occasions and I know how personal they are to you!

I would like to express gratitude to many others for their support and assistance in various aspects of this project. Contribution of so many great people at the IRDB 3rd floor and the college made this project a success. Thank you to Drs. Goncalo Correia, Samit Kundu, Pamela Pruski and Sherrianne Ng for your input in data preparation and modelling. I would also like to thank Prof. Suks Minhas and Dr. Channa Jayasena for their insightful advice in male reproduction and urology.

I am grateful to Dr. Shirin Khanjani for laying the foundation of this project and her support and input in development of this study. Dr. Khanjani also greatly supported me in obtaining an 'Honorary Research Associate' position at CRGH for sample recruitment. I have so many wonderful people to thank at CRGH including Dr. Jara Ben Nagi for continuous support, liaising with the clinical team, and making me feel so welcome at the clinic. I would also like to thank everyone else at CRGH including consultants, embryologists, andrologists, nurses and support staff for all their kind help and support.

I would like to extend my deepest gratitude to Prof. David A. MacIntyre, my primary supervisor. David's management of every aspect of this project and my personal development was instrumental, and I will be eternally grateful to you. David's passion for science is truly infectious and his attention to detail is inspirational. Thank you, David, for rescuing this project and supporting me throughout the tough times.

Lastly, I'd like to thank my friends and family for all your love and support. To my parents and my sister Sherry, you are my rock. You always believe in me and encourage me to reach new heights and push the boundaries of success.

AMA	Advanced Maternal Age
ART	Assisted Reproductive Technologies
BV	Bacterial Vaginosis
CCA	Canonical Correlation Analysis
CRGH	Centre for Reproductive & Genetic Health
CVF	Cervico-Vaginal Fluid
CST	Community State Type
CGH	Comparative Genomic Hybridization
DNA	Deoxyribonucleic Acid
DESI-MS	Desorption Electrospray Ionization Mass Spectrometry
DMSO	Dimethyl Sulfoxide
ECM	Embryo Culture Media
EMT	Endometrial thickness
E2	Estradiol
ER	Estrogen Receptor
EMMPRIN	Extracellular Matrix Metalloproteinase Inducer
FRT	Female Reproductive Tract
FISH	Fluorescence *in situ* Hybridization
FSH	Follicle Stimulating Hormone
FF	Follicular Fluid
FERC	Frozen Embryo Replacement Cycles
GPCR	G Protein-Coupled Receptors
GALP	Galanin-Like-Peptide
GC-MS	Gas Chromatography-Mass Spectrometry
GR	Glucocorticoid Receptor
GnRHa	GnRH agonists
GnRH	Gonadotropin-Releasing Hormone
HRA	Health Research Authority
hr-NGS	High-Resolution Next Generation Sequencing
hCG	Human Chorionic Gonadotropin
HFEA	Human Fertilisation and Embryology Authority
HGP	Human Genome Project
HIV	Human Immunodeficiency Virus
hMG	Human Menopausal Ggonadotropin
HMP	Human Microbiome Project

HPG	Hypothalamic-Pituitary-Gonadal
IVF	In Vitro Fertilisation
IRDB	Institute of Reproductive and Developmental Biology
IL	Interleukin
ICSI	Intracytoplasmic Sperm Injection
LIF	Leukemia Inhibitory Factor
LPS	Lipopolysaccharide
LC-MS	Liquid Chromatography-Mass Spectrometry
LDL	Low-Density Lipoprotein
LH	Luteinizing Hormones
MHC	Major Histocompatibility Complex
MFI	Male Factor Infertility
MS	Mass Spectrometry
MMP-8	Matrix Metalloproteinase
NICE	National Institute for Health and Care Excellence
NIH	National Institutes of Health
NK cells	Natural Killer cells
NKT cells	Natural Killer T cells
NPY	Neuropeptide Y
NGS	Next generation sequencing
NLR	NOD-Like Receptors
NMR	Nuclear Magnetic Resonance
OHSS	Ovarian Hyperstimulation Syndrome
OS	Oxidative Stress
PPAR	Peroxisome Proliferator-Activated Receptors
PBS	Phosphate-Buffered Saline
PCOS	Polycystic Ovary Syndrome
PCR	Polymerase Chain Reaction
PMN	Polymorphonuclear Leukocytes
POR	Poor Ovarian Responders
PGD	Preimplantation Genetic Diagnosis
PGT	Preimplantation Genetic Testing
POF	Premature Ovarian Failure
PTB	Preterm Birth
POI	Primary Ovarian Insufficiency
P4	Progesterone

PR	Progesterone Receptor
PG	Prostaglandin
qPCR	Quantitative PCR
ROS	Reactive Oxygen Species
rFSH	recombinant FSH
RPL	Recurrent Pregnancy Loss
RHD	Rel Homology Domain
RNA	Ribonucleic Acid
rRNA	Ribosomal RNA
STAT3	Signal Transducer and Activator of Transcription 3
SDF	Sperm DNA Fragmentation
SAC	Spindle Assembly Checkpoint
SAC	Spindle-Assembly Checkpoint
SOP	Standard Operating Procedures
TUNEL	Terminal deoxynucleotidyl transferase biotin-dUTP Nick End Labeling
TESE	Testicular Sperm Extraction
TLR	Toll-like receptors
TUV	Transvaginal Ultrasonography
TBE	Tris/Borate/EDTA
TEP	Trophectoderm Projections
UV	Ultraviolet
UI	Unexplained Infertility
UN	United Nations
VVC	Vulvovaginal Candidiasis
WHO	World Health Organisation
ZP	Zona Pellucida
α-MSH	α-melanocyte stimulating hormone

1 CHAPTER I

1.0 INTRODUCTION

***

Aspects of this introduction have been published in the following book chapter:
Shahriar Mowla, Phillip R. Bennett and David A. MacIntyre, The Vaginal Microbiome, in The Handbook of Genetic Diagnostic Technologies in Reproductive Medicine: Improving Patient Success Rates and Infant Health. Edited By Carlos Simón and Carmen Rubio, Taylor and Francis Publishing. 2021 (1).

1.0 Human fertility

For more than 50 years, global fertility rates have been in decline. In 1950, women gave birth on average to 4.7 children in their lifetime. By 2017 this average had almost halved to 2.4 and is projected to further fall below 1.7 by 2100 (2). There are multiple factors thought to be contributing to this including social-structural conditions, greater access to contraception and more women choosing to receive education and to work (3). As a result, women are starting families later in life, which coincides with a reduction in their natural fecundity. An association between advanced maternal age and adverse pregnancy outcomes was first reported by Naeye and colleagues in 1983 (4), and according to a 2015 United Nations (UN) report, the mean maternal age has continued to rise over the last 3 decades, particularly in developed countries (5).

According to the National Institute for Health and Care Excellence (NICE), it is estimated that infertility affects 1 in 7 couples in the UK. Infertility is defined as failure to achieve a pregnancy after 1 year of unprotected intercourse and can be caused by various factors including ovulatory and uterine disorders, tubal damage, and male factor infertility (6). Around 15% of couples fail to conceive naturally beyond 1 year and although many have the potential for natural conception, idiopathically they fail to achieve pregnancy (7, 8). Data published by the Human Fertilisation and Embryology Authority (HFEA) indicates that unexplained infertility accounts for 24% of all infertility cases (9).

Assisted reproduction is defined as any reproductive technique or treatment that involves handling of eggs or embryos (10). Initially intended to treat women with tubal factor infertility, *in vitro* fertilisation (IVF) was developed by Steptoe and Edwards with the first successful pregnancy achieved in 1978 and subsequently the birth of first IVF baby, Louise Brown (11).

Since then, IVF has evolved both technically and in its application and is now widely used to treat a range of infertility factors (12). Development of super-ovulatory protocols in recent decades, has resulted in improved pregnancy rates and fewer cycle cancellations and the ability to cryopreserve surplus gametes, has largely eliminated the need for additional fresh cycles if a patient requires future embryo transfers (13). Between 1991 and 2016, there have been 1.1 million IVF cycles in the UK alone. In 2016, 68,000 IVF cycles in the UK resulted in over 20,000 births (14).

1.1 Reproductive endocrinology

Production and regulation of sex hormones is the central component of reproductive function. This is largely mediated by the female Hypothalamic-Pituitary-Gonadal (HPG) axis. Secretion of GnRH by hypothalamic neurons in a pulsatile manner stimulates the anterior pituitary gland to produce and secrete Luteinizing Hormone (LH) and Follicle Stimulating Hormone (FSH) (15). Gonadotropin-Releasing Hormone (GnRH) is a small decapeptide of 10 amino acids. The central amino acid sequence of Tyr-Gly-Leu-Arg, is a non-conserved segment which can vary among different species (16). The frequencies and amplitude of GnRH pulses directly control and alter the secretion patterns of FSH and LH (17, 18). Increased frequency of GnRH pulses is favourable for LH secretion whereas slow pulsing results in greater FSH release (19). FSH is a 35.5 kDa glycoprotein hormone, made up of α and β subunits. The α subunit of FSH consists of 96 amino acids and is identical to LH, TSH and hCG (20). The β subunit is unique and interacts with the FSH receptors to carry out the biological effects (21).

The pituitary expresses cell-surface GnRH receptors that are important in regulation of FSH and LH production. GnRH signalling on the anterior pituitary gland is transmitted via G Protein-Coupled Receptors (GPCR). The pituitary GnRH receptor cDNA encodes a protein of 328 amino acids and are from the 7-transmembrane family of receptors (22). This receptor lacks the typical intracellular carboxy terminus and has a relatively short third intracellular loop (23). These properties of the receptor are important for the internalisation and desensitisation of many GPCRs (24).

Collectively, LH and FSH stimulate the ovaries for steroidogenesis and gametogenesis (25). Hormones such as Estradiol (E2), Progesterone (P4) and inhibin secreted by the ovaries, control the secretion of gonadotrophins by a feedback mechanism to anterior pituitary gland and hypothalamus. This feedback mechanism also accounts for initiation of the mid-cycle LH surge and suppression of gonadotrophin release in the luteal phase of the menstrual cycle (Figure 1.1).

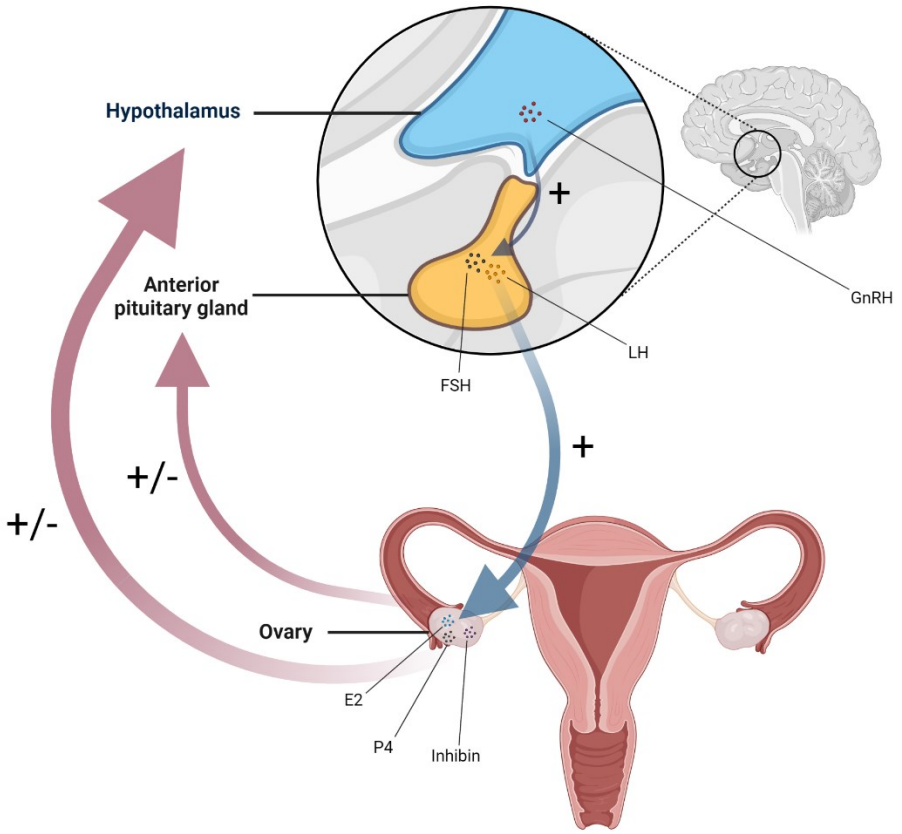


Figure 1.1: Hypothalamic, pituitary, and gonadal axis of the female. During the follicular phase of the cycle, E2 downregulates (-) GnRH. At midcycle, E2 upregulates (+) GnRH, LH and FSH. Simultaneously, FSH is downregulated (-) by inhibin which leads to a strong LH surge prior to ovulation. During the luteal phase, E2 and P4 strongly downregulate (-) GnRH, LH and FSH which in the absence of fertilisation, provide the hormonal environment required for menses. Created in Biorender.com.

Several neuropeptides and hormones are directly and indirectly involved in regulating the production of GnRH. These neuropeptides and hormones are also involved in mediation of food intake as well as the fertility axis, which act on GnRH depending on the estrogenic state when E2, oxytocin, Galanin-Like-Peptide (GALP), Galanin, Kisspeptin, α-melanocyte stimulating hormone (α-MSH) and Neuropeptide Y (NPY) directly stimulate production of GnRH. Additionally, leptin and insulin have an indirect impact on stimulation of GnRH at these times. When E2 levels are low, galanin, Kisspeptin, α-MSH and NPY inhibit GnRH production (26).

1.1.1 Estradiol

Estradiol (E2) is a key estrogen steroid hormone involved in the development and regulation of the female reproductive system. In non-reproductive aged women, E2 is synthesized in extragonadal sites such as the kidney, adipose tissue, skin, and brain. Extragonadal E2

functions as a paracrine and intracrine regulator of tissue specific functions (27, 28). Ovarian-synthesized endocrinological E2 is the main source of E2 in reproductive aged women. It is produced primarily in the theca cell layer of the antral follicle which expresses LH receptors that assist in the conversion of cholesterol into precursor androgens. The granulosa cell layer of the follicle express FSH receptors which are involved in the conversion of androgens to E2 as described below. The action of LH and FSH hormones on theca and granulosa cells are collectively referred to as the '2-cell, 2-gonadotrophin system' (Figure 1.2) (29).

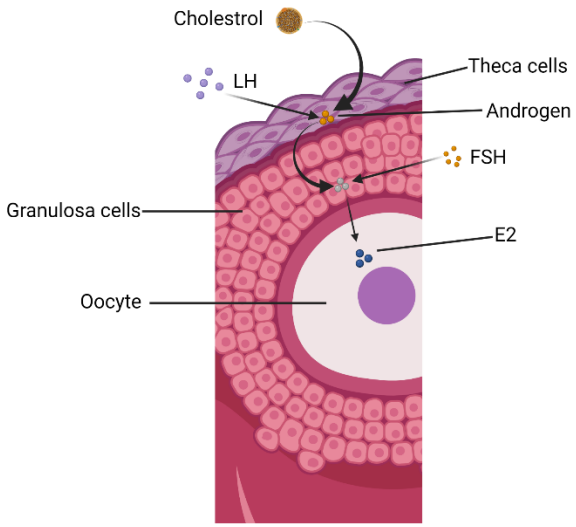


Figure 1.2: E2 biosynthesis in the ovaries. LH and FSH bind to their respective receptors in Theca and Granulosa cells for E2 synthesis in the oocyte. Created in Biorender.com.

The process of steroidogenesis is mediated by several key enzymes including cytochrome P450s, oxido-reductases and steroid reductases which are located in the endoplasmic reticulum and mitochondria (30). Circulating cholesterol enters cells via Low-Density Lipoprotein (LDL) receptors. Cholesterol is then converted into E2, P4, testosterone and cortisol as outlined in Figure 1.3 (30).

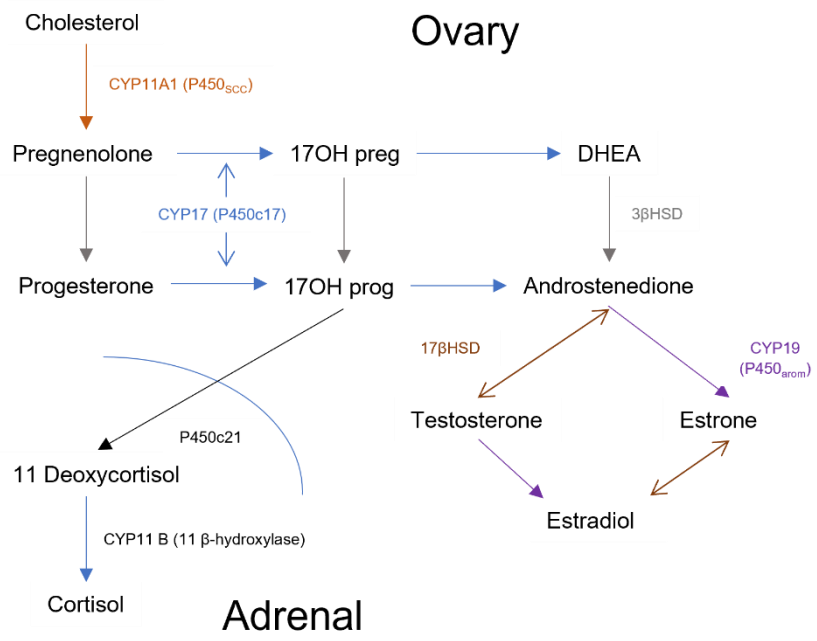


Figure 1.3: Enzymatic regulation of steroidogenesis. Cholesterol is converted to biologically active steroid hormones via a series of enzymatic reactions. Various steroidogenic tissues synthesize steroid hormones via cell-type-specific patterns assisted by specific steroidogenic enzymes.

1.1.2 Progesterone

Progesterone (P4) is the most important progestogen inside the body which act on the uterus to prepare a maternal environment for embryo implantation and growth. Following the mid-cycle LH surge in late follicular phase, P4 secretion increases, which in turn leads to increased FSH concentrations (31). The luteal phase marks P4 preparation of the endometrium to accept and nourish the embryo if fertilisation occurs (32). Increasing pulsatile P4 encourages capillary growth and maturation which allows them to permeate granulosa cells. This causes a major increase in vascularization in the endometrium (33).The *corpus luteum* continues P4 secretion for the first 10 weeks of pregnancy followed by the placenta in the later stages of pregnancy (34). In the absence of implantation P4 levels decrease, and the process of endometrial sloughing is initiated. Due to coiling and constriction of spiral arterioles, the bleeding event of menstruation follows (31). P4 is involved in numerous biological processes during pregnancy including regulation of inflammatory mediators. Low P4 concentrations can increase risk of miscarriage and premature delivery (35).

1.2 Assisted Reproductive Technologies (ART)

1.2.1 IVF Treatment protocols

IVF protocols involve pharmacological manipulation of hormones via suppression of the pituitary followed by controlled ovarian hyperstimulation to achieve maturation of oocytes but also prevent a LH surge which would result in a premature ovulation. Gonadotrophins are central in fertility treatments and ovarian stimulation. In early 1900s, pituitary regulation of gonadal function was first described which paved the way for later gonadotrophin use in artificial ovarian stimulation (36, 37). In the 1940s, human menopausal gonadotropin (hMG) was developed consisting of FSH and LH at 1:1 ratio from post-menopausal urine and later used commercially (38). hMG was first used in infertility treatment in the 1960s for anovulatory women and in the 1980s for anovulatory and for multi-follicle stimulation in IVF cycles (38, 39). Highly purified urinary FSH was developed in the 1990s from hMG using antibody based purification techniques followed by recombinant FSH (rFSH) using recombinant DNA technologies (40). Purified urinary and recombinant gonadotrophins were superior in quality and effectiveness in comparison with earlier hMG urinary products (38). Modern treatments use exogenous gonadotrophins in the form of highly purified hMG and rFSH which maintain the FSH and LH required for the development of many follicles needed for multiple oocyte collection for IVF cycles (41).

Pituitary suppression is an essential part of IVF protocols which is achieved by GnRH analogues. This process can be achieved using GnRH agonists (GnRHa) and antagonists (figure 1.4). This results in E2 withdrawal and a temporary, yet reversable, hypogonadotropic state (42). Subsequently a pharmacological dose of FSH induces the growth of multiple follicles followed by an LH-like exposure to trigger oocyte maturation. Human Chorionic Gonadotropin (hCG) is homologous with LH and can activate a common G-protein coupled receptor and thus is commonly included in protocols to trigger oocyte maturation (43).

GnRHa can be administered as an intra-muscular or subcutaneous injection or as a nasal spray. Through binding to GnRH receptors in the pituitary, GnRHa initially induces gonadotropin release (flare-up effect). Following days of continuous administration, they cause a dramatic decrease in circulating FSH and LH concentrations by desensitization (44).

GnRHa have greater affinity for the GnRH receptor and greater resistance to enzymatic breakdown as well as prolonged half-life (3 hours for Leuprolide compared with 2-4 minutes for native GnRH) (45). These characteristics make them an effective method for pituitary suppression. Once GnRHa is bound to its receptor, the complex is removed from the cell surface (desensitisation) and the complex is uncoupled from the effector system (down-

regulation). This leads to a temporary hypogonadotropic state. Clinically, duration of GnRHa administration can vary according to patient's clinical history and demographics. GnRHa protocols include ultra-short, short as well as long follicular and luteal phase. The GnRHa protocol is however associated with higher risk of Ovarian Hyperstimulation Syndrome (OHSS) (44, 46).

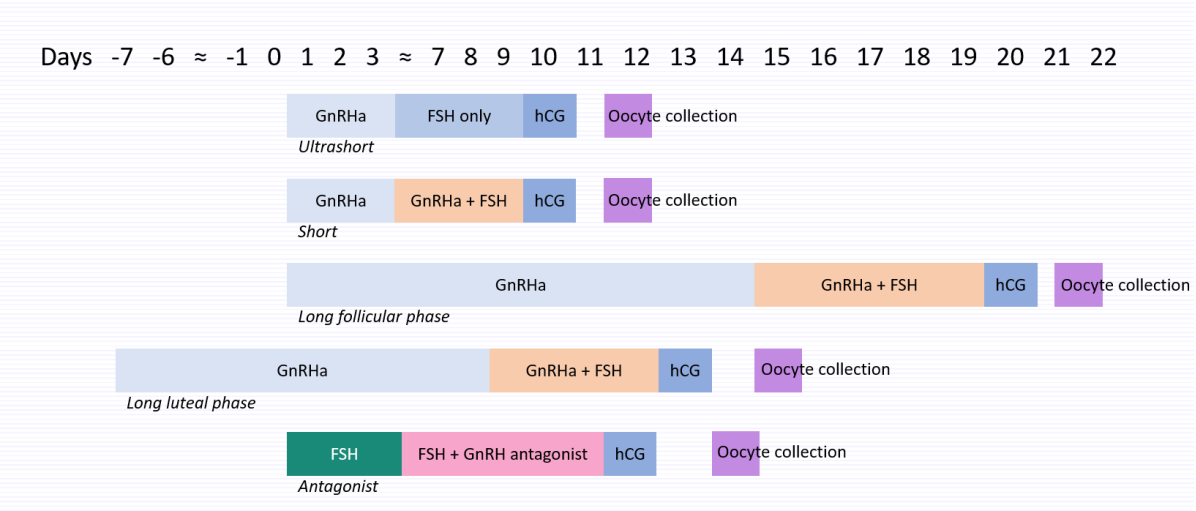


Figure 1.4: Diagrammatic representation of IVF protocols. Demonstration of pituitary suppression, ovarian stimulation and oocyte collection using GnRH analogues (13).

1.2.2 Intracytoplasmic Sperm Injection (ICSI)

The introduction of ICSI represents a major advancement in artificial reproductive treatment options. ICSI involves injecting sperm directly inside the oocyte, thereby bypassing the Zona Pellucida (ZP) (47). This advanced procedure, is particularly beneficial for men with severe male factor infertility and now accounts for many fresh Assisted Reproductive Technology (ART) cycles in addition to conventional IVF (48).

1.2.3 Preimplantation genetic diagnosis and screening

There are various factors that influence the outcome of ART treatments. These include the quality of chosen sperm and egg to create an embryo and the maternal environment in which the embryo is nurtured and developed until birth. Genetic screening of embryos helps minimise embryological factors associated with failure such as aneuploidy (49). Aneuploidy remains the leading genetic cause of pregnancy loss with at least 5% occurrence rate in all clinically recognised pregnancies (50). It has long been recognised that advanced maternal age is strongly associated with aneuploidies. In 1933, the link between maternal age and Down's syndrome was first reported decades before it was understood that the condition is caused by trisomy 21 (51). Other exogenous and endogenous factors contributing to age-related oocyte

aneuploidy include recombination failure, chromosome cohesion deterioration, Spindle Assembly Checkpoint (SAC) dysregulation, abnormalities in post-translational modification of histones and tubulin, and mitochondrial dysfunction (52).

Preimplantation Genetic Testing (PGT) tools are increasingly used for screening and identifying chromosomally normal embryos to improve chances of ART success and avoid transmission of genetic abnormalities to the offspring (53). In the United States, the rate of PGT increased from 4% in 2005 to over 22% in 2015 (54). PGT collectively refers to Preimplantation Genetic Screening for aneuploidy (PGT-A), monogenic conditions (PGT-M), polygenic conditions (PGT-P), structural rearrangements (PGT-SR), and Preimplantation Genetic Diagnosis (PGD) for single gene disorders (55, 56).

PGD was first developed in 1967 by Gardner and Edwards who successfully predicted sex of rabbit fetuses at the blastocyst stage (57). In their experiments, blastocysts were held by negative pressure on a flame-polished pipette while a small cone of ZP was sucked into a second pipette. A small incision was made on the cone and a column of trophoblasts (typically between 200-300 cells) were biopsied. Cells were fixed and stained and scored manually for sex chromatin during a procedure that took up to 2 hours. During this time embryos were kept at room temperature before being subsequently transferred into the recipient females. In 1990, PGD was successfully used to detect adrenoleukodystrophy and other X-chromosome linked disorders for humans (58).

Implementation of PGD to ART cycles has revealed the relatively high prevalence of genetic aberrations harboured by human embryos (59, 60). However, a potential limitation of PGD testing is the concept of mosaicism. Mosaicism occurs when the embryos contain more than one cytogenetically distinct cell line due to errors in chromosome segregation during mitotic divisions (61). Conventionally, most studies on PGD relied on Fluorescence *in situ* Hybridization (FISH) which can provide information on the cytogenetic status of every cell. These studies have reported varying degrees of mosaicism in human embryos ranging from 30% to 90% (61-63). These studies typically examine only one-third or a half of the chromosome in each cell.

In recent years, more sensitive and comprehensive technologies such as array Comparative Genomic Hybridization (CGH) and High-Resolution Next Generation Sequencing (hr-NGS) have become preferable to FISH due to their ability to provide information on copy numbers of all chromosomes (64, 65) (Table 1.1).

Table 1.1: Comparison of complete chromosomal screening methods (66). aCGH: Array Comparative Genomic Hybridization, SNP microarray: Single Nucleotide Polymorphism. qPCR: quantitative Polymerase Chain Reaction. NGS: Next Generation Sequencing. Complete CA: Complete Chromosomal Aneuploidy.

Method	Cost	Complexity	Time (h)	Abnormalities detected	Limitations	Resolution
aCGH	Medium	Medium	~12h	Complete CA and translocations	False positives and unable to detect mosaicism	Medium
SNP microarray	High	High	Up to 72h	Complete CA, parental origin, and translocations	Unable to detect balanced chromosomal rearrangements, and unable to detect mosaicism	High
qPCR	Low	Low	4h	Complete CA	Unable to detect segmental aneuploidy, and unable to detect mosaicism or translocations	Low
NGS	High	High	<24h	Complete CA, mosaicism, mitochondrial copy number, single-gene disorders, and translocation	Limited ability to detect balanced chromosome translocations	High

Table 1.2: Comparison of biopsy techniques for preimplantation genetic testing.

Biopsy technique	Cells collected	Time of biopsy collection	Advantages	Limitations/Disadvantages
Polar Body Biopsy	Polar body from an oocyte	Before embryo cleavage	Removal of polar bodies have no influence on further development of embryos (67).	Only maternal chromosomes or genes are analysed. Limited information can be obtained from a single cell (67).
Cleavage Stage biopsy	1-2 blastomeres from a 6-8 cell embryo	Cleavage stage	Both maternal and paternal meiotic errors are detected, as well as some mitotic errors (68).	Removal of cells at cleavage stage can slow down the development of the embryo to the blastocyst stage (69). It may also affect implantation and pregnancy rates (70). Mosaicism detection degree is variable (68).
Trophectoderm biopsy	5-10 trophectoderms from a 70-100 cell embryo	Blastocyst stage	Overall high implantation rates following transfer of euploid embryos (71).	possibility of false positive or negative due to different cell lineages to the inner cell mass (72) Increased risk of preeclampsia (55).

1.2 The Microbiome

The human body is colonised by complex communities of microorganisms that play important symbiotic roles in many aspects of human physiology including metabolism, pathogen resistance and immune homeostasis (73-76). The assemblage of these microorganisms, which include bacteria, viruses, fungi and archaea, in a specific niche is referred to as the 'microbiota' (77). The term 'microbiome' is often used interchangeably with microbiota but actually refers to the entire habitat, including the microbiota, their genomes, and surrounding biochemical milieu (78).

1.2.1 Human Microbiome

While the completion of Human Genome Project (HGP) in 2001 is widely considered a major advancement in scientific knowledge (79), many in the scientific community recognised that the genetic information encoded in the human genome alone represented just a small fraction of the total genetic information carried within the human body as a whole (80). As such the Human Microbiome Project (HMP) a multi-component community resource was launched in 2007 by the National Institutes of Health (NIH) in America and was completed in 2012 (81). The project aimed to apply cutting edge molecular techniques to catalogue and characterise the human microbiome from multiple body sites of healthy volunteers and begin to determine the impact of microbiome alteration on health and disease, and to produce a readily available standardised data resource to promote broader studies on human microbiome. Part of the HMP focused on characterising the microbiota of the vagina and showed that compared with other body sites studied such as the skin and gut, bacterial diversity and richness of the vagina was low and often dominated by species of *Lactobacillus*. It is now recognised that as many as 100 trillion microbes are estimated to reside in and on the human body. These have evolved to contribute to niche-specific symbiotic relationships between microbe and host that helps to maintain states of health (82). As described below, these relationships begin to form in early life and have profound and long-lasting consequences on host health and disease.

1.2.2 Antenatal to Adult Microbiome

Historically the human fetus was considered to be nourished and matured *in utero* in a sterile environment (83). Using sensitive molecular based tools such as next generation sequencing, recent studies have suggested that the fetus may be exposed to low levels of microbes, which could be harboured in the placenta (84), and that initial immune 'training' of the fetus may start prior to birth (85-88). It is however widely considered that the first major microbial seeding

event of the new-born occurs during birth where it is exposed to a wide range of microbes from a variety of sources including the maternal lower reproductive and digestive tracts. To begin to examine the source of the early life microbiome, Dominguez-Bello et al. examined skin, oral, nasal and meconium samples of 10 neonates (4 born vaginally, 6 via caesarean section) immediately after birth. Their results indicated that the microbiome of neonates is highly influenced by the mode of delivery. Vaginally delivered babies were dominated by communities resembling the vaginal microbiota i.e., *Lactobacillus, Prevotella* and *Sneathia spp.,* while C-section born babies were hosting microbiota resembling the mother's skin flora such as *Staphylococcus, Corynebacterium,* and *Propionibacterium* species. Furthermore, the pyrosequencing of the samples showed undifferentiated communities across the samples collected from different body sites of neonates contrary to the highly differentiated communities of their mothers regardless of the mode of delivery (88).

In addition to the delivery method, the microbiome of healthy neonates depends on gestational age, breastfeeding, exposure to antibiotics and the length of time spent at the hospital (89-91). Following birth, the gut microbiome of humans gradually becomes richer and more diverse during infanthood and by the age of 3 it resembles the microbiota composition of an adult (92, 93).

Evidence also indicates that microbial composition is again restructured in the elderly. A study in 2011 found that *Bacteroidetes* was the dominant phylum in 57% and *Firmicutes* in 40% of faecal samples collected from 161 elderly subjects (94). In comparison, faecal samples of a younger adult control population were dominated by *Bacteroidetes* in only 41% and *Firmicutes* in 51%. Furthermore, exposure to antibiotics correlated with increased levels of *Bacteroidetes* and decreased levels of *Firmicutes, Actinobacteria,* and *Proteobacteria*. The study also concluded that the composition of intestinal microbiota of the elderly had more individual variation compared with younger adult population (94, 95).

Dietary changes, immune dysfunction, frequent exposure to medications including antibiotics, gastric atrophy, damaged dentition and salivary function are all factors that may contribute to microbiome changes in older adults (96). Subsequently, it has been proposed that changes in the microbiota of the elderly may lead to additional chronic health conditions and increase mortality rates of most infections at least 3-fold compared with younger adults with the same disease (97).

1.2.2.1 Menopause

Menopause marks the end of menstruation due to cessation of follicular activity. During the peri-menopause phase, women often express symptoms such as irregular menstrual cycles,

cramps, and tenderness of breasts. Additional symptoms as a result of E2 depletion include vasomotor symptoms, migraines, vaginal dryness and atrophy of tissue (98). The onset of menopause directly influences the microbial composition of the vagina. Imbalance of microbiota is marked by depletion of healthy *Lactobacilli* and increased presence of *G. vaginalis* and *Candida*, the main causes of Bacterial Vaginosis (BV) and vulvovaginal candidiasis (VVC), respectively (99, 100). Consistent with a role in shaping *Lactobacillus* species dominance in the vaginal niche, reduced E2 following the menopause correlates with decreased glycogen levels and vaginal epithelium thinning that in turn associates with increased bacterial diversity (101). Consistent with this, administration of E2 replacement therapy is considered an effective way to prevent urogenital infections in post-menopausal women by promoting vaginal dominance of *Lactobacillus* species (102).

1.2.2 Characterisation of Microbiota: From Culture-Based Methods to Metataxonomic Profiling

Characterisation of the microbiome by culture has proved challenging due to the complex nutritional requirements of different bacterial species (103). There are potentially thousands of different bacterial species present in a given niche that require different growth conditions. Further, isolated strains may behave differently in culture than in their natural environment (104). Therefore, producing an accurate catalogue of clinically relevant species by conventional microbiological means is highly challenging, if not impossible (105, 106). It has been estimated that 80%-99% of bacteria cannot be cultivated (104). Anaerobic organisms are particularly challenging and are often underrepresented by culture growth (107).

One solution to this is to detect and identify species directly from a sample or site using taxonomic information contained within microbial genomes. This requires sensitive and specific methods that can accurately characterise genomic information of potentially highly complex microbial communities. These approaches emerged in the 1970s with the development of DNA sequencing methods, which were initially costly and labour intensive (108). Sanger sequencing, developed in 1977, offered a faster and more accurate technique and paved the way for modern sequencing technologies (109). Some limitations associated with Sanger sequencing include suitability to sequence short pieces of DNA (300 to 1000 base pairs) and the fact that the quality of sequence is generally not great in the first 15 to 40 bases where the primers bind (110). These limitations were overcome through the advent of next generation sequencing (NGS) approaches which offered cheaper, faster and less labour intensive DNA sequencing, capable of performing whole genome sequencing within a day regardless of the genome size (111). The principle of NGS is the construction of a sequencing library and clonal amplifying of DNA fragments *in vitro.* In addition, array based sequencing of

NGS involves DNA fragments being multiplexed and immobilised on a solid substrate (112). One application of this method involves the amplification and sequencing of specific bacterial genes such as the 16S rRNA gene. The 16S rRNA gene contains 9 'hyper variable' regions (V1-V9). The hyper variable segments are attached to conserved stretches which enable PCR amplification or target sequences by universal primers (113). These regions express high sequence diversity in different species and are used to develop species-specific hybridization probes and PCR primers with the ability to detect and identify species and in some cases species strains (114). This approach is referred to as 'metataxonomics'. Metataxonomics involves amplification of sequencing of short-length regions of microbial taxonomic marker genes including the commonly targeted hypervariable regions of bacterial 16S rRNA gene (115).

1.2.3.1 Conventional approaches for bacterial detection in the reproductive tract

Culture and microscopy remain the mainstay techniques used for investigating microbes isolated from the vagina and low reproductive tract in clinical environments. Results are often combined with symptomatic assessments for the purpose of diagnosis. For example, bacterial vaginosis (BV) is microbiologically characterised as displacement of commensal *Lactobacillus* species with an overgrowth of typically, strict anaerobes, many of which are considered potential pathogens of the cervicovaginal niche. The Amsel Criteria, first described in 1983, is based upon a combined assessment of both clinical symptoms (e.g. fishy odour, pH, and white discharge) and microscopic features of vaginal secretions that include presence of vaginal epithelial cells coated by gram-variable bacteria referred to as Clue cells (116). The Nugent Criteria is often employed for diagnosis of BV in research settings and relies upon microscopic evaluation and grading for the presence or absence of three key bacterial morphotypes; i) large gram-positive rods, ii) small gram-variable rods and iii) curved gram-variable rods (117). These morphotypes were thought to correspond to the genera *Lactobacillus, Gardnerella* and *Mobiluncus* respectively, although recent molecular analyses of the *Mobiluncus* morphotypes indicates that they are more likely other BV-associated bacteria such as BV-associated bacterium-1 (BVAB1) (118), now referred as *Candidatus* Lachnocurva vaginae (119).

The first culture independent study on vaginal bacteria was done in 2002 in a cohort of 20 postmenopausal women (120). The authors used a combination of Polymerase Chain Reaction (PCR) and denaturing gradient gel electrophoresis. Since then, phylogenetic analysis of 16S ribosomal rRNA (rRNA) gene sequencing has been widely used for assessment of reproductive tract microbiome composition.

1.3 Reproductive tract microbiome

There is now substantial evidence implicating the vaginal microbiome in reproductive tract health and disease. As technology has developed, the ability to characterise the composition of the reproductive tract microbiome of both females and males has improved and provided new insights into how commensal and pathogenic microbes can interact with the host to protect against, or potentiate, pathology and disease. Like other body sites that have been studied in greater detail (e.g., oral cavity and gut), the lower female reproductive tract hosts a thriving microbiota, the composition of which is subject to change throughout a woman's lifespan. There is growing recognition that specific vaginal microbiota associate with states of good reproductive health and can therefore be considered "optimal". In contrast, other microbiota compositions are more frequently observed prior to or during a shift toward a pathogenic state and are thus considered "suboptimal". The endogenous and exogenous factors that influence colonisation of different vaginal microorganisms, and how the host responds to them, are critical in determining their role in the niche.

While studies in new era of metataxonomic technology have mostly focused on female reproductive tract, there is increasing evidence that the male reproductive tract harbours a microbiota, despite being traditionally considered sterile in absence of infections. However, the origin, microbiota-host interactions, and impact of microbiota on male reproductive functions remains unclear with only a handful of studies to date with contrasting findings (121-125).

1.3.1 Female reproductive tract microbiome

As early as the late 19th century, vaginal bacteria had begun to be linked to states of reproductive health and pathology. Investigating the concept that vaginal bacteria may be involved in post-partum sepsis, Albert Döderlein discovered and described for the first time *Lactobacillus* species, which were present in high abundance in the vaginal secretions of many women (126). Soon after it was noted that in the absence of the *Lactobacillus* species, the vagina would instead be often colonised by "diphtheroids, enterococci and staphylococci" (127). Culture and microscopy would continue to be the main tools used for investigating vaginal microorganisms for at least the next century. These studies enabled important associations to be made between 'abnormal' vaginal microbial communities, typically described as those depleted of *Lactobacillus* species with increased diversity of facultative or strict anaerobes, and a range of poor reproductive health outcomes including increased risk

of sexually transmitted infections (128, 129) and pregnancy complications such as miscarriage and preterm birth (130-132).

In 2011, a study by Ravel and colleagues provided a more in depth characterisation of the vaginal microbiota in a large (n=396) and ethnically diverse cohort of reproductive aged women (133). Investigating samples collected from a similar number of asymptomatic Asian, Black, Hispanic, and White women, the study showed that bacterial profiles of the vagina could be classified into 5 so-called “community state types” (CSTs) that were characterised by the presence or absence of four *Lactobacillus* species; CST I- *L. crispatus* dominated, CST II- *L. gasseri* dominated, CST III- *L. iners* dominated and CST V- *L. jensenii* dominated. A fifth group termed CST IV, was characterised by a lack of *Lactobacillus* species, and increased relative abundance of typically strict anaerobes that had previously been linked with BV including *G. vaginalis, Prevotella, Dialister* and *Atopobium* species. Importantly, the study also reported that the bacterial composition of the vaginal microbiome is influenced by ethnicity of the host. Vaginal CSTs from White (89.7%) and Asian (80.2%) women were most commonly those dominated by *Lactobacillus* species. In comparison, only 59.6% of Hispanic and 61.9% of Black women had CSTs dominated by *Lactobacillus* species. Numerous studies have since confirmed the relationship between ethnicity and vaginal microbiome composition (134-137) and the broad compositional characteristics of the original CSTs, sometimes now referred to as ‘vagitypes’ or ‘vaginal microbial communities’, have been consistently observed in other populations (134, 138-141). As the volume of vaginal microbiome studies increases, it becomes clearer that additional, rarer vaginal CSTs exist, and efforts are now being made to standardise how CSTs are calculated and described to improve comparability of data across studies (142). To this extent, the VALENCIA algorithm, a nearest centroid classification algorithm, has been recently developed to categorise vaginal microbial communities based on composition and structure with high reproducibility (Figure 1.5) (142). This method maps vaginal microbiota profiles to a large dataset of more than 13,000 samples classifying samples initially into 1 of 7 CSTs that are akin to the original CST classifications described by Ravel (133) before being further subclassified into 1 of 13 CSTs (see Figure 1.5): CST I-*L. crispatus* dominated, CST II-*L. gasseri* dominated, CST III-*L. iners* dominated, and CST V-*L. jensenii* dominated. CST I and CST III are split into 2 sub-CSTs A and B. CST I-A and CST III-A represent samples with high relative abundance of *L. crispatus* and *L. iners* respectively and CST I-B and CST III-B represent samples with lower relative abundance of *L. crispatus* and *L. iners*. The 3 remaining CSTs do not have high relative abundance of *Lactobacillus* are called CST IV-A, CST IV-B and CST IV-C. CST IV-A is characterised by high relative abundance of *Candidatus* Lachnocurva vaginae (BVAB1) and a moderate relative abundance of *G. vaginalis*. CST IV-B is characterised by high relative abundance of *G. vaginalis* and low

relative abundance of *Candidatus Lachnocurva vaginae.* CST IV-C is characterised by low relative abundance of *Lactobacillus, G. vaginalis*, *Candidatus Lachnocurva vaginae, A. vaginae* and high relative abundance of facultative and strictly anaerobic bacteria.

Samples can then be mapped in higher resolution to the 7 CSTs are further broken down into 13 sub-CSTs. Similarly, to the CST classifications first published by Ravel the *Lactobacillus* dominated CSTs are as follows: CST IV-C is divided into 5 sub-CSTs as follows: CST IV-C0 signifies an even community with moderate amounts of *Prevotella*, CST IV-C1 is dominated by *Streptococcus*, CST IV-C2 is *Enterococcus* dominated, CST IV-C3 is *Bifidobacterium* dominated, and CST IV-C4 is *Staphylococcus* dominated (Figure 1.5).

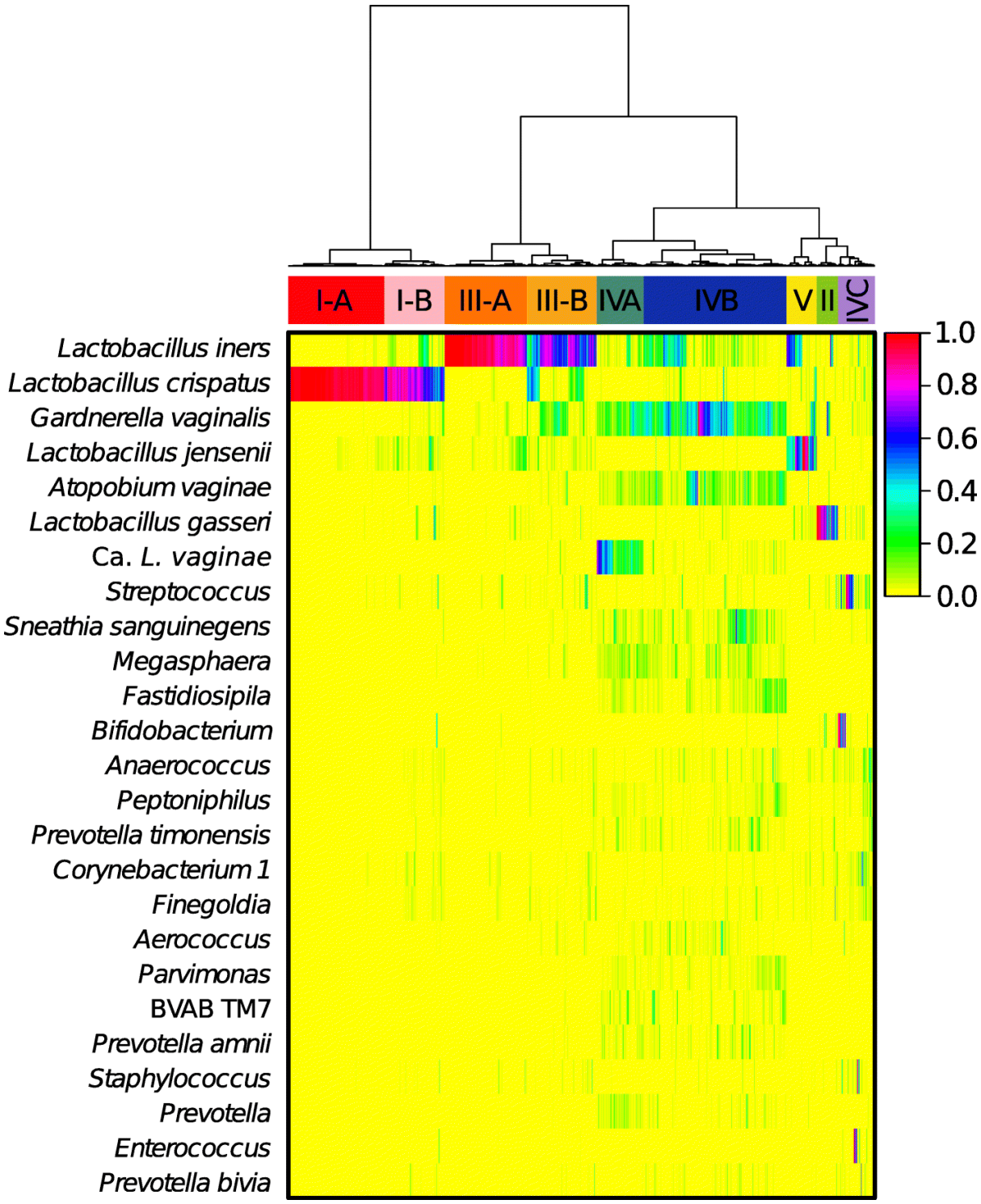


Figure 1.5: Vaginal microbiome of non-pregnant women of reproductive age. Produced by France et al. (2020), the vaginal microbiome sub-CSTs.

1.3.1.1 Factors influencing the composition of the vaginal microbiome

Despite its comparative simplicity, the compositional structure of the vaginal microbiota is dynamic (138) and it changes throughout a women's lifespan. These changes often occur in

concert with circulating hormonal levels, particularly E2. Soon after birth, colonisation of the vagina begins under the influence of high circulating maternally derived E2 concentrations (143). This leads to increased storage of glycogen in the vaginal epithelia, which when broken down into complex sugars by host α-amylase, can be used preferentially as energy sources by *Lactobacillus* species, which were seeded there during delivery.

As maternal E2 is metabolised, glycogen levels are depleted and a shift towards a high-diversity community structure depleted in *Lactobacillus* species is observed, which is accompanied by increased pH, the vaginal microbiota composition becomes more similar to reproductive-age women, characterised by increased *Lactobacillus* species dominance and reduced diversity (144). The highly estrogenic state of pregnancy, caused by feto-placental production of E2, further supports *Lactobacillus* species dominance of the vagina (145, 146).

Post-delivery, disturbance of biochemical microenvironment of the vaginal mucosa caused by passing of amniotic fluid and bleeding during delivery combined with a rapid decline in maternal E2 (147) sees vaginal microbiota increase in richness and diversity (145). This shift towards CST-IV profiles have been shown to persist in some women for up to one year following delivery (148). Other host factors that influence the composition of the vaginal microbiota include menses (138, 149-151), hormonal contraceptives (152-154), antibiotics (155-158) and sexual activity (152, 159, 160).

In a recent study of 26 college-aged women who self-sampled daily for 10 weeks, changes in vaginal microbiota composition were also associated with diet and exercise (151). This finding highlights the potential of lifestyle change as a means for non-invasively manipulating vaginal microbiota composition. Figure 1.6 provides a schematic summary of factors influencing vaginal microbiota.

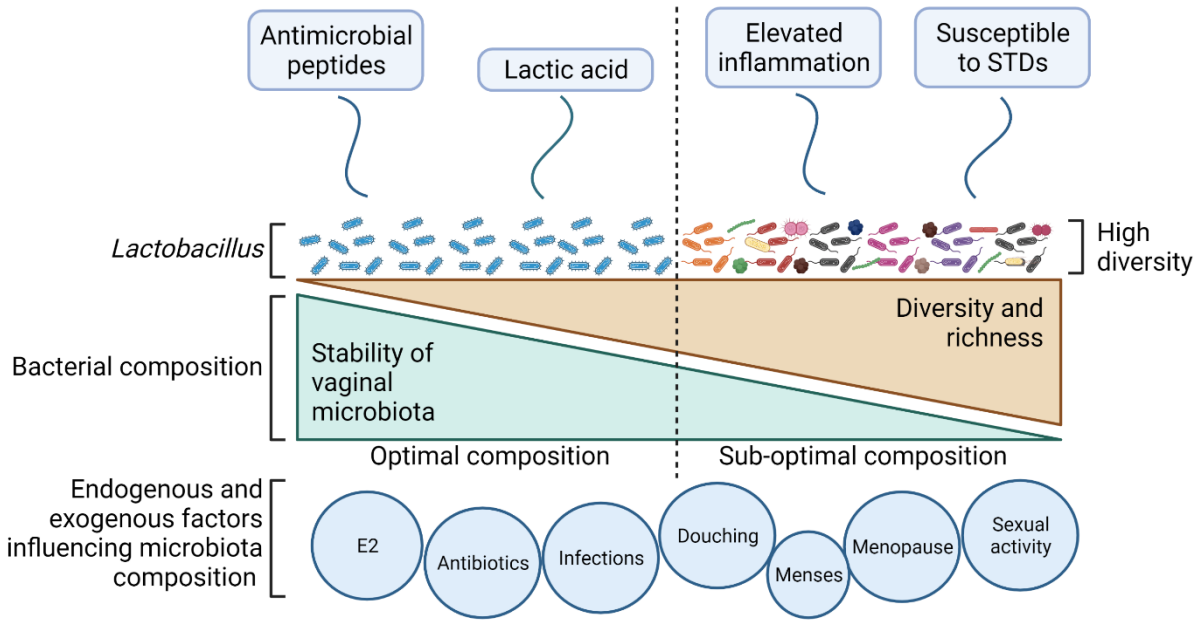


Figure 1.6: Overview of factors influencing vaginal microbiota composition and stability and its relationship with health and disease states. *Lactobacillus* species are more stable and are considered optimal compositions in the vaginal milieu. Created in Biorender.com.

1.3.1.2 Vaginal microbiota, pathogen colonisation and host response

There are distinct anatomical, immunological, and morphological differences between the lower (vagina and ectocervix) and upper (uterus and endocervix) reproductive tract that reflect their unique functions (Figure 1.7). For example, the vaginal epithelia consists of multiple protective layers of non-keratinised stratified squamous epithelial cells that can vary in thickness from a few to 45 cells (161). In comparison, the epithelia of the upper reproductive tract consist of a single layer of columnar epithelial cells. In the vagina, cells in the apical layer undergo cornification, a process by which they lose their nuclei and intracellular organelles (162). These cells are exfoliated approximately every four hours into the vaginal lumen (161) assisting in the removal of invading pathogens (163, 164). Mitosis in the basal layer promotes renewal of the epithelium (161) with an estimated turnover of approximately 96h (165).

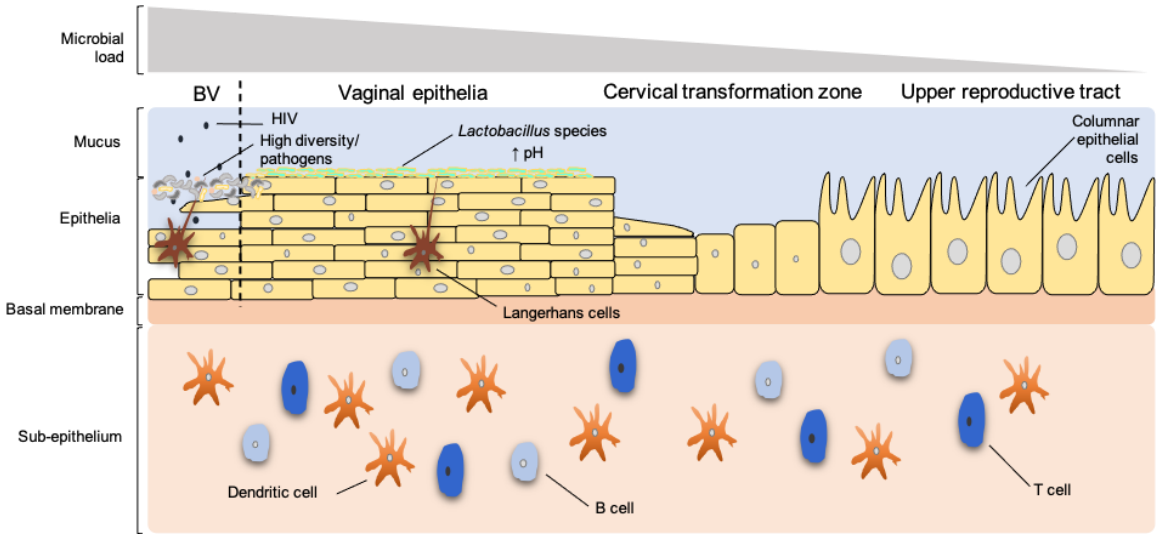


Figure 1.7: Microbiota-host interactions at epithelial mucosal interface throughout the reproductive tract. Vaginal epithelia act as a barrier to pathogens. Damaged vaginal epithelia make the host susceptible to infections.

The lower reproductive tract has evolved alongside a high bacteria load compared to the upper reproductive tract. This is largely due to the cervix which acts as both a physical and immunological barrier between the upper and lower reproductive tract (166, 167). Mucus produced by the cervix is predominantly composed of water and highly glycosylated proteins called mucins that can act as sites of attachment and adhesion as well as energy substrates for microbiota (168).

Mucus production by the cervix is driven by E2 and as levels rise, viscosity typically decreases which is important for allowing the passage of spermatozoa through the mucus (169). During pregnancy, the cervical mucus forms a plug that seals the cervix helping to prevent ascending infection from the vagina (170, 171). The mucosal layer is also enriched by proteins and metabolites produced by both host and microbial cells that regulate its function. For example, specific isoforms of lactic acid produced by *Lactobacillus* species can alter viscosity and thus the viral trapping capacity of cervical mucus (172-174). Lactic acid also decreases mucosal pH to a level (4.0 ± 0.5) which is microbicidal for many pathogens. Secretion of biosurfactants and bacteriocins and competitive exclusion through displacement and inhibitory adhesion are additional strategies by which *Lactobacillus* species help to protect against pathogen colonisation in the lower reproductive tract (133, 175-177).

While *Lactobacillus* species are widely considered to be important components of a healthy vaginal microbiome, increasing evidence suggests that *L. iners,* a common species frequently isolated from the vagina, may act as an intermediatory between optimal and sub-optimal vaginal microbiomes (178). The genome of *L. iners* is unusually small (1.3 Mbp) compared

with *L. crispatus* (3-4 Mbp) and contains genes encoding for iron-sulfur proteins, unique σ-factors as well as a pore-forming toxin called inerolysin (179). Complex nutritional requirements have also likely contributed to its apparent tolerance of potentially pathogenic species that provide it with metabolic breakdown products leading it to be frequently detected in both healthy and pathogenic states (178).

1.3.1.3 Vaginal microbiome and pregnancy outcomes

Given its important role in mediating immune response and inflammation within the reproductive tract, there is growing interest in understanding the relationship between the vaginal microbiome and reproductive health and disease states. In reproductive aged women, vaginal microbiota communities dominated by *Lactobacillus* species have been shown to provide protection against a wide range of pathologies and diseases including BV (180, 181), pelvic inflammatory disease (182), candidiasis (183) and various sexually transmitted infections such as HIV, HSV-2 (184-186) and human papilloma virus, the latter being causally linked to the development of cervical cancer (187, 188). In a recent study, regression of untreated cervical intraepithelial neoplasia 2, the pre-invasive precursor of cervical cancer, is associated with dominance of vaginal microbiota by *Lactobacillus* species (189). Data also indicated that vaginal microbiota may harbour the capacity to modulate the efficacy of some therapeutic interventions. The topical pre-exposure prophylactic, Tenofovir, is superior in preventing HIV acquisition in women with *Lactobacillus*-dominated vaginal microbiota compared to women colonised predominately by *G. vaginalis* and BV-associated bacteria (190).

There is also substantial evidence that the vaginal microbiota influences the reproductive success of the host. Vaginal microbiota composition has recently been associated with infertility (191-194) and has even been proposed as a predictive biomarker for *in vitro* fertilisation success (195, 196). Despite differences in design and techniques used to assess microbiota composition, these studies are in general agreement that *Lactobacillus* species dominance of the vaginal niche associates with successful embryo implantation whereas *Lactobacillus* species depletion and overgrowth of facultative anaerobes associates with poorer rates of success. The importance of *Lactobacillus* species dominance continues into pregnancy. Vaginal microbiota depleted of *Lactobacillus* species have recently been linked with first trimester miscarriage (197) and early data suggests that women who suffer unexplained recurrent miscarriage have higher prevalence of potential pathogens including *Atopobium*, *Prevotella* and *Streptococcus* species (198).

The vast majority of research on the pregnancy vaginal microbiome to date has been focused toward understanding its relationship with preterm birth (115), which continues to be the leading cause of childhood mortality worldwide (199). Vaginal pathogen infection (200) or pathologies such as BV (201, 202) and aerobic vaginitis (200) have long been recognised to increase preterm birth risk. However, recent application of metataxonomic profiling approaches in pregnancy have provided new insights into the relationship between vaginal microbiota composition and Preterm Birth (PTB) (115, 203). Numerous studies across different global populations have now shown that in women of White ethnic backgrounds, there exists a positive association between increased vaginal microbial diversity and risk of PTB (135, 204-209). In contrast, studies of Black pregnant women have not shown any relationship between vaginal microbiota composition and preterm risk (210) or have reported decreased vaginal diversity in women subsequently experience preterm birth (211, 212). These findings suggest that the influence of ethnicity on the vaginal microbiota extends to its association with certain pathologies, including preterm birth. A summary of studies investigating the relationship between the vaginal microbiota and IVF success is presented in Table 1.3.

Table 1.3: A summary of studies investigating the relationship between the vaginal microbiota and IVF success.

Authors	Date published	No. of subjects	Protocol	Sampling	Relationship between vaginal microbiota and IVF success	Significant impact on outcome?
Ralph et al. (213)	1999	867	Gram stain	On the day of oocyte retrieval.	BV does not affect the conception rate in women undergoing IVF but may increase risk of miscarriage in the first trimester	N
Liversedge et al. (214)	1999	301	Gram stain	On the day of oocyte retrieval.	presence of BV does not have an adverse impact on embryo implantation rates and treatment outcomes	N
Eckert et al. (215)	2003	91	Gram staining and culture	On the day of embryo transfer.	Reduced concentration of *Lactobacillus* spp. may be associated with decreased conception rates and increased rates of early pregnancy loss.	Y
Selman et al. (216)	2007	152	Culture	On the day of embryo transfer.	The cohort of patients who tested positive for Entrobacteriaceae and *Staphylococcus* species had significantly lower pregnancy rates compared with the negative cohort	Y

Hyman et al. (217)	2012	30	16S rRNA sequencing	Ultrasound, oocyte retrieval, embryo transfer and 6-8 weeks gestation.	Diversity of vaginal species is dependent on E2/P4 serum level. The diversity on the day of embryo transfer correlates with outcome of the IVF treatment (samples comprised solely of *Lactobacillus* spp. being favourable for lower diversity).	Y
Mangot-Bertrand et al. (218)	2012	307	Nugent score and qPCR	On the day of oocyte retrieval.	BV positive patients had a lower embryo implantation rate than BV negative patients. This difference was not statistically significant.	N
Haahr et al. (219)	2016	130	qPCR	2-4 weeks prior to start of IVF treatment.	High concentrations of *G. vaginalis* and *Atopobium vaginae* are associated with low clinical pregnancy rates.	Y
Haahr et al. (195)	2018	120	V4 hypervariable region of the 16S rRNA gene and qPCR	First consultation before initiation of the IVF treatment.	No association between CSTs of the vagina and reproductive outcomes are established. However high Shannon diversity index (>0.93) is associated with low pregnancy and live birth rates. Abnormal vaginal microbiota (diagnosed by qPCR) is	Y

					significantly associated with poor reproductive outcome.	
Wee et al. (191)	2018	31 (65 samples collected)	V1-V3 hypervariable regions of the 16S rRNA gene	During hysteroscopy examination. Vaginal and cervical swabs and endometrial biopsy.	Vaginal microbiome composition is associated with successful fertility outcomes. Trend of *Gardnerella* in the cervix and *Ureaplasma* in the vagina were associated with women with history of infertility.	Y
Koedooder et al. (196)	2019	303 (192 samples used for analysis). IVF population, vaginal swabs.	IS-pro technique (16S-23S rRNA gene)	Sample collection prior to start of the IVF or IVF-ICSI procedure.	Women with a low percentage of *Lactobacillus* in their vaginal samples are less likely to have successful embryo implantation.	Y
Vergaro et al. (220)	2019	150	qPCR (gDNA)	On the day of embryo transfer	Bacterial compositions associated with BV do not affect live birth rates at the time of embryo transfer.	N
Fu et al. (221)	2020	67 (recurrent implantation failure	V3-V4 hypervariable regions of the	1 month and 7 days before embryo transfer	Vaginal *Lactobacillus* positively correlates with successful pregnancy in patients undergoing IVF. Patients with recurrent implantation failure	Y

		n=27, control group n=40)	16S rRNA gene		contained significantly less *Lactobacillus* and more pathogens compared to the control group	
Kong et al. (193)	2020	555 (475 included)	V4 hypervariable region of the 16S rRNA gene	Before endometrium preparation.	Lower abundance of *Lactobacillus* and higher abundance of *Gardnerella* and *Prevotella* are detected in patients that did not achieve pregnancy following IVF.	Y
Zhao et al. (192)	2020	122 (secondary infertility patients n=30, controls n=92)	V1-V2 hypervariable region of the 16S rRNA gene	Vaginal swabs: 1 sample in early follicular phase and 1 sample following GnRH agonist and r-hCG administration.	Secondary infertility was associated with reduced α-diversity compared with healthy women in follicular phase but no after ovulation. *Bifidobacterium* was associated with unsuccessful IVF treatments.	Y
Hao et al. (222)	2021	124 (IVF patients)	V3-V4 hypervariable regions of the 16S rRNA gene	On the day of embryo transfer.	*Lactobacillus* species are more abundant in non-pregnant patients than pregnant in fresh IVF cycles. No difference was observed in frozen IVF cycles.	Y

1.3.1.4 Upper reproductive tract microbiome

Several studies have reported a connection between the presence of pathogenic bacteria in the uterus and pelvic inflammatory diseases (223-225). Furthermore, presence of Streptococcaceae and Staphylococaceae is significantly higher in cystic fluid of women with ovarian endometrioma compared with a control group (226). Early research on the microbiota of human endometrium suggested that in the absence of infections, the uterine cavity is free from microorganisms (227, 228). Since then, accumulating data have demonstrated that the upper female reproductive axis is not sterile and harbours an active microbial ecosystem (229). Most abundant phyla found in the endometrium include: Firmicutes, Bacteroidetes and Proteobacteria and similarly to the vagina, *Lactobacillus* is the most abundant genus (230-232).

The origin of upper reproductive tract microbiota is still debated. Studies have found that radioactively labelled particles are transported from the vagina to the uterus in 2 minutes during both follicular and luteal phases (233). This suggests that fluids and particles can move from the lower and upper reproductive tract freely. In theory, the origin of endometrial microbiome could be of hematogenous bacteria ascending from the vagina or other factors such as gynaecological interventions or IVF. A study by Mitchell and colleagues analysed swabs from the endometrium and upper endocervix (231). They reported presence of low biomass bacteria in said organs and concluded that either the cervix serves as a partial filter on ascending microbiota from the vagina or the endometrial immune response eliminates most of the ascending bacteria. Another study reported that the endometrial bacteria resemble CSTs of the lower reproductive tract and most likely originate from the vagina (234). Further supporting that theory, Walther-Antonio et al. found that microbiome present throughout the reproductive tract organs including vagina, cervix and fallopian tubes is highly correlated within an individual (235). On the contrary, Chen and colleagues reported the existence of unique microbiome compositions in the cervix, uterus and fallopian tubes independent of that of the vagina (230). Furthermore, Moreno and colleagues found that microbial communities from endometrial fluid and vaginal aspirates within the same study subjects presented differences in some women (232). Table 1.4 summarises studies on endometrial microbiota.

Table 1.4: A summary of studies investigating the endometrial microbiota.

Study	Date	Design and cohort	Method	Findings
Aagaard et al. (84)	2014	Case cohort study of 320 patients (89 preterm, 231 term)	16S rRNA and whole genome shotgun sequencing	Unique placental microbiome with non-pathogenic commensal microbiota: *Firmicutes*, *Tenericutes*, *Proteobacteria*, *Bacteroidetes* and *Fusobacteria* phyla. The profiles resembled the oral microbiome. 16S analyses showed an association between placental microbiome with a remote history of antenatal infections like urinary tract infection in the first trimester as well as preterm birth.
Mitchel et al. (231)	2015	Swabs collected prior to hysterectomy from endometrium and upper endocervix for 58 women.	Selective PCR assays for 12 bacterial species: *L. iners, L. crispatus, L. jensenii, G. vaginalis, A. vaginae, Megasphaera spp, Prevotella spp, Leptotrichia/Sneathia,* BVAB1, BVAB2, BVAB3, and a broad range 16S rRNA gene assay	Endometrial cavity was not sterile in most women undergoing hysterectomy. Presence of low biomass microbiota in the endometrium was not associated with inflammation.

Moreno et al. (236)	2016	Paired samples of endometrial fluid and vaginal aspirates in pre-receptive and receptive phases within the same cycle. Endometrial fluid at pre-receptive and receptive phases within the same cycle. 13 fertile women to identify the existence of an endometrial microbiota. 22 fertile women to investigate the hormonal regulation of the endometrial microbiota during receptivity. 35 infertile women undergoing IVF to assess the reproductive impact of an altered endometrial microbiota.	V3-V5 hypervariable regions of the 16S rRNA gene	Distinct bacterial communities in the uterine cavity were different to the vaginal communities in some subjects. Presence of non-*Lactobacillus* dominated microbiota in a receptive endometrium was associated with significant decrease in implantation, pregnancy, ongoing pregnancy, and live births.
Walther-Anthonio et al. (235)	2016	Vaginal, cervical, Fallopian, ovarian, peritoneal, and urine samples. 17 patients with endometrial cancer. 4 patients with endometrial hyperplasia. 10	V3-V5 hypervariable regions of the 16S rRNA gene	Microbiome from all sample collection sites correlated within an individual. There was a structural microbiome shift in cancer and hyperplasia cases.

		patients with benign uterine conditions		Detection of *Atopobium vaginae* and *Porphyromonas* spp Combined with high pH was associated with endometrial cancer.
Franasiak et al. (237)	2016	33 patients undergoing euploid single embryo transfer. The most distal 5-mm portion of the transfer catheter tip was used for analysis.	V2-4-8, and V3-6,7-9 hypervariable regions of 16S rRNA gene	*Lactobacillus* was the top genus for patients who achieved pregnancy and those who did not (followed by *Flavobacterium*).
Chen et al. (230)	2017	Samples from 6 locations (lower third of the vagina, posterior fornix, cervical mucus, endometrium, left and right fallopian tubes, peritoneal fluid) were collected for 110 symptomless women.	V4-V5 hypervariable regions of 16S rRNA	Distinct microbial communities in cervical canal, uterus, fallopian tubes, and peritoneal fluid, were different from that of the vagina. The vaginal sample collection sites and the cervical mucus were predominantly made up of *Lactobacillus* species. *Lactobacillus* constituted for 30.6% of endometrial samples, 1.7% of fallopian tube samples and even lower in peritoneal fluid from the pouch of Douglas.
Wee et al. (191)	2018	A retrospective pilot study for 31 women to determine whether the reproductive tract microbiota differs between women with a history of infertility and fertile women during hysteroscopy examination. Vaginal and cervical	V1-V3 hypervariable regions of the 16S rRNA gene	Vaginal microbiome composition was associated with successful fertility outcomes. Trend of *Gardnerella* in the cervix and *Ureaplasma* in the vagina were associated with women with history of infertility.

		swabs as well as endometrial biopsies.		
Kyono et al. (238)	2018	Endometrial fluid samples collected using IUI catheter for 92 women undergoing IVF	16S rRNA gene sequencing	Pregnancy rates were higher for *Lactobacillus* dominated endometrial samples but not significantly different.
Carosso et al. (239)	2020	15 predominantly Caucasian patients undergoing IVF. Vaginal swabs and assessment of embryo transfer catheter tip on the day of embryo transfer.	V3-V4-V6 hypervariable regions of the 16S rRNA gene	Increase in endometrial *Prevotella* and *Atopobium* as well as decrease in *Lactobacillus* following ovarian stimulation was associated with reduced implantation rates following IVF.
Riganelli et al. (240)	2020	Endometrial and vaginal samples from a cohort of 34 predominantly Caucasian women with history of implantation failure. Vaginal fluid with cytobrush and endometrial biopsies with IUI catheter collected at day 21of menstrual cycle before start of IVF	V4-V5 hypervariable regions of the 16S rRNA gene	Endometrial microbiota were more diverse compared with vaginal microbiota. Lactobacilli were exclusively detected in the endometrial compositions of patients with unsuccessful IVF outcomes.
Chen et al. (241)	2021	94 infertile patients: 25 with chronic endometritis and 69 without chronic endometritis. Endometrial fluid with IUI	V4 hypervariable region of the 16S rRNA gene	High abundance of *G. vaginalis* was observed in patients with chronic endometritis. *G. vaginalis* was also associated with unsuccessful IVF outcomes.

		catheter, 3-5 days after secretory phase.		
Diaz-Martinez et al. (242)	2021	48 patients undergoing IVF treatments. Vaginal swabs and transcervical endometrial tissue.	V3-V4 hypervariable regions of the 16S rRNA gene	Higher abundance of *Lactobacillus* species was associated with greater clinical pregnancy rates.
Ichiyama et al. (243)	2021	145 patients with recurrent implantation failure and 21 controls in an Asian population. Vaginal swabs and transcervical endometrial tissue with pipette on day 5-7 after ovulation	16S rRNA gene sequencing	Vaginal microbiota of patients with recurrent implantation failure had lower abundances of *Lactobacillus* compared with controls. Endometrial bacteria compositions were not significantly difference between recurrent implantation failure patients and controls.
Moreno et al. (244)	2022	342 asymptomatic women undergoing IVF	V2-4-8 and V3-6, 7-9 hypervariable regions of the 16S rRNA gene.	*Lactobacillus* species are enriched in patients with live births outcomes. A dysbiotic endometrial microbiota including *Atopobium*, *Bifidobacterium*, *Gardnerella*, *Staphylococcus* and *Streptococcus* were associated with unsuccessful outcomes.

1.3.2 Semen and male reproductive tract microbiome

Male reproductive potential is decreasing. Several congenital and acquired factors are contributing to this trend. Among the known pathological factors' urogenital abnormalities, varicocele, endocrine abnormalities, primary and secondary testicular failure, genetic disorders including chromosomal abnormalities, immunological factors, cancer, are known to be the leading contributors of male factor infertility (245). Lifestyle changes also protect/damage male fertility potential. Exposure to toxins (pesticides and air pollution) radiation, unbalanced diet, smoking, excessive alcohol consumption, and lack of physical activity are all associated with suboptimal semen (245-247). Additionally, infections of the urogenital tract such as prostatitis and epididymitis are long understood to be potential causes of male infertility.

1.3.2.1 Sperm

Sperm cells are highly specialised cells that deliver the male pronucleus to the oocyte. The structure of the sperm is unique, divided into 4 parts: head, neck (connecting piece), midpiece and tail (248). The head contains the nucleus covered by a nuclear envelope (NE) and protected by perinuclear theca (PT) that is made up of densely coiled chromatin (haploid DNA) fibres (249). The acrosome is also placed in the sperm head. A sac-like secretory granule derived from the golgi apparatus, covered by membranes (250). The acrosome contains several enzymes that assist in the process of physiological acrosome reaction by binding the anterior sperm head plasma membrane with ZP membrane. These enzymes include: acid glycohydrolases, proteases, and esterases that are secreted at the site of sperm-ZP biding (251).

The tail is made up of two pieces: midpiece and principal piece. The midpiece assist in optimised motility and efficiency to reach the oocyte for fertilisation and contains mitochondria that generate energy by oxidative phosphorylation (252). The principal and end pieces beat and propel the sperm forward (253).

1.3.2.2 Seminal fluid

Ejaculated semen is not homogenous as it comprises of a mixture of secretions from the sex glands with varying compositions (254). Secretions from epididymis, seminal vesicles, prostate, bulbourethral grands and periurethral glands vary in consistency and collectively account for >90% the semen volume and only come into contact as they are pushed down the penile urethra (254, 255).

The composition of the ejaculate is an important factor in optimal sperm function. There are key differences in the composition of semen *in vitro* compared with *in vivo* environments. During intercourse, the initial sperm rich portion of the ejaculate with zinc-rich prostatic fluid mixes with cervical mucus and is pushed up the cervical canal without full compositional homogenisation with the rest of the ejaculate (256). *In vitro* semen analysis consists of the collection of the entire ejaculate in a collection pot and analysis only commences upon liquefaction of the sample (usually 20-30 minutes post ejaculation). Following this process, sperm that are trapped in a gel-like matrix of proteins from seminal vesicles, reach their motility potential and increased osmolarity due to actions of prostatic serine proteases (257, 258).

Semen contains cellular components other than sperm, some of which have relevant clinical associations. These cells include epithelial cells of genitourinary tract origin, as well as leukocytes and immature germ cells (collectively referred to as round cells) (259). Excess of leukocytes ($>10^6$/mL) in semen may indicate an underlying genital tract infection and is referred to as leukocytospermia (260). There is no consensus on prevalence of leukocytospermia in fertile and infertile men. Studies have found that leukocytes are significantly higher in semen of infertile patients compared with controls, including associations with sperm count and motility (261-264). Conversely, others reported higher concentrations of leukocytes in fertile patients (265, 266). There are also reports suggesting no link between increase of leukocytes in semen and sperm function, or fertility (267, 268)

The laboratory analysis and processing of seminal fluid is based on the WHO (World Health Organisation) laboratory manual was first published in 1980 and it is currently at its 6th edition (258). Seminal analysis is the most basic procedure to evaluate male fertility using microscopy. WHO sets the standards in various aspects such as: basic examination, preparation and cryopreservation and quality assessment and control. Microscopic assessment of semen consists of sperm concentration, sperm motility and sperm morphology. Extended examinations often carried out including detection of leukocytes, immature germ cells, sperm antibodies, sperm aneuploidy, DNA fragmentation and Reactive Oxygen Species (ROS).

1.3.2.3 Sperm DNA fragmentation and ROS in semen

Sperm DNA content is essential for normal fertilisation, gamete development, embryo implantation and successful pregnancy. DNA damage is linked to fertility complications such as recurrent miscarriages (269, 270). To avoid damage, sperm DNA is highly condensed and compactly packed in sperm (271). This involves the DNA being wrapped around histone proteins which are replaced by protamines for effective condensation leading to inactivity of

transcription (272, 273). Sperm DNA damage can affect both mitochondrial and nucleus DNA and can be induced by several mechanisms including apoptosis during spermatogenesis and DNA strand breakdown during chromatin remodelling. The process of chromatin remodelling incurs torsional stress, which is created and repaired during chromatin arrangement (274). Failure to repair the nicks leads to DNA damage (275). Chromatin damage can occur in single or double strands, deletions, or DNA crosslinking (intra- and inter-strand cross-linkage) (276). Any DNA related defect can result in Sperm DNA Fragmentation (SDF). Double strand breaks are particularly implied to affect embryo development and reduced implantation rates (277). There are repair mechanisms by which oocytes can repair moderate SDF. An effective repair mechanism depends on the cytoplasmic and genomic quality of the oocyte and age of the female partner (278).

The exact underlying mechanisms leading to SDF are not yet fully explored. ROS are implicated as one of the leading contributors to sperm DNA damage during sperm transport through the seminiferous tubules and the epididymis (278). An increase of 25% in concentration of free radicals is associated with a 10% increase in sperm DNA strand breaks (279). ROS are short lived, highly reactive free radicals formed by partial reduction of oxygen (Figure 1.8). At cellular level, relatively low concentrations of ROS are required for optimal sperm function by assisting in capacitation, the acrosome reaction, and sperm maturation (280). Physiological concentrations of ROS are involved in intracellular signal transmissions to downstream targets and are required for oxidation of cysteine-thiol groups of protamines, which is required for chromatin compaction and stabilization (281).

High levels of ROS are combated by antioxidants due to their ability to neutralise ROS and restoration of oxidative balance (282). Excessive amounts of ROS however, exhaust the antioxidant reserves in semen and result in a condition known as Oxidative Stress (OS) (283). High concentrations of ROS result in apoptosis, oxidization of lipids, amino acids, carbohydrates, and DNA damage by fragmentation all of which reduce the fertility potential of men (284, 285).

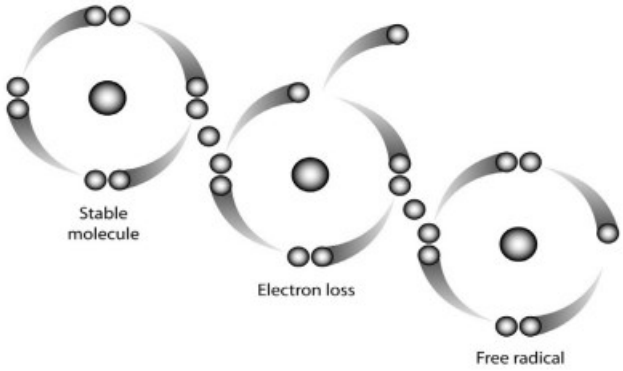


Figure 1.8: Schematic representation of free radical formation. Produced by Agarwal et al. (2008)(286).

ROS can be generated in high amounts by Polymorphonuclear Leukocytes (PMN); therefore, infections are known to increase excessive ROS generation within the seminal milieu (287, 288). High abundance of PMNs in semen account for up to 1000-fold increase of ROS compared to endogenous levels produced by sperm (278, 289). In response to bacteria, local PMNs generate ROS which is accompanied by loss of sperm motility and vitality (289-291). Additionally, elevated ROS in semen is associated with impaired sperm capacitation, acrosome reaction, and sperm-oocyte fusion (292-294).

While some bacteria can lead the production of ROS through the action of PMNs, some bacteria can scavenge ROS. *Lactobacillus gasseri* are gram-positive bacilli which can protect the mice embryonic fibroblast cells from oxidative stress by instigating expression of genes associated with oxidative stress (295). Probiotic lactic acid bacteria are equipped with oxygen consuming and antioxidant enzymes such as lactate oxidase that aid in maintenance of intracellular redox balance (296).

1.3.2.4 Overview of male reproductive tract bacteria and origins of semen bacteria

Constituents of semen including lipids, sugars, saccharides, nucleic acids, proteins and peptides, and its slightly basic pH of between 7.2 and 8 provides a suitable habitat for bacterial colonisation (297). The origin of seminal bacteria is a debated topic and is likely multifactorial. Unlike the female reproductive tract, the male reproductive tract is a closed circuit and is not in direct contact with the environment. It is therefore possible that bacteria present in semen originate from organs sourcing the seminal fluid. The majority of the seminal fluid is secreted by the seminal vesicles and prostate gland that contain several biochemically important substances such as fructose, acid phosphatases and zinc (298). Comparison of tumour and non-tumour prostatic tissues have shown differences in microbial compositions including detection of *Streptococcus* exclusively in non-tumour prostate tissues (124). Furthermore, presence of microbial communities residing in the seminal vesicles have been confirmed in mice (123). However, it remains unclear where these species might originate from.

The testes contribute millions of sperm to the seminal fluid that are suspended in a secretion from Sertoli cells assisting in transport of sperm through the genital ducts (298). A testicular microbial signature associated with azoospermia has been reported by Alfano et al. and is characterised by increased abundance of Actinobacteria and Firmicutes and higher bacterial loads compared with normozoospermic men using Microdissection Testicular Sperm Extraction (microTESE) (125). In another study on testicular sperm samples collected from infertile men, Molina et al. reported presence of low biomass testicular bacterial signatures (299). Following stringent decontamination protocols, the authors reported that between 50% to 70% of all bacterial reads were due to contaminants. There were however, 10 genera specific to testicular sperm following decontamination: *Blautia, Cellulosibacter, Clostridium XIVa, XIVb, and XVIII, Collinesella, Prevotella, Prolixibacter, Robinsoniella,* and *Wandoina*. The most prevalent taxon was *Prevotella*, which was present in 90% of the samples analysed.

Emerging evidence also suggests that couples commonly share bacteria between their reproductive tracts. This was outlined in women with BV-associated bacterial markers and their close resemblance with bacteria of penile skin and urethral microbiota including taxa such as *Prevotella* and *Gardnerella* (300). In a study by Mandar et al., 85% of detected phylotypes were shared between seminal and vaginal communities including high abundance taxa such as: *Lactobacillus*, *Veillonella*, *Streptococcus*, and *Porphyromonas* (301). Furthermore, dominance of *G. vaginalis* in the vaginal bacteria was significantly associated with inflammation in the male genital tract (301). The mechanism by which microbial homogeneity is maintained between vaginal fluid and semen is suggested to be stochastic rather than being driven by deterministic forces (302).

1.3.2.4.1 Bacteria and male fertility

There are various mechanisms by which bacteria could reduce the fertility potential of men. One such mechanism is through direct contact with sperm cells. The surface of sperm is rich in glycoproteins making it susceptible to bacterial interactions such as receptor-ligand bindings (303). Bacteria equipped with attachment organelles such as flagella, pili or type-1 fimbriae can directly attach to mannose receptors on surface of sperm cells (304). The adhesion phenomena impact sperm motility and normal morphology, as well as agglutinations and subsequent apoptosis (303, 305). Table 1.5 summarises some of the mechanisms by which bacteria negatively impact sperm cells.

As previously mentioned, high abundance of leukocytes in semen are a primary source of ROS generation. In response to bacteria, local leukocytes produce ROS which is accompanied by loss of sperm motility and vitality (289-291). Bacterial infections can lead to tissue damage and inflammation which reduce the male fertility potential by negatively affecting spermatogenesis and testosterone synthesis (306). Through inflammation, the host responds to infections which causes leucocytes to migrate to the site of the infection. Inflammatory mediators such as TNF-α, IL-1β and IL-6 can inhibit testosterone synthesis in Leydig cells and induce apoptosis of immature sperm cells (307).

Table 1.5: A summary of studies investigating mechanisms by which bacteria negatively impact sperm cells.

Bacteria	Impact on semen quality/reproductive tract	Mechanism of interaction
E. coli	Reduced sperm motility, vitality and morphologically normal forms (308).	Sperm adhesion mediated by mannose and mannose-binding receptors present on the surface of both sperm and bacteria (309). This phenomenon impairs mitochondrial function possibly due to membrane damage caused by mitochondrial-induced ROS generation via lipid peroxidation (310). Hemolysin (hlyA) secretion: a virulence factor involved in premature acrosomal activation and sperm DNA damage.(311).
C. trachomatis	Infection of testicular cell populations by hijacking testicular macrophages (312)	Interaction with CD14 on sperm surface through LPS leading to lipid peroxidation, sperm DNA damage and caspase-mediated apoptosis (313).
N. gonorrhoeae	Twice as common in semen of infertile men (314).	Induction of apoptosis and production of oxidation intermediates in semen by promoting IL-1β (315, 316).
U. urealyticum	Implicated in the pathogenesis of epididymitis, prostatitis, and urethritis (317).	Adhesion to sperm decreases sperm motility (exact mechanism unclear) (318). Metabolic products including H_2O_2 and OH- are toxic to sperm (319).

1.3.2.4.1 Bacteria detection in semen: culture-based and metataxonomic studies

Detection of bacteria in semen samples is referred to as bacteriospermia. Prevalence of bacteriospermia in culture-based studies spans from 6% to 68% with an average of 37% according to 17 major studies between 1995 and 2018 (304, 320-335). Collectively, these studies found that prevalence of *Escherichia* (19%), *Staphylococcus* (15%), *Enterococcus* (15%), *Enterococcus* (15%) and *Ureaplasma* (7%) to be detected in both fertile and infertile men. Although some of these studies did not find any relationship between bacteria and suboptimal semen parameters (320, 326, 331, 336), others reported significant impacts. Frequent detection of *U. urealyticum*, *E. faecalis*, and *M. hominis* were particularly associated with sub-optimal seminal parameters. Bacteriospermia associated with suboptimal seminal parameters include: reduced sperm count (304, 321-323, 329), reduced morphologically normal forms (304, 323), reduced sperm motility (321-323, 329, 332), increased DNA fragmentation index (304), lower mitochondrial membrane potential (304), and protamine deficiency (321, 322).

PCR is another widely used method to identify bacteria in semen samples. PCR detects presence of targeted bacterial species (337). Studies using this approach have mostly focused on identification of widely recognised pathogens including *C. trachomatis*, *Ureaplasma* species and *Mycoplasma* species. Numerous studies have described the presence of these pathogens in semen samples of men seeking fertility treatments. Prevalence of *C. trachomatis* ranges from >3% to 40% in ethnically diverse cohorts (338-342). However generally, *C. trachomatis* has not been linked to adverse seminal parameters (338, 340, 341), although one study suggested it may be associated with reduced sperm motility (339). *U. urealyticum* has been reported to significantly reduce parameters of sperm quality such as concentration (343, 344), motility and morphology (344). Similarly, *Mycoplasma* species are associated with reduced sperm concentration, motility, and morphology (342, 345).

Several studies have used metataxonomic approaches for the investigation of seminal microbiota (121, 346-350) but results have been inconsistent (Table 1.6). These studies suggest that *Lactobacillus* (>20%), *Corynebacterium* (>6%), *Staphylococcus* (>6%), *Prevotella* (>6%), *Streptococcus* (>5%), *Peptoniphillus* (>5%), *Finegoldia* (>4%), and *Anaerococcus* (>4%) are amongst the most abundant taxa detected in semen. Three studies suggested a significant relationship between microbial compositions and health (346, 347, 350). In one study *Lactobacillus* was higher in optimal samples and in another, low abundance of *Lactobacillus* associated with suboptimal microscopic semen parameters.

Table 1.6: A summary of studies investigating relationship between seminal microbiota and their relationship with health.

Study	Date	Design and Cohort	Target for molecular characterisation of microbiota	Compositional relationship with health?	Findings
Hou et al. (346)	**2013**	77 men, 19 sperm donors and 58 infertility patients	V1-V2 hypervariable regions of the 16S rRNA gene	N	*Anaerococcus* negatively associated with sperm quality.
Weng et al. (347)	**2014**	96 men from couples suffering from: male factor, female factor, or unknown aetiology	V4 hypervariable region of the 16S rRNA gene	Y	*Lactobacillus* and *Gardnerella* abundances significantly higher in normal samples, *Prevotella* significantly higher in low-quality samples.
Monteiro et al. (348)	**2018**	118 men, 29 healthy controls and 89 infertility cases	V3-V6 hypervariable regions of the 16S rRNA gene	Y	High abundance of *Neisseria*, *Aerococcus*, *Actinobaculum Klebsiella* and *Pseudomonas* and low abundance of *Lactobacillus* associated with suboptimal microscopic semen.
Baud et al. (349)	**2019**	94 men, 26 patients with normal spermiogram, 68 with abnormal parameters	V1-V2 hypervariable regions of the 16S rRNA gene	N	Microbiota were broadly classified as *Prevotella*, *Lactobacillus* and polymicrobial. *Prevotella* was associated with high bacterial load. *Prevotella* relative abundance was increased in samples with defective sperm motility while *Staphylococcus* was increased in the corresponding control group. In addition, increased relative abundance of *Lactobacillus* in samples with normal sperm morphology.

Yang et al. (350)	**2020**	159 patients including 22 with oligoasthenospermia, 58 with asthenospermia, 8 with azoospermia, 13 with oligospermia and 58 healthy controls	V1-V2 hypervariable regions of the 16S rRNA gene	Y	Bacterial compositions of dysspermic samples higher in β-diversity compared with controls. Relative abundance of *Ureaplasma, Bacteriodes, Anaerococcus, Finegoldia, Lactobacillus*, and *Acinerobacter iwoffii* significantly higher in asthenospermia. Relative abundance of *Lactobacillus* high in oligoasthenospermic samples.
Lundy et al. *(121)*	**2021**	37 men. 12 men with proven paternity, 25 men with primary idiopathic infertility. Compared functional profiles of the gut, semen and urine	V3-V4 hypervariable regions of the 16S rRNA gene	N	Seminal microbiome has modest similarity to urinary microbiome. Vasectomy alters seminal microbiome indicating testicular or epididymal contribution to seminal microbiota. Infertility is associated with increased seminal α-diversity and increased *Aerococcus*. *Prevotella* was inversely associated with sperm concentration, and *Pseudomonas* was directly associated with total motile sperm count.
Molina et al. (299)	**2021**	24 testicular biopsies from 11 men comprising a total of 307 testicular maturing sperm	V3-V4 hypervariable regions of the16S rRNA gene	N/A	Testicular sperm samples are associated with a high degree of contaminants (50%-70% of all detected bacteria). Testicles, harbour low-biomass microbial signatures potentially contributing to seminal microbiome composition. *Prevotella* was identified in over 90% of the testicular samples and was highly abundant among immature sperm.

Okwelogu et al. (351)	**2021**	36 couples undergoing IVF provided seminal fluid and vaginal swabs	V4 hypervariable region of the 16S rRNA gene	Y	Microbiota of normal semen samples corresponded with vaginal swabs of their partners including high abundance of *Lactobacillus* and *Gardnerella.* Azoospermia was associated with high abundance of *Mycoplasma* and *Ureaplasma*.
Yao et al. (352)	**2022**	87 semen samples including 33 with normal seminal leukocyte count and 54 samples with leukocytospermia	V3-V4 hypervariable regions of the 16S rRNA gene	Y	Increased α-diversity was associated with leukocytospermia. Samples with normal leukocyte counts were associated with enrichment of *Lactobacillus* and leukocytospermia samples were associated with *Streptococcus* enrichment.

1.4 Reproductive tract mucosa: key modulators between host immunity and environment

The immunology of the Female Reproductive Tract (FRT) is highly complex. It has evolved to selectively tolerate high abundance of commensal bacteria whilst identifying and eradicating pathogens with high sensitivity (353). This is in part achieved through differential expression of pathogen recognition receptors such as Toll-like receptors (TLRs) and nucleotide-binding oligomerization domain (NOD)-like receptors (NLRs) throughout the FRT, which sense the presence of pathogens by recognising highly conserved molecular structures called pathogen-associated molecular patterns (PAMPs) (354). Once activated, they drive a proinflammatory cascade that leads to the production of cytokines and chemokines involved in recruitment of white blood cells such as neutrophils that can clear the invading pathogen through phagocytosis.

As discussed earlier, *Lactobacillus* species can avoid activation of inflammation by producing high levels of the anti-inflammatory compound lactic acid. However, immune homeostasis is a delicate multifactorial balance. Certain bacterial stimulations can initiate a cascade of immune responses that result in secretion of local cytokines (355). Colonisation of facultative anaerobic bacteria such as *G. vaginalis* and *Prevotella* species are associated with an inflammatory response (355-357). The impact of disrupted vaginal microbiota on local immune response has been studied in both pregnant and non-pregnant subjects. A study on cervical secretions of a non-pregnant cohort reported that increased concentrations of TNF-α and IL-1β were significantly associated with BV (358). Similarly, studies on cervical mucus and vaginal fluid of pregnant women found associations between vaginal bacterial dysbiosis and production of cytokines; elevated levels of IL-1α and IL-1β in subjects with BV during early pregnancy (359, 360) and increased concentrations of IL-1α and IL-8 in patients diagnosed with BV at screening of preterm birth (361).

At conception, sperm cells with ‘non-self’ allogeneity need to reach the site of fertilisation in the FRT and the semi-allogeneic embryo must be tolerated by the local immune system for healthy development (362). Highly regulated inflammation is also a critical component of implantation. Remodelling of the endometrial spiral arteries, regulation of decidualisation, differentiation and proliferation of the endometrium, apposition of the blastocyst, embryonic epithelial/stromal interactions and acceptance of the semi-allogenic conceptus are all tightly regulated by cytokines as well as serum hormones (363-369).

Endometrial preparation for implantation is a proliferative, E2 mediated phase that occurs in what is known as the putative implantation window (370). This process occurs between days

19-23 of the menstrual cycle during which decidual cells develop from transformed endometrial stromal cells (371). During this period, the endometrium becomes more receptive for the arrival of the blastocyst and is assisted by immune cells, cytokines, chemokines, adhesion molecules and growth factors (372). Although questions remain regarding the molecular pathways of window of implantation, it is understood that E2 and P4 play a major role in regulating this period (363). Additionally, paracrine signalling between the activated blastocyst and the uterus are thought to further contribute to the timing of this phenomenon and the receptivity of the endometrium (373).

The functions of the E2 and P4 hormones are mediated via their respective intracellular receptors (ER and PR), which are members of the nuclear family of ligand-dependant transcription factors (374). Sex hormones can also regulate host response to microbial stimuli via nuclear receptor proteins such as Peroxisome Proliferator-Activated Receptors (PPARs) (375). Further, E2 plays an important role is mediating expression of endosomal TLRs and TLR8 expression (376, 377).

Over the course of the menstrual cycle with fluctuations of hormones, migration patterns of macrophages, B cells and neutrophils into the vagina vary depending on the levels of sex hormones (378, 379). During the menstrual cycle, immune cells are abundantly present and are distributed in the stroma and epithelia of the FRT. The cyclical secretion of E2 and P4 also shapes the immune cell infiltrate into the Fallopian tubes, uterus, cervix, and the vagina. Leukocytes make up 6-20% of the total number of cells within the FRT (378). Furthermore, NK cells are abundantly present in addition to T-lymphocytes ($CD4^+$ and $CD8^+$) (380).

Vaginal mucosa consists of three layers with specialised functions. The outer layer is lubricated by cervical mucus which contains immunological mediators such as chemokines, interleukins, complements and antibodies (381, 382). The middle mucosal layer is a site of glycogen production in direct correlation with serum E2 and the basal layer is made up of actively dividing cells.

Secretions of the lower female reproductive tract assist in modulation of innate immunity and have several contributing components (166). These include exfoliated epithelial cells as well as cervical, endometrial and oviductal mucus (383). The amount and characteristics of these fluids are in direct correlation with serum E2 and P4 (384). Additionally, secretions of sebaceous, sweat, Bartholin's and Skene's glands also contribute to these secretions (383). Proteomic analysis of Cervico-Vaginal Fluid (CVF) has confirmed presence of proteins with defensive properties such as haptoglobin, defensins, lactoferrin, azurocidin and dermcidin (385).

1.4.1 Reproductive tract immune regulation and embryo implantation

Post fertilisation, the embryo must first successfully break out of its glycoprotein outer layer called the zona pellucida (ZP), through a process called zona hatching (386). This phenomenon is thought to be controlled by both cellular and molecular factors. The process is initiated by a hydrostatic pressure build up as the blastocyst expands and is aided by zona lysins (387, 388). The blastocyst of a number of species including humans, also express cytoplasmic protrusions from the trophectoderms called Trophectoderm Projections (TEP) (389). TEP have been described to induce rupture of ZP through which the embryo exits (390). Although *in vitro* hatching of human embryo has not been studied as comprehensively as other mammalian species, evidence suggests that it follows a similar sequence of events (389), resulting in the spontaneous hatching of the embryo from the ZP (391).

The remodelling of the endometrial tissue in preparation for implantation is both structural and functional (392) and hormonally regulated. This process requires binding of E2 and P4 with their respective receptors to regulate gene transcription. There are two isoforms of steroid nuclear E2 receptors (ERα and ERβ) and P4 receptors (PR-A and PR-B) (393, 394). ERα stimulate uterine epithelia proliferation in preimplantation by inducing production and secretion of Leukemia Inhibitory Factor (LIF) from uterine glands which regulates the window of implantation (395). PRs preparation of endometrium is by inhibition of epithelial proliferation and modulating of epithelial-stroma crosstalk (396). Loss of PRs in the uterine epithelium is a requisite for embryo implantation. As demonstrated in mice studies, conditional expression of PR-A transgene in the epithelia results in inhibition of embryo implantation (397). The PR molecules comprise of domains allowing for ligand binding, DNA binding and transcription activation. PR-B is the larger isoform containing additional 164 amino acids and amino terminus (398), which forms an additional domain and more transcription activity (399). Expression of epithelial PR-A and PR-B reduce LIF transcription by impairing ERα occupancy at the promoter of LIF (400). In preparation for embryo implantation, PRs signalling acts on reduced transcription of LIF and upregulation of SGK1 gene expression and P13K-SGK1 activities (401).

Following fertilisation and embryonic migration, the embryo adheres to the surface of the endometrium and implants. Implantation can be viewed as the invasion of the semi-allogeneic embryo to the maternal tissue to gain access to the nutrients that are essential for its survival and growth (370). Paternal antigens presented by the developing fetus are tolerated by the maternal immune system throughout gestation via a poorly understood mechanism that

involves several immune factors in addition to complex bidirectional communications between the embryo and endometrium (402).

Following the recognition of the unique immunological relationship between fetus and maternal tissue in the 1950s (403), a number of hypotheses emerged to account for the lack of fetal rejection by the immune system. None of these theories however were convincing nor universally accepted. Amongst the proposed theories were the following: the trophoblast can act as a mechanical barrier which keeps the immune cells out of reach (403), the maternal immunity is systemically suppressed during this period (404), there are no class I Major Histocompatibility Complex (MHC) molecules in the trophoblast (405), and the immune system is locally suppressed (406).

The process of zona hatching may be linked to the peri-implantation process (407). Although an independent biological phenomenon, zona hatching shares several molecular factors with embryo-epithelial interactions during the peri-implantation period. Peri-implantation is a process involving morphological and biochemical changes taking place in the endometrium. Under the influence of E2 and P4, endometrial stromal cells proliferate changes in the epithelium (373). In addition to the hormones, several cytokines, Prostaglandins (PG) and other growth factors play a role in regulation of the peri-implantation interaction (Table 1.7).

Table 1.7: Cytokines, PGs and growth factors involved during the embryo-epithelial interaction. m: mice studies. h: human studies.

Compound	Biological role
HB-EGF	Stimulates trophoblast outgrowth and blastocyst growth. Induced in the luminal epithelium by the blastocyst at the site of apposition (366).[m]
IL-1	Induces production of LIF, GM-CSF and CSF-1 (408, 409)[h]. The IL-1 family regulate communication between blastocyst and endometrium (367)[h/m].IL-1β induces COX-2 gene expression (410)[h].
IL-1ra	May prevent implantation by blocking embryonic attachment (411)[m].
IL-11	Involved in the decidualisation of the stromal cells (369)[h].
IL-15	Upregulated during decidualisation (368)[h].
IFN-γ	LIF inhibitor (408).[h]
IGFBP-1	Involved in endometrial function and regulates endometrial changes (412)[h], present in the decidual cells and regulated by trophoblasts (413)[m].
LIF	Involved in differentiation of the endometrium (369)[h].
GM-CSF	Involved in trophoblast differentiation (409) [h]. May be involved in preparation of the uterus for implantation (414)[m].
PGE_2	Induces endometrial proliferation (415).[h]
TNF-α	Induces secretion of LIF, GM-CSF and CSF-1 (408, 409)[h]. Involved in endometrial changes (416)[h].

Modification of the endometrium under the control of E2 and P4 are essential for the 3 phases of implantation: apposition, attachment and invasion (417). Prior to the penetration of the hatched blastocyst into the decidua, the polar trophectoderm is orientated towards the epithelial surface (367). Apposition of the embryo is aided by several immune analytes including HB-EGF and LIF. The concentration of HB-EGF is increased in the luminal epithelium around the embryo aiding the attachment and reduced concentrations of LIF are associated with failed implantation (418, 419). The striking upregulation of LIF during the implantation period at the time of increased concentration of E2, suggests that it plays an important role in the paracrine signalling of implantation in mice studies (419, 420).

4.2 Immune regulation of pregnancy

Depending on the cytokines produced, immune function can conventionally be divided into Th1 and Th2 responses. During human pregnancy, signals from the fertilised ovum mediate the recognition of pregnancy by the maternal immunity (421). A potential signal to mediate acceptance of fetal alloantigens by the maternal immune system is the intrauterine predominance of Th2-type immunity throughout the pregnancy (422, 423). Therefore a Th2-

type cytokine predominance could be crucial in embryo development and pregnancy outcome (424).

This theorem was further reinforced by the findings of Bates and colleagues. They reported heighted levels of Th1-type cytokines in 46 pregnant women with history of idiopathic Recurrent Pregnancy Loss (RPL) (425). Further evidence has suggested that a more complex network of cytokines is involved in successful embryo implantation than previously reported as Th2-type dominance immunity was observed in recurrent abortion cases (426). Moreover, despite the strong correlation between Th1-type immunity and fetal rejection, presence of individual Th1 cytokines including IL-2 and IFN-γ after the early stages of pregnancy is not a necessity for the rejection process (427).

Evidence suggests that a more complex network of cytokines are involved in successful embryo implantation than the Th1-Th2 paradigm (427). a healthy pregnancy will occur because of a discrete balance between Th1 and Th2 type cytokines. Agarwal et al. suggested that cytokines themselves possess immunoregulatory characteristics that shift the balance towards Th2-type dominance. Fetal and placental cells are known to secrete both Th1 and Th2-type cytokines. Production of Th1 type cytokines such as TNF-α, TNF-β, IL-1, IL-2, IL-8 and IFN-γ as well as the Th2-type cytokines IL-4, IL-5, IL-6 and IL-10 by the feto-placental cells, exemplifies the complex relationship between these cytokines (428).

A major group of Th2 type cytokines involved in successful embryonic implantation is the IL-6 family. This group includes numerous cytokines including IL-6, IL-11 and LIF. Members of the IL-6 family possess anti- and pro-inflammatory characteristics and express cellular signalling through gp130 (370). furthermore, the IL-6 family members are one of the main activators and stimulants of Signal Transducer and Activator of Transcription 3 (STAT3) (429).

In addition to implantation, there are several cytokines that play a vital role in placentation and parturition. A dysregulation of cytokine secreting immune cells can lead to inadequate fetal growth, spontaneous abortion, maternal physiological complications or even fetal and maternal death (430). IL-4 and IL-10 are anti-inflammatory cytokines that play an important role in the resolution of the inflammation by suppression of pro-inflammatory dominance throughout pregnancy (430). Several immune cells produce IL-4 including natural killer T (NKT) cells, basophils, eosinophils, and mast cells (431, 432). IL-4 regulates the polarisation of naïve Th-cells into Th2 in addition to binding to IL-4Rα receptors on Th2 cells which generates Th2 responses (430).

1.4.2.1 Activation of inflammation

In humans, there are two major cell signalling pathways regarded as important regulators of immunity and inflammation: NF-κB and glucocorticoid-mediated signal transduction cascades (433). These cellular signalling pathways have diametrically opposed functions in regulation of immune responses. NF-κB is the most studied inflammatory pathway and was identified by Sen and Baltimore in 1986 using electrophoretic mobility shift assay with end-labelled DNA fragments as an enhancer-binding protein controlling Igκ-light chain gene expression in B cells (434). Subsequent studies found that in addition to B cells, NF-κB is expressed in other immune cells such as in activation, differentiation and effector functioning of T-cells (435, 436). NF-κB represent a family of inducible transcription factors that mediate the transcriptional activation of numerous cytokines and cytokine-induced genes in immunological responses (437). Conversely, Glucocorticoid Receptor-α (GR) is known to suppress the expression of many cytokines and related genes activated by NF-κB (433). The mechanism of interaction between NF-κB and GR are understood to be as mutual transcriptional antagonists (438).

NF-κB transcription factor family includes a collection of proteins that share a highly conserved DNA-binding and dimerization domain called the Rel Homology Domain (RHD) (439). Members of the Rel subfamily are c-Rel, RelB and RelA and *Drosophila* Dorsal and diff (440). In addition, there are two more structurally related members of NF-κB family called NF-κB1 (p50) and NF-κB2 (p52). These factors mediate the transcription of target genes by binding to a specific DNA element called κB enhancer as numerous hetero- or homodimers (441). NF-κB is activated via two major signalling pathways, canonical and noncanonical (442). The canonical activation pathway responds to stimuli such as ligands of cytokine receptors, pattern recognition receptors, TNF receptors, T-cell receptors, and B-cell receptors (443). In contrast, the noncanonical activation pathway responds to specific stimuli including LTβR, BAFFR, CD40, and RANK which are ligands of the TNFR superfamily (444). Unlike the functional application of canonical NF-κB which is in almost all aspects of immunological responses, the noncanonical NF-κB pathway applies to specific aspects of the adaptive immunity (445). Both canonical and noncanonical pathways are based on inducible phosphorylation of IκB proteins by IκB-kinase (IKK) which contains two catalytic subunits: IKKα (IKK1) and IKKβ (IKK2) in addition to the regulatory subunit IKKγ (433). IκBs are a family of endogenous inhibitors that sequester NF-κB in inactive form in the cytoplasm prior to expression of extracellular stimuli (442).

Table 1.8: NF-κB target genes involved in inflammation activation and progression.

Immune components	Gene	Resulting actions
Dendritic cells	Inflammatory gene induction	Maturation (446)
T-cells	IL-12, IL-23, RORγt, T-cell receptors α and β	Differentiation, activation, memory T-cells (433)
Macrophages	Proinflammatory gene induction	Production of proinflammatory cytokines and chemokines, M1 polarization (447)
Neutrophils	Inflammatory gene induction	Anti-apoptosis, recruitment (448)
Anti-apoptotic factors	Fas, Bcl-2, c-FLIP, Caspases, IAPs, BFL-1, Survivin	Cell survival (449, 450)
Cell cycle regulators	Bcl-2L1, PAI2, Cyclin	Cell survival, proliferation (451, 452)
Cytokines	IL-1, IL-2, IL-6, IL-12, TNF-α	Proliferation, inflammatory response, angiogenesis (453)
Chemokines	MCP-1, IL-18, RANTES, MIP-2, CXCL1, CXCL8, CXCL10	Angiogenesis (448, 454)
Adhesion molecules	ICAM-1, VCAM-1, ECAM-1, MMPs	Adhesion, invasion, metastasis (455, 456)

The negative interactions between NF-κB p65 (Rel A) and E2 receptors are comprehensively documented (457, 458). In the context of reproduction, the anti-inflammatory impact of E2 is highlighted by reduction of symptoms of rheumatic arthritis, inflammatory bowel disease and multiple sclerosis during pregnancy (459). Sun and colleagues suggested that the mechanism of interaction between E2 receptors and NF-κB is the impact of E2 on blocking IκBα phosphorylation (460). This action ensures the sustained presence of the inhibitory subunit of NF-κB resulting in obstructing activation. Additional *in vivo* and *in vitro* studies have also researched the role of E2 in modulation of the immune response by reciprocal inhibitory effect of E2 on NF-κB. An *in vivo* study by Quaedackers found that ERα and NF-κB subunits p50 and p65 directly interact following E2 stimulation (461). Similarly, Feldman and colleagues reported an inhibitory interaction between E2 receptors and NF-κB p65 (462).

As mentioned earlier, E2 acts on the endometrium by E2 receptors ERα and ERβ which are expressed in epithelial and stromal cells (463, 464). Immunocytochemical analysis of endometrial biopsies and cultured endometrial epithelial cells suggest that NF-κB p65 and p50 are increased during the mid-secretory phase (465). It has also been reported that the expression of IκBα is reduced at the mid-secretory phase (466).

The host's response to pathogens and microbial products such as Lipopolysaccharides (LPS) and PAMPs, activate the NF-κB pathway to modulate a series of cellular events leading to an immune response (467). Following bacterial stimulation, immune receptors such as TLRs are activated to mediate the NF-κB signalling pathway. NF-κB translocate from cytoplasm to the nucleus and binds to DNA to regulate downstream gene transcription (468).

1.5 Metabolome of the cervicovaginal mucosa

Metabolomics is a term defined as the untargeted identification and quantification of low molecular weight products of metabolism (469). The metabolic profile of biological samples contain thousands of molecular components that illustrate the biochemical events occurring in a complex biological system (470). Metabolomics aim to identify and comprehensively quantify the entire endogenous and exogeneous metabolites present to determine the functional status of a biological system (471). Recent studies have identified metabolic biomarkers in embryonic culture fluid, follicular fluid, and urine (472-474).

As highlighted earlier, vaginal bacteria produce metabolites and chemical compounds (e.g., lactic acid) that play functionally important roles in regulating microbe-host responses in the female reproductive tract. Several metabolomic profiling studies have shown that a shift from *Lactobacillus* species dominance towards diverse anaerobic species is accompanied by metabolomic changes in CVF (475, 476).

In pregnancy, several studies have shown that metabolomics approaches can detect changes in microbial associated metabolites that associated with risk of poor pregnancy outcomes including preterm birth. For example, using Nuclear Magnetic Resonance (NMR) spectroscopy, Amabebe and colleagues reported high CVF acetate levels, likely derived from microbiota, to be predictive of preterm delivery (477). These results were in line with previous findings of a similar experiment using Gas Chromatography-Mass Spectrometry (GC-MS) on identification of metabolite markers several weeks before term and pre-term outcomes (478). There were however limitations associated with the study design, i.e., inclusion of a limited number of analytes as well as only having one patient in the low-risk group hence lacking a control population. Another limitation associated with LC-MS and NMR based metabolomics approaches is the processes of substantial sample preparation, sample processing and large analytical platforms that are not conductive for bedside patient diagnostics (479).

To address these limitations, the MacIntyre and Takats laboratory recently developed Direct Swab Analysis by Desorption Electrospray Ionization Mass Spectrometry (DESI-MS). DESI-MS enables robust and reproducible acquisition of mucosal metabolic profiles directly from mucosal swabs within minutes and facilitates exploration of both the host and local microbiota derived metabolites (480). DESI-MS is an untargeted technique performed in ambient conditions by directing charged electro-sprayed aqueous droplets at the surface of interest in air. The charged particles will then stimulate the sample to produce gaseous ions that are carried to a mass spectrometer (481). DESI-MS analysis does not require sample preparation

which enables it for bedside patient diagnostics of robustly predicting microbiota composition and host inflammatory responses (480, 482, 483).

1.6 Hypothesis, aims and objectives

1.6.1 Hypothesis

This thesis sets out to test two major hypotheses that reflect our current understanding of microbiota-host interactions in the reproductive tract in the context of early reproductive success, specifically in patients undergoing fertility treatment:

1. Hormonal manipulation during IVF treatment modifies vaginal microbiota-host immune response, which are collectively important for subsequent success of IVF.

2. Semen harbours a microbiota that modulates parameters of sperm quality and function.

1.6.2 Aims and objectives

The following aims were devised to test these hypotheses:

- Longitudinal assessment of the relationship between sex hormones, immune analytes, and bacteria at high and low estrogenic states throughout fresh IVF cycles and to identify whether these relationships are related to treatment outcomes. It was also aimed to assess whether these relationships are reflected in the metabolome.
- Longitudinal assessment of the relationship between bacterial compositions in frozen IVF cycles and treatment outcomes using embryos with and without preimplantation genetic testing.
- Characterisation of seminal bacteria and assessment of their relationship with seminal quality and function parameters.

2 CHAPTER II

2.0 METHODS AND MATERIALS

2.1 Participants and study design

Samples used during the work described in this thesis were derived from several patient cohorts. Firstly, sample recruitment was undertaken as part of the ART I study: 'Discovery of Biomarkers for Successful Assisted Reproduction'. This was a cohort study which aimed to recruit women struggling to conceive following at least 1 year of unprotected intercourse. These women attended the IVF clinic at Wolfson Fertility Centre, Hammersmith hospital (Imperial College Healthcare NHS Trust, W12 0HS) where they were undergoing IVF, ICSI or FERC (Frozen Embryo Replacement Cycles) procedures (Figure 2.1). Ethics approval for the study was obtained from Health Research Authority (HRA) (REC:16/LO/1286). All patients recruited provided informed written consent prior to sample collection. Sample collection was performed in line with the standard operating procedures. Sample collection took place between Jan 2017 and Aug 2017. Patients were aged between 18-45 years of age and were HIV and Hepatitis C negative.

Sample recruitment also took place as part of the ART II study: 'The Dynamics of Vaginal Microbiome in Frozen-Thawed Embryo Replacement Cycles'. Samples were collected at The Centre for Reproductive & Genetic Health (CRGH, 230-232 Great Portland Street, London, W1W 5QS). Ethics approval for the study was obtained from the CRGH internal review board (IRB-0002C07.10.2019). This was a cohort study in which participants provided informed written consent prior to sample collection. The aim of this phase of the study was to recruit patients undergoing frozen embryo replacement cycles. We were particularly interested in patients with euploid embryos (Figure 2.1). 34 of the cycles included for ART II, underwent PGS/PGD prior to embryo transfer. As per the ART I cohort, these subjects were aged between 18-45 years of age and were viral negative (HIV and Hepatitis C negative). The recruitment took place between Aug 2019 and Mar 2020. The recruitment process abruptly stopped due to the rapid spread of the Covid-19 in London at that time. Several patients already taking part in the study subsequently cancelled their cycles in Mar 2020 with the view to continue once the impact of the pandemic was under control.

Finally, semen samples were collected as part of the 'Relationship Between Seminal Microbiome, Sperm Quality Parameters and Sperm DNA Fragmentation' study. Samples were collected at The Centre for Reproductive & Genetic Health (CRGH, 230-232 Great Portland Street, London, W1W 5QS). Ethics approval was granted by the Internal Review Board at

CRGH (IRB-0003C07.10.19). Following informed written consent, participants provided a one-time semen sample at the time of their appointment at the Andrology clinic at CRGH. Sample collection took place between November 2019 and March 2020. Sample recruitment stopped in Mar 2020 due to the impact of Covid-19 pandemic in London.

An additional cohort of men took part in the study recruited by study collaborators Tharu Tharakan and Linda Farahani. Ethical approval was granted by the West London and GTAC Research Ethics Committee (14/LO/1038). Ethical guidelines for human research were adhered to, and all participants provided written informed consent. Samples were recruited between January 2019 and March 2020. Participants in the study group were recruited from the recurrent miscarriage clinic at St. Mary's Hospital (Praed street, London W2 1NY). Participants in the control group were recruited through local posters at two hospital sites St. Mary's Hospital and Hammersmith Hospital, London (72 Du Cane Road, London W12 0HS). Inclusion criteria for both groups were men aged 18-60 years old and BMI < 35kg/m^2. To be included in the study group participants must have had at least two consecutive miscarriages, and to be included in the control group, the participants must have a history of conceiving and having a child with their partner. Exclusion criteria were a confirmed female cause for RPL, current symptoms of genitourinary tract infections, alcohol excess, hormone therapy, smoking within the last 6 months, and active treatment for severe systemic disease. Sample collection at multiple centres were as follows:

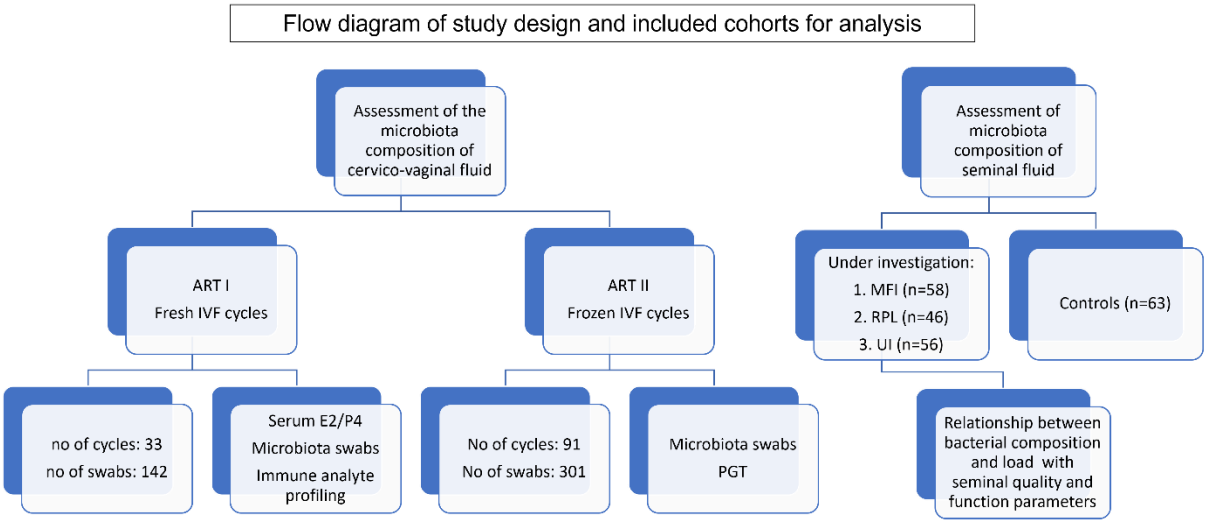


Figure 2.1: Flow diagram of the study design and included cohorts in this thesis. The microbiota of the cervico-vaginal tract was studied using both fresh and frozen IVF cohorts. The ART I arm of the study included analysis of serum hormones, and immune analyte profiling in relation to microbiota of the cervico-vaginal tract. ART II arm of the study included analysis of euploid embryo transfers. Collectively, both cohorts aimed to assess whether microbiota compositions are associated with clinical treatment outcomes. Additionally, quantitative, and compositional analysis of seminal microbiota aimed to assess whether the bacterial communities associated with seminal quality and function parameters.

2.2 Role of the PhD candidate

Sample collection for ART I was performed by Dr Shirin Khanjani, prior to commencement of this PhD project. All subsequent laboratory work including sample processing, DNA purification and extraction, cytokine profiling and analysis were done by myself. Much of the laboratory work took place at Institute of Reproductive and Developmental Biology (IRDB). Microplates plates for cytokine analysis were processed and prepared at the IRDB except the final stage of processing using the Bio-Rad analyser (Luminex), which was done at the department of infectious diseases (8th floor, Commonwealth building, Hammersmith campus, Imperial College London Healthcare Trust, W12 0HS). For cytokine analyses performed as part of the ART I study cohort, MSc student Jingyi Xie, assisted me in processing the samples.

For the ART II and seminal microbiome study, I partook in the study design alongside my primary supervisor Prof David MacIntyre, Prof Philip Bennett, and Dr Shirin Khanjani. In addition, Dr Jara Ben-Nagi (consultant Gynaecologist and specialist in reproductive medicine and surgery at CRGH) played an instrumental role in supporting the ART II study being undertaken at CRGH. This included assisting with application for local ethics approval and designing the patient information sheet. To facilitate recruitment, I obtained the position of 'Honorary Research Associate' at CRGH which allowed me to coordinate with various departments at the centre to collect samples at the time of patient appointments. I personally attended baseline scans and initial nurse appointments, embryo transfer clinics and subsequent pregnancy scans. My responsibilities also included processing, logging, and storage of samples, as well as recording relevant clinical data for patients, assistance in sample collection and general study management.

Dr Yun Lee, (Project Manager, IRDB) assisted in the development of laboratory analysis strategies and development of a suitable DNA extraction protocol for the seminal microbiome study. Given that seminal bacteria are low in biomass compared with bacteria that reside in the vagina, it was important to make sure the protocol was fully validated prior to analysis of the samples. The sperm microbiome study was collaborative work with another research group at Imperial College London. Dr Channa Jayasena (Reader in Reproductive Endocrinology) was the lead collaborator as well as Dr Tharu Tharakan (Clinical Research Fellow) and Dr Linda Farahani (Clinical Research Fellow) who recruited additional study cohorts in addition to the CRGH cohort. I was solely responsible for DNA extraction, PCR amplification, and sequencing analysis of these additional samples. Upon receipt of the processed sequencing data, I performed all subsequent statistical and bioinformatical analysis for interpretation and presentation of the data under the supervision of Prof. David MacIntyre and in collaboration with Drs Channa Jayasena, Tharu Tharakan and Linda Farahani.

Metabolic profiling of vaginal swabs using DESI-MS analysis was performed by Dr Pamela Pruski. Data was processed by Dr Gonçalo Correia. I performed subsequent statistical analyses, interpretation, and presentation of the data was performed under the supervision of Prof. David MacIntyre, Dr Pamela Pruski and Dr Gonçalo Correia.

2.4 Sample collection

The manual of sampling procedures (Version 1: 12 Jan 2017) was the operational guideline for sample collections used in this study (Coordinating author: Shirin Khanjani). The content of this guideline was made available to all involved in this study to ensure the strict guidelines were followed and chances of contamination due to incorrect sample collection were minimised. Liquid Amies elusion swabs were used for collection and transport of the vaginal microbiome samples.

2.4.1 Collection method for microbiome swabs

The procedure for collecting vaginal swabs for microbiome analysis and immune profiling was as follows:

1. Healthcare professionals collecting the samples washed and dried their hands thoroughly and put on sterile gloves.
2. The participants passed urine and were asked to undress from the waist down and lie on the bed covered with a clean sheet.
3. The external genitalia were cleaned with sterile cotton wool and sterile water.
4. The labia were parted, and the swab inserted into the mid-vagina and rotated for 15 seconds.
5. Swabs were removed from the vagina and placed inside the protective cover.
6. Samples were labelled with date, sample timepoint and a uniquely assigned study number.
7. Samples were immediately placed on ice and were transported to a freezer (stored at -80°) until the day of analysis.
8. The details were then recorded on the password protected sample log only accessible to myself and the clinical supervisor.

2.4.2 Materials for microbiome sample collection and storage

Materials used for vaginal microbiome swabs is as follows:

- Sterile vaginal examination pack
- Sterile water
- Microbiome swab (VWR Transport swabs with medium 710-0438)
- Dry ice for transport of the samples from the clinic to the research laboratory
- -80°C freezer

2.4.3 Collection methods for semen samples

Semen samples were produced by means of masturbation. Patients were asked to wash and dry their hands thoroughly and capture the entire sample in the sterile pots provided. The pots were labelled with patient name, date of birth and other relevant information. Upon completion, they then placed the collection pot inside a hatch from which the laboratory staff collected it. It was then placed in an incubator at 37°C for a minimum of 20 mins prior to analysis and taking an aliquot for storage. The aliquots were collected in sterile cryovials and stored at -80°C until the day of analysis. The cryovials were labelled with unique study identification numbers. The information was then recorded into password protected sample logs, only accessible to myself and the clinical supervisor.

2.4.4 Materials for semen sample collection and storage

- Standard sterile semen collection pots
- Sterile cryovials
- Suitable 37°C incubator
- Dewar tanks for temporary storage of samples prior to transport to the lab
- Dry ice for transport of the samples from the clinic to the research laboratory
- -80°C freezer

2.5 Materials for DNA extraction

- 5ml sterile syringes (Medicina)
- 1.5 ml microcentrifuge tubes
- Pipettes and pipette tips
- Vortexer
- 37°C water bath
- 56°C heating block
- Lysozyme (Sigma L6876) 10 mg/ml in filter sterilised 10mM Tris. HCl (pH 8.0)
- Mutanolysin (Sigma, M9901/10KU) dissolved in sterile water (25U/µl)
- Lysostaphin (Sigma, L9043) dissolved in 20 mM NaOAc (4000U/ml)
- $T_{10}E_{50}$ buffer (10 mM Tris. 50 mM EDTA)
- 12% Triton (diluted in H_2O)
- Ethanol (96-100%)

- Standard PBS (Phosphate-buffered saline)
- QIAamp DNA mini kit (Qiagen)*
- Bleached and rinsed 0.1mm diameter zirconia/silica beads
- Tissue Lyser LT Qiagen
- 5x reaction buffer
- Forward primer 10 µM (27F-5'- AGAGTTTGATCCTGGCTCAG-3')
- Reverse primer 10 µM (338R-5'-GCTGCCTCCCGTAGGAGT-3')
- OneTaq DNA polymerase (NEB M0480)
- 10 mM dNTP (Sigma)
- DNase/RNase free H_2O (VWR)
- Agarose (Invitrogen)
- 1x TBE (Tris/Borate/EDTA)
- SYBR safe DNA stain (Invitrogen)
- 100bp Hyper-ladder (Bioline)
- 6x Tritrack DNA loading dye (thermo Scientific)
- QIAamp DNA mini kit (51306) includes the following reagents and consumables:
    - QIAamp Mini Spin Columns
    - 2 ml collection tubes
    - Buffer AL (lysis buffer, 12 ml)
    - Wash buffer AW1 concentrate (19 ml)
    - Wash buffer AW2 concentrate (13 ml)
    - Elution buffer AE (15 ml)
    - Proteinase K (1.25 ml)

2.6 DNA extraction laboratory procedures

DNA extraction was performed using the QIAamp DNA mini kit as per manufacturer's instructions (484). Swabs were removed from -80˚C storage on the day of the analysis and placed on wet ice to thaw. To extract the entire content of the swabs, a sterile 5ml syringe was used to squeeze the sponge as thoroughly as possible. This recovered a volume of approximately 500µl of the swab solution. For swabs that appeared dry and contained a lower solution volume than 500µl, PBS was added, and the sponge was massaged with the swab tip thoroughly to resuspend all contents of the swab. A record of dry samples that required PBS as well as swabs that appeared bloody were taken.

The recovered swab solutions were collected in an Ultraviolet (UV) radiated 2ml Eppendorf tube and centrifuged at 6,200 x g for 10 mins. The supernatant was carefully removed and placed in a prechilled 1.5ml tube and stored at -20˚C for future cytokine analysis. To the pellet, 300µl of enzymatic master mix was added (see Table 2.1). For each batch of extractions performed, a negative control swab was taken. For this, a swab was removed from the manufacturers packaging, waved in air, and underwent the same entire extraction protocol as previously described.

Table 2.1: Contents and volumes of the enzymatic master mix.

Lysozyme 10mg/ml	50 µl
Mutanolysin 25U/µl	6 µl
Lysostaphin 4000U/ml	3 µl
TE	41 µl
12% Triton	30 µl
PBS	170 µl
Total	300 µl

After addition of the enzymatic master mix, the samples were pulse vortexed to mix the pellet with the enzymes and incubated at 37˚C for 1 hour. Following the incubation period, samples were pulse centrifuged to bring down any condensation gathered on the inside the lid or on the sides of the tubes. After completion of the enzymatic lysis, the cells in the solution were further disrupted by bead beating. A total of 100mg of bleached and rinsed 0.1mm diameter zirconia/silica was added to each tube and oscillated at 25 Hz for 1 min using a Tissue Lyser. The samples were then pulse spun and 200µl of the solution was transferred to a sterile 1.5ml tube with care taken not to carry forward any beads into the new tube. A total of 20µl of proteinase K was added to each tube along with 200µl of buffer AL and mixed. The samples were then incubated at 56˚C for 30 mins before adding 200µl of absolute ethanol was added and pulse vortex and pulse centrifugation. The solution was then added to a QIAamp (Qiagen) mini spin column in a 2 ml collection tube without wetting the rim of the column. The caps were then firmly shut, and the tubes were centrifuged at 6,200 x g for 1 min. The collection tubes were then discarded, and the columns were placed in fresh 2ml collection tubes. Next, 500µl of AW1 buffer was added without wetting the column rim and the tubes were centrifuged at 6,200 x g for 1 min. Columns were then placed in a fresh collection tube and 500µl of AW2

buffer was added. Column lids were firmly shut, and the tubes were centrifuged at 17,000 x g for 3 mins. The columns were placed in a fresh collection tube and centrifuged at 17,000 x g for 1 min to eliminate the chance of possible AW2 buffer carryover.

The extraction continued by placing the columns in a sterile 1.5µl tube and 100µl of AE buffer was added. The solutions were then incubated at room temperature for 10 mins and further centrifuged at 17,000 x g for 1 min. 5µl of the eluates were aliquoted for PCR to confirm successful extraction. 20µl of the eluates were separately aliquoted, stored at -20˚C and sent for sequencing to Research and Testing Lab in Texas USA, using Illumina MiSeq platform (Illumina, Inc. San Diego, California) (on 25/04/18 for ART I).

2.7 Polymerase Chain Reaction (PCR) Amplification

PCR was carried out to amplify the extracted DNA and confirm the presence of bacterial DNA using 16S barcode primers; forward primer 27F-5'- AGAGTTTGATCCTGGCTCAG-3', reverse primer 338R-5'-GCTGCCTCCCGTAGGAGT-3'. The PCR cycle setting was set for 95°C for 1 min, then 30 cycles for 95°C for 30 secs, 55°C for 30 mins and 72°C for 1.30 mins. For PCR analysis of the eluates, a mix of required components were prepared as outlined in Table 2.2.

Table 2.2: Contents and volumes of the PCR mix.

Reagents	Volume
5x reaction buffer	10µl
dNTP	1µl
Forward primer 10µl	1µl
Reverse primer 10µl	1µl
Taq polymerase	0.25µl
DNase free H_2O	31.75µl
Total	45µl

Following the completion of PCR, a 1.5% agarose gel was prepared by dissolving agarose in 100ml 1x TBE. This solution was heated for approximately 3 mins for all the agarose powder to dissolve. It was then cooled and 1µl of SYBR safe gel stain was added and left in a plate to solidify. 1x TBE was also used as the running solution of the electrophoresis process. Samples in PCR tubes were mixed with 7µl of loading dye and briefly mixed using a vortexer. A 100bp hyper-ladder DNA marker was loaded in a well for each row. A 20µl aliquot of each sample containing the DNA tracker was loaded in each well in addition to a positive Group B *Streptococcus* (GBS DNA) and negative control (blank swab). Samples were separated by electrophoresis at 140V for 10 mins and fluorescent bands were visualised by UV trans illumination (example provided in Figure 2.1).

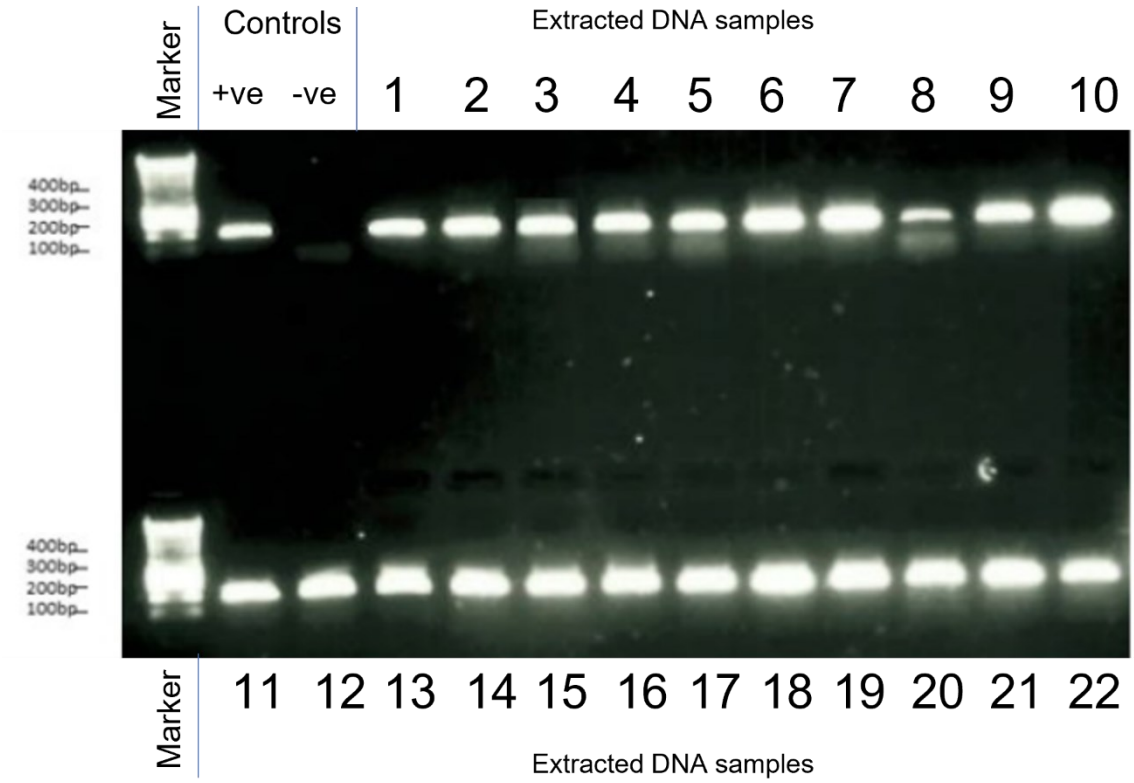


Figure 2.2: Demonstration of successful DNA amplification. Molecular weight marker, positive (+ve and -ve controls) and detected bacterial DNA amplicons labelled 1-22.

2.8 Materials required for immune analyte profiling

The materials used for cytokine analysis were as follows:

- Magnetic Luminex® Screening Assay Human Premixed Multi-Analyte Kit (17-plex) (R&D Systems, Inc., Minneapolis, USA)
    - Human standard cocktails A, B, C, I, K and O
    - Human premixed Biotin-Ab cocktail
    - Streptavidin-PE concentrate
    - Diluent RD2-1
    - Calibrator diluent RD6-52
    - Wash buffer concentrate
    - Microplate
    - Certificate of analysis
- Mixing bottles
- Multi-channel pipette and tips
- Distilled H_2O
- 500ml graduated cylinder

- Horizontal orbital microplate shaker (0.12” orbit)
- Microcentrifuge
- Polypropylene test tubes
- Plate sealers
- Microplate magnet (Bio-Rad Laboratories, California, USA)

2.9 Sample preparation for immune analyte analysis

Cell-free supernatants from the cervico-vaginal swabs prepared during DNA extraction were removed from the freezer and thawed on ice. The samples were centrifuged at 17,000 x g for 10 mins in a cold centrifuge for further purification. The supernatants were then transferred into fresh Eppendorf tubes.

Cell-free supernatants were analysed using multiplex cytokine kits – Magnetic Luminex® Screening Assay Human Premixed Multi-Analyte Kit (17-plex) (R&D Systems, Inc., Minneapolis, USA). Based on available literature, an array of 17 pro- and anti-inflammatory cytokines were identified for analysis: GM-CSF, IFN-γ, IGFBP-1, IL-1β, IL-1ra, IL-4, IL-6, IL-8, IL-10, IL-11, IL-12, IL-17a, IL-18, LIF, Leptin and TNF-α.

2.9.1 Sample preparation for immune analyte analysis: additional notes

Concentrations of IL-1ra in all samples and 41% of IL-8 readings were above the upper limit of specificity for the assay. Therefore, samples were diluted 1:20 before repeating assays for IL-1ra and IL-8.

2.10 Reagent and standards preparation for immune analyte profiling

Reagents were stored in a cold room as per the instructions from the manufacturer. Prior to use all reagents were brought back up to room temperature and were gently agitated to ensure any precipitates were reconstituted. Based on the chosen analytes, 6 standard cocktails were provided in the multi-analyte kit. Standard cocktails (A, B, I, O, C and K) were reconstituted with Calibrator Diluent RD6-52 according to the manufacturer’s guidelines provided in the certificate of analysis (Table 2.3) Following reconstitution, standard cocktails were kept at room temperature for 15 mins and were gently agitated prior to making serial dilutions.

Table 2.3: Standard cocktails and reconstitution volumes for immune analyte analysis.

Standard cocktails	Reconstitution volume (ml)
A	0.0225
B	0.25
I	0.25
O	0.2
C	0.25
K	0.225

2.11 Immune analyte profiling: laboratory procedure

Serial dilutions were prepared in 6 Eppendorf tubes (1.5ml). Standard 1 was prepared by combining 100µl of each standard cocktail (combined total of 600µl) added to 400µl Calibrator Diluent RD6-52 into standard 1 tube, making up a total volume of 1000µl. Serial dilutions of the standard cocktails continued with addition of 200µl of Calibrator Diluent RD6-52 into the 5 remaining Eppendorf tubes. Then 100µl of Standard 1 was added to Standard 2. This process continued with addition of 100µl from Standard 2 to 3 and so on to complete a serial dilution. Contents of each tube were mixed before each transfer. A total volume of 50µl of each standard was added in designated wells on each 96-well plate. Samples were also loaded in designated wells in 50µl volumes. All standards and samples were loaded in duplicates. Calibrator Diluent RD6-52 was added in 2 wells to act as 'blank'. A cocktail made up of an equal volume of each of the samples was prepared, of which 50µl was included in duplicate on each plate to serve as a control for plate-to-plate variation.

To each well, 50µl of Microparticle Cocktail mix was added. The Microparticle Cocktail mix was created by mixing 500µl of the Microparticle Cocktail with 5ml of Diluent RD2-1. The plate was then immediately sealed with a foil sealer to protect the samples from light. The plate was then placed on a horizontal orbital microplate shaker at 62 x g for 2 hours at room temperature. After incubation, the microplate was secured on a microplate magnet for the washing stages. Following 1 min of resting on the magnet, the liquid was discarded and 100µl of Wash Buffer

was added to each well. Following another minute of rest on the magnet, the wash buffer was discarded before repeating the washing procedure 3 more times.

A Biotin-Antibody cocktail was prepared by mixing 500µl of Biotin-Antibody cocktail concentrate to 5ml of Diluent RD2-1 in a foiled Falcon tube to protect the solution from light. A total of 50µl of the diluted Biotin-Antibody cocktail was added to each well and the plate was sealed and placed on the microplate shaker (62 x g) for 1 hour before washing 3 times. Streptavidin-PE was then prepared by pulse centrifugation and vortexing. A total of 220µl Streptavidin-PE concentrate was added to 5.35ml of Wash Buffer in a polypropylene amber bottle for protection from light. To each well, 50µl of diluted Streptavidin-PE was then added, the plate sealed and placed on the microplate shaker at 62 x g for 30 mins before washing as previously described. The microparticles were then resuspended in 100µl of Wash Buffer and incubated for an additional 2 mins on the microplate shaker at 62 x g immediately before placing the microplate in the Bio-Rad analyser. The analysis was performed within 90 mins of the final washing step. Data was acquired using a Bio-Rad Bioplex® 200 system (Bio-Rad Laboratories, California, USA). Standard curves calculated for each analyte are shown in Appendix Figure 1.

2.12 Quantitative bacteriology

2.12.1 Materials

- StepOne© qPCR machine (ThermoFisher Scientific, UK)
- 5µl bacterial DNA isolated from vaginal swabs or semen samples
- *E. coli* DNA (Sigma, D4889 1U)
- PCR grade H_2O (Cambio, UC-17000-10, quaranteed DNA free)
- Platinum PCR Supermix UDG Containing Rox (LifeTech, Cat No. 11730-017)
- BactQuant forward primer at 100µM (Sigma, 0.025 µmol synthesis scale, desalted)
    - Sequence: 5’ CCT ACG GGA GGC AGC A
- BactQuant reverse primer at 100µM (Sigma, 0.025 µmol synthesis scale, desalted)
    - Sequence: 5’ GGA CTA CCG GGT ATC TAA TC
- BactQuant Probe (LifeTech, Cat. No. 4316034, 6000pmol scale)
    - Sequence 5’ 6FAM-CAG CAG CCG CGG TA-MGBNFQ
- 1.5ml microcentrifuge tubes
- Optical 96-Well Reaction Plate (Starlab semi-skirted Cat. No. E1403-7700)
- Plate Seal EU opti-seal optical disposable adhesive (100) Cat. No. BP231 Appleton Woods

2.12.2 Quantitative bacteriology laboratory procedure

For a subset of women with samples collected at embryo transfer for both ARTI and ARTII cohorts as well as for the semen samples, bacterial load was estimated by determining the total number of 16S rRNA gene copies per sample (485). A known concentration of *E. coli* DNA was used to create a ten-fold standard curve from 3 to 300,000 copies of 16S DNA. The *E. coli* standards and the 5µl of samples DNA templates were combined with a platinum PCR supermix UDG containing 50nM Rox, BactQuant forward and reverse primers, and probe and loaded in duplicates onto a PCR plate. Following a 2 min centrifugation the plate was transferred to the StepOne© qPCR machine. PCR parameters were ser to hold at 50°C for 2 min, 95°C for 10 secs, followed by 40 cycles of 95°C for 15 secs and 60°C for 1 min before a final holding stage of 4°C until plate retrieval (Figure 2.2). StepOne© software was used to calculate the 16S DNA copy number of the sample in template in relation of the *E. coli* standard curve (example provided in Figures 2.3 and 2.4). Template free PCR controls were included in each run to exclude contamination of PCR reagents.

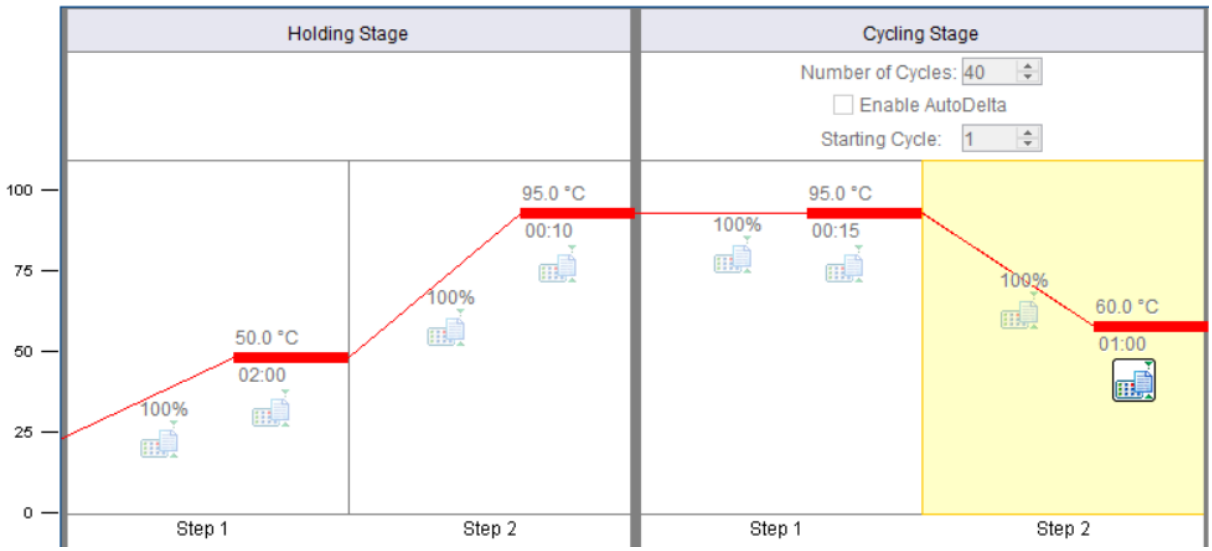


Figure 2.3: PCR cycle conditions. Holding stage, followed by a total of 40 cycles before a final holding stage of 4°C.

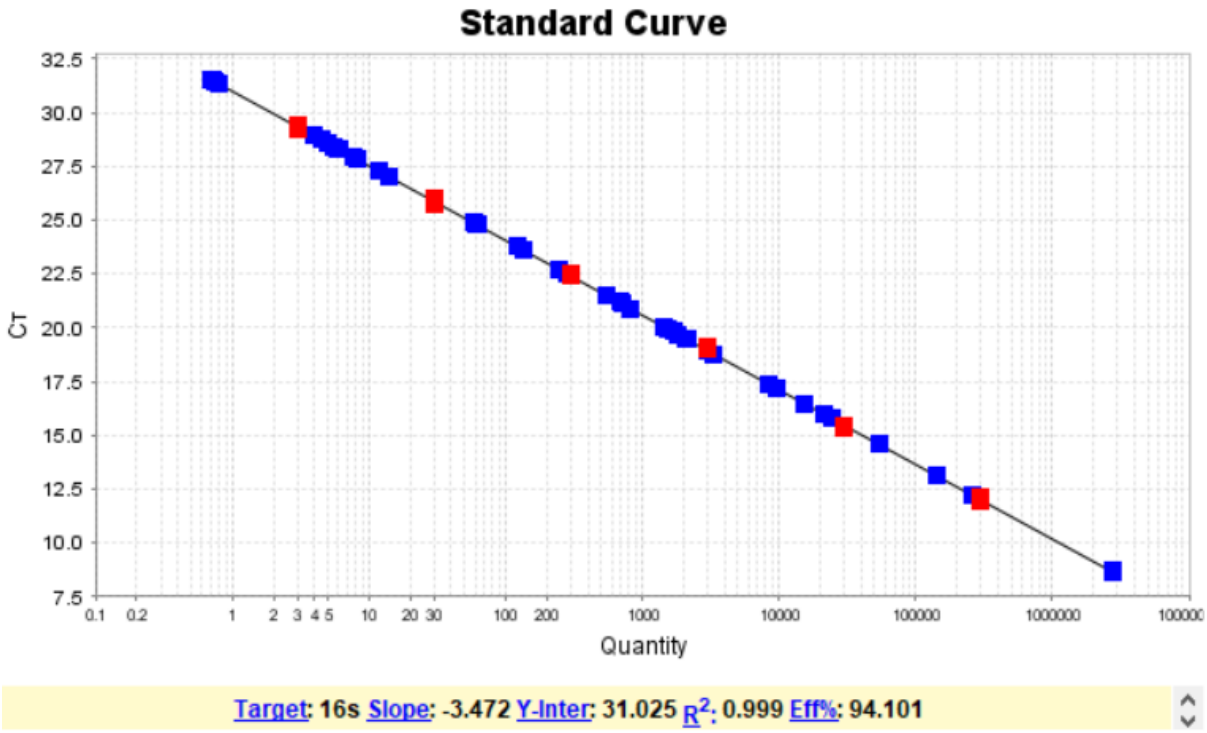


Figure 2.4: BactQuant Standard curve. A standard curve generated from serial dilutions of *E. coli* standards (red squares) was used to calculate the number of 16S rRNA genes detected within biological samples (blue squares).

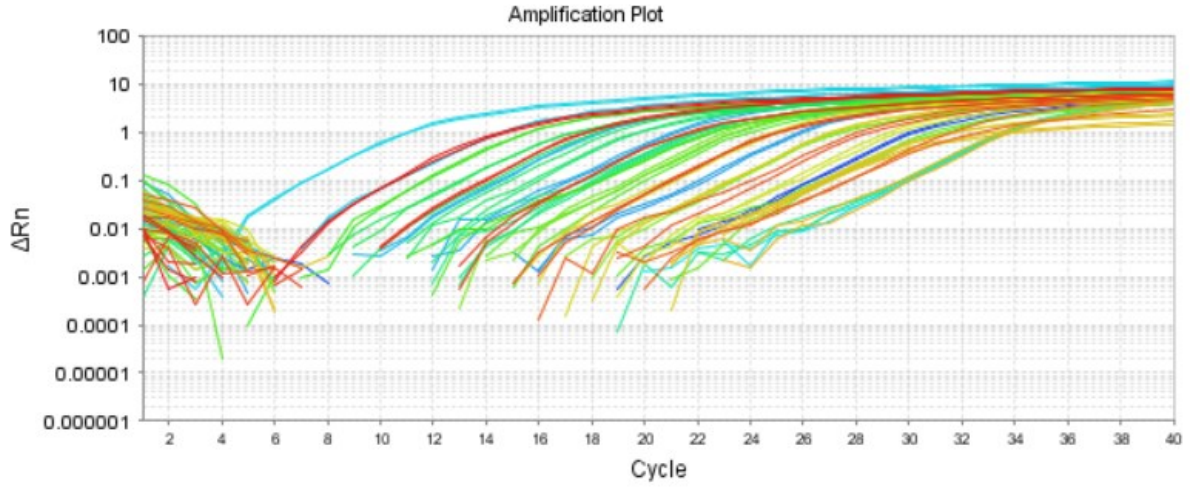


Figure 2.5: BactQuant Amplification plot. Amplification plot for biological samples and standard preparations of *E. coli* at known concentrations (indicated in red).

The bacterial load for semen samples is reported as 16S rRNA copy numbers per 1 mL of semen. This included identifying the number of 16S rRNA copies associated with each bacterial species as outlined in Appendix figure 3.

2.14 Assessment of semen quality and function

Aliquots from semen samples were used for routine semen analysis, ROS assessment, DNA fragmentation analysis, and genomic assessment of seminal microbiota.

2.14.1 Routine semen analysis

Semen analysis was carried out by qualified Andrologists in the Andrology Departments of both Hammersmith Hospital and CRGH according to WHO 2010 guidelines and UK NEQAS accreditation (248). Microscopic and macroscopic semen qualities were assessed within 60 mins of sample production. This included: measurement of semen volume, sperm concentration, total sperm count, progressive motility and total motility count, morphological assessment, anti-sperm antibodies and leucocyte count.

2.14.2 ROS analysis

ROS levels in semen samples was analysed in the Andrology laboratory using an in-house developed chemiluminescence assay validated by Vessey et al. (486). In this assay, Luminol is oxidised in the presence of ROS, which generates chemiluminescence. ROS is measured indirectly by measuring the chemiluminescence generated using a CE marked luminometer (GloMax°Promega Corporation) (486). In advance of ROS measurement, a 100 mmol/L luminol (5-amino-2,3-dihydro-1,4-phthalazinedione; Sigma-Aldrich) stock solution was prepared in dimethylsulfoxide (DMSO). The stock solution generally remains stable for up to 15 weeks. Due to light sensitivity of the assay, the analysis was done in dark and in an aluminium foil covered polystyrene Falcon tube. All reagents stored at 4°C, were brought to room temperature before analysis. A luminol working solution (5 mmol/L luminol prepared in DMSO), negative controls (400µl PBS with 10µl 5 mmol/L luminol working solution), and positive control samples (395µl PBS, 5µl 30% H_2O_2 (VWR), and 10µl 5 mmol/L luminol working solution). On the morning of each analysis, the luminometer was calibrated using the negative and positive controls. All samples were mixed gently immediately before placing the tubes in the luminometer. Sperm concentration of >1 M/mL is required for this assay. This is because ROS measurement could be unreliable in lower than 1 M/mL sperm concentrations (487). A total of 400µl of semen was aliquoted using a positive displacement pipette and placed into a 1.5 mL microfuge tube. Following this, 10µl of the luminol working solution was added and gently mixed before taking readings in the luminometer. This process is time sensitive and was done at exactly 20 mins of sample production (minimum amount of time for semen to reach liquefaction). A total of 10 consecutive readings were recorded at 1 min apart. The ROS

value was obtained by subtracting control mean from the test mean and correcting it for sperm concentration. Results are therefore reported as 'relative light units per second per million sperm'. The upper limit of optimal ROS was internally determined at 3.77 RLU/sec/10^6 sperm (95% CI).

2.14.3 Sperm DNA fragmentation assessment

2.14.3.1 TUNEL assay

The TUNEL (Terminal deoxynucleotidyl transferase biotin-dUTP Nick End Labeling) assay was used to determine the sperm DNA fragmentation index. Following determination of semen concentration and motility, samples were aliquoted into 2 tubes to run the patient negative sample in duplicates, and 2 tubes for patient test samples in duplicate. Semen was added into the tubes and spun at 300 x g for 7 mins. Seminal plasma was then removed.

A hydrogen peroxide solution was diluted in PBS at a 1:15 ratio from the stock solution (30% H_2O_2). Sperm was resuspended in 1mL of the diluted H_2O_2 solution and placed in a heater at 50°C for 1 hour. It was then centrifuged for 7 mins at 250 x g followed by supernatant removal and adding 1mL of PBS. The tube was then centrifuged for 7 mins at 250 x g. After the supernatant was removed, 1mL of PBS was added and centrifugation was repeated. The supernatant was again removed and 1mL of PBS was added. Together with the test and negative samples, the sample was centrifuged for 7 mins at 250 x g. Samples then underwent fixation and permeabilization. For this, a 3.7% paraformaldehyde solution was prepared by diluting 10mL of stock formaldehyde 37% solution in 90mL of PBS (1X). After removing the supernatant from the samples and sperm controls, 1mL of the 3.7% paraformaldehyde was added. The samples were incubated at room temperature for 15 mins, they were then centrifuged for 4 min at 600 x g. Samples were then washed with PBS and centrifuged for an additional 4 min at 600 x g. Supernatant was removed and 1mL of ice cold 70% ethanol was added. Samples were then incubated at 4°C for 15-30 min.

Stain preparation was done using the reagents and in the same sequence as presented in Table 2.4, with all procedures taking place in the dark.

Table 2.4: Reagents and volumes used for TUNEL assay.

Staining solution	Volume per 1 assay
Reaction buffer	10.00µl
TdT Enzyme	0.75µl
FITC-dUTP	8.00µl
Distilled H_2O	32.25µl
Total volume	51.00µl

Reaction buffer (stored at 4°C), as well as TdT enzyme and FITC-dUNP (stored at -20°C) were placed in room temperature for 20 mins to thaw. TdT enzyme was spun for 5 mins at 250 x g to bring the reagent to the bottom of the tube. TdT enzyme was omitted from negative controls. The pellets in each tube were then resuspended in 50µl of the staining solution. Sperm was incubated in the staining solution for 60 mins at 37°C covered in aluminium foil. 1.0mL of Rinse buffer was then added to each tube and centrifuged for 7 mins at 250 x g and supernatant was discarded. Cell rinsing, centrifugation and supernatant discard steps were repeated. The pellet was then resuspended in 0.5mL of PI/RNase staining buffer. The cells were then incubated for 30 mins at room temperature in the dark.

2.14.3.2 Comet assay

DNA fragmentation analysis on 40 samples was done using the Comet assay. The samples were sent to Examen Lab (Belfast, UK) for analysis. The alkaline Comet assay is a single cell gel electrophoresis assay, which was optimised for human sperm application (488, 489).

2.15 Materials required for metabolome analysis

Materials used for metabolome analysis included the following:

- HPLC grade methanol (Sigma-Aldrich, St Louis, MO)
- HPLC grade Water (Sigma-Aldrich, St Louis, MO)
- Transwab Amies medical swabs (MWE medical wire, Wiltshire, UK)

2.16 Metabolome analysis using DESI-MS

The Desorption electrospray ionisation mass spectrometry (DESI-MS) instrument used consists of an electronic spray emitter and automated rotatable swab holder aided by a 3D manual moving stage. A rotor for controlled rotation is designed on the sample holder as well as a plastic tube for stabilisation and prevention of sideway tripping during rotation. The spray was then directed towards the inlet capillary of an LTQ-Orbitrap Discovery mass spectrometer (Thermo Scientific, Bremen, Germany). A batch and run-order randomisation process was carried out prior to analysis to avoid bias due to analytical batch and run order effects.

Table 2.5: Source Parameters and DESI-MS Instrumental Settings.

Nebulising gas pressure	7 bar	Microscans	1
Spray voltage	4.3 kV	Mass range	50-1000
Capillary temperature	250°C	Mass resolution	30.000
Capillary voltage	50 V	Tip-to-surface height	<2 mm
Solvent flow rate	10µL min^{-1}	Distance inlet-sample	2 mm
Tube lens voltage	120 V	Angle tip-sample	50°
Spray solvent	Methanol/water (95:5, v/v)	Angle inlet	10°
Max. injection time	500 ms	Distance tip-inlet	4.5 mm

2.17 Metabolome analysis laboratory procedure

Swabs were fixed into the swab holder and positioned in front of the mass spectrometer inlet capillary. The DESI sprayer was directed to the centre of the swab, with a tip-sample distance of 1.5-2 mm and altitude difference of 2 mm between the tip and the inlet capillary. The entire surface of the swabs was analysed by DESI through clockwise rotation of the swab towards the MS capillary. A mixed methanol/water solution (95:5, v/v) spray solvent was used for desorption of the sample material. Full scan mass spectra (*m/z* 50-1000, *R* = 30.000 (fwhm)) were recorded in the negative and positive ion mode.

2.17.1 Mass spectral data pre-processing

Raw mass spectral data were converted from proprietary Thermo .raw files into the .mzML open format via the ProteoWizard msConvertGUI (Vanderbilt University, Nashville, TN, USA)(490), and centroided using the vendor algorithm implemented in the msconvert tool. The mzML files were then opened in Python3 using the pymzml package. Each sample acquisition was processed by grouping centroids across scans using a Python implementation of MALDIquant's *binPeaks* function, with *tolerance=15* ppm and *grouper='strict'*. An average mass spectrum was then obtained by averaging all the peaks present in more than 25% of the scans measurement. Peaks from the averaged spectra were then grouped across multiple samples using MALDIquant-*binPeaks* algorithm, with *tolerance=15* ppm, and *grouper='relaxed'*. Peaks which were not present in at least 25% of the samples were excluded. The *m/z* values for the MS features in the final data matrix were re-calibrated using a linear calibration function fitted to the observed *m/z* values matching the endogenous lactate (89.02442 $[M-H]^-$), cholesterol sulphate (465.3044 $[M-H]^-$) and PG (36:1) (775.5489 $[M-H]^-$) signals. An example of representative DESI-MS spectral profile of a vaginal swab sample is provided in Appendix Figure 2.

2.18 16S rRNA data processing

The 16S rRNA gene sequences were analysed using the bioinformatics software package Mothur (491) using the MiSeq SOP Pipeline to analyse multiplex sets of data on a single run. The paired reads were assembled using make.contigs which extract the sequences and quality score data from the fastq files, and creates the reverse complement of the reverse read and assembles the paired end reads into a contig. We used the kmer searching method using the Silva bacterial database (www.arb-silva.de/) for sequence alignment, with the flip parameter set to true which allows the reverse complement of the sequence to be aligned for better results. For classifications of the sequences we used a RDP database and reference sequence files and used the Wang method (492). 16S rRNA gene sequence reads were quality checked and normalised to the lowest number of reads in Mothur.

Using Mothur and the Vegan package in the R statistical package (493), the Alpha diversity index was calculated. The Simpson index was used for this purpose as it includes both species richness and evenness of abundance among the species present in samples (494).

The raw counts at species and genera level were centered-log-ratio (CLR) transformed using the *propr* R package. Taxa with a zero count in more than 25% of the samples were excluded from the analysis after performing the CLR transformation.

2.19 Statistical analysis

Longitudinal analyses were performed with linear mixed effect models in R, with models created and fitted using the R package "*lme4"* and the restricted maximum likelihood estimation method. For each marker, a model with the structure Marker ~ Stage + (1|Subject) was fitted, where the mean level of each marker is regressed against the fixed-effect Stage (the treatment time-points) and between subject variability is modelled as a random effect (random intercept per subject). Immune and hormone markers were log transformed after addition of a constant offset (*c=1)*, while for analysis of 16S rRNA taxa the CLR transformed values were used. The hypothesis that the variance explained by the "Staqe" fixed-effect coefficient was significantly larger than zero was tested with ANOVA, using the *anova* function and the statistical testing interface of the package *lmerTest*. The degrees of freedom were estimated with the Kenward-Roger approximation implemented in the *pbkrtest* package. Associations between immune markers and microbial taxa were estimated using standard linear regression models, with the formula log (Marker + 1) ~ clr(Taxa). This model structure estimates the expected mean log-transformed (after addition of a constant *c=1)* values of hormone and immune marker concentration conditional on the CLR transformed microbial taxa counts. For both standard and mixed effect linear model analyses, the false discovery rate correction and q-values were estimated using the Benjamini-Hochberg method, using the implementation in the base R function *p.adjust.* Box-and-whiskers plots were generated with *ggplot2*. Regularized canonical correlation analysis was performed in R, with the *mixOmics* package. Cytokine data was log transformed after addition of a constant offset *c=1* to account for zero values, and microbial taxa counts were CLR transformed as described above. The shrinkage parameters were chosen automatically using 5-fold cross-validation, with the *tune.rcc* function of the *mixOmics* package, and final models fitted with the *rcc* function, with the argument *method='ridge'*. Canonical coordinate plots were drawn in *ggplot2*. Random forest models were trained in R using the *randomForest* and *caret* packages. The cytokine values and metataxonomic species counts were log and CLR transformed in the same manner as in the linear regression analysis. The reported model performance metrics were estimated with repeated (n=15) 3-fold cross validation.

To determine which statistical tests needed to be performed, several analyses and examinations of the datasets were performed in GraphPad Prism (GraphPad Software Inc, CA, USA) (version 9.3.1). The Shapiro-Wilk's test was performed to assess the normality of data distributions. For non-normally distributed data, comparison of means was performed in more than 2 groups, a non-parametric ANOVA test in form of Kruskal-Wallis test with Dunn's

multiple comparison tests were performed. For non-normally distributed data for 2 groups, Mann-Whitney tests were performed. For correlation analysis, the Spearman r test was done.

3 CHAPTER III The cervicovaginal microbiota and host response in women undergoing fresh IVF cycle treatments

3.0 INTRODUCTION

Lactobacillus species contribute in various ways to the maintenance of vaginal health (181). In addition to the production of lactic acid, *Lactobacillus* species inhibit the growth of pathogenic bacteria by competitive exclusion as well as production of bacteriostatic and bactericidal substances (133). Several studies have demonstrated the ability of *Lactobacillus* species to adhere to the epithelial cell wall which enables the long-term colonization of these bacteria in the vagina (495, 496) and comparative genomic analyses suggest that *L. crispatus* contains core proteins and bacteriocin-like substances with potential for competitive exclusion of *G. vaginalis* and other pathogens (497).

In early pregnancy, loss of *Lactobacillus* species from the vaginal niche is associated with decreased conception rates and increased rates of early pregnancy loss (498). As outlined in the introduction chapter (Table 1.3), most studies suggest dominance by *Lactobacillus* species associates with improved embryo implantation during IVF treatments (499). In contrast, BV associated bacteria such as *G. vaginalis* and *Prevotella* species are associated with unsuccessful embryo implantations (218, 500). However, the relationship between IVF success and the vaginal microbiome remains unclear with several studies reporting no relationship between vaginal microbiota composition and IVF success (1).

It is now well established that E2 plays an important role in shaping a healthy vaginal microbiome. Elevated concentrations of E2 promote the deposition of glycogen in vaginal epithelial cells (501), which is then broken down by α-amylase into complex oligomers of glucose that are metabolised by *Lactobacilli* as a preferential energy source (502). Dominance by *Lactobacillus* species contributes to the increasing acidity of the vagina and protection against pathogenic colonisation (Figure 1.7) (503). However, as alluded to in section 1.4 (page. 45 and 46), sex hormones also play a critical role in regulating innate immunity. The immune response plays an important role in endometrial remodelling, acceptance of the semi-allogenic embryo and a healthy ongoing pregnancy. Several components of the immune system play a critical role in implantation, apposition and attachment of the embryo to the endometrium (417). Locally, E2 engages with immunity through receptors ERα and ERβ which are expressed in epithelial and stromal cells (463, 464). Immune cells such as uNK cells also express E2 receptors (ERβ1), NK cells secrete immune mediators such as IFN-γ and IL-18 which assist in embryo implantation and successful pregnancy (504-506). The interaction

between sex hormones, microbiota of the reproductive tract and host immune response is poorly defined, particularly in the context of IVF and early pregnancy events.

During IVF treatment, hormonal levels of patients are artificially manipulated via pituitary suppression and ovarian stimulation to supraphysiological concentrations (Figure 1.4). This provides a unique opportunity to examine the relationship between host immune response in the lower reproductive tract to vaginal microbiota in differing hormonal contexts. The hypothesis of the work presented in this chapter is that changes the levels of key sex hormones, namely P4 and E2, lead to differences in host response to vaginal microbiota and that this interplay is reflective of the underlying reproductive potential of the host and is therefore predictive of IVF success. To test this hypothesis, this chapter aimed to study these interactions throughout 5 major timepoints during the treatment cycle and to elucidate whether these relationships have biomarker capabilities in predicting the clinical outcomes of fresh IVF cycles.

3.1 Results: Patient recruitment and sample collection

As summarised in Figure 3.1, a total of 53 patients were recruitment from the ART1 study as part of these investigations. After excluding samples from cancelled embryo transfer cycles, a total of 142 swabs collected from 33 women undergoing fresh embryo transfer cycles and 20 swabs from 7 women undergoing frozen embryo transfer cycles were available for analysis.

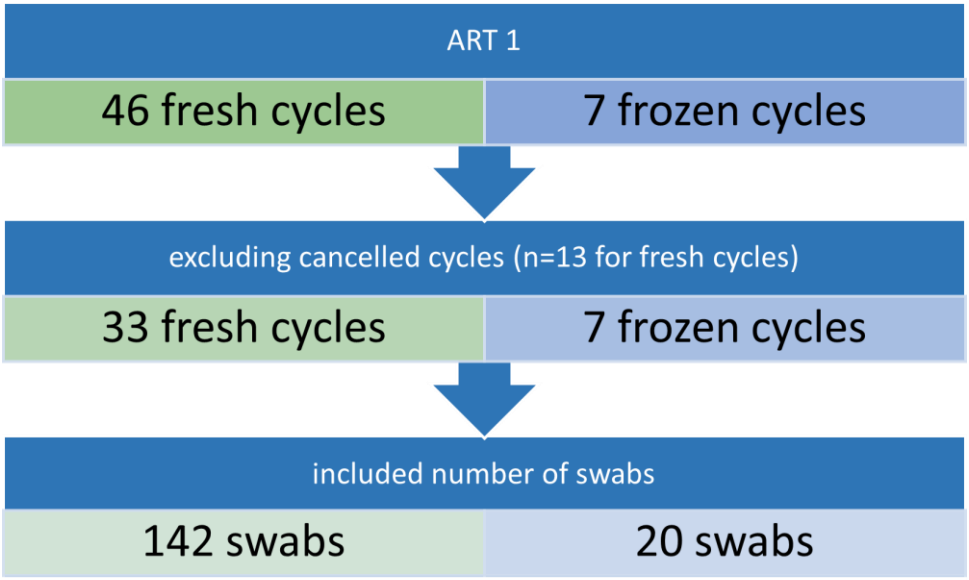


Figure 3.1: Summary of patients recruited and sampled in the ART1 study.

3.2 Assessment and comparison of E2 and P4 levels throughout fresh and frozen IVF cycles

Initial analyses aimed to compare the concentration of circulating E2 and P4 at equivalent treatment stages of women undergoing fresh and frozen IVF cycles (Figure 3.2). In women undergoing fresh cycles, treatment to induce pituitary suppression led to a significant reduction in both P4 and E2. Ovarian stimulation induced a major rise in circulating E2, peaking at an average of 6000 pmol/L, which was largely maintained throughout egg collection and embryo transfer. Concentrations of P4 increased slightly at egg collection but most substantially at the time of embryo transfer, reaching a maximal average of 420nmol/L. In contrast, in women undergoing frozen cycles, a significant reduction of P4 was not observed at pituitary suppression compared to coordination appointment. Significantly higher levels of E2 (mean = 2060 pmol/mL ± 1751 Std) and P4 (mean = 59 nmol/mL ± 59) were observed at the time of embryo transfer.

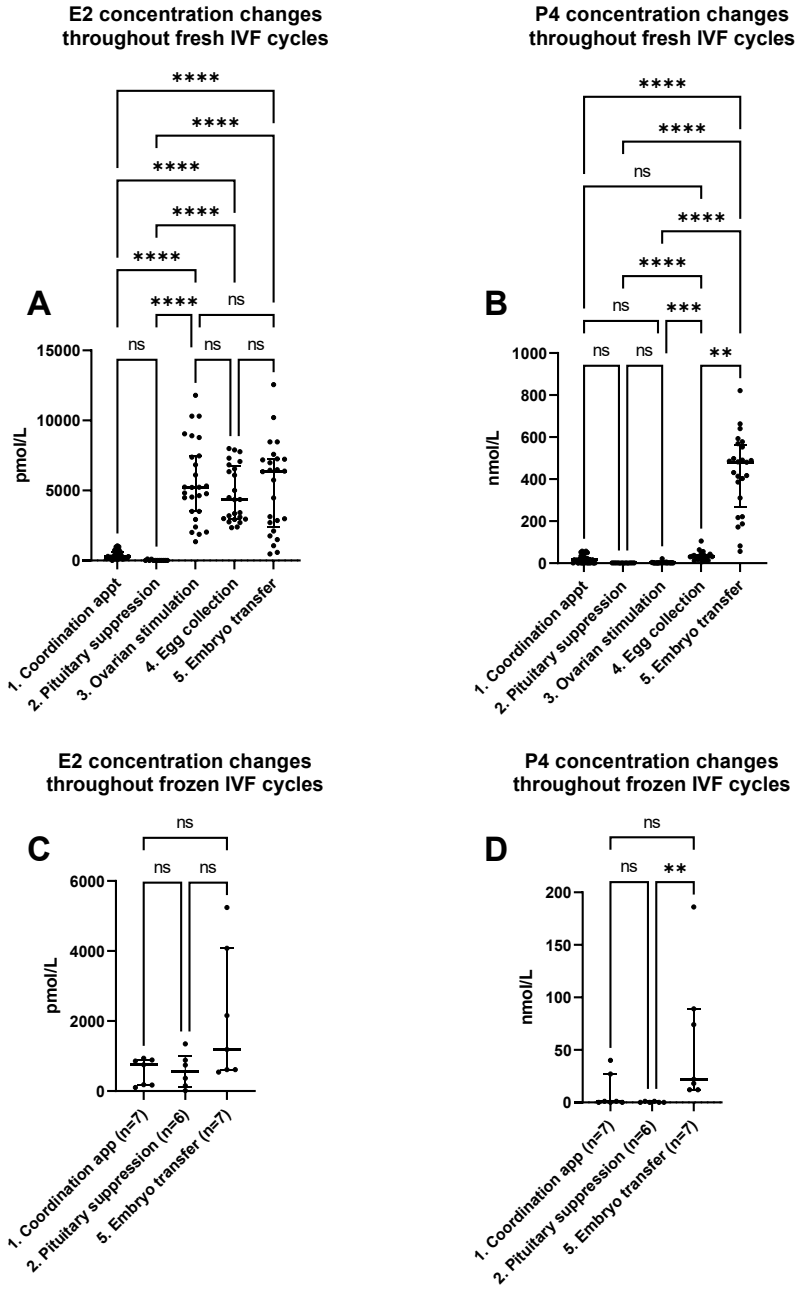


Figure 3.2: Concentrations of serum E2 and P4 for fresh and frozen IVF cycles. A) E2 concentrations changed significantly throughout fresh IVF cycles (Kruskal-Wallis p<0.0001), Supraphysiological concentrations of serum E2 are reached due to ovarian stimulation protocol and remain high until the day of embryo transfer. B) P4 concentrations change significantly throughout fresh IVF cycles (Kruskal-Wallis p<0.0001), high concentrations are observed on the day of egg collection and further significant increase is observed on the day of embryo transfer. C) E2 concentrations throughout frozen IVF cycles did not change significantly (Kruskal-Wallis p=0.17). however, higher concentrations were observed for 3 patients. D) P4 concentrations throughout frozen IVF cycles change significantly (Kruskal-Wallis p=0.002). P4 concentrations were low as a result of pituitary suppression but they were not significantly different to coordination appointment using post-hoc testing (Dunn's multiple comparison test p=0.90). Subsequently, P4 levels significantly increased from pituitary suppression to embryo transfer (Dunn's multiple comparison test p=0.005).

Comparison of hormonal levels between fresh and frozen IVF cycles indicated significant differences in concentrations of E2 at equivalent stages of treatment (Figure 3.3). While levels of E2 at the coordination appointment were similar, levels were significantly higher in women undergoing frozen cycle at pituitary suppression (583.3 ± 502.1 v 24.5 ± 34.0, p=0.001, Mann-Whitney T-test). However, at embryo transfer, serum levels of E2 were significantly higher in the fresh IVF cohort compared with the frozen (5238 ± 3197 v 2061 ± 1892, p=0.001, Mann-Whitney T-test).

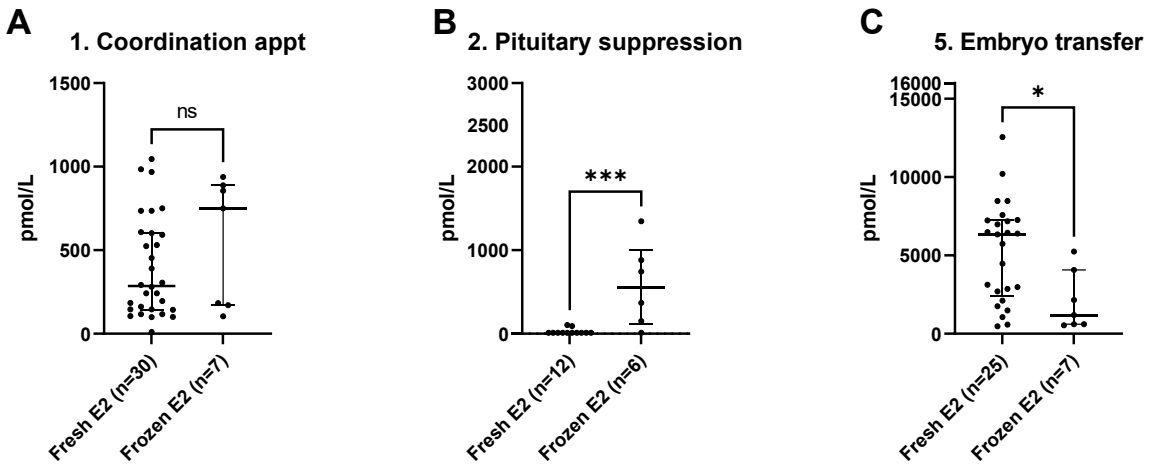


Figure 3.3: Comparison of E2 concentrations between fresh and frozen IVF cycles at comparable stages of sample collection. A) At the time of the coordination appointment samples were hormonally unregulated and no significant differences between fresh and frozen E2 concentrations were observed (393.6 ± 298.8 v 555.7 ± 381.9, p=0.33). B) During pituitary suppression, endogenous circulating hormones were artificially suppressed using GnRH analogues. Circulating E2 concentrations were significantly lower in fresh cycles compared with frozen cycles (24.5 ± 34.0 v 583.3 ± 502.1 p=0.001). C) At embryo transfer supraphysiological concentrations of E2 in fresh cycles due to ovarian stimulation protocols were significantly higher than frozen cycles (5238 ± 3197 v 2061 ± 1892 p=0.01). Mann-Whitney T-tests.

Concentrations of P4 were comparable between fresh and frozen patient cohorts at coordination appointment (17.8 ± 19.4 v 9.9 ± 16.5, P=0.12; Mann-Whitney T-test) and during pituitary suppression (0.7 ± 0.4 v 0.4 ± 0.4, P=0.14; Mann-Whitney T-test). However, at embryo transfer P4 levels were significantly higher for the fresh IVF cohorts (425.5 ± 187.8 v 59.0 ± 64.2, P<0.0001, Mann-Whitney T-test).

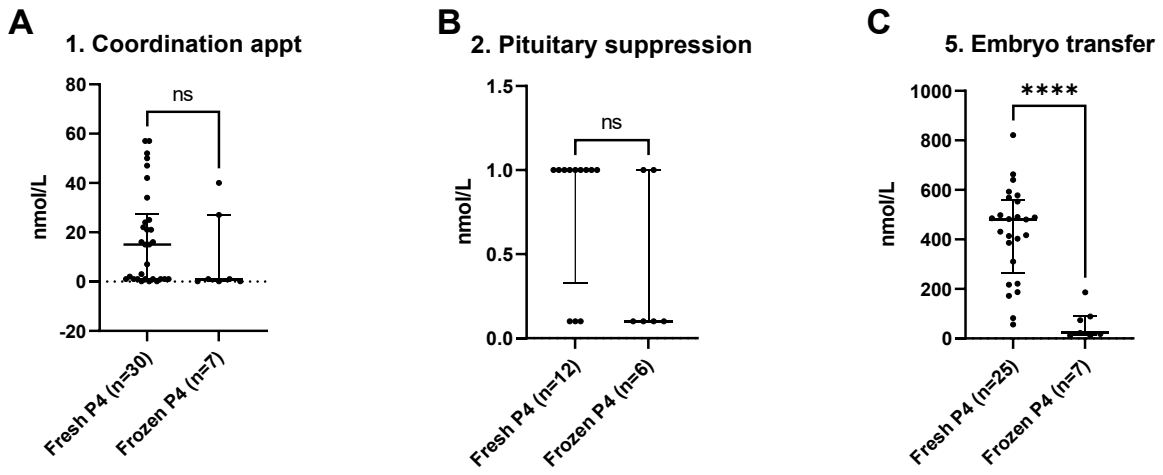


Figure 3.4: Comparison of P4 concentrations between fresh and frozen IVF cycles at comparable stages of sample collection. A) No significant differences between fresh and frozen P4 concentrations (17.8 ± 19.4 v 9.9 ± 16.5, P=0.12) were observed at the coordination appointment or at B) pituitary suppression, where endogenous circulating hormones were artificially suppressed using GnRH analogues (0.7 ± 0.4 v 0.4 ± 0.4, P=0.14). C) At embryo transfer P4 concentrations were significantly higher on the day of embryo transfer in fresh IVF cycles (425.5 ± 187.8 v 59.0 ± 64.2, P<0.0001). Mann-Whitney T-tests.

Given that women undergoing frozen cycles had significantly different hormonal levels at equivalent stages of treatment, subsequent analyses designed to examine the relationship between hormones and immune analytes and their relationship to outcome were limited to only those women undergoing fresh IVF cycles (n=33). Additional analyses of the frozen IVF cycles (n=7) are presented in Chapter 4. Using a locally estimated scatterplot smoothing (LOESS) fit method, a smoothed line of best fit was applied to the available E2 and P4 datasets for the fresh cycle patient cohort (Figure 3.5). As shown by the individual patient level datapoints, at this time of sample collection during the coordination appointment, patients were at various stages of their monthly cycle.

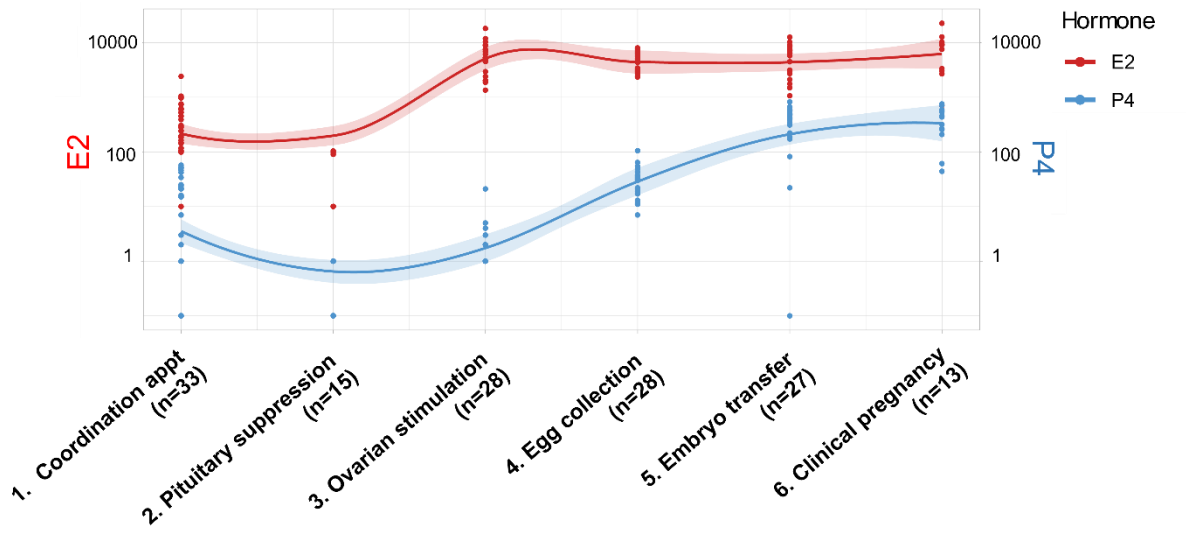


Figure 3.5: Longitudinal E2 and P4 concentrations throughout fresh IVF cycles. LOESS fit method (507). Note: data points for some sample collection timepoints are overlapping.

Data for P4 and E2 were available at pituitary suppression for n=15 women, with levels of both hormones found to be decreased at this stage. Following ovarian stimulation, E2 and P4 levels increased. At egg collection, embryo transfer and during clinical pregnancy, E2 levels remained high and during these stages, P4 levels continued to increase. A summary of mean fold changes calculated for E2 and P4 across the treatment stages of fresh cycles is presented in Table 3.1.

Table 3.1: Summary of E2 and P4 fold change during hormonal manipulations of fresh IVF cycles.

Fold changes	E2	P4
1. Coordination appt to 2. Pituitary suppression	16-fold ↓	23-fold ↓
2. Pituitary suppression to 3. Ovarian stimulation	246-fold ↑	3-fold ↑
3. Ovarian stimulation to 4. Egg collection	1.2-fold decrease ↔	14-fold ↑
4. Egg collection to 5. Embryo transfer	1.1-fold increase ↔	13-fold ↑

3.3 Patient demographics for fresh IVF cycles

A summary of key patient metadata for the women undergoing fresh cycles is presented in Table 3.2. Of the 33 cycles included in this study, 17 resulted in pregnancy (51%) of which there were 15 live births (45%). Caucasian patients were more likely to have a successful embryo implantation compared with other ethnicities (13 v 4, p=0.01, Fisher's exact test). The non-Caucasian cohort was made up of patients who self-identified as Indian (n=8), Arab (n=2), Black/African (n=2), Pakistani (n=1), Chinese (n=1) and mixed race (n=1). No other significant differences in key clinical and patient factors between women who has a successful IVF outcome and those who did not was observed.

Table 3.2: Patient demographics and clinical outcomes for women undergoing fresh IVF cycles. For statistical comparison of categorical variables, Fisher's exact test was used. For statistical comparison of continuous variables, unpaired T-test was used. Where continuous data was unavailable for some patients, the final sample size is indicated.

Factor	**Pregnant (n=17)**	**Not pregnant (n=16)**	**p-value**
Ethnicity			
Caucasian (n=18, 55%)	13 (72%)	5 (28%)	0.01*
Asian/Black (n=15, 45%)	4 (27%)	11 (73%)	
Age			
<30 (n=3, 9%)	1 (33%)	2 (67%)	0.99
30-36 (n=19, 58%)	10 (53%)	9 (47%)	
>36 (n=11, 33%)	6 (55%)	5 (45%)	
Suppression protocol used			
GnRH antagonist (n=11, 36%)	5 (45%)	6 (55%)	0.71
mid-luteal protocol (GnRHa) (n=20, 61%)	11 (60%)	9 (40%)	
Microdose flare up protocol (n=1, 3%)	0 (0%)	1 (100%)	
Infertility diagnosis			
Male and female (n=3, 10%)	2 (67%)	1 (33%)	NA
Female factor (n=6, 20%)	2 (33%)	4 (67%)	
Male factor (n=11, 35%)	6 (55%)	5 (45%)	
Unexplained (n=11, 35%)	6 (55%)	5 (45%)	
BMI (mean±SD)	24.3±2.94 (n=7)	24.6±3.14 (n=10)	0.86
AFC (mean±SD)	19±13 (n=12)	19±11 (n=15)	0.95
AMH (mean±SD)	25.6±14.9 (n=11)	23.3±12.8 (n=11)	0.69
Baseline FSH (mean±SD)	5.93±1.72 (n=10)	5.6±2 (n=6)	0.80
Baseline LH (mean±SD)	5.43±1.82 (n=7)	7.38±3.31 (n=5)	0.27
Days of stimulation (mean±SD)	12±2 (n=8)	12±1 (n=10)	0.65
Cumulative FSH dose (mean±SD)	3332±1841 (n=8)	3329±1475 (n=10)	0.99
Day of trigger from start of stimulation (mean±SD)	13±2.4 (n=8)	13±1.3 (n=10)	0.64
Follicles ≥14mm (mean±SD)	12.1±5.2 (n=8)	11.7±5.5 (n=10)	0.87
Number of eggs collected (mean±SD)	11.4±6.6 (n=8)	12.8±5.5 (n=10)	0.64
Number of eggs fertilised (mean±SD)	7.7±3.58 (n=8)	8.6±5.37 (n=10)	0.58
Vaginal pH at first sample collection (mean±SD)	4.5±0.5 (n=8)	4.5±0.5 (n=10)	0.99

3.4 Assessment of cervicovaginal (CVF) immune analytes across fresh IVF cycles

A total of 17 immune analytes were examined in samples collected from women undergoing fresh IVF cycles (Table 3.3). To determine whether the immune analytes were changing across each of the sample collection timepoints, a linear mixed effects model was used. The model included stages 1 to 5 of sample collection irrespective of clinical outcomes. Samples collected during clinical pregnancy were plotted for comparison but were excluded from the mixed effects modelling. A total of four analytes, IGFBP-1, IL-1β, IL-1ra and IL-8 were found to significantly changes in concentration across the stages of sample collection. To account for multiple testing, adjusted p-values (q-values) were calculated using the Benjamini-Hochberg procedure.

Table 3.3: Longitudinal changes across stage for immune analytes. p-values for changes for immune analytes. Linear mixed effects modelling to assess whether immune analyte concentrations change significantly based on cross-sectional data collection timepoints. IGFBP-1, IL-1β, IL-1ra and IL-8 concentrations undergo significant changes throughout fresh IVF cycles. q-values indicate adjusted p-values using the Benjamini-Hochberg procedure.

Immune analytes	p-value	q-value
GM-CSF	0.98	0.98
IFN-γ	0.90	0.98
IGFBP-1	**<0.0001**	**0.0001**
IL-1β	**0.001**	**0.01**
IL-1ra	**0.04**	0.16
IL-2	0.84	0.98
IL-4	0.96	0.98
IL-6	0.29	0.98
IL-8	**<0.0001**	**<0.0001**
IL-10	0.90	0.98
IL-11	0.48	0.98
IL-12 p70	0.63	0.98
IL-17a	0.92	0.98
IL-18	0.75	0.98
Leptin	0.47	0.98
LIF	0.87	0.98
TNF-α	0.62	0.98

Levels of the four analytes found to change across treatment stages are presented in Figure 3.6. Compared to the time of the coordination appointment, concentrations of IGFBP-1, increased at pituitary suppression before decreasing during ovarian stimulation, egg collection and embryo transfer. IL-1β concentrations were lowest during ovarian stimulation when E2 levels were high and P4 low. The concentrations were at a similar range for other stages of sample collection.

Concentrations of IL-1ra were comparable at the coordination appointment, during ovarian stimulation and at egg collection. Higher concentrations were observed for some patients at pituitary suppression and embryo transfer. During pituitary suppression, concentrations of IL-1ra appeared to be bimodally distributed with 6 patients exhibiting with high IL-1ra levels of whom 5 went on to have successful clinical outcomes. Concentrations of IL-8 were observed to increase from the coordination appointment to pituitary suppression in absence of E2. Increased E2 at ovarian stimulation coincided with a reduction in concentrations of IL-8. The concentrations of IL-8 then progressively increased as the treatment progressed.

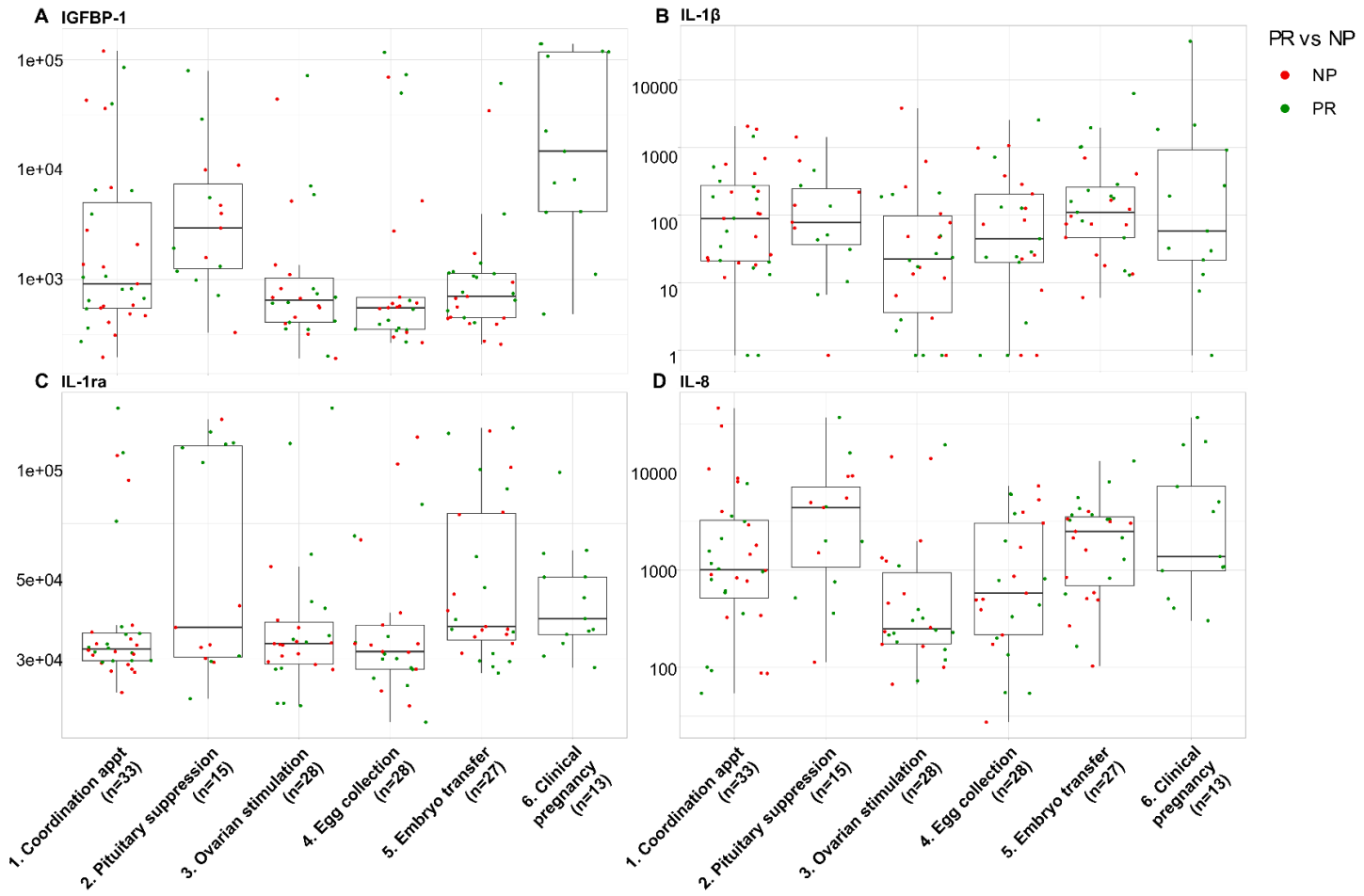


Figure 3.6: Longitudinal concentration of immune analytes across stages of sample collection. A) IGFBP-1 ($p<0.0001$, $q=0.0001$), B) IL-1β ($p=0.001$, $q=0.01$), C) IL-1ra ($p=0.04$, $q=0.16$), D) IL-8 ($p<0.0001$, $q<0.0001$) throughout fresh IVF cycles (concentrations measured in pg/mL). PR: pregnant, NP: not pregnant.

3.5 Relationships between immune analytes and hormones across fresh IVF cycles

Given that the concentration of some CVF immune analytes appeared to change across treatment cycles in concert with the manipulation of hormonal levels in these patients, a direct assessment of the relationship between cytokines and circulating E2 and P4 was next performed using all available samples, regardless of the stage of sample collection. An inverse correlation between levels of E2 and IGFBP-1 ($p<0.0001$), IL-1ra ($p=0.04$), IL-6 ($p=0.005$), IL-8 ($p=0.001$), IL-18 ($p=0.04$), LIF ($p=0.03$), and TNF-α ($p=0.02$) was observed (see Figure 3.7). However, no significant relationships were detected between immune analytes and P4 levels.

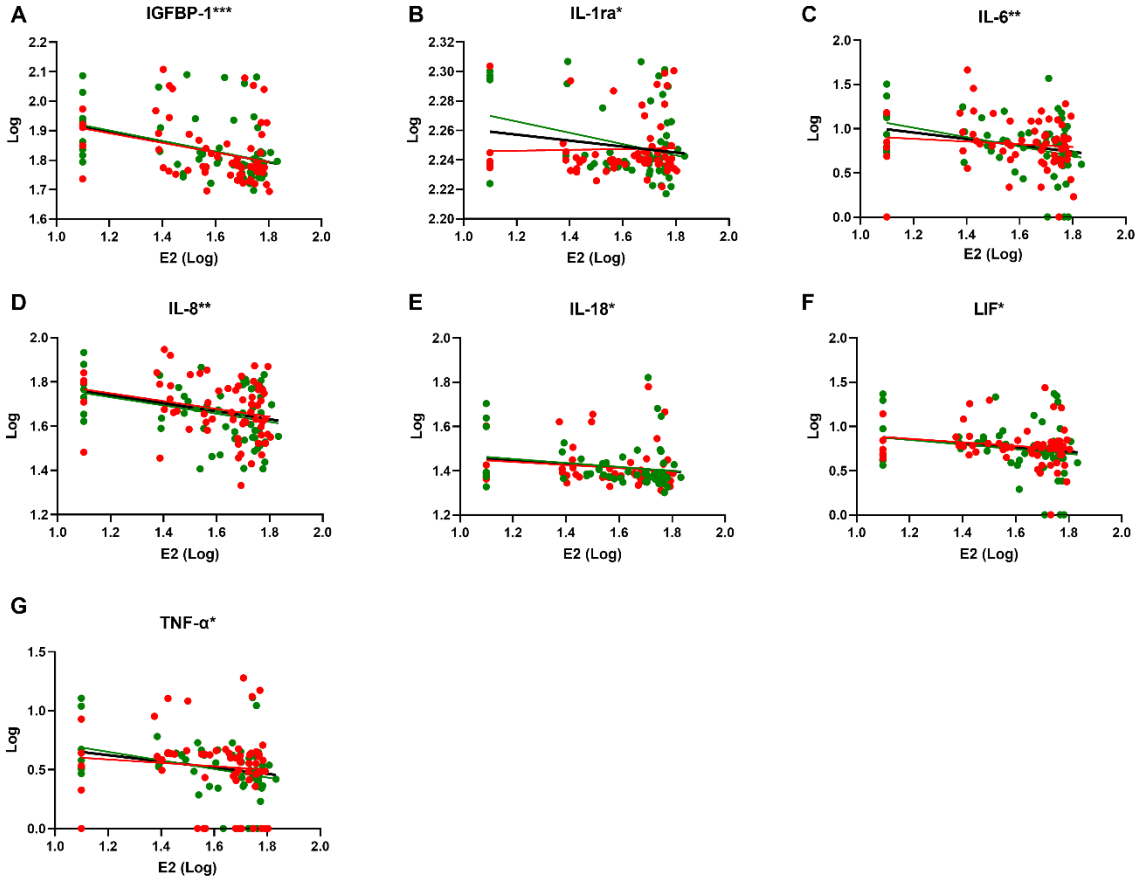


Figure 3.7: Linear regression between immune analytes and E2. A) IGFBP-1 ($p<0.0001$), B) IL-1ra ($p=0.04$), C) IL-6 ($p=0.005$), D) IL-8 ($p=0.001$), E) IL-18 ($p=0.04$), F) LIF ($p=0.03$), and G) TNF-α ($p=0.02$) for all available samples (n=128). (●) Red dots indicate unsuccessful outcomes, (●) green dots indicate successful outcomes. Three regression lines are presented on each plot; the black line indicates the average linear regression for all samples, the green (successful clinical pregnancy) and red lines (unsuccessful outcome) represent the relationship in respect to the outcome of the treatment cycle. The reported statistical significance is for the average linear regression for all samples.

3.5.1 Cross sectional analysis of immune analyte and hormone relationships at different clinical stages

Further assessment of the relationship between immune analytes and hormones was performed within each of the 5 stages of sample collection. For these analyses, only those analytes found to have a significant relationship with either E2 or P4 are presented.

3.5.1.1. Coordination appointment

For samples collected at the coordination appointment, IGFBP-1 (p=0.002), IL-1β (p=0.02), IL-6 (p=0.002), IL-8 (p=0.01), and LIF (p=0.01) were found to be negatively correlated with E2 (Figure 3.8). In samples with subsequent successful clinical outcome, a similar relationship was observed for IL-1β (p=0.01) IL-6 (p=0.002), and IL-8 (p=0.01). For samples with unsuccessful outcomes, a negative correlation between E2 was only observed for IGFBP-1 (p=0.03). No relationship between P4 levels and any of the CVF immune analytes was identified at this stage of sample collection.

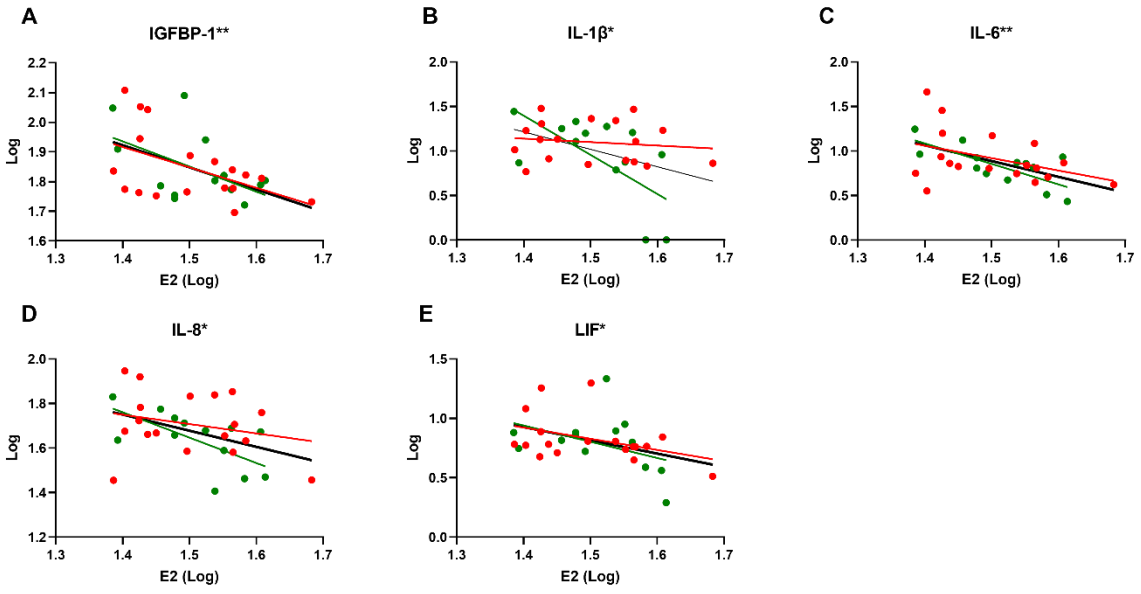


Figure 3.8: CVF immune analytes significantly correlated with serum E2 at the time of coordination appointment. Linear regression identified a significant negative correlation between E2 and A) IGFBP-1 (p=0.002), B) IL-1β (p=0.02), C) IL-6 (p=0.002), D) IL-8 (p=0.01), and E) LIF (p=0.01), (n=32). The reported statistical significance is for the average linear regression for all samples (black line). (●) Red dots and lines indicate unsuccessful outcomes, (●) green dots and lines indicate successful outcomes.

3.5.1.2. Pituitary suppression

At the time of pituitary suppression when levels of E2 and P4 were suppressed, no associations between any of the studied immune analytes and hormones were identified.

3.5.1.3. Ovarian stimulation

In samples collected at the time of ovarian stimulation where serum levels of E2 and P4 were significantly increased, an inverse relationship between IFN-γ (p=0.04) and IL-1β (p=0.04) with E2 was observed (Figure 3.9). IFN-γ was also significantly inversely correlated with E2 in patients who subsequently had successful outcomes (p=0.01) but not for patients with unsuccessful outcomes (p=0.91). CVF levels of IL-1β were inversely correlated with E2 (p=0.04) and a similar trend was observed when sub-analyses were performed in patients with successful (p=0.06) and unsuccessful (p=0.33) outcomes. No significant relationship between CVF immune analytes and P4 levels was observed at this stage of sample collection.

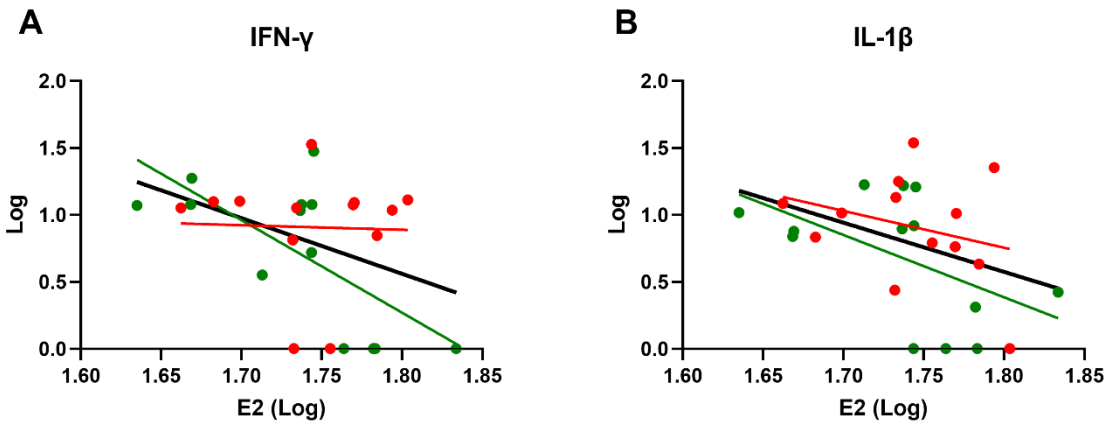


Figure 3.9: Linear regression between immune analytes and E2 throughout ovarian stimulation. Linear regression identified a significant negative correlation between E2 and A) IFN-γ (p=0.04), and B) IL-1β (p=0.04), (n=26). The reported statistical significance is for the average linear regression for all samples (black line). (●) Red dots and lines indicate unsuccessful outcomes, (●) green dots and lines indicate successful outcomes.

3.5.1.4. Egg collection

In samples collected at egg collection where P4 levels had continued to increase no significant relationship between any of the studied immune analytes and E2 or P4 levels were observed.

3.5.1.5. Embryo transfer

Similarly, no significant correlations between the immune analytes and E2 or P4 levels were observed at the time of embryo transfer however there was a trend towards a positive relationship between IL-1ra and E2 (p=0.07).

A summary of the relationships between the immune analytes and E2 for all available data and at each stage of sample collection throughout fresh IVF cycles is provided in Table 3.4. Analysis of all available samples identified inverse relationships between IGFBP-1, IL-1ra, IL-6, IL-8, IL-18 and LIF. These relationships were also observed for IGFBP-1, IL-6, IL-8 and LIF for samples collected at coordination appointment. Furthermore, IL-1β also had an inverse correlation with E2 for samples collected at coordination appointment. No significant relationships were maintained throughout pituitary suppression. The inverse relationship observed between IL-1β and E2 was also observed for samples collected throughout ovarian stimulation as well as IFN-γ. For samples collected on the day of egg collection, no significant correlations between any of the studied immune analytes and E2 were observed. For samples collected prior to embryo transfer, IL-1ra trended towards a positive correlation with E2. No other significant associations were observed on the day of embryo transfer.

Table 3.4: Overview of the relationship between immune analytes and E2. Significant inverse relationships are noted using 'inverse' for each immune analyte where applicable. Negative but non-significant slopes are indicated using light amber and positive but non-significant slopes are indicated using light grey.

				Relationship with E2		
Cytokines	All samples (n=128)	1. Coordination appt (n=32)	2. Pituitary suppression (n=15)	3. Ovarian stimualtion (n=27)	4. Egg collection (n=24)	5. Embryo transfer (n=27)
IFN-γ				inverse		
IGFBP-1	inverse	inverse				
IL-1β		inverse		inverse		
IL-1ra	inverse					
IL-6	inverse	inverse				
IL-8	inverse	inverse				
IL-18	inverse					
LIF	inverse	inverse				
TNF-α	inverse					

3.5.2 Paired analyses of hormone and immune analyte relationships at different clinical stages of IVF treatment

For a subset of the patient cohort, longitudinal sampling was performed across successive sample collection stages. This provided an opportunity to further examine within patient changes in serum hormones and immune analytes using paired analyses.

3.5.2.1 Coordination appointment to pituitary suppression

A total of 15 patients had hormonal and CVF immune analyte data available at both coordination appointment and at the time of pituitary suppression. Changes in concentration of serum hormones and immune analytes from the hormonally unregulated state were assessed at coordination appointment to pituitary suppression (Figure 3.10). On average, E2 concentrations were reduced by 16-fold (393.6 pmol/L ± 293.8 v 24.5 pmol/mL ± 32.5) and P4 concentrations by 23-fold (17.8 nmol/L ± 19.0 v 0.7 nmol/mL ± 0.4) based on untransformed serum concentrations (Table 3.1). While the pituitary suppression protocols for IVF resulted in a systemic suppression of E2 in all patients, P4 levels were not suppressed in 3/15 patients. For 1 patient whose eventual treatment outcome was unsuccessful, P4 levels increased between these stages whereas for 2 patients, P4 levels remained in the same low range (eventual treatment outcome was successful in both cycles).

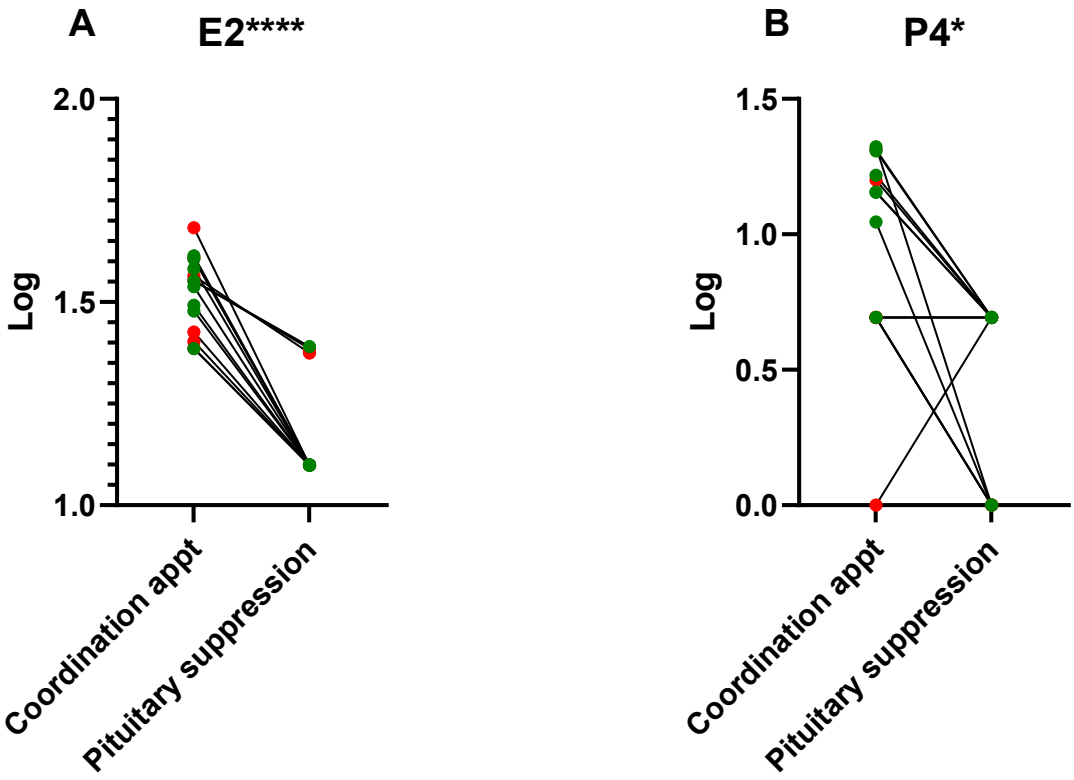


Figure 3.10: Within patient hormone level changes from coordination appointment to pituitary suppression. Hormonal concentrations are presented on a natural logarithmic scale. Concentration of A) E2 ($p<0.0001$), were reduced for all 15 patients throughout pituitary suppression. Suppression of serum hormones for B) P4 ($p=0.02$) were not uniformly decreased for all 14 patients for which data was available. Pairwise Wilcoxon signed rank tests (●) Red dots indicate unsuccessful outcomes, (●) green dots indicate successful outcomes.

Examination of CVF immune analytes across these stages indicated that IL-1ra was the only analyte that significantly changed following pituitary suppression with a significant increase in concentration observed (Figure 3.11). This increase was particularly evident in 5/15 patients with levels of the IL-1ra remaining similar across the two stages for the remaining patients.

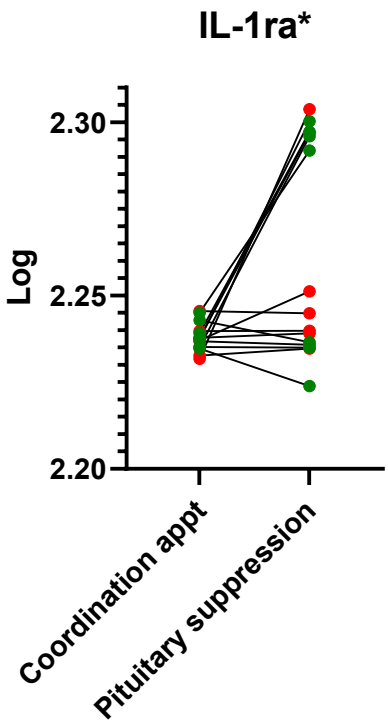


Figure 3.11: Within patient IL-1ra concentration changes from coordination appointment to pituitary suppression. IL-1ra concentrations are presented on a natural logarithmic scale. IL-1ra concentrations on average increased from a hormonally unregulated state throughout pituitary suppression for 15 patients (31754 pg/mL ± 2899 v 69491 pg/mL ± 45457). Pairwise Wilcoxon signed rank test (p=0.01). (●) Red dots indicate unsuccessful outcomes, (●) green dots indicate successful outcomes.

3.5.2.2 Pituitary suppression to ovarian stimulation

A total of 12 patients had serum sampling collected sequentially at both pituitary suppression and during ovarian stimulation. Ovarian stimulation was associated with an average 246-fold increase for E2 compared with levels observed at pituitary suppression (24.5 pmol/L ± 32.5 v 6031.9 pmol/mL ± 3606.2) and patient level analyses indicated a major rise in E2 for all 12 patients. An average 3-fold increase for P4 was observed across the two timepoints (0.7 nmol/L ± 0.3 v 2.3 nmol/mL ± 3.7), however the patient level response was variable. Four patients have a major increase in P4 levels during ovarian stimulation whereas for the remaining 8 patients, a minor increase was observed. The level of P4 increase did not associate with subsequent clinical success of the IVF cycle treatment (Figure 3.12).

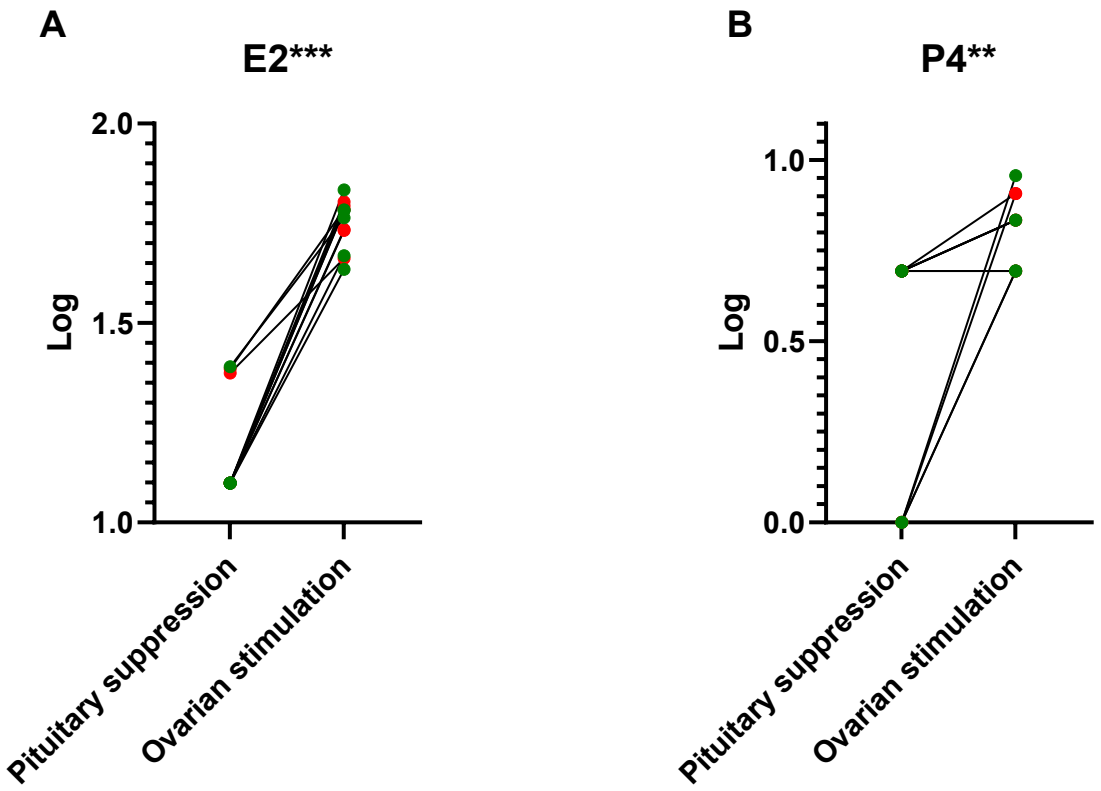


Figure 3.12: Within patient E2 and P4 changes from pituitary suppression to ovarian stimulation. Hormone concentrations are presented on a natural logarithmic scale. Concentrations of A) E2 ($p<0.0001$) increased for all 12 patients in this analysis. Concentrations of B) P4 ($p=0.04$), also increased for the same 12 patients in the transition from pituitary suppression to ovarian stimulation. Pairwise Wilcoxon signed rank tests. (●) Red dots indicate unsuccessful outcomes, (●) green dots indicate successful outcomes. Note: data points for some sample collection timepoints are overlapping.

CVF samples were collected sequentially across pituitary suppression and ovarian stimulation for n=13 women. A significant reduction in IL-1ra was observed (72272 pg/mL ± 46062 v 41680 pg/mL ± 32870, p=0.02) and a trend decrease in IL-4, IL-1β, IL-6, IL-8, and TNF-α, and IGFBP-1 was also observed from pituitary suppression to ovarian stimulation (Figure 3.13).

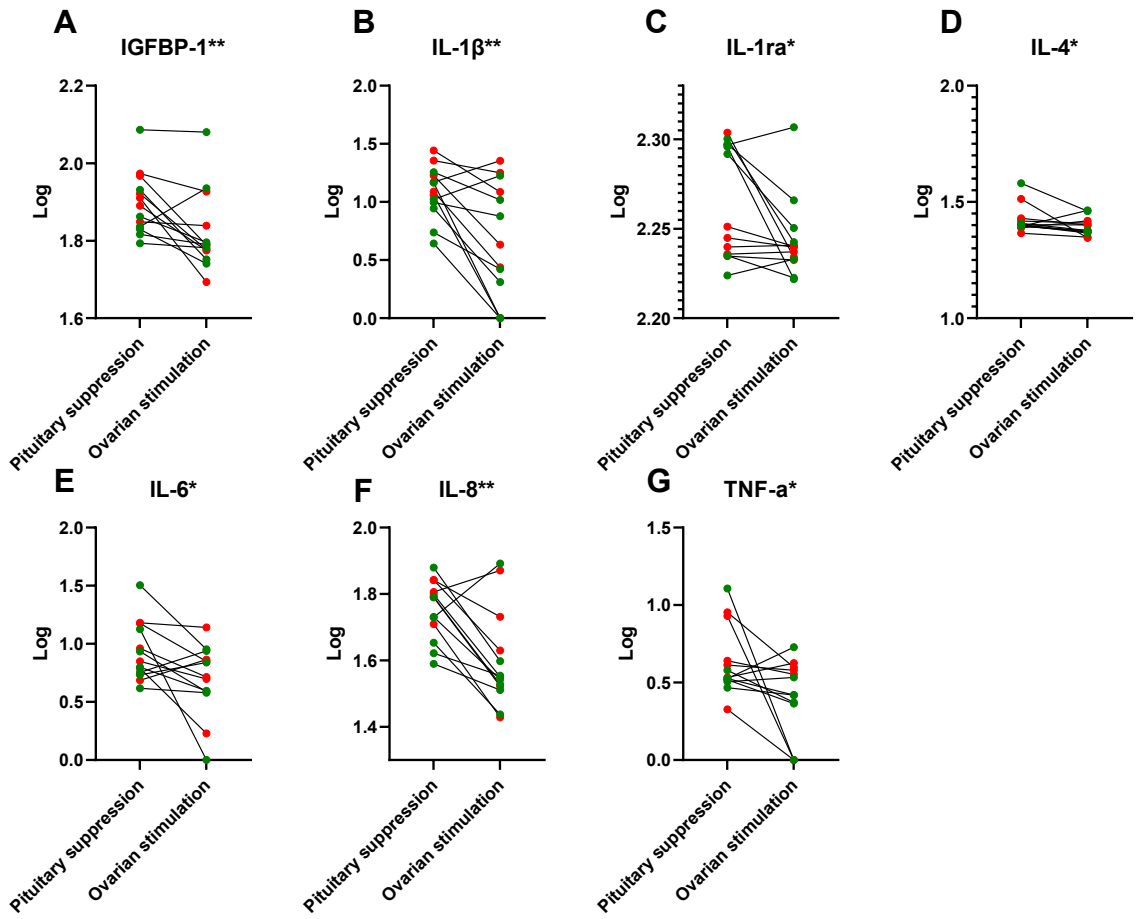


Figure 3.13: Within patient Immune analyte concentration changes from pituitary suppression to ovarian stimulation. Immune analytes are presented on a natural logarithmic scale. During the transition from pituitary suppression to ovarian stimulation, concentration of 7 immune analytes were significantly reduced for n=13 patients with sequential samples available at both time points. A) IGFBP-1 (9649 pg/mL ± 21260 v 6841 pg/mL ± 19565, p=0.006, n=13), B) IL-1β (240 pg/mL ± 395 v 97 pg/mL ± 180, p=0.004, n=13), C) IL-1ra (72272 pg/mL ± 46062 v 41680 pg/mL ± 32870, p=0.02, n=13), D) IL-4 (112 pg/mL ± 109 v 71 pg/mL ± 28, p=0.04, n=13), E) IL-6 (61 pg/mL ± 182 v 5.1 pg/mL ± 7.3, p=0.02, n=13), F) IL-8 (4673 pg/mL ± 4524 v 2891 pg/mL ± 6216, p=0.003, n=13), and G) TNF-α (17.7 pg/mL ± 29 v 4.4 pg/mL ± 3.1, p=0.02, n=13). Pairwise Wilcoxon singed rank tests. (●) Red dots indicate unsuccessful outcomes, (●) green dots indicate successful outcomes.

3.5.2.3 Ovarian stimulation to egg collection

While the transition from ovarian stimulation to egg collection did not correspond to a change in serum E2 concentrations, a major (average 14-fold) and consistent increase in serum P4 concentrations were observed in paired samples collected from n=22 women (Figure 3.14).

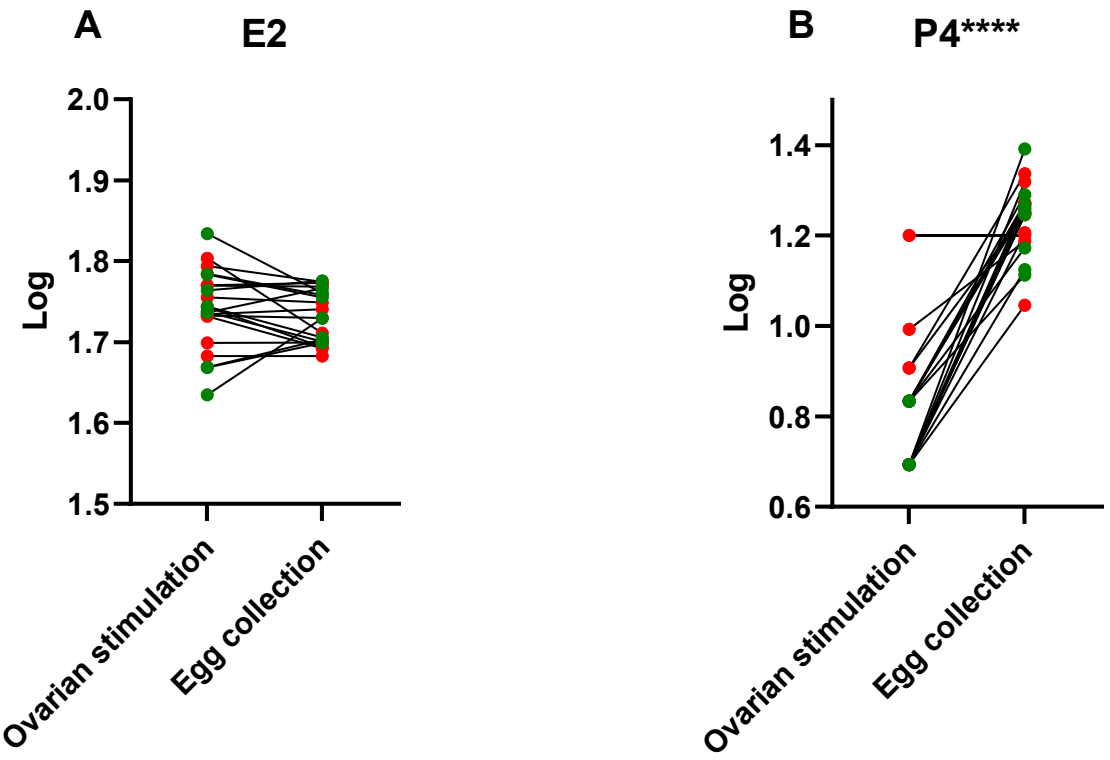


Figure 3.14: Within patient E2 and P4 changes from ovarian stimulation to egg collection. Hormone concentrations are presented on a natural logarithmic scale. Concentration of A) E2 ($p=0.23$, $n=22$) did not significantly change during this transition. Concentration of B) P4 ($p<0.0001$, $n=22$) increased significantly. Pairwise Wilcoxon signed rank tests. (●) Red dots indicate unsuccessful outcomes, (●) green dots indicate successful outcomes.

No significant changes in the concentration of CVF immune analytes were observed between the transition from ovarian stimulation to egg collection.

3.5.2.4 Egg collection to embryo transfer

A total of 24 women had sequential serum hormone levels and CVF analyte data available. Consistent with continuation of P4 support in IVF protocols, the concentration of serum P4 increased further from egg collection to embryo transfer (33.3 pmol/mL ± 20 v 425 pmol/mL ± 184). This increase was observed in 23 out of 24 patient treatment cycles (see Figure 3.15). E2 levels did not significantly change within the same time span (Figure 3.15).

.

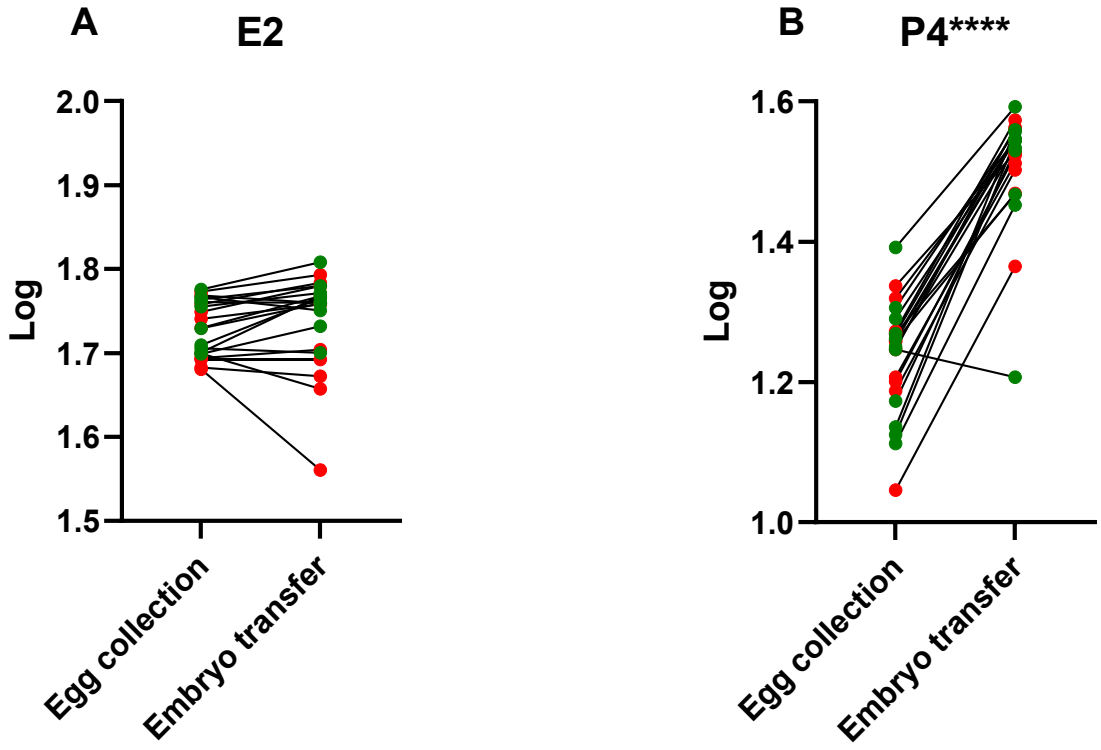


Figure 3.15: Within patient E2 and P4 changes from egg collection to embryo transfer. Hormone concentrations are presented on a natural logarithmic scale. Concentration of A) E2 ($p=0.06$, $n=24$) did not significantly change during this transition. Concentration of B) P4 ($p<0.0001$, $n=24$) increased significantly. Pairwise Wilcoxon signed rank tests. (●) Red dots indicate unsuccessful outcomes, (●) green dots indicate successful outcomes.

CVF samples were collected sequentially across egg collection to embryo transfer for n=24 women. A significant increase in IL-1β (273 pmol/mL ± 572 v 523 pmol/mL ± 1311), IL-1ra (41471 pmol/mL ± 26278 v 57803 pmol/mL ± 34944) and IL-8 (1858 pmol/mL ± 2279 v 2895 pmol/mL ± 2933) were observed (Figure 3.16).

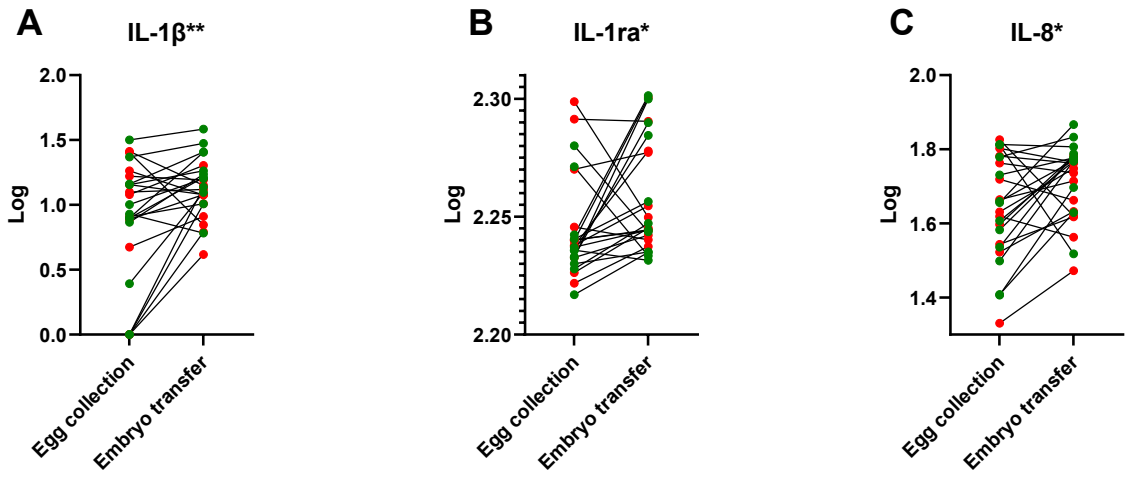


Figure 3.16: Within patient Immune analyte concentration changes from egg collection to embryo transfer. Immune analyte concentrations are presented on a natural logarithmic scale. During the transition from egg collection to embryo transfer, concentration of 3 immune analytes were significantly increased for n=24 patients with sequential samples available at both time points. A) IL-1β (273 pg/mL ± 572 v 523 pg/mL ± 1311, p=0.006), B) IL-1ra (41471 pg/mL ± 26278 v 57803 pg/mL ± 34944, p=0.01), and C) IL-8 (1858 pg/mL ± 2279 v 2895 pg/mL ± 2933, p=0.01). Pairwise Wilcoxon signed rank tests. (●) Red dots indicate unsuccessful outcomes, (●) green dots indicate successful outcomes.

3.6 The relationship between immune analytes and clinical outcomes

To examine potential relationships between CVF immune analyte levels at each stage of sample collection with subsequent clinical outcomes, 2 main approaches were used. Firstly, concentrations of immune analytes were compared between successful and unsuccessful clinical outcomes at each sampling stage. Secondly, the differences of regression slopes between immune analytes and serum hormones for patients with respect to clinical outcomes were compared.

At coordination, pituitary suppression, ovarian stimulation and egg collection, no differences in mean concentrations of any assessed CVF analyte were detected between women who went on to experience a successful IVF treatment outcome compared to those who had an unsuccessful outcome (Table 3.5).

Table 3.5: Cross-sectional immune analyte concentration changes according to treatment outcomes. Concentrations of immune analytes were compared cross-sectionally using non-parametric Mann-Whitney tests. Differences in concentrations of immune analytes based on clinical outcomes were only observed at the time of embryo transfer. IGFBP-1, IL-1β and IL-8 concentrations are higher in samples with successful embryo implantation.

Analytes	1. Coordination appointment (n=33)	2. Pituitary suppression (n=15)	3. Ovarian stimulation (n=28)	4. Egg collection (n=28)	5. Embryo transfer (n=27)
GM-CSF	0.47	0.57	0.38	0.86	0.90
IFN-γ	0.51	0.96	0.67	0.82	0.29
IGFBP-1	0.62	0.55	0.98	0.65	**0.02***
IL-1β	0.56	0.77	0.42	0.49	**0.03***
IL-1ra	0.39	0.88	0.98	0.25	0.36
IL-2	0.72	0.46	0.33	0.73	0.95
IL-4	0.62	0.77	0.73	0.43	0.60
IL-6	0.34	0.94	0.18	0.44	0.19
IL-8	0.21	0.46	0.22	0.65	**0.04***
IL-10	0.28	0.17	0.47	0.99	0.21
IL-11	0.31	0.50	0.46	0.93	0.86
IL-12p70	0.95	0.13	0.66	0.47	0.85
IL-17a	0.20	0.77	0.82	0.82	0.53
IL-18	0.54	0.94	0.88	0.62	0.36
Leptin	0.64	0.44	0.55	0.24	0.40
LIF	0.89	0.94	0.88	0.41	0.55
TNF-α	0.85	0.49	0.41	0.56	0.77

At the time of embryo transfer, the mean concentration of IGFBP-1 (p=0.02, Mann-Whitney T-test), IL-1β (p=0.03) and IL-8 (p=0.04) were significantly higher in patients with successful clinical outcomes, however, significance did not withstand correction for multiple testing (q>0.05, Benjamini-Hochberg) (Figure 3.17).

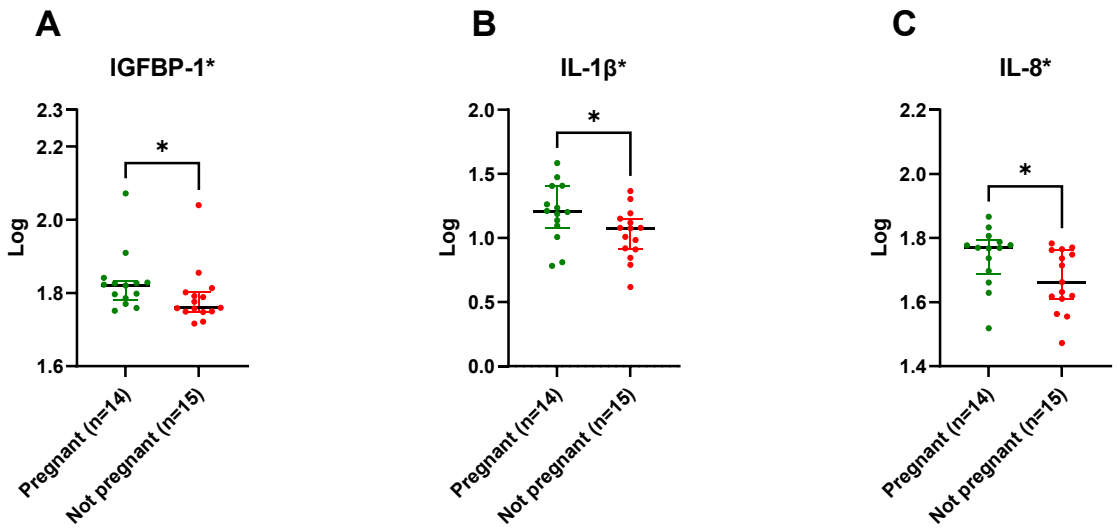


Figure 3.17: Comparison of immune analyte concentrations from samples collected on the day of embryo transfer with respect to clinical outcomes. Concentration of three immune analytes were significantly higher for patients with successful treatment outcomes. Immune analyte concentrations are presented on a natural logarithmic scale. Using Mann-Whitney T-tests, concentration of A) IGFBP-1 (p=0.02), B) IL-1β (p=0.03), and C) IL-8 (p=0.01) were significantly higher for women with successful clinical outcomes.

Regression analysis of all available data for serum E2 and P4 levels with immune analyte data (n=128) only identified a significant relationship between IL-1ra and E2 with respect to clinical outcomes (p=0.03) (See Table 3.6). When similar regression analyses were performed at each sampling timepoint, a significant difference in slopes between clinical outcome groups was identified at the coordination appointment between IL-1β and E2 (p=0.01). The differences in the relationship between IL-1β and E2 in successful and unsuccessful clinical outcome is presented in Figure 3.18 where a negative correlation is observed only in women experiencing a successful outcome.

Table 3.6: The relationship between immune analytes and E2 with respect to clinical outcomes. Based on all available data, a significant difference in slopes between clinical outcome groups was observed between IL-1ra and E2 (p=0.03). At coordination appointment timepoint, a significant difference in slopes between clinical outcome groups was identified between IL-1β and E2 (p=0.01). Significant relationships (p<0.05) are noted using green colour. Light blue colour represents p-values between 0.05 and 0.09.

	Immune analytes relationship with E2: slope comparison between successful and unsuccessful outcomes					
analytes	All samples (n=128)	1. Coordination appt (n=32)	2. Pituitary suppression (n=15)	3. Ovarian stimualtion (n=27)	4. Egg collection (n=24)	5. Embryo transfer (n=27)
GM-CSF	0.42	0.6	0.67	0.73	0.81	0.92
IFN-γ	0.07	0.84	0.46	0.09	0.07	0.98
IGFBP-1	0.86	0.74	0.36	0.14	0.74	0.55
IL-1β	0.5	**0.01**	0.11	0.6	0.24	0.1
IL-1ra	**0.03**	0.21	0.52	0.87	0.42	0.86
IL-2	0.58	0.39	0.92	0.66	0.9	0.37
IL-4	0.27	0.31	0.72	0.76	0.51	0.78
IL-6	0.14	0.41	0.12	0.41	0.5	0.46
IL-8	0.93	0.23	0.14	0.45	0.63	0.29
IL-10	0.26	0.16	0.68	0.68	0.27	0.47
IL-11	0.85	0.91	0.6	0.87	0.68	0.39
IL-12 p70	0.98	0.63	0.85	0.95	0.36	0.83
IL-17a	0.84	0.55	0.63	0.19	0.64	0.69
IL-18	0.8	0.46	0.38	0.77	0.44	0.55
Leptin	0.61	0.58	0.69	0.98	0.71	0.44
LIF	0.78	0.66	0.91	0.32	0.97	0.71
TNF-α	0.35	0.68	0.29	0.16	0.09	0.84

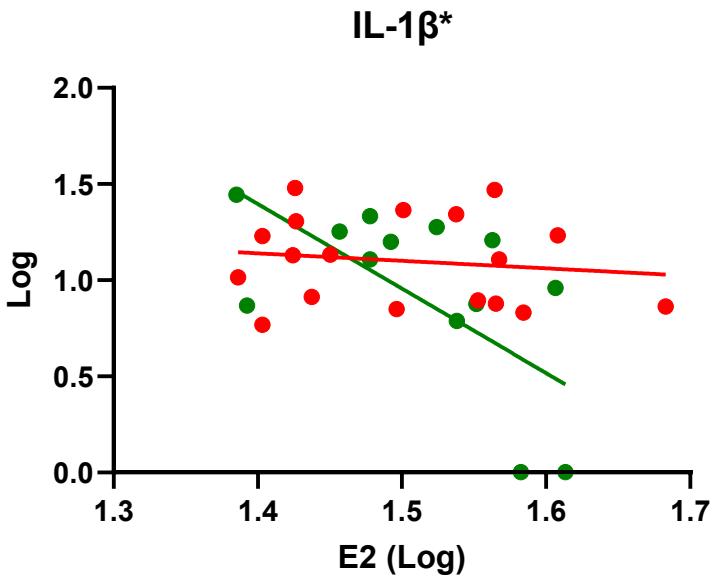


Figure 3.18: Comparison of regression slopes between successful and unsuccessful outcomes for IL-1β and E2 at the coordination appointment timepoint. A significant difference in slopes between clinical outcome groups was observed between IL-1β and E2 using linear regression modelling (n=32, p=0.01). (●) Red dots and lines indicate unsuccessful outcomes, (●) green dots and lines indicate successful outcomes.

Using all available data (n=128) for CVF cytokines and P4, a significant difference in the relationship between IL-1ra and P4 in the different outcome groups was observed (p=0.04) (Table 3.7). However, no differences in the interrelationships between immune analytes and P4 levels of women with successful or unsuccessful treatment outcomes was observed within any of the specific sampling timepoints.

Table 3.7: The relationship between immune analytes and P4 with respect to clinical outcomes. Based on all available data, a significant difference in slopes between clinical outcome groups was observed between IL-1ra and P4. (p=0.04). No differences in slopes between clinical outcome groups were observed for any of the immune analytes at specific sampling timepoints.

	Immune analytes relationship with P4: slope comparison between successful and unsuccessful outcomes					
analytes	All samples	1. Coordination appt (b=33)	2. Pituitary suppression (n=15)	3. Ovarian stimualtion (n=26)	4. Egg collection (n=25)	5. Embryo transfer (n=32)
GM-CSF	0.37	0.41	0.45	0.11	0.64	0.45
IFN-γ	0.07	0.17	0.37	0.08	0.42	0.67
IGFBP-1	0.93	0.81	0.58	0.27	0.27	0.81
IL-1β	0.56	0.3	0.23	0.88	0.15	0.94
IL-1ra	**0.04**	0.89	0.63	0.11	0.93	0.31
IL-2	0.42	0.93	0.18	0.13	0.52	0.53
IL-4	0.27	0.65	0.46	0.09	0.56	0.69
IL-6	0.92	0.35	0.87	0.76	0.4	0.59
IL-8	0.35	0.36	0.8	0.35	0.15	0.88
IL-10	0.71	0.73	0.17	0.61	0.66	0.5
IL-11	0.61	0.72	0.31	0.08	0.08	0.96
IL-12 p70	0.81	0.48	0.25	0.14	0.23	0.9
IL-17a	0.71	0.25	0.39	0.15	0.82	0.62
IL-18	0.71	0.19	0.65	0.14	0.19	0.53
Leptin	0.71	0.45	0.4	0.79	0.86	0.56
LIF	0.78	0.98	0.39	0.059	0.97	0.62
TNF-α	0.36	0.21	0.82	0.24	0.79	0.68

3.7 Metataxonomic characterisation of vaginal bacteria during IVF

Although the focus of the analyses described in this chapter are primarily directed toward samples collected from women undergoing fresh IVF cycles, metaxonomic characterisation of the vaginal microbiota was initially conducted on samples collected from both the ART1 cohort (predominantly fresh cycles, n=40), and ART2 cohort (exclusively frozen IVF cycles, n=91) to ensure data processing was consistent across cohorts enabling later downstream comparison of resulting data.

In total, 11,967,926 sequence reads were generated from all available vaginal samples (n=460) analysed in these studies. These were derived from 3,209 distinct ASVs which could be mapped to a total of 295 bacterial species. Due to the large number of samples analysed, the sequence data had to be generated across 2 different Illumina Miseq sequencing runs. To assess any possible run-to-run bias, 5 samples from ART1 (run 1) were re-sequenced with samples from the ART2 cohort (run 2). In run 1, 53 species were detected in these 5 samples compared with 23 in run 2 indicating that there were more rare taxa detected in run 1. Consistent with this, there were also more sequences generated per sample for run 1 (mean = 27,018) than run 2 (mean = 15,861) for these 5 samples indicating a slight difference in sequencing depth. Despite this, compositional structures of the 5 samples where highly similar between the 2 runs (see Figure 3.19).

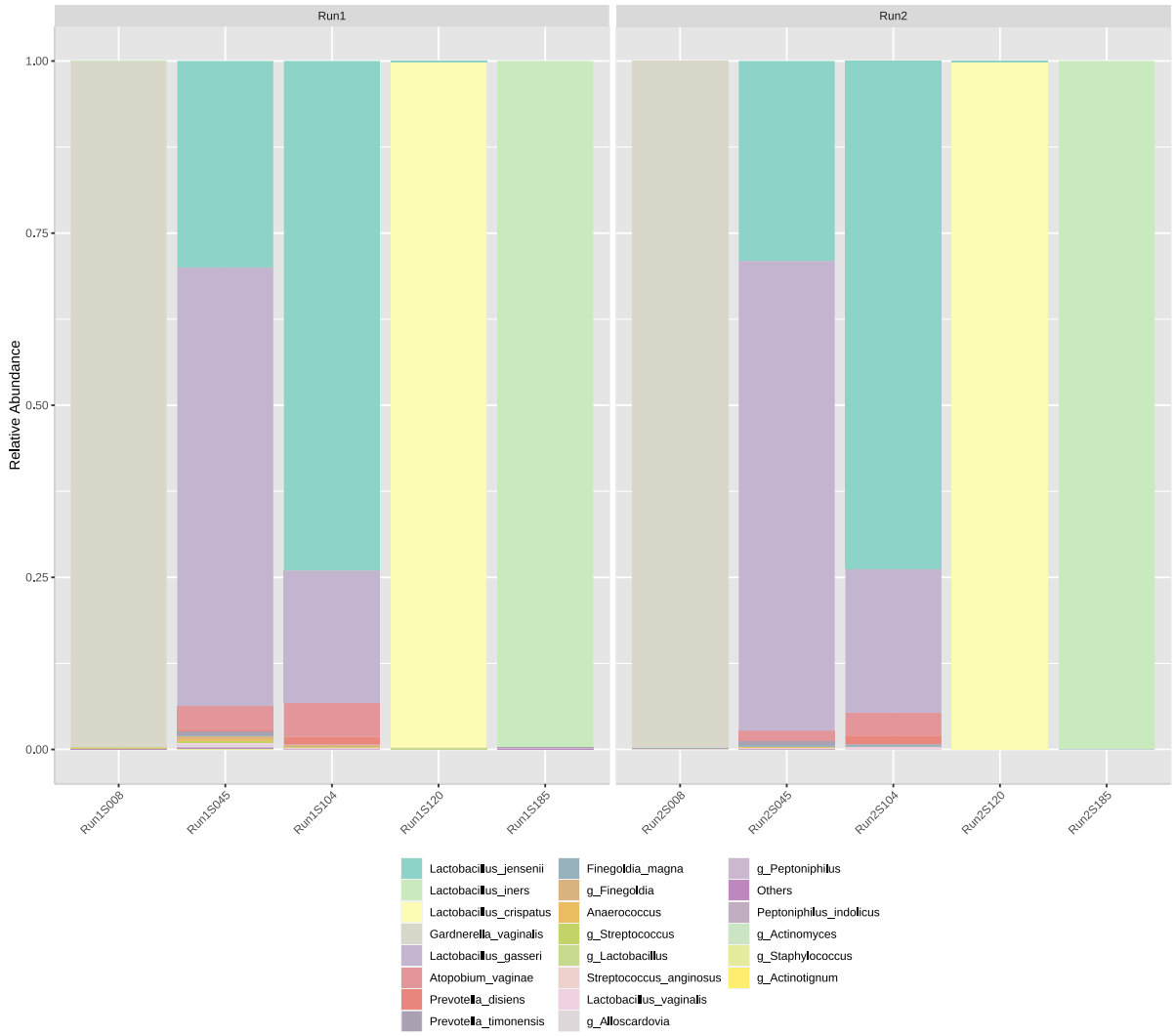


Figure 3.19: Assessment of run-to-run sequencing variation in vaginal microbiota profiles.

Different batches of consumables and kits can contribute to run-to-run variation of rare taxa that are largely derived from environmental sources and/or differences in sequencing depth. To account for this, rare taxa detected in only one or the other sequencing run were excluded from the data set. In total, 2 031 ASVs that were only detected in run 2 (corresponding to 133 species) and 792 in run 1 (corresponding to 35 species) where removed from the dataset (see Figure 3.20). Although a large number of ASVs, this corresponded to only 2.4% of all sequencing reads from the dataset and consisted of rare and low abundance species, many of which were recognised as environmental and kit contaminants. Therefore, subsequent downstream analyses consisted for 386 ASVs corresponding to127 species.



Figure 3.20: Venn diagram describing the number of species detected in each run. A total of 35 species only detected in run 1 and 133 species only detected in run 2 were excluded from the downstream analyses. The analyses consisted of a total of 127 species detected in both runs.

Several patients made repeat clinical visits within a short time window which led to them being sampled twice. In total 3 patients provided repeated vaginal swab sample from ART1 (all for frozen cycles a pituitary suppression) and 29 from ART2 (2 at coordination appointment, 10 at pituitary suppression, and 17 clinical pregnancy). For data exploration and assignment of vaginal microbiota profile community state types, these repeat sample collections were included. However, for comparative analyses, only one sample per patient, per timepoint was included. For the repeated samples from coordination appointed, the second samples were consistently used as it would temporally be closer to the beginning of IVF treatment. For repeated samples collected during pituitary suppression, the second sample collected at a time when the endometrium was deemed suitable for treatment to proceed was therefore more reflective of suitably prepared endometrium was consistently used.

3.7.1 Microbiota characterisation and data exploration

After removal of rare taxa associated with run-to-run variation, there was a total of 10,460,027 sequence reads included in the dataset, with run 1 accounting for 5,699,615 and run 2 accounting for 4,760,412 sequence reads. Data was then imported to Microbiome Analyst (ver 2.0) (508) for further processing and analyses. A total of 6 samples were excluded from analysis due to low sequence read counts (<1000 reads). A further 22 ASVs with <2 counts across the total data set were eliminated. Thus, the final dataset used for analyses consistent of 364 ASVs.

3.7.2 Vaginal microbiome composition

To begin, each sample was initially classified into microbiota profile based on the highest relative abundance of dominant species (509, 510). There were 24 taxa identified that accounted for at least 30% relative abundance of all species identified in any given sample (Figure 3.21). Of these *L. crispatus* dominance was the most prevalent (n=152), followed by *L. iners* (n=89) and *G. vaginalis* (n=62). There were 4 taxa-types classified at genera level as their corresponding sequences could not be confidently assigned to species level: *Bifidobacterium* (n=4), *Lactobacillus* (n=3), *Klebsiella* (n=2), and *Corynebacterium* (n=1). For 3 patients, Enterobacteriaceae (family) was the highest taxonomic resolution that could be achieved. For 2 samples, relative abundance of the top taxa did not reach 30%, these samples were classed as 'other'. The most abundant feature for sample ART2S211 was *Corynebacterium* (genera) with 27% abundance and the most abundant feature for sample ART2S289 was *Corynebacterium sundsvallense* with 22% abundance.

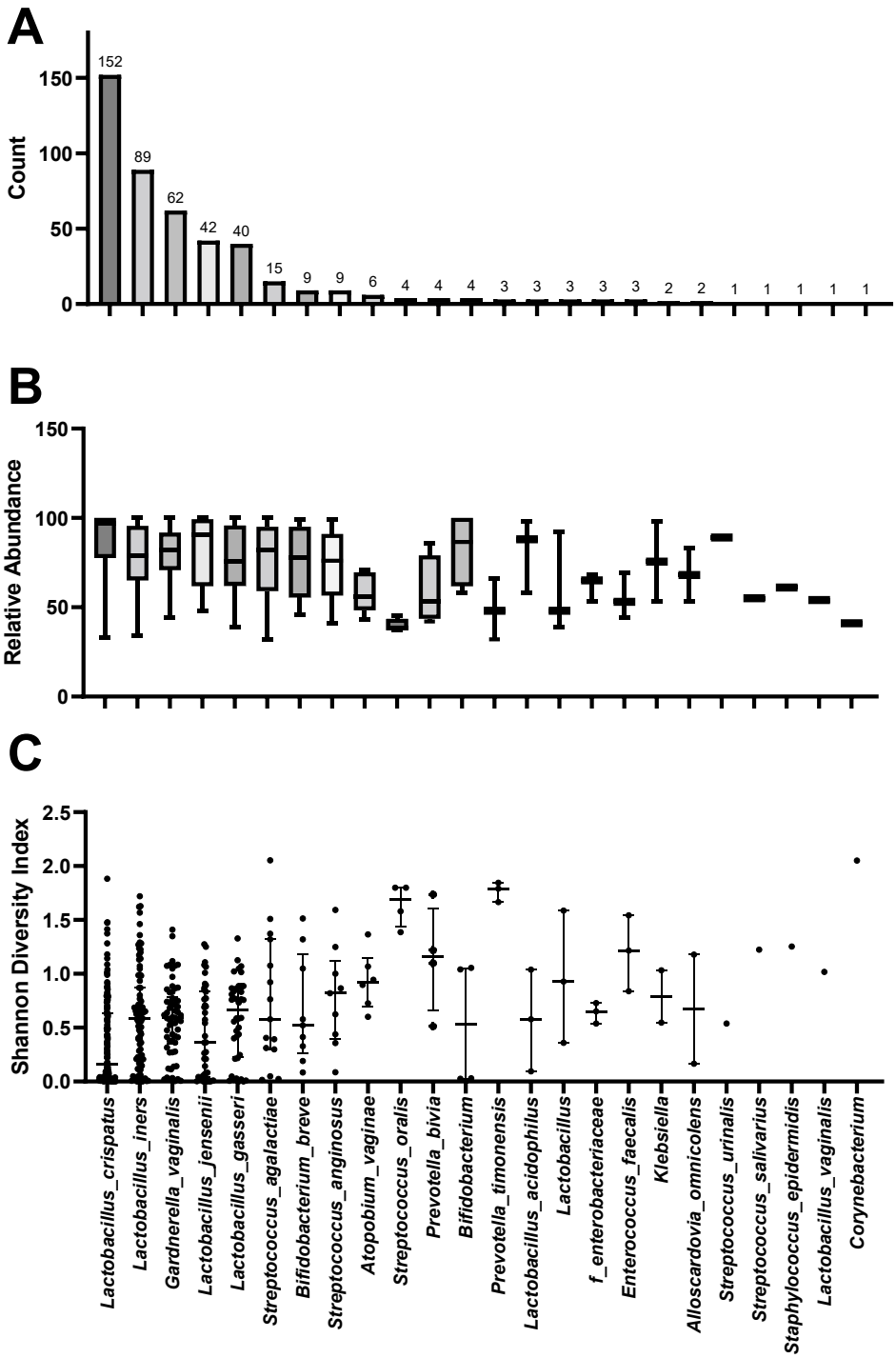


Figure 3.21: Vaginal microbiome compositions. A) Bar charts demonstrating the number of samples within each dominant species group, B) Plots representing the relative abundance of species, whiskers representing minimum and maximum, and C) Shannon diversity index of each dominant species group with bounds of the box representing interquartile ranges, centre line median.

3.7.2.1 Co-occurrence relationships of the most abundant vaginal taxa

A prevalence filter of 25% was applied to the data to identify the most abundant and frequently observed taxa across samples in the dataset. This resulted in the identification of 12 taxa that were identified in at least 25% of all samples assessed. These included *L. crispatus*, *L. gasseri*, *L. iners* and *L. jensenii, G. vaginalis*, *S. anginosus*, *P. bivia*, *P. timonensis*, *L. vaginalis*, *F. magna*, *P. indolicus* and *D. micraerophilus*. Subsequent analyses including the relationship between microbiota and hormones, microbiota and immune analytes and univariate relationships between bacteria and outcome were performed using these 12 species.

Examination of co-occurrence between these species was performed using Pearson's correlation coefficient (Figure 3.22). *L. vaginalis* was positively correlated with several other species including *L. iners, L. crispatus, L. jensenii* and *L. gasseri,* as well as *F. magna, P. indolicus* and *D. micraerophilus. L. iners* positively correlated with several other taxa such as *G. vaginalis, L. jensenii, P. bivia, P. timonensis, L. vaginalis,* and *D. micraerophilus*. *L. iners* negatively correlated with *L. gasseri*. *L. crispatus* was positively correlated with *L. jensenii*, *P. bivia*, *L. vaginalis* and *D. micraerophilus* and was negatively correlated with *S. anginosus*.

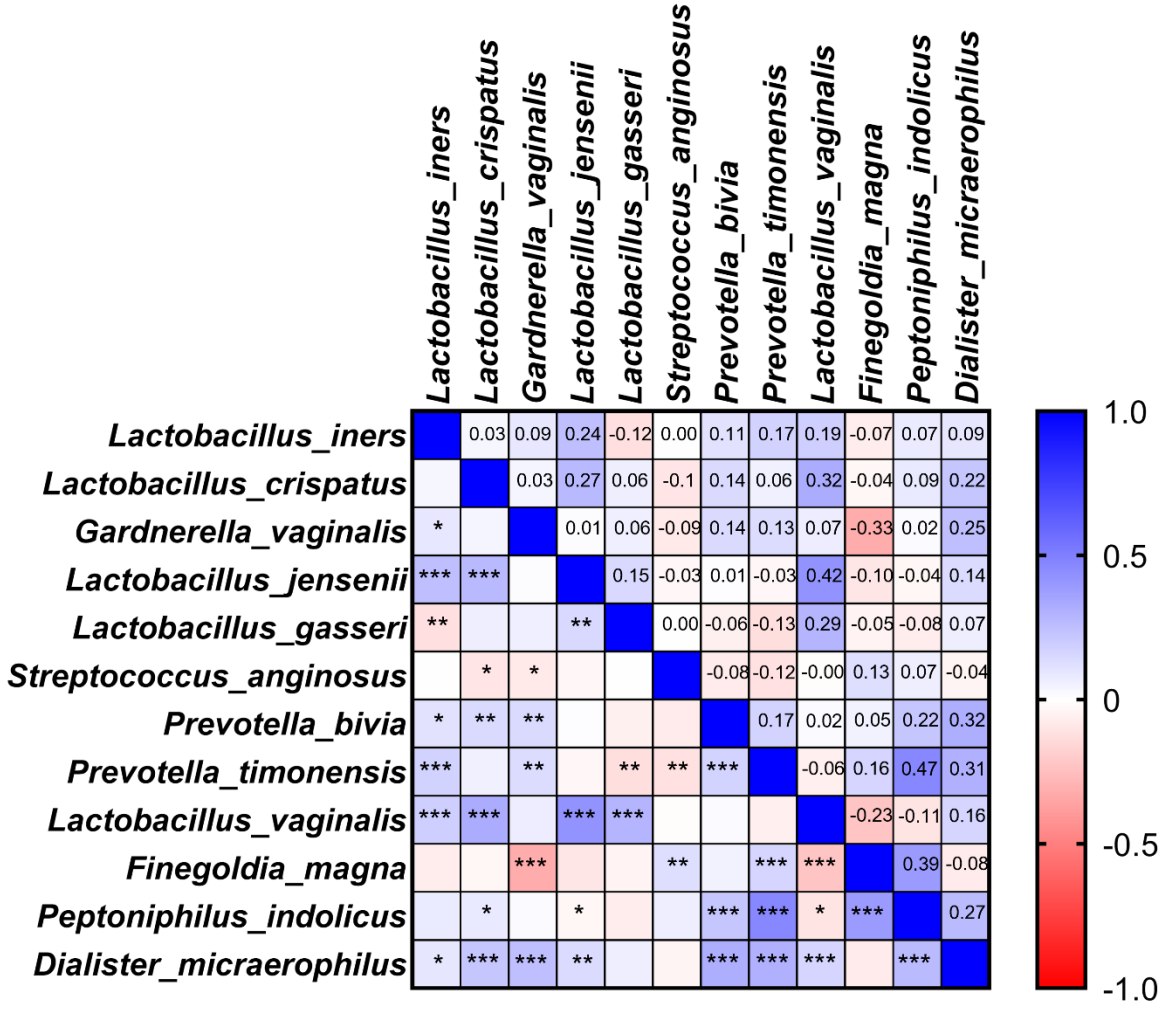


Figure 3.22: Correlation plot for highly abundant species with 25% prevalence inclusion threshold. Correlation matrix using Spearman correlation strength is indicated (*** p<0.001, ** p<0.01, and * p<0.05). Blue boxes: positive correlation, red boxes: inverse correlations.

3.7.2.2 Assignment of vaginal microbiota community state types (CSTs)

Samples were next categorised into CST classifications using the VALENCIA algorithm, a centroid clustering method that provides a standardised approach to classify vaginal bacterial profiles on the basis of a common compositional structure (142). In total, n=158 number of sample were classified as CST I (*L. crispatus* dominated), n=49 as CST II (*L. gasseri* dominated), n=84 as CST III (*L. iners* dominated), n=126 as CST IV (a combination of n=60 IV-B, *G. vaginalis* dominated and n=66 IV-C, dominated by a diverse array of facultative and strictly anaerobes), and n=45 as CST V (*L. jensenii* dominated).

3.8 Characterisation and comparison of vaginal microbiota in fresh IVF cycles

The analysis for the rest of this chapter is restricted to the fresh IVF cycles where serum hormone and immune analyte data was available for each patient. The analyses focused on the relationship between highly abundant taxa with hormones and immune analytes as well as the relevance of these relationships with clinical outcomes.

The microbiological significance of CST classifications in the fresh IVF cohorts are highlighted using richness and diversity indices. Bacterial richness and diversity were found to be significantly different between the CSTs. (Kruskal-Wallis tests, $p=0.0005$ and $p<0.0001$ respectively). Due to low prevalence of CST II in the fresh IVF cycles ($n<5$), this CST was excluded from statistical analysis. CST I had significantly lower richness than CST IV (Dunn's multiple comparison $p=0.0012$). Similar differences in diversity (assessed using Simpson's index) between CST I and CST IV were observed (Dunn's multiple comparison $p<0.0001$). CST I diversity was also significantly lower than CSTs III and V (Dunn's multiple comparison $p<0.0001$ and $p=0.0074$ respectively) (Figure 3.23).

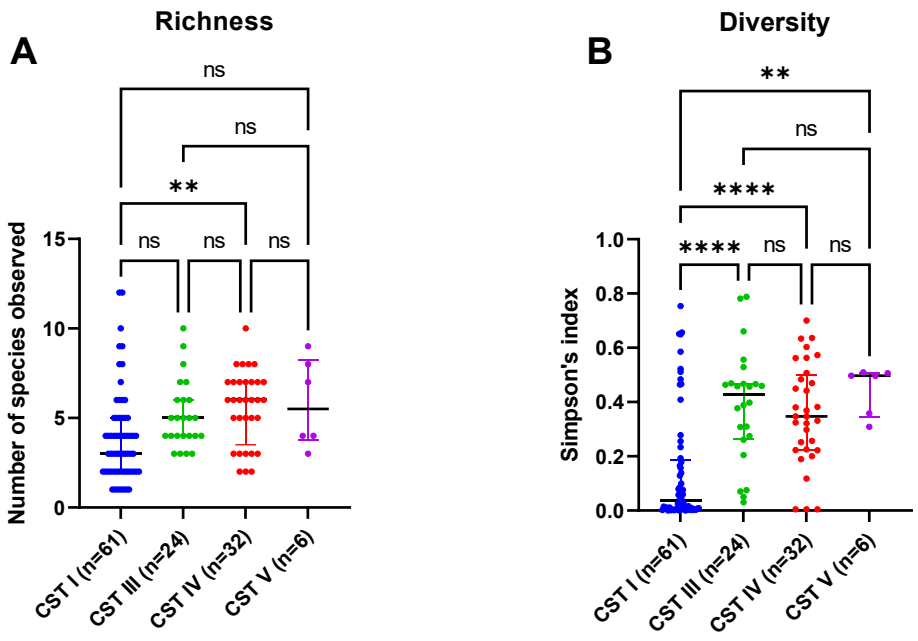


Figure 3.23: Ecological parameters of vaginal bacteria based on CST classifications in fresh IVF cycles. A) Species richness was significantly different between the CSTs (Kruskal-Wallis test p=0.0005). Dunn's multiple comparison test was used as a post-hoc test for between group comparisons. CST I richness was significantly lower than CST IV (Dunn's multiple comparison p=0.0012). There were no other between group significant differences in species richness based on CST classifications. B) Diversity was significantly different between CSTs (Kruskal-Wallis test p<0.0001). CST I diversity was significantly lower than CSTs III, IV and V using Dunn's multiple comparison tests (p<0.0001, p<0.0001 and p=0.0074 respectively).

The prevalence of these CSTs was then compared across the clinical stages of women undergoing fresh IVF treatment cycles (Figure 3.24). As the sample size of CST II samples was <2 at pituitary suppression, egg collection and embryo transfer, a contingency analysis could not be performed. Additionally, more than 20% of the data had less than 5 samples per CST, another condition which was not met for the test to be valid. To overcome this, samples assigned as *Lactobacillus* species type CSTs were combined into a 'Lacto-dominant' group and were compared CST IV samples. No statistical significance between prevalence of *Lactobacillus* dominated samples and CST IV dominated samples was observed across treatment stages (X^2, p=0.67). Furthermore, the prevalence of CST I compared to the combination of the other 4 CSTs did not differ across the treatment timepoints (X^2, p=0.72).

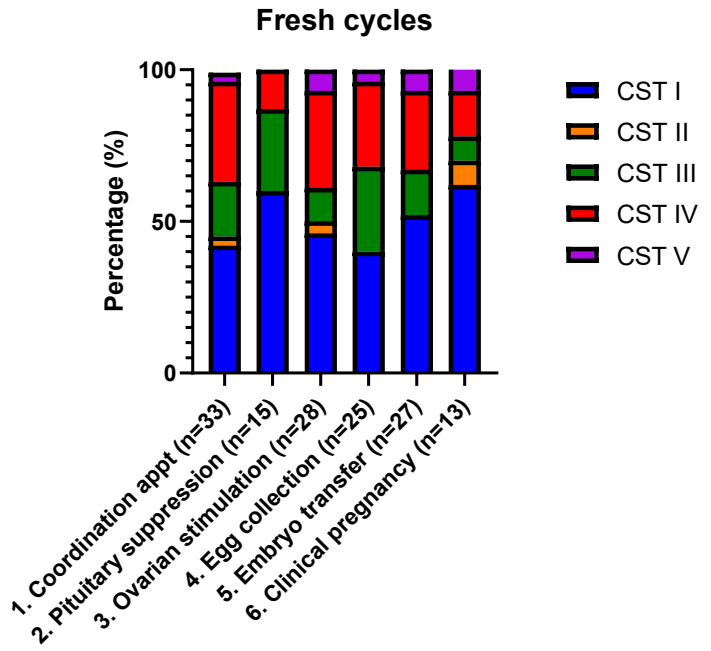


Figure 3.24: CST representations at various stages of sample collection for fresh IVF cycles. CST I is the most prevalent CST across all stages of sample collection, on average up to half of samples collected were classified as CST I. Prevalence of CSTs II and V were low across stages of sample collection with no representation throughout pituitary suppression for either CST. There were also no samples classified as CST II on the days of egg collection and embryo transfer. Prevalence of Lacto-dominant samples were not significantly different across stages of sample collection for fresh IVF cycles.

To determine whether any specific taxa were significantly changing across each of the sample collection stages irrespective of clinical outcomes, a linear mixed effects model was used (Table 3.8). The analysis included stages 1 to 5 of sample collection. As shown in Figure 3.25, stage 6 was plotted for comparison but was excluded from the mixed effects modelling. Significant changes were observed for *P. timonensis* and *F. magna. F. magna* changes were also significant based on the adjusted p-value. There were no significant changes in abundance of other highly abundant taxa such as *L. crispatus, L. iners*, or *G. vaginalis* which is in concert with prevalence of CST Lacto-dominant and CST IV not changing significantly throughout the fresh IVF cycles.

Table 3.8: Longitudinal abundance changes for highly abundant taxa. ANOVA linear mixed effects modelling of highly abundant taxa based on cross-sectional data collection timepoints. *P. timonensis* and *F. magna* changed significantly throughout sample collection timepoints. adjusted p-values (q-values) were calculated using the Benjamini-Hochberg procedure.

Bacterial	p-value	q-value
L. iners	0.64	0.64
L. crispatus	0.31	0.41
G. vaginalis	0.55	0.61
L. jensenii	0.26	0.41
L. gasseri	0.14	0.41
S. anginosus	0.09	0.37
P. bivia	0.37	0.45
P. timonensis	**0.04**	0.23
L. vaginalis	0.29	0.41
F. magna	**0.0001**	**0.002**
P. indolicus	0.26	0.41
D. micraerophilus	0.29	0.41

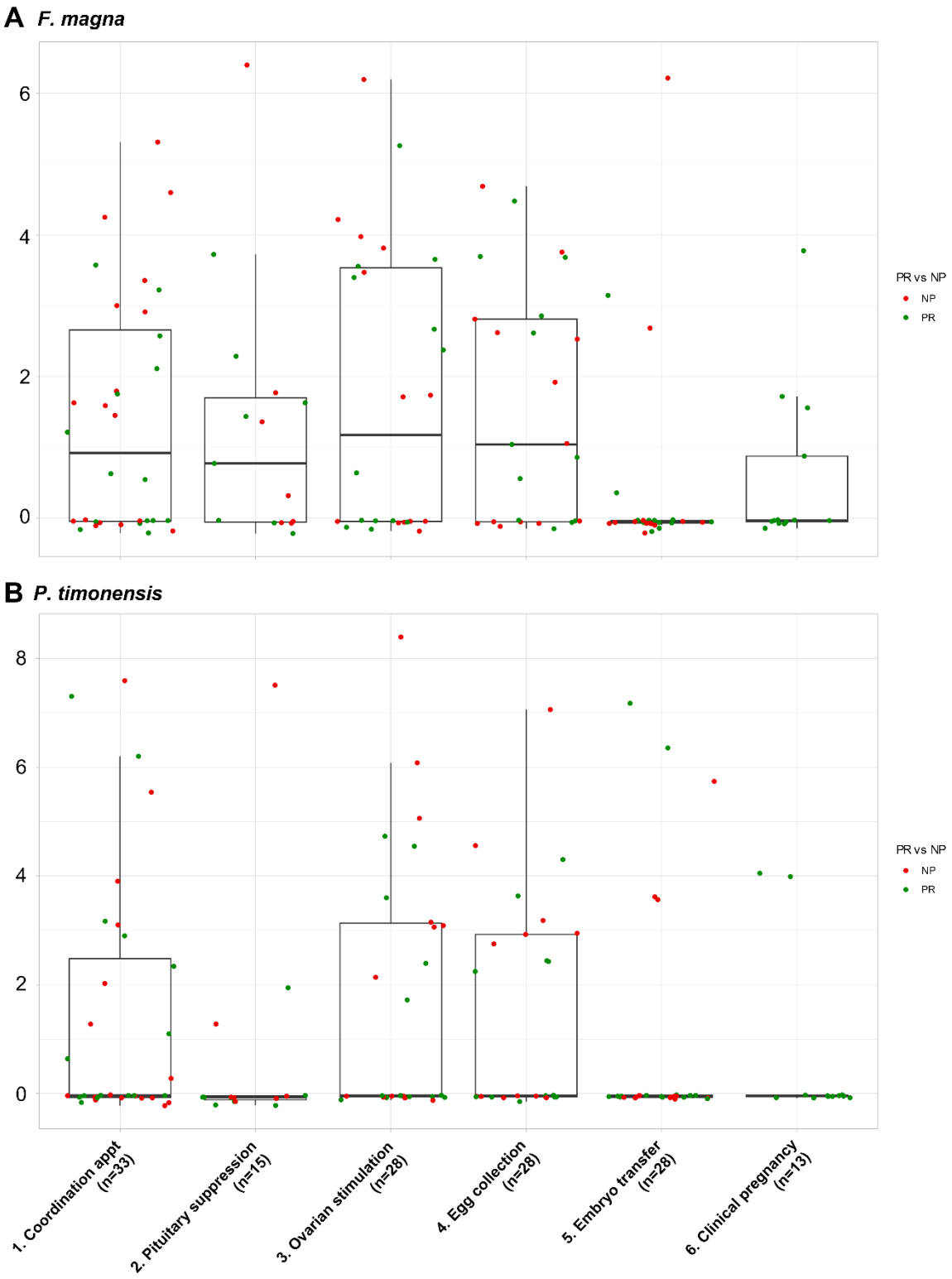


Figure 3.25: Longitudinal relative abundance changes of taxa. A) *F. magna* (p=0001, q=0.002), and B) *P. timonensis* (p=0.04, q=0.23) changed significantly throughout sample collection timepoints. PR: pregnant, NP: Not pregnant.

The next set of analyses addressed whether the prevalence of CSTs related to clincal outcomes at each of the sample collection timepoints. First, data were assessed based on prevalence of CST I compared to the combination of the other 4 CSTs (Table 3.9). There were no associations with treatment outcomes at any stages of sample collection. Next, samples were categorised into Lacto-dominant and CST IV classifications. Similarly, there were no relationships with prelavence of Lacto-dominant samples and outcome (Table 3.10).

Table 3.9: Cross-sectional CST representations according to outcome for fresh IVF cycles: CST I vs other CSTs. There were no strong associations between prevalence of CST I with clinical outcomes at any stages of sample collection throughout fresh IVF cycles (Fisher's exact test p-values).

1. Coordination appointment	**CST I**	**Other CSTs**	**p-value**
Pregnant (n=16)	7 (44%)	9 (56%)	0.99
Not pregnant (n=17)	7 (41%)	10 (59%)	
2. Pituitary suppression			
Pregnant (n=8)	5 (62%)	3 (38%)	0.61
Not pregnant (n=7)	3 (43%)	4 (57%)	
3. Ovarian stimulation			
Pregnant (n=13)	8 (62%)	5 (38%)	0.23
Not pregnant (n=13)	4 (31%)	9 (69%)	
4. Egg collection			
Pregnant (n=12)	7 (58%)	5 (42%)	0.1
Not pregnant (n=14)	3 (21%)	11 (79%)	
5. Embryo transfer			
Pregnant (n=14)	8 (57%)	6 (43%)	0.44
Not pregnant (n=14)	5 (36%)	9 (64%)	

Table 3.10: Cross-sectional CST representation according to outcome for fresh IVF cycles: CST Lacto-dominant vs CST IV. There were no strong associations between prevalence of CST Lacto-dominant with clinical outcomes at any stages of sample collection throughout fresh IVF cycles (Fisher's exact test p-values).

1. Coordination appointment	**CST Lacto-dominant**	**CST IV**	**p-value**
Pregnant (n=16)	12 (75%)	4 (25%)	0.70
Not pregnant (n=17)	11 (65%)	6 (35%)	
2. Pituitary suppression			
Pregnant (n=8)	7 (88%)	1 (12%)	0.56
Not pregnant (n=7)	5 (71%)	2 (29%)	
3. Ovarian stimulation			
Pregnant (n=13)	10 (77%)	3 (33%)	0.23
Not pregnant (n=13)	7 (54%)	7 (46%)	
4. Egg collection			
Pregnant (n=12)	10 (83%)	2 (17%)	0.21
Not pregnant (n=14)	8 (57%)	6 (43%)	
5. Embryo transfer			
Pregnant (n=14)	12 (86%)	2 (14%)	0.20
Not pregnant (n=14)	8 (57%)	6 (43%)	

3.8.1 Stability of vaginal microbiome throughout fresh IVF cycles

Given that at each timepoint there were no relationship with outcome (Tables 3.9 and 3.10), the next analysis aimed to assess the microbiota stability for each patient based on clinical treatment outcomes. The study of vaginal microbiome stability was based on CST classifications for the samples collected (Figure 3.26). A cycle with a stable vaginal microbiome was defined as one where the same CST was observed for all samples assessed. The samples collected at 6-8 weeks gestation were excluded as they were collected up to 2 months following the completion of the IVF cycles. Repeat sample collections were taken into consideration where available. Patient 52 (not pregnant) was excluded due to only having 1 sample available for analysis.

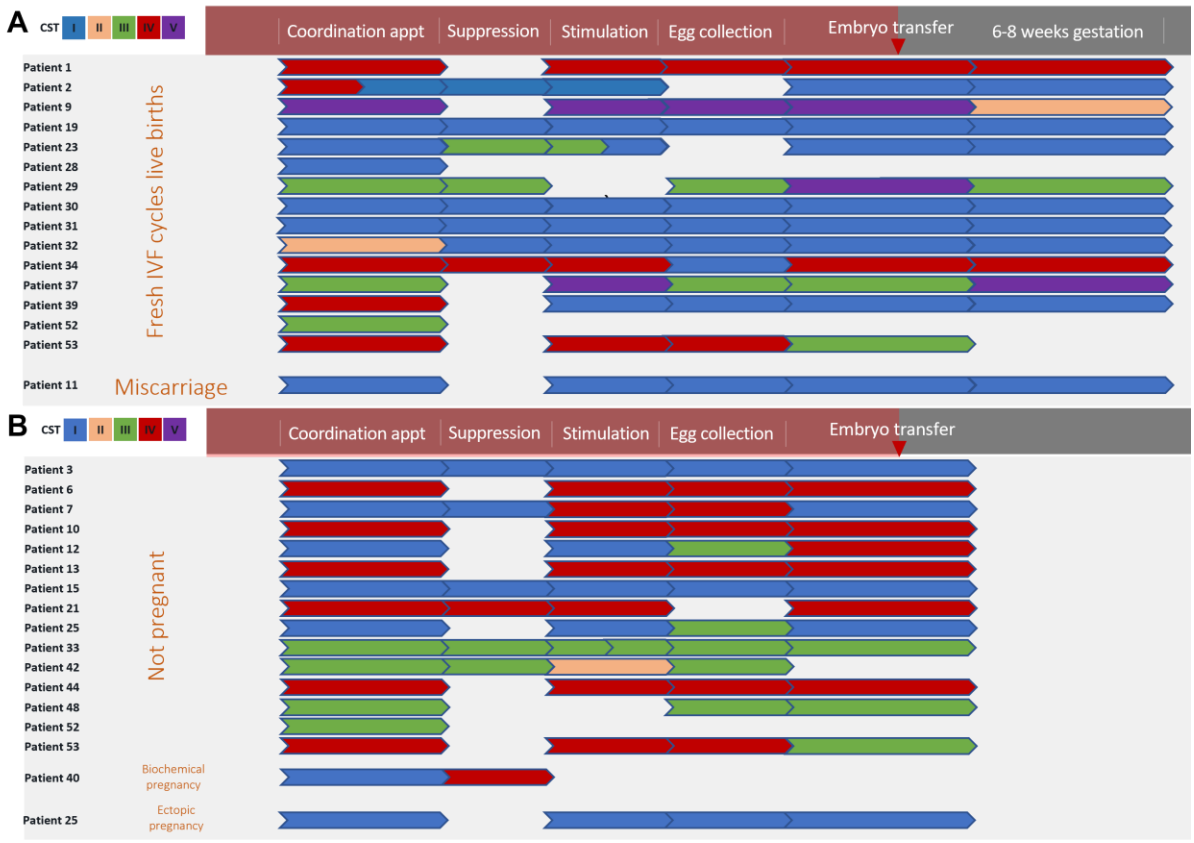


Figure 3.26: Within patient sample collection timeline for fresh IVF cycles. A) cycles with successful clinical pregnancy outcomes, B) cycles with unsuccessful clinical pregnancy outcomes.

There were 16 cycles with successful clinical pregnancies in the fresh IVF cohort. In this cohort, 6 cycles maintained the same CST from the first sample collection point to embryo transfer (38%). The rate of CST stability was higher in patients who did not have successful clinical pregnancies with 9 out of 16 cycles remained stable throughout the treatment (56%). The difference in CST stability rates according to clinical pregnancy was not significantly different (p=0.47, Fisher's exact test).

3.8.2 Assessment of bacterial load for samples collected on the day of embryo transfer for fresh IVF cycles

Having examined microbiota composition, the next set of analyses aimed to determine whether bacterial load within samples is associated with clinical outcomes. Bacterial load was first analysed for samples collected on the day of embryo transfer based on CST classifications of samples. There were no significant differences between CSTs based on bacterial load (Kruskal-Wallis test p=0.10) (Figure 3.27).

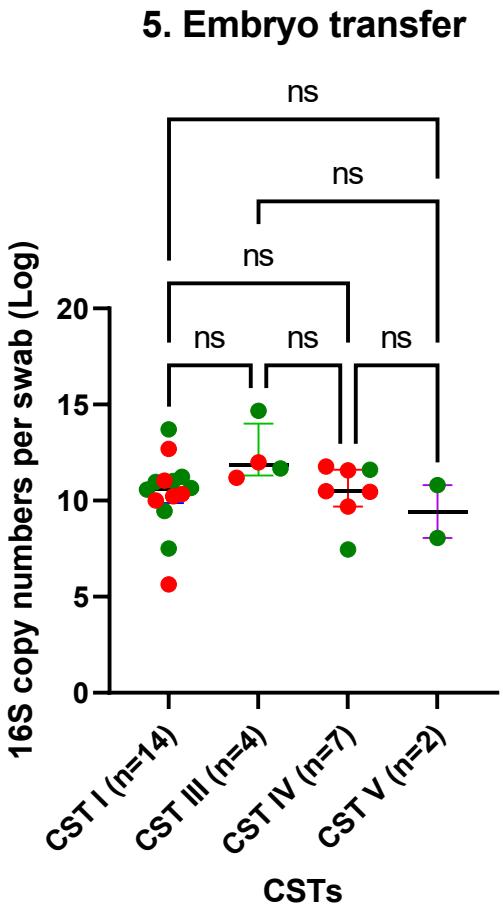


Figure 3.27: CSTs and bacterial load for samples collected on the day of embryo transfer. There were no significant differences in bacterial load based on CSTs ($p>0.05$ for all). Kruskal-Wallis test ($p=0.10$), Dunn's multiple comparisons indicated on the plot ($p>0.05$ for all). (●) Red dots and lines indicate unsuccessful outcomes, (●) green dots and lines indicate successful outcomes.

There were no significant differences in bacterial load based on clinical outcomes for samples collected on the day of embryo transfer using Mann-Whitney test ($p=0.90$) (Figure 3.28).

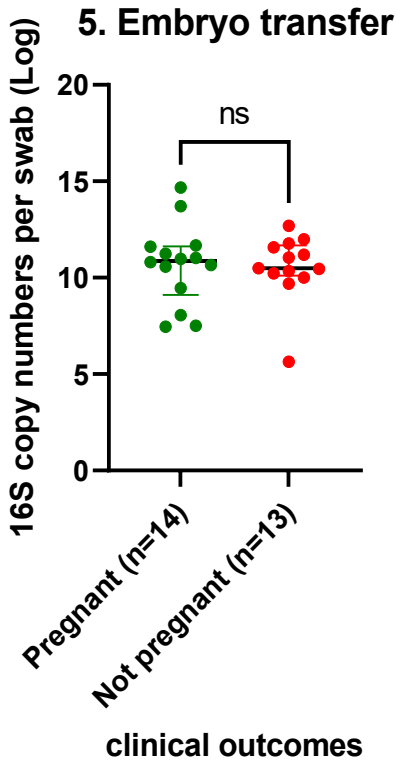


Figure 3.28: Clinical outcomes and bacterial load for samples collected on the day of embryo transfer. There were no significant differences in bacterial load based on clinical treatment outcomes. Mann-Whitney test (p=0.90).

3.8.3 The relationship between highly abundant taxa and hormones

The relationship between highly abundant taxa and the hormones were first analysed for all available samples regardless of stages of sample collection. There were no correlations observed between the relative abundance of the highly abundant taxa and E2. *F. magna* (p=0.004, q=0.04) and *S. anginosus* (p=0.04, q=0.24) had an inverse correlation with P4. Relative abundance of *L. crispatus* with respect to E2 (p=0.80, q=0.87) and P4 (0.82, q=0.82) were not significant. This trend was similarly observed for *L. jensenii* with E2 (p=0.60, q=0.87) and P4 (p=0.43, q=0.66) as well as *L. gasseri* with E2 (p=0.044, q=0.87) and P4 (p=0.37, q=0.66). Furthermore, *G. vaginalis* did not have any linear correlations with E2 (p=0.87, q=0.87) and P4 (p=0.74, q=0.81), across the entire dataset (see Table 3.11).

Table 3.11: Linear regression R2 values for the highly abundant taxa and serum hormones for all available samples. *F. magna* (p=0.004, q=0.04) and *S. anginosus* (p=0.04, q=0.24) had an inverse correlation with P4. R^2 values in bold indicate a significant p-value and thick cell-border indicate a significant q-value (n=128).

species	E2	P4
Lactobacillus_iners	-0.005	-0.001
Lactobacillus_crispatus	0.002	0.003
Gardnerella_vaginalis	0.000	0.000
Lactobacillus_jensenii	0.001	0.004
Lactobacillus_gasseri	0.005	-0.009
Streptococcus_anginosus	-0.016	**-0.027**
Prevotella_bivia	-0.015	-0.010
Prevotella_timonensis	0.000	-0.013
Lactobacillus_vaginalis	0.001	0.003
Finegoldia_magna	-0.003	**-0.059**
Peptoniphilus_indolicus	0.000	-0.013
Dialister_micraerophilus	-0.002	-0.002

3.8.3.1 Cross-sectional analysis of highly abundant taxa and hormones

In samples collected at coordination appointment, *S. anginosus* was negatively correlated with E2 (p=0.004, q=0.04). The inverse relationship between *S. anginosus* and E2 trended throughout pituitary suppression and ovarian stimulation, however, did not reach significance. In samples collected at coordination appointment, *P. indolicus* also inversely correlated with E2 (p=0.03, q=0.19). No other species correlated with E2 or P4 at this stage of sample collection. Throughout pituitary suppression, *L. jensenii* positively correlated with P4 (p=0.03, q=0.38). For samples collected during ovarian stimulation, there were no correlations between highly abundant taxa and serum hormones. For samples collected on the day of egg collection, *P. bivia* inversely correlated with E2 (p=0.03, q=0.21) and P4 (p=0.03, q=0.47). Furthermore, *L. jensenii* positively correlated with E2 (p=0.02, q=0.21). On the day of embryo transfer, there were no significant correlations between taxa and serum hormones (Figures 3.29 and 3.30).

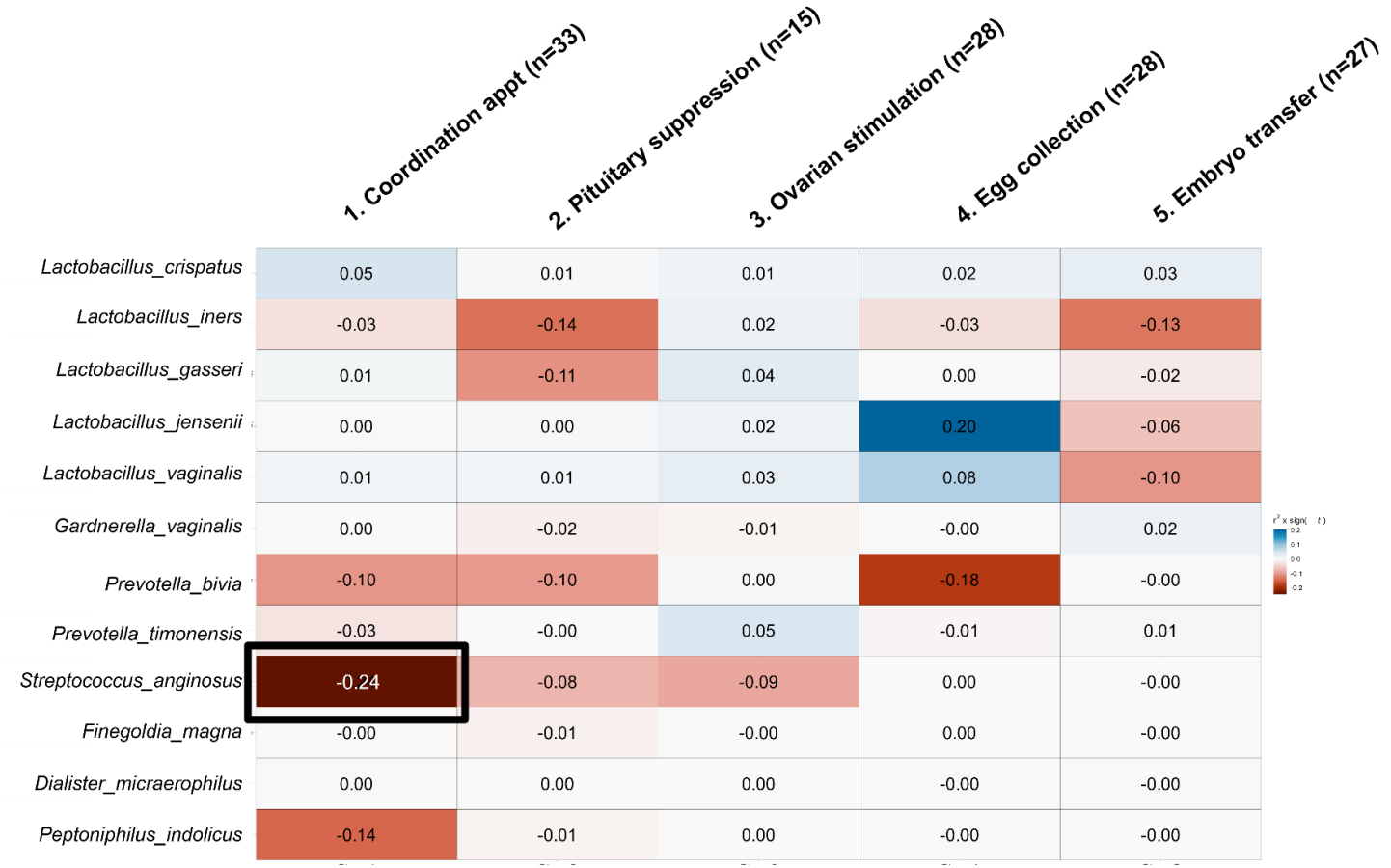


Figure 3.29: Cross-sectional linear regression R2 values of CLR transformed abundance of highly abundant taxa with E2 levels. *Streptococcus anginosus* inversely correlated with E2 concentrations at coordination appointment. This correlation was significant based on adjusted p-value (p=0.004, q=0.04). No other correlation withstood the correction for multiple comparison testing (n=128).

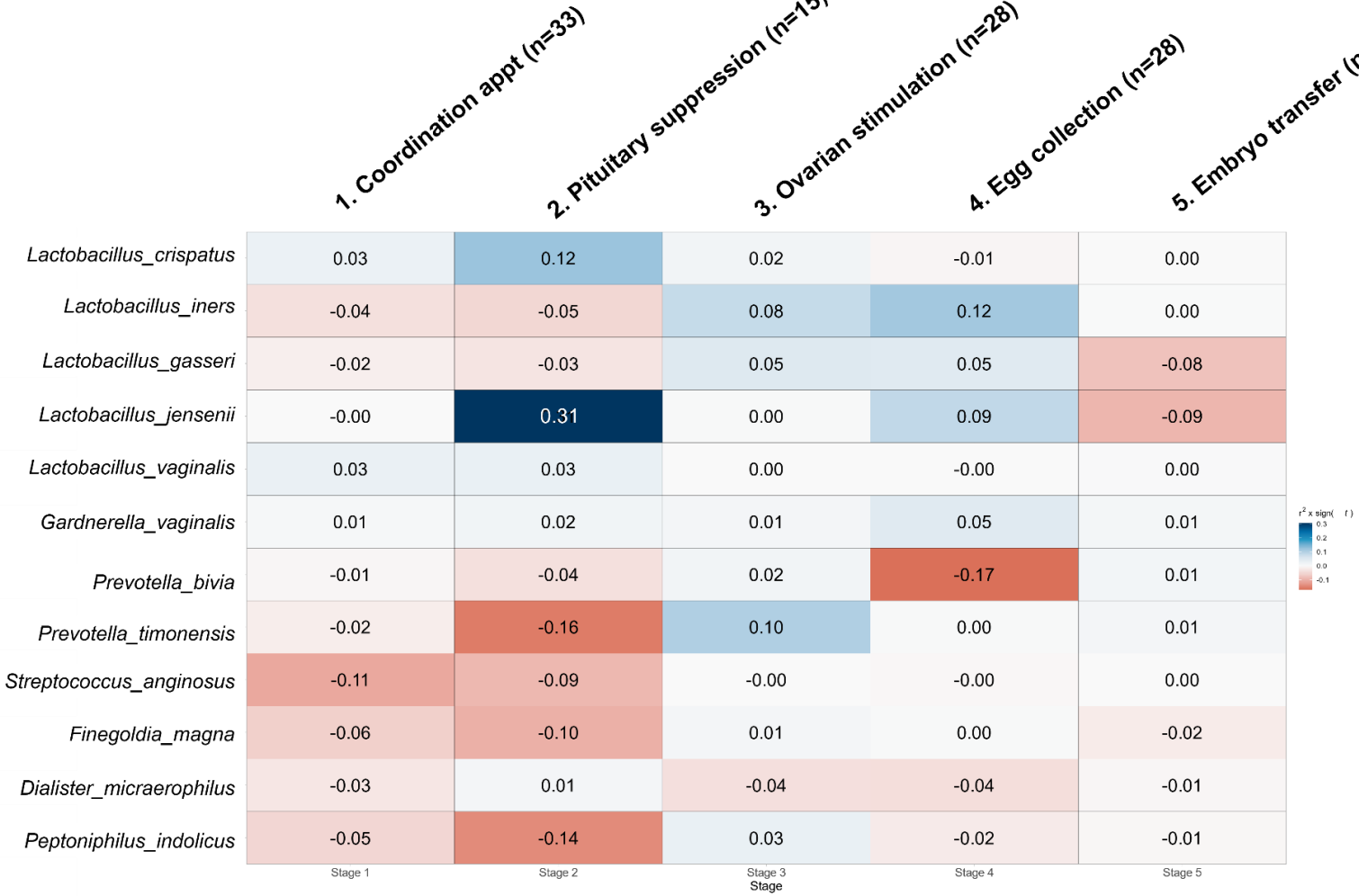


Figure 3.30: Cross-sectional linear regression R2 values of CLR transformed abundance of highly abundant taxa with P4 levels. No correlations were significant based on multiple comparison corrected p-value (n=128).

Figures 3.31-3.34 show significant correlations of CLR transformed abundance of highly abundant taxa with serum hormones at each stage of sample collection. Three regression lines are presented on each plot; the black line indicates the overall linear regression relationship, whereas the green and red lines show the regression lines with respect to the outcome of the treatment cycle. The reported significance in figure legends is the overall significance.

3.9.3.1.1. Coordination appointment

For samples collected at coordination appointment, *L. iners* inversely correlated with E2 (p=0.04, q=0.19). This trend was strongly observed in patients with successful outcomes (n=14, p=0.0004) but not in patients with unsuccessful outcomes (n=18, p=0.82) (Figure 3.31).

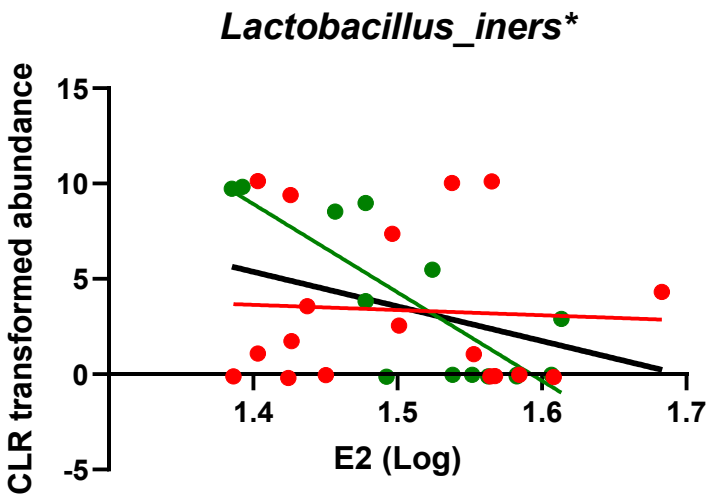


Figure 3.31: Linear regression between CLR transformed abundance of *L. iners* with E2 for samples collected at coordination appointment. (p=0.04, n=32), (●) Red dots and lines indicate unsuccessful outcomes, (●) green dots and lines indicate successful outcomes.

P4 did not correlate with any of the highly abundant taxa at this stage of sample collection.

3.9.3.1.2. Pituitary suppression

For samples collected throughout pituitary suppression, there were not any significant correlations between any of the highly abundant taxa and E2 concentrations. *L. jensenii* and P4 positively correlated (p=0.03, q=0.38) (Figure 3.32).

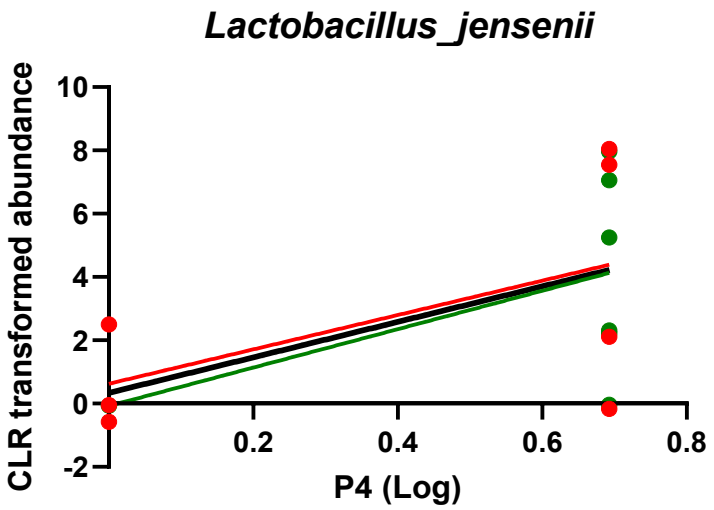


Figure 3.32: Linear regression between CLR transformed abundance of *L. jensenii* with P4 for samples collected throughout pituitary suppression. (p=0.03, n=15). (●) Red dots and lines indicate unsuccessful outcomes, (●) green dots and lines indicate successful outcomes.

3.9.3.1.3. Ovarian suppression

For samples collected throughout ovarian stimulation, there were no significant correlations between the abundance of highly abundant taxa and hormone levels.

3.9.3.1.4 Egg collection

For samples collected on the day of egg collection, *P. bivia* (p=0.03, q=0.83) and *L. jensenii* (p=0.02, q=0.63) correlated with E2 positively and inversely respectively. *P. bivia* also negatively correlated with P4 (p=0.04, q=0.99) (Figure 3.33). The positive correlation between *L. jensenii* and E2 at this stage was also observed for patients who had successful treatments (n=11, p=0.01) but not for patients who did not have successful treatment outcomes (n=13, p=0.49) (Figure 3.34). The inverse relationship between *P. bivia* and E2 however was only

observed in patients with unsuccessful treatments (n=13, p=0.03) but not patients with successful treatments (n=11, p=0.18).

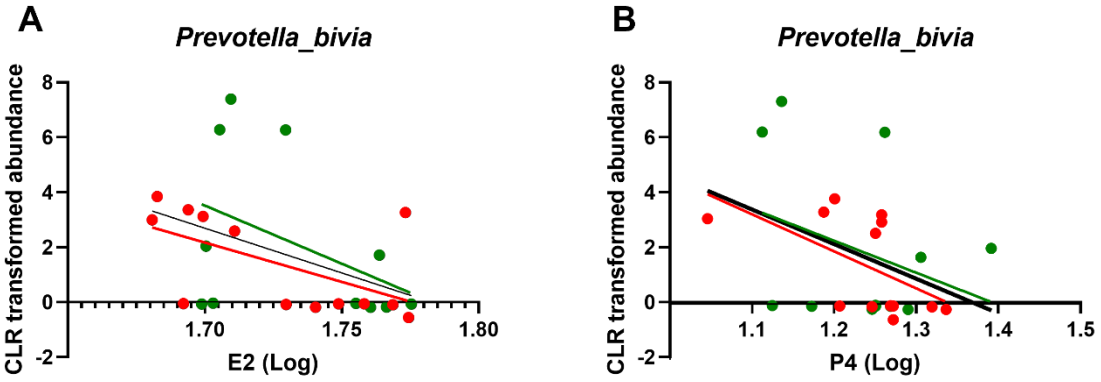


Figure 3.33: Linear regression between CLR transformed abundance of *P. bivia* with serum hormone concentrations for samples collected on the day of egg collection. A) E2 (p=0.02, n=24), and B) P4 (p=0.04, n=25). (●) Red dots and lines indicate unsuccessful outcomes, (●) green dots and lines indicate successful outcomes.

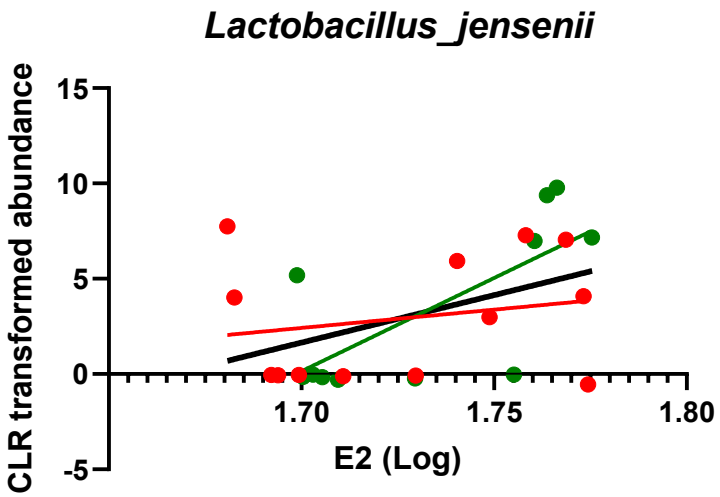


Figure 3.34: Linear regression of *L. jensenii* with E2 for samples collected on the day of egg collection. (p=0.02, n=24). (●) Red dots and lines indicate unsuccessful outcomes, (●) green dots and lines indicate successful outcomes.

3.9.3.1.5 Embryo transfer

For samples collected on the day of embryo transfer, there were no significant correlations between the abundance of highly abundant taxa and serum hormones.

3.8.4 Relationship between vaginal taxa with hormones and immune analytes

Potential interactions between major vaginal bacteria, immune analytes and hormones were investigated using Canonical Correlation Analysis (CCA). The data modelling using CCA illustrates the relationship between the major taxa with hormones and immune analytes by demonstrating the main sources of variance within the dataset. Like the regression analysis, the interplay between the inflammatory analytes and taxa composition were demonstrated for the entire dataset and at each stage of sample collection.

Analysis on all available data across the whole dataset suggested that many immune analytes correlate with several BV associated taxa. *F. magna, P. indolicus, D. micraerophilus, P. bivia* and *P. timonensis* are positioned closely with immune analytes such as IL-18, IFN-γ, IL-6, IGFBP-1, and TNF-α on the plot indicated a positive correlation (Figure 3.35). *Lactobacillus* species, with the exception of *L. iners*, were closely associated with one another as well as E2, P4 and IL-1ra. Furthermore, *L. crispatus* was anti-correlated with pro-inflammatory cytokines, particularly IL-8 and IL-1β.

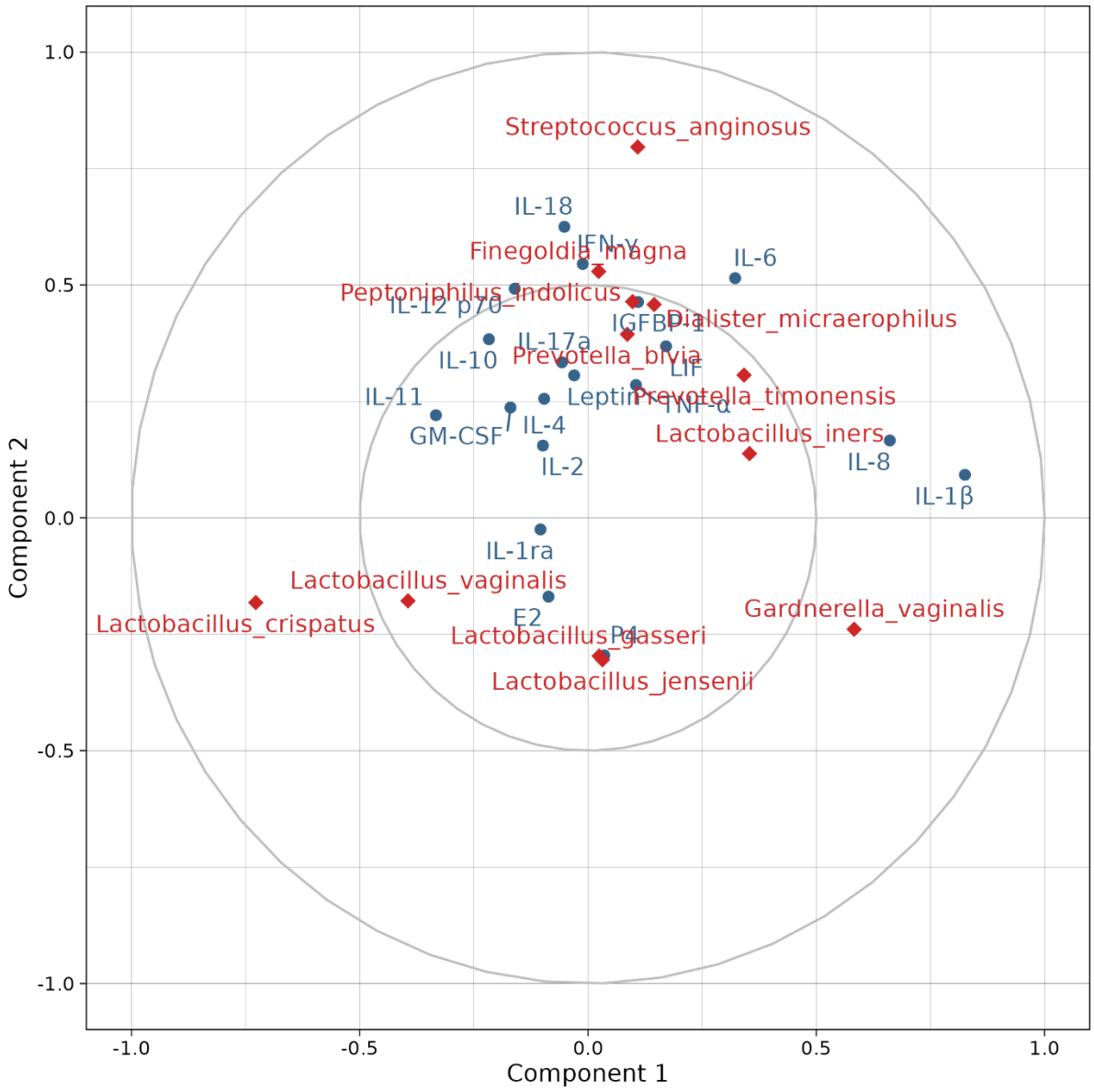


Figure 3.35: CCA variance plot across all stages of sample collection. CCAs for the first 2 principal dimensions of the relationship between microbiota, immune analytes, and serum hormones. Bacteria are indicated in red. Immune analytes and serum hormones are indicated in blue (n=128).

To assess specific linear relationships between vaginal taxa and immune analytes, samples were first analysed across the whole dataset (Figure 3.36). There were 28 significant relationships identified, 10 of which withstood correction for multiple testing. *L. crispatus* negatively correlated with IL-1β ($p<0.0001$, $q<0.0001$) and IL-8 ($p=0.0005$, $q=0.006$) (Figure 3.37). *L. iners* positively correlated with IL-8 ($p=0.002$, $q=0.01$) (Figure 3.38). *L. vaginalis* ($p=0.004$, $q=0.01$) (Figure 3.39) and *G. vaginalis* (Figure 3.40) correlated with IL-β inversely and positively respectively ($p<0.0001$, $q<0.0001$) (Figure 3.39). *S. anginosus* positively correlated with 4 analytes: IFN-γ ($p=0.002$, $q=0.03$), IGFBP-1 ($p=0.001$, $q=0.01$), IL-6

(p=0.001, q=0.01), and IL-18 (p<0.0001, q=0.0005) (Figure 3.41). *D. micraerophilus* with IL-18 (p=0.007, q=0.04) (Figure 3.42).

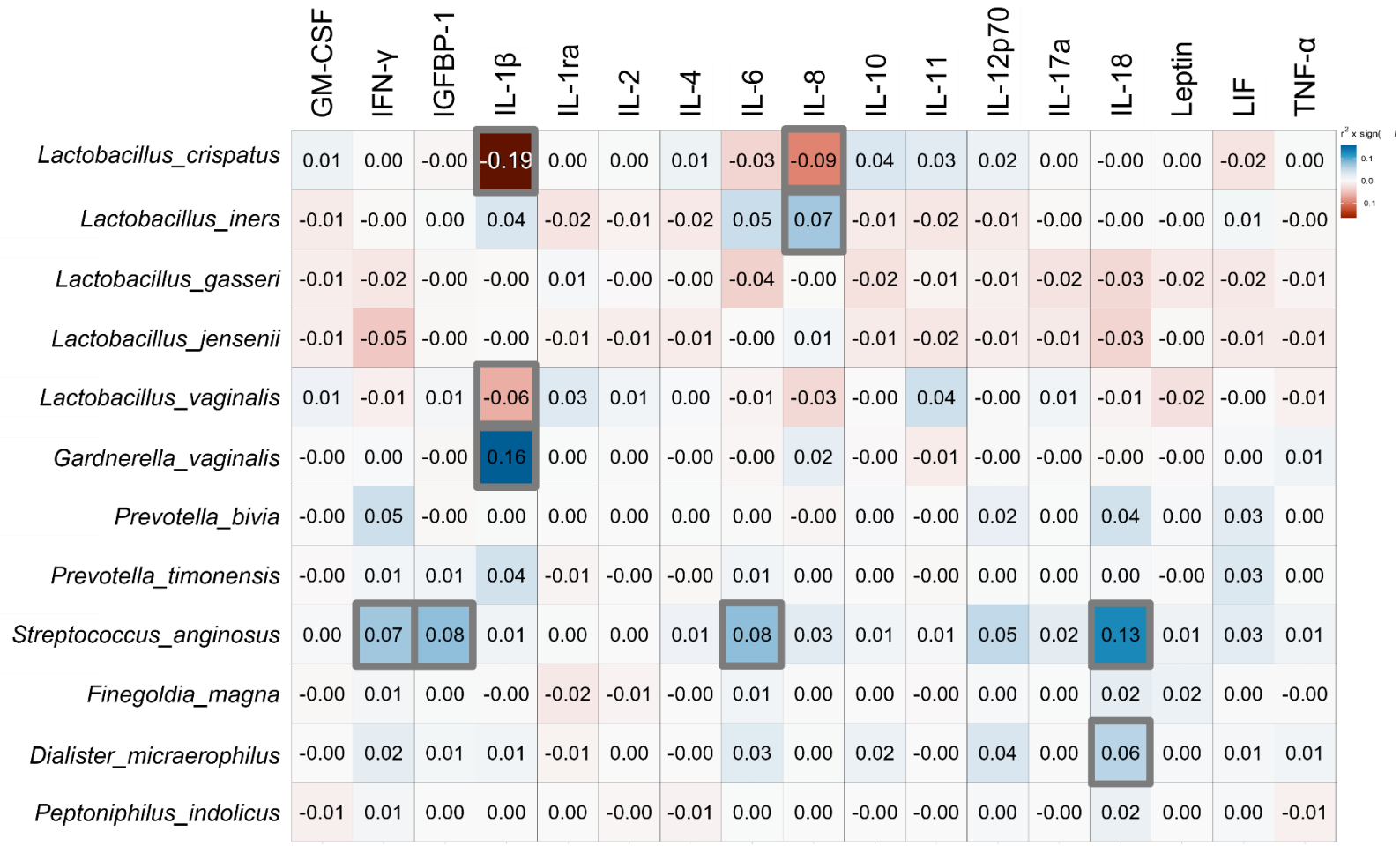


Figure 3.36: Linear regression R2 values for highly abundant taxa and immune analytes across the whole dataset. Several positive and inverse associations were observed. The blue shades represent positive associations and red shades inverse associations. thick cell-borders indicate a significant q-value (n=128).

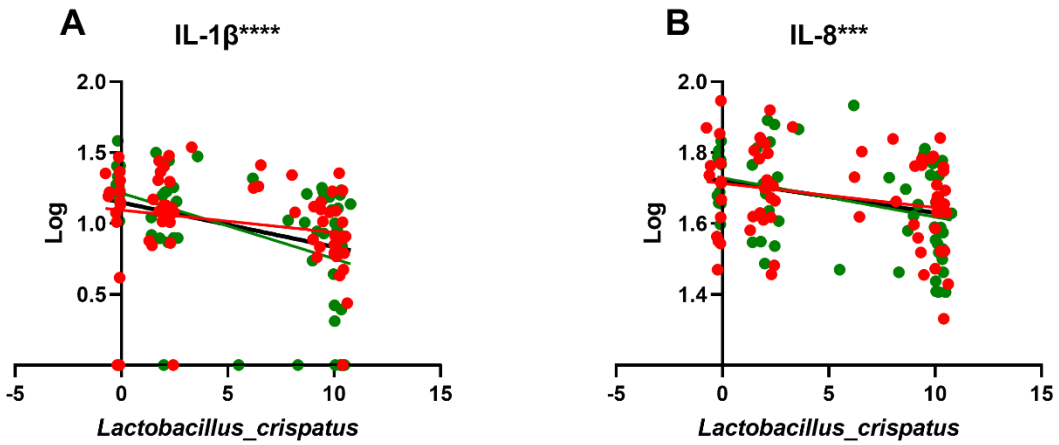


Figure 3.37: Linear regression of *L. crispatus* and immune analytes across the whole dataset. A) CLR transformed relative abundance of *L. crispatus* inversely correlates with IL-1β ($p<0.0001$, $q<0.0001$, $R^2=0.18$). B) CLR transformed relative abundance of *L. crispatus* inversely correlates with IL-8 ($p=0.0005$, $q=0.006$, $R^2=-0.09$) (using all available data n=128). (●) Red dots indicate unsuccessful outcomes, (●) green dots indicate successful outcomes.

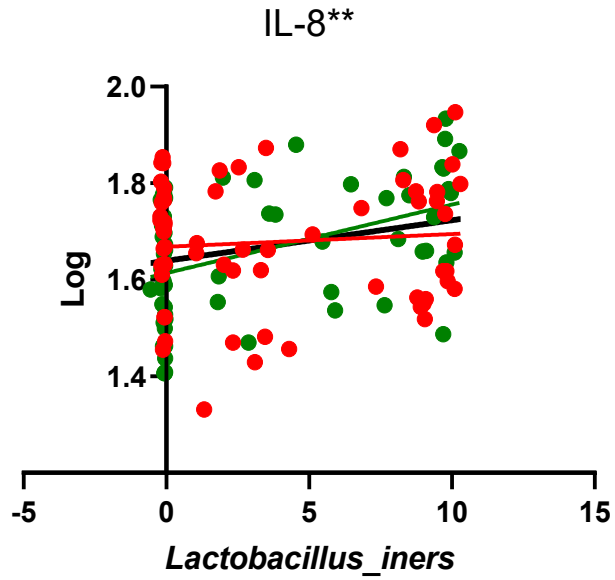


Figure 3.38: Linear regression of *L. iners* and IL-8 across the whole dataset. CLR transformed relative abundance of *L. iners* positively correlates with IL-8 ($p=0.002$, $q=0.01$, $R^2=-0.07$, n=128). (●) Red dots and line indicate unsuccessful outcomes, (●) green dots and line indicate successful outcomes.

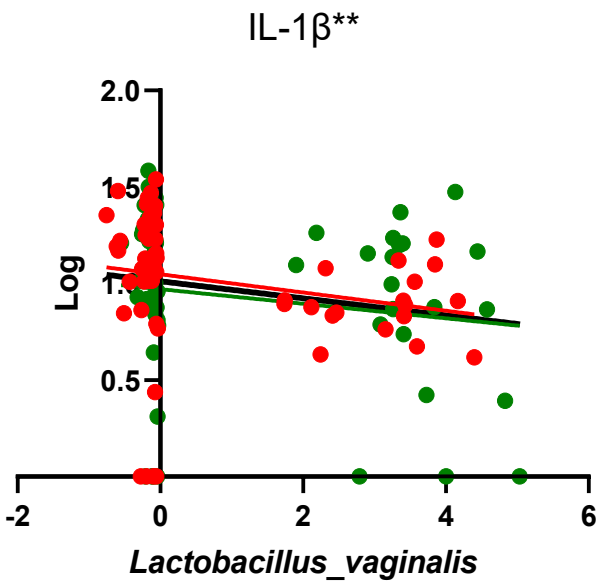


Figure 3.39: Linear regression of *L. vaginalis* and IL-1β across the whole dataset. CLR transformed relative abundance of *L. vaginalis* inversely correlates with IL-1β (p=0.004, q=0.01, R^2=-0.06, n=128). (●) Red dots and line indicate unsuccessful outcomes, (●) green dots and line indicate successful outcomes.

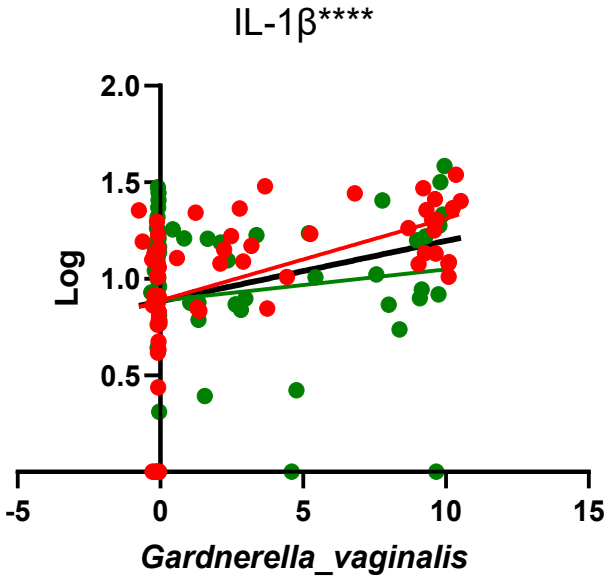


Figure 3.40: Linear regression of *G. vaginalis* and IL-1β across the whole dataset. CLR transformed relative abundance of *G. vaginalis* positively correlates with IL-1β (p<0.0001, q<0.0001, R^2=-0.15, n=128). (●) Red dots and line indicate unsuccessful outcomes, (●) green dots and line indicate successful outcomes.

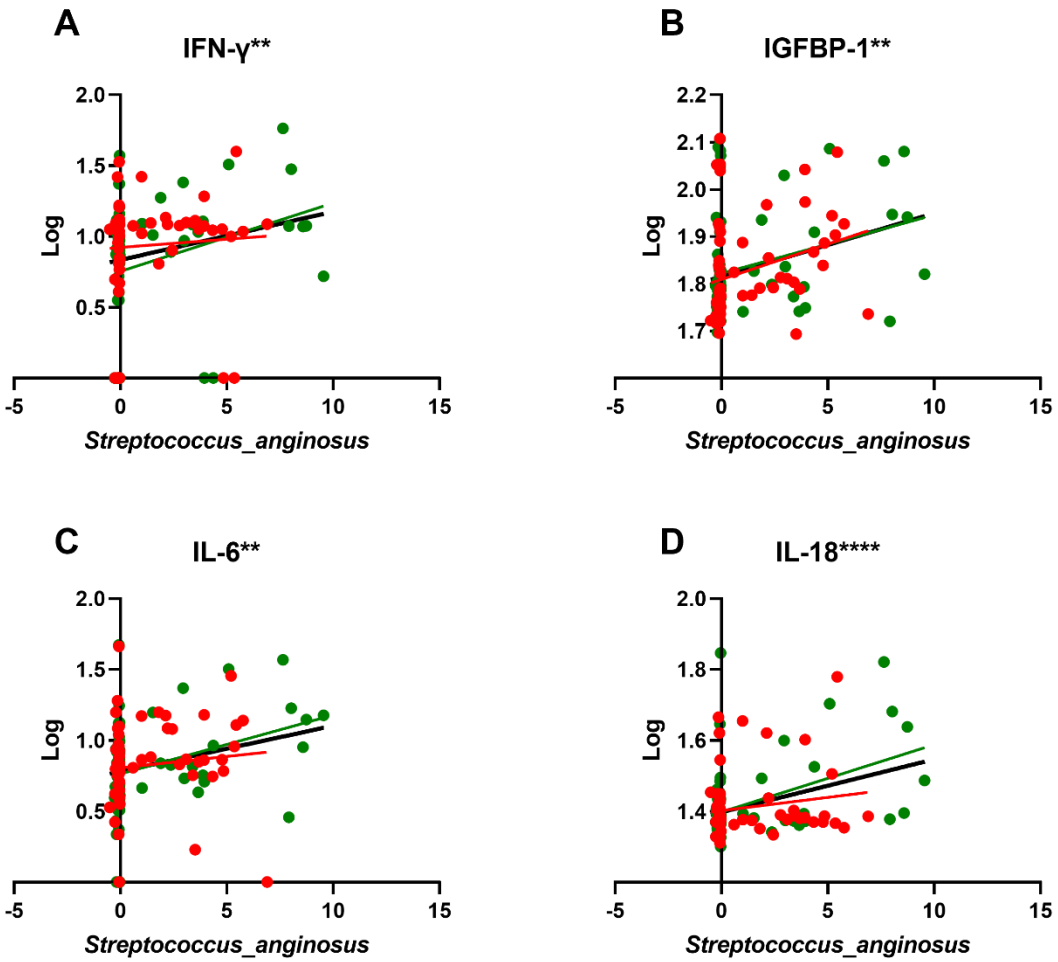


Figure 3.41: Linear regression of *S. anginosus* and immune analytes across the whole dataset. CLR transformed relative abundance of *S. anginosus* positively correlates with A) IFN-γ (p=0.002, q=0.03, R^2=-0.07), B) IGFBP-1 (p=0.001, q=0.01, R^2=-0.07), C) IL-6 (p=0.001, q=0.01, R^2=0.08), and D) IL-18 (p<0.0001, q=0.0005, R^2=0.12) (n=128). (●) Red dots and line indicate unsuccessful outcomes, (●) green dots and line indicate successful outcomes.

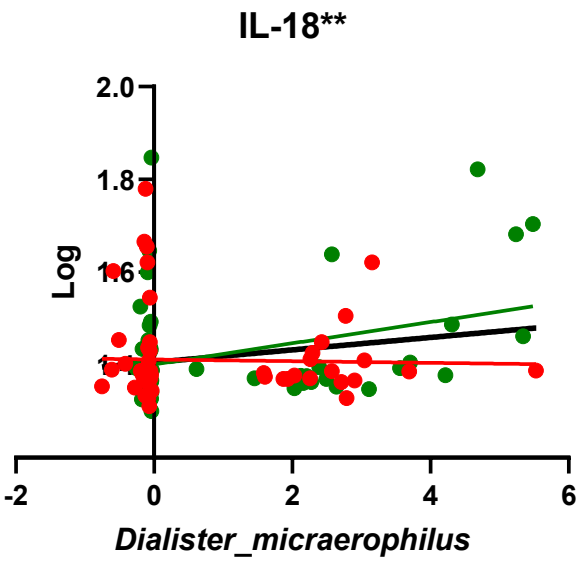


Figure 3.42: Linear regression of *D. micraerophilus* and IL-18 across the whole dataset. CLR transformed relative abundance of *D. micraerophilus* positively correlates with IL-18 (p=0.007, q=0.04, R^2=0.05, n=128). (●) Red dots and line indicate unsuccessful outcomes, (●) green dots and line indicate successful outcomes.

3.8.4.1 Coordination appointment

For samples collected at coordination appointment, immune analytes appeared in 2 distinct clusters with relation to vaginal taxa. The cluster containing IGFBP-1, IL-1β, IL-6 and IL-8 anti-correlated with *L. crispatus* and correlate with *P. indolicus, P. timonensis, F. magna* and *L. iners*. The cluster containing Leptin, IL-10, IL-2, IL-11, IL-12p70, IL-4, IFN-γ, GM-CSF, IL-17a, IL-1ra, LIF and TNF-α closely correlated with one another as well as *P. bivia* and *G. vaginalis*. *L. gasseri* closely associated with E2 (Figure 3.43).

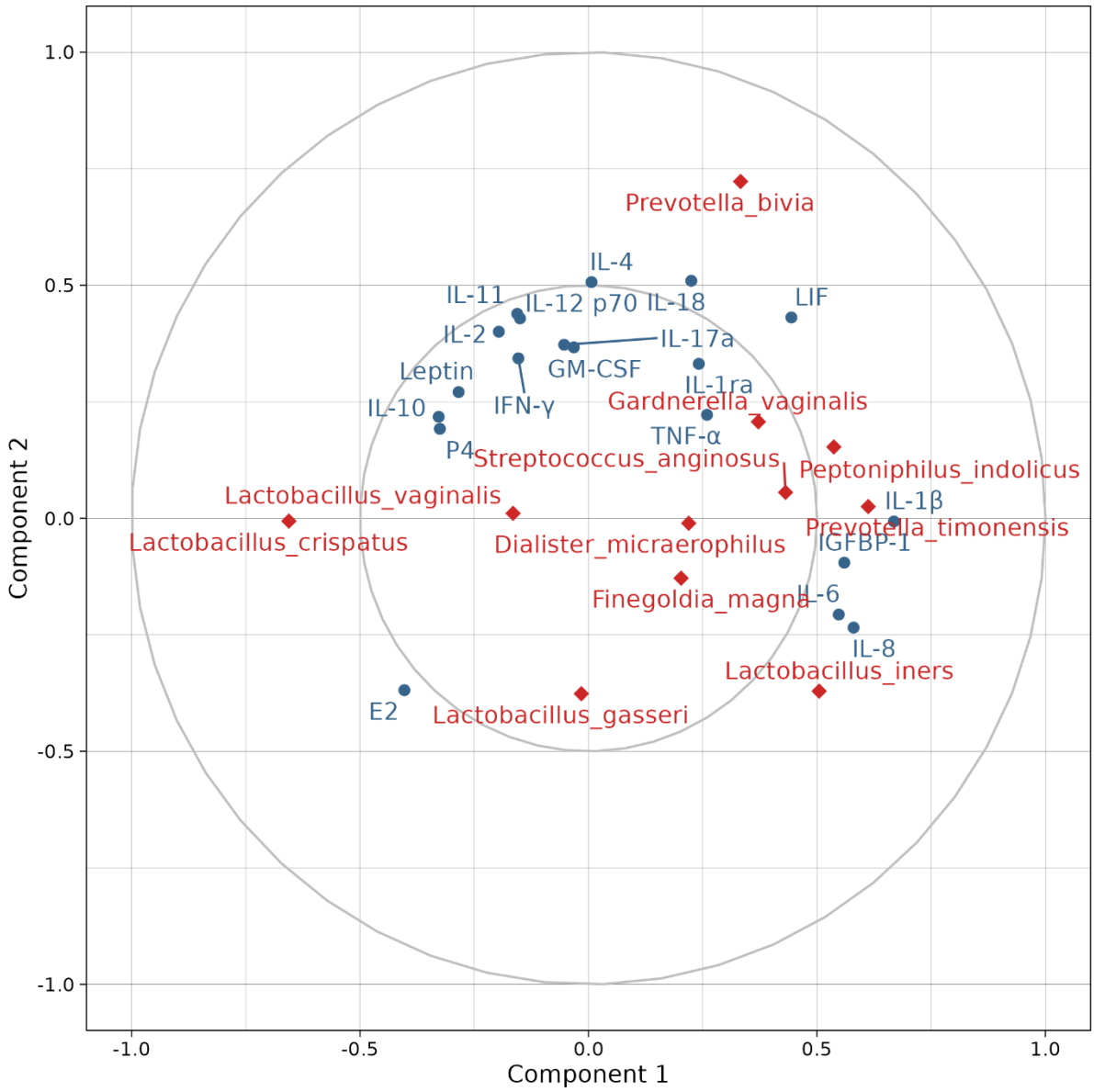


Figure 3.43: CCA variance plot for samples collected at coordination appointment. CCAs for the first 2 principal dimensions of the relationship between microbiota, immune analytes, and serum hormones. Bacteria are indicated in red. Immune analytes and serum hormones are indicated in blue (n=33).

Four significant relationships were identified after p-values were adjusted for multiple testing (Figure 3.44). These were a negative relationship between *L. crispatus* with IL-1β (p=0.003, q=0.03) (Figure 3.45), a positive relationship between *P. indolicus* with IL-1ra (p=0.003, q=0.04) (Figure 3.46). *P. bivia* was positively associated with IL-18 (p=0.001, q=0.01) and LIF (p=0.0006, q=0.008) (Figure 3.47).

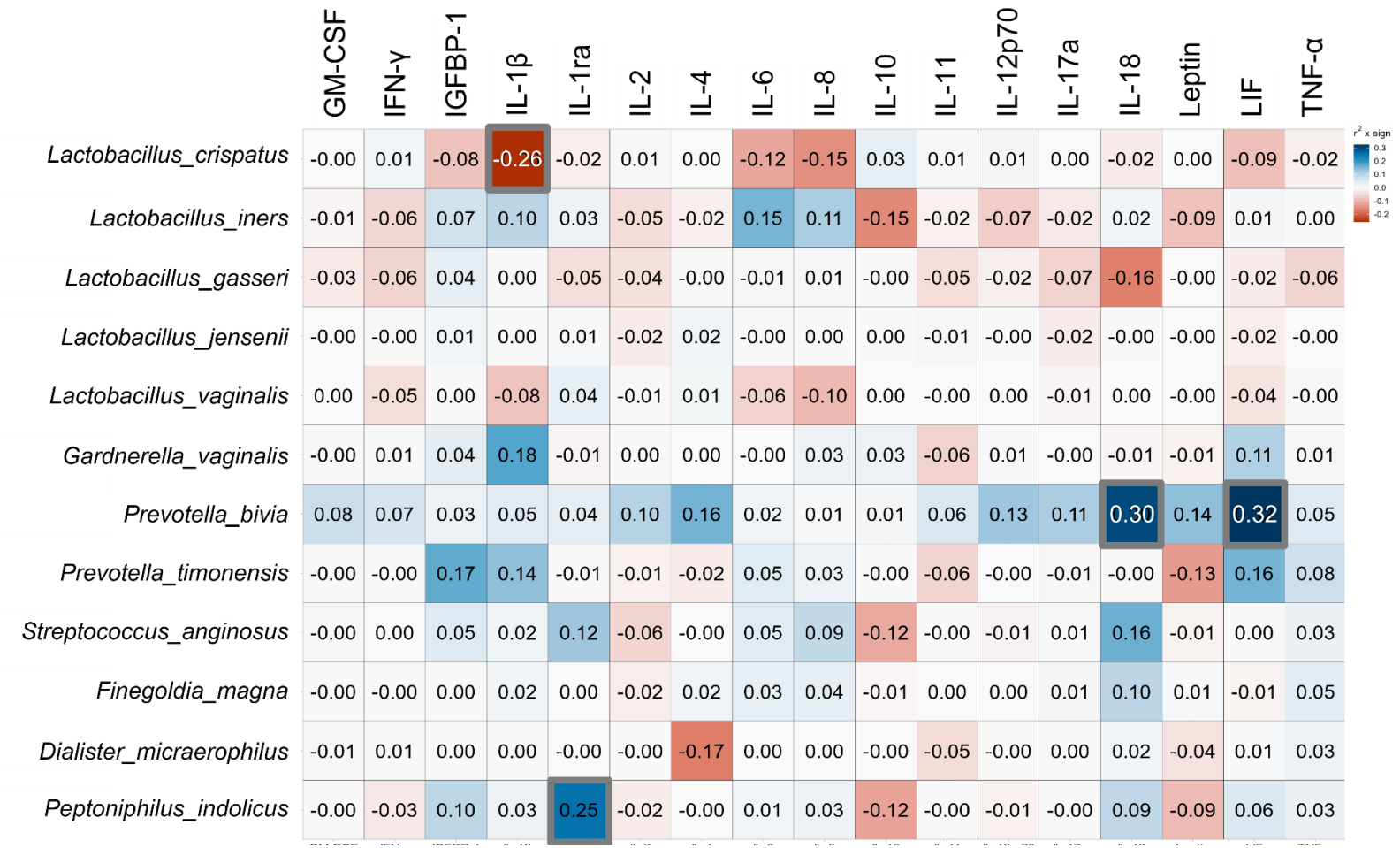


Figure 3.44: Linear regression R2 values for highly abundant taxa and immune analytes for samples collected at coordination appointment. Thick cell-borders indicate a significant q-value Several positive and inverse associations were observed. The blue shades represent positive associations and red shades inverse associations. thick cell-borders indicate a significant q-value (n=33).

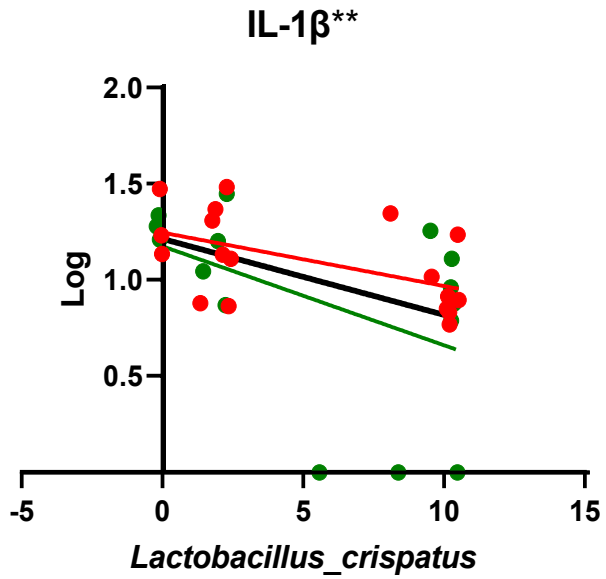


Figure 3.45: Linear regression of *L. crispatus* and IL-1β for samples collected at coordination appointment. CLR transformed relative abundance of *L. crispatus* inversely correlates with IL-1β (p=0.003, q=0.03, R^2=0.01, n=33). (●) Red dots and line indicate unsuccessful outcomes, (●) green dots and line indicate successful outcomes.

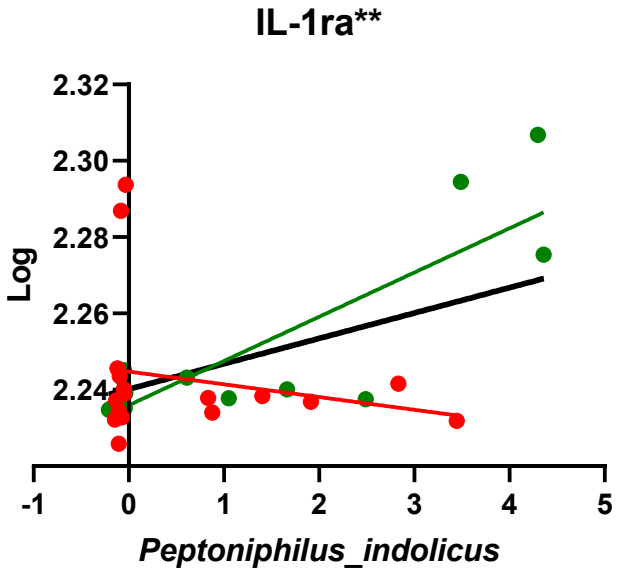


Figure 3.46: Linear regression of *P. indolicus* and IL-1ra for samples collected at coordination appointment. CLR transformed relative abundance of *P. indolicus* positively correlates with IL-1ra (p=0.003, q=0.04, R^2=0.29, n=33). (●) Red dots and line indicate unsuccessful outcomes, (●) green dots and line indicate successful outcomes.

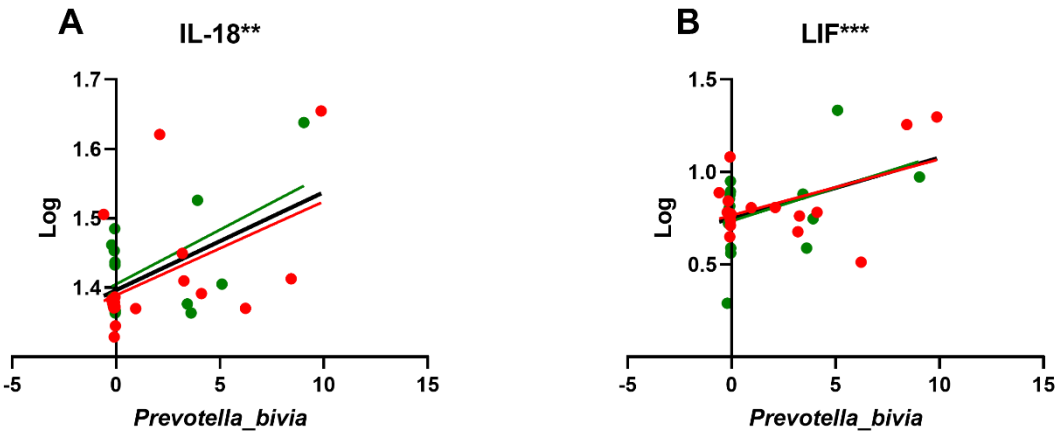


Figure 3.47: Linear regression of *P. bivia* and immune analytes for samples collected at coordination appointment. CLR transformed relative abundance of *P. bivia* positively correlates with A) IL-18 (p=0.001, q=0.01, R^2=0.08), and B) LIF (p=0.0006, q=0.008, R^2=0.05) (n=33). (●) Red dots and line indicate unsuccessful outcomes, (●) green dots and line indicate successful outcomes.

3.8.4.2 Pituitary suppression

For samples collected throughout pituitary suppression, *L. crispatus* and *L. gasseri* anti-correlated with several immune analytes notably IL-1β. E2 was very close to the origin reflecting the very low circulating concentration of E2 at this stage of sample collection. The immune analytes are closely associated with one another, and several BV associated bacteria as well as *L. iners* (Figure 3.48).

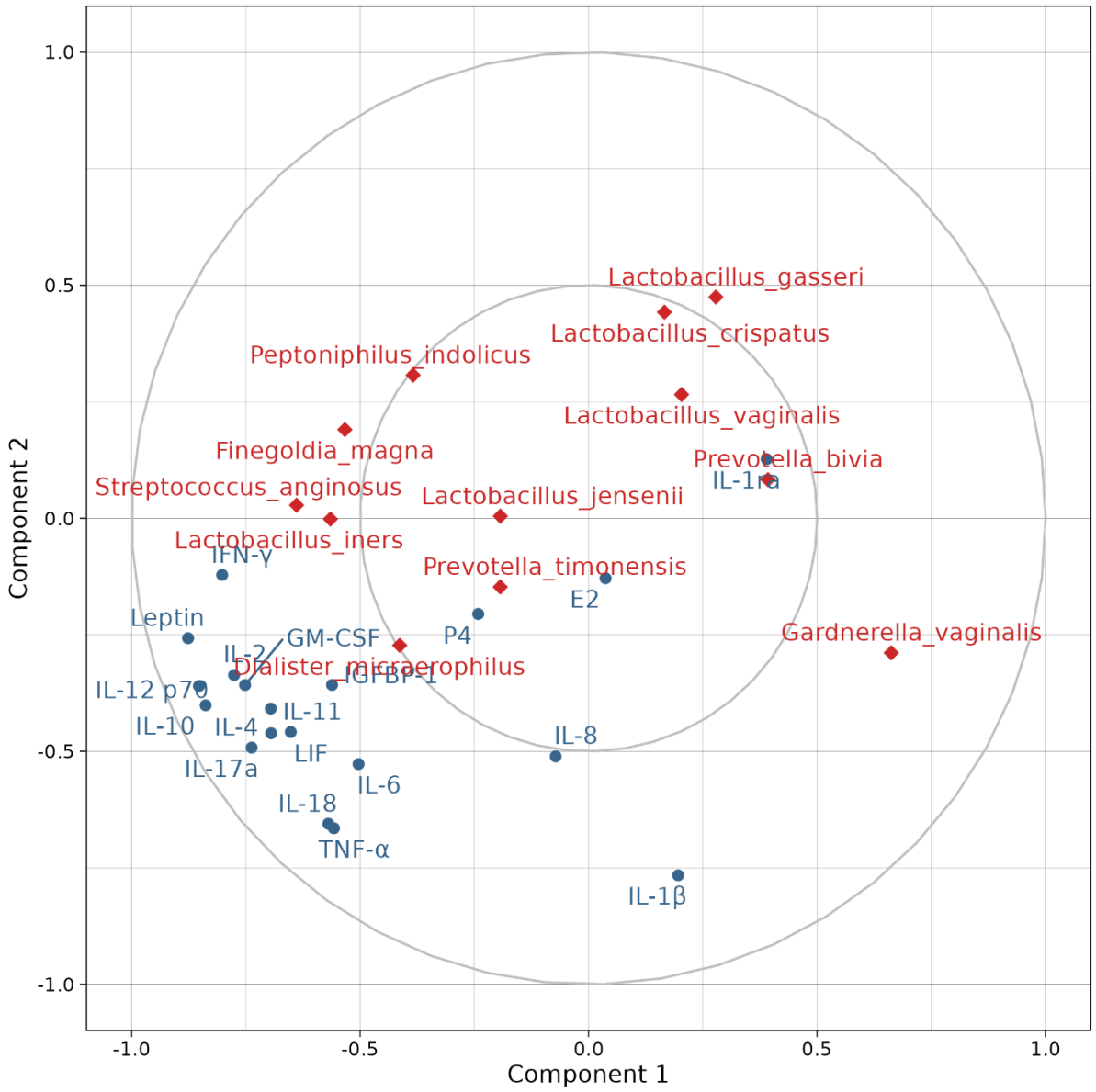


Figure 3.48: CCA variance plot for samples collected throughout pituitary suppression. CCAs for the first 2 principal dimensions of the relationship between microbiota, immune analytes, and serum hormones. Bacteria are indicated in red. Immune analytes and serum hormones are indicated in blue (n=15).

Due to a smaller number of samples available for analysis throughout pituitary suppression (n=15), the R^2 values appeared inflated, however, there were not any significant relationships between highly abundant taxa and immune analytes with respect to the adjusted p-values (Figure 3.49).

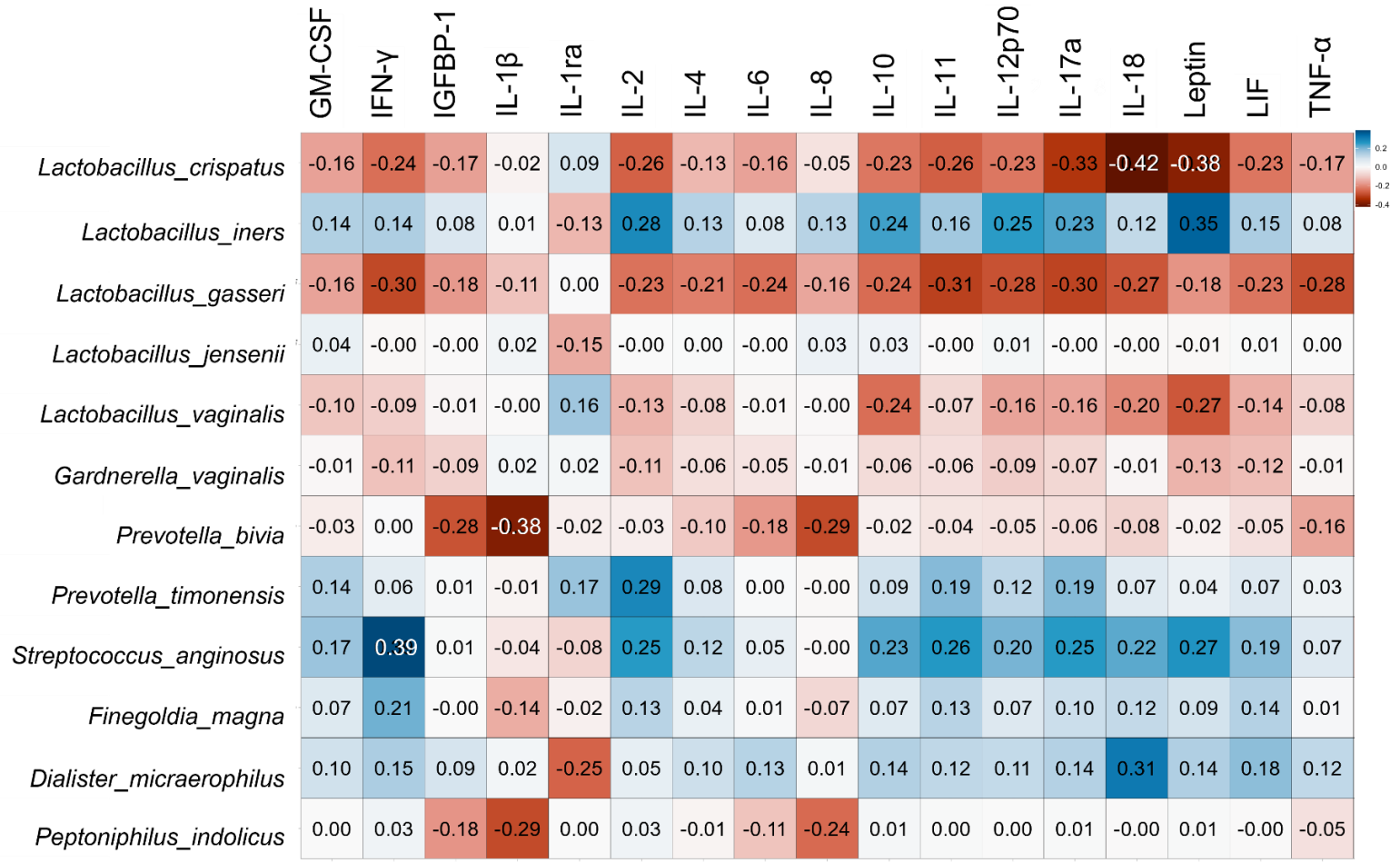


Figure 3.49: Linear regression R2 values for highly abundant taxa and immune analytes for samples collected throughout pituitary suppression. There were no significant associations based on adjusted p-values (n=15).

3.8.4.3 Ovarian stimulation

The interplay between the analytes and taxa composition changed throughout ovarian stimulation compared with pituitary suppression. At high estrogenic state, *S. anginosus, D. microraephilus* and *F. magna* were closely associated with several immune analytes. *L. crispatus* and *L. vaginalis* were positively associated with IL-1ra and E2 but anti-correlated with IL-1β (Figure 3.50).

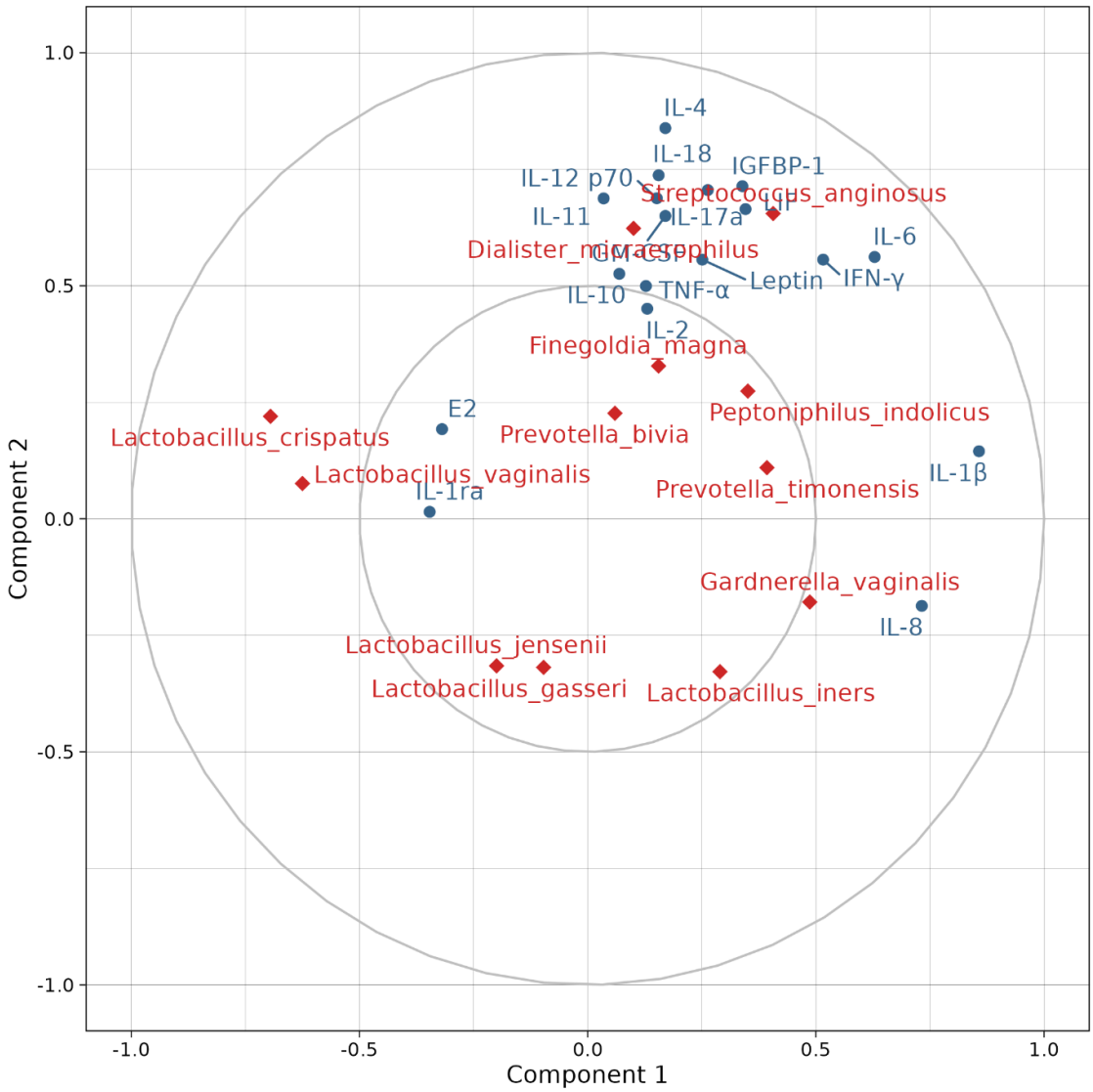


Figure 3.50: CCA variance plot for samples collected throughout ovarian stimulation. CCAs for the first 2 principal dimensions of the relationship between microbiota, immune analytes, and serum hormones. Bacteria are indicated in red. Immune analytes and serum hormones are indicated in blue (n=28).

There were 5 significant relationships identified (Figure 3.51). *S. anginosus* was positively associated with IGFBP-1 (p=0.002, q=0.02) and IL-6 (p=0.002, q=0.03) (Figure 3.52); *D. micraerophilus* was positively associated with IL-4 (p=0.0002, q=0.003), IGFBP-1 (p=0.002, q=0.02) and IL-6 (p=0.002, q=0.03) (Figure 3.53). All observed correlations were positive.

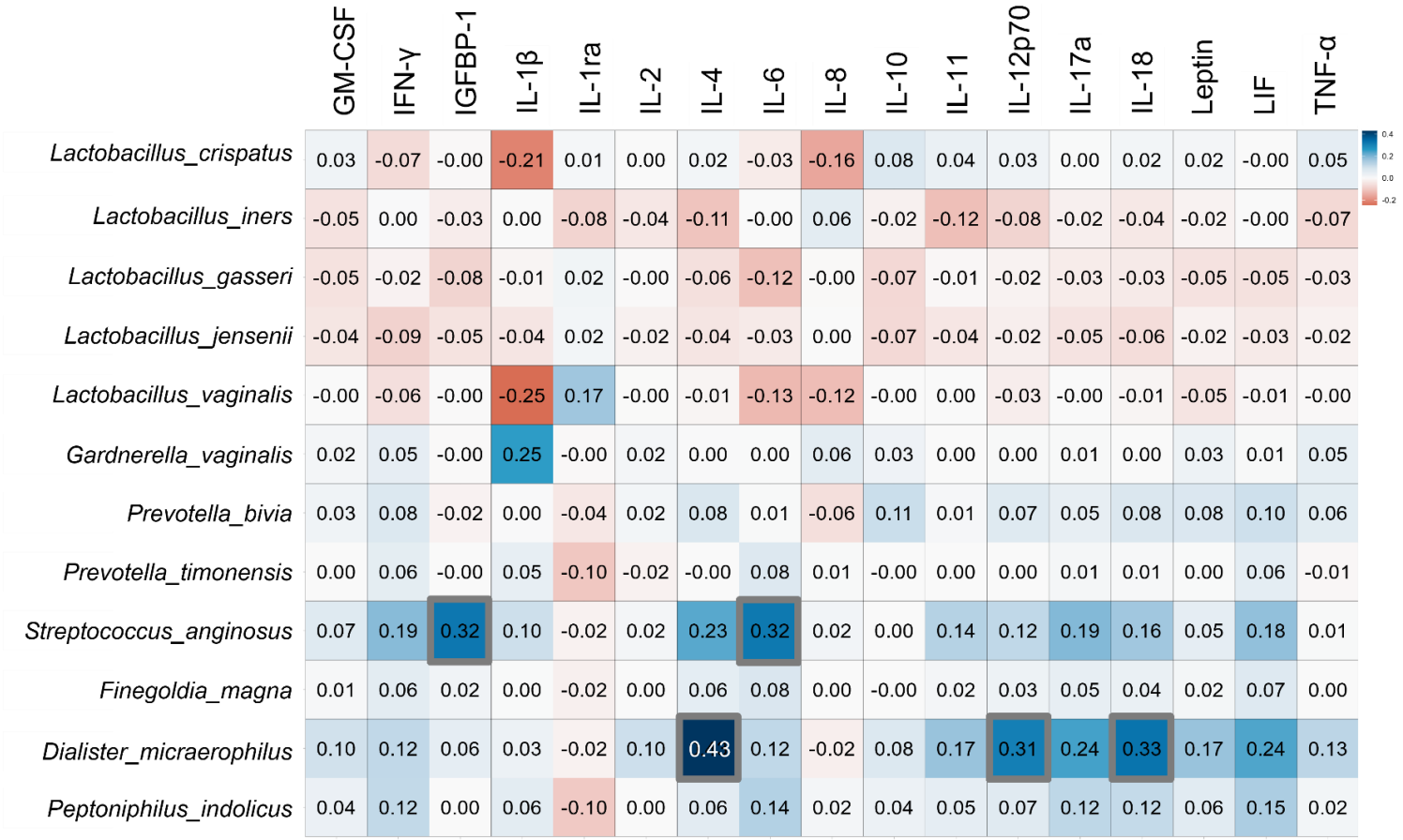


Figure 3.51: Linear regression R2 values for highly abundant taxa and immune analytes for samples collected throughout ovarian stimulation. Several positive and inverse associations were observed. The blue shades represent positive associations and red shades inverse associations Thick cell-borders indicate a significant q-value (n=28).

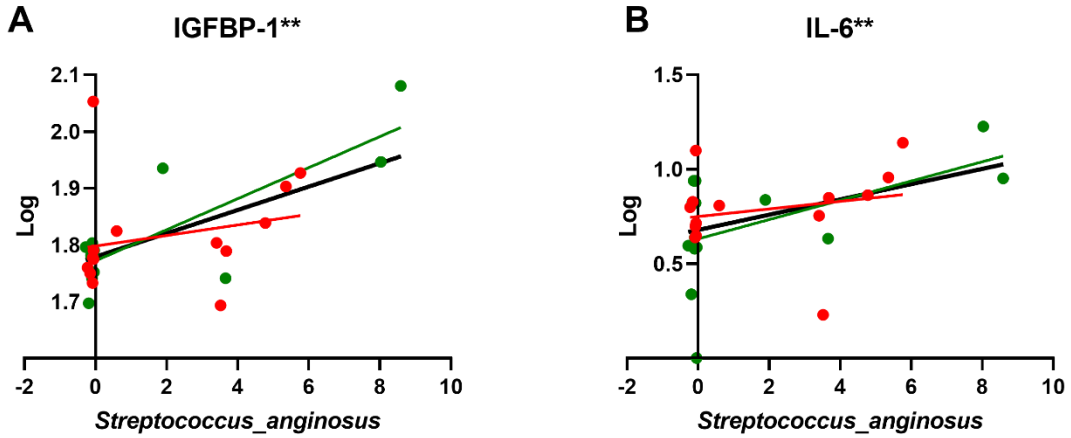


Figure 3.52: Linear regression of *S. anginosus* and immune analytes for samples collected throughout ovarian stimulation. CLR transformed relative abundance of *S. anginosus* positively correlates with A) IGFBP-1 (p=0.002, q=0.02, R^2=0.32), and B) IL-6 (p=0.002, q=0.03, R^2=0.32) (n=28). (●) Red dots and line indicate unsuccessful outcomes, (●) green dots and line indicate successful outcomes.

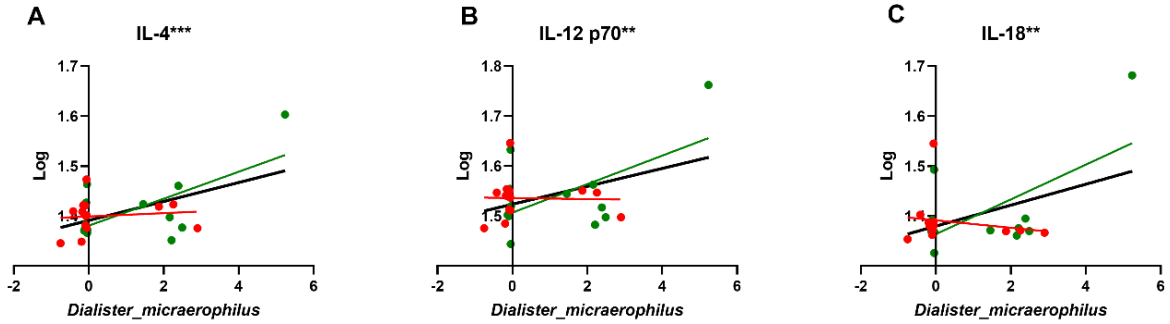


Figure 3.53: Linear regression of *D. micraerophilus* and immune analytes for samples collected throughout ovarian stimulation. CLR transformed relative abundance of *D. micraerophilus* positively correlates with A) IL-4 (p=0.0002, q=0.003, R^2=0.43), B) IL-12p70 (p=0.003, q=0.03, R^2=0.30), and C) IL-18 (p=0.002, q=0.03, R^2=0.33) (n=28). (●) Red dots and line indicate unsuccessful outcomes, (●) green dots and line indicate successful outcomes.

3.8.4.4 Egg collection

For samples collected on the day of egg collection, IL-12p70, IL-10, IFN-γ and IL-18 were closely associated. Another cluster of analyses including TNF-α, IL-4, GM-CSF, IL-2 and IL-17a also correlated with one another. IL-1ra correlated with *L. gasseri* and *L. vaginalis*. *L. iners* correlated with P4. *L. crispatus* anti-correlated with IL-1β (Figure 3.54).

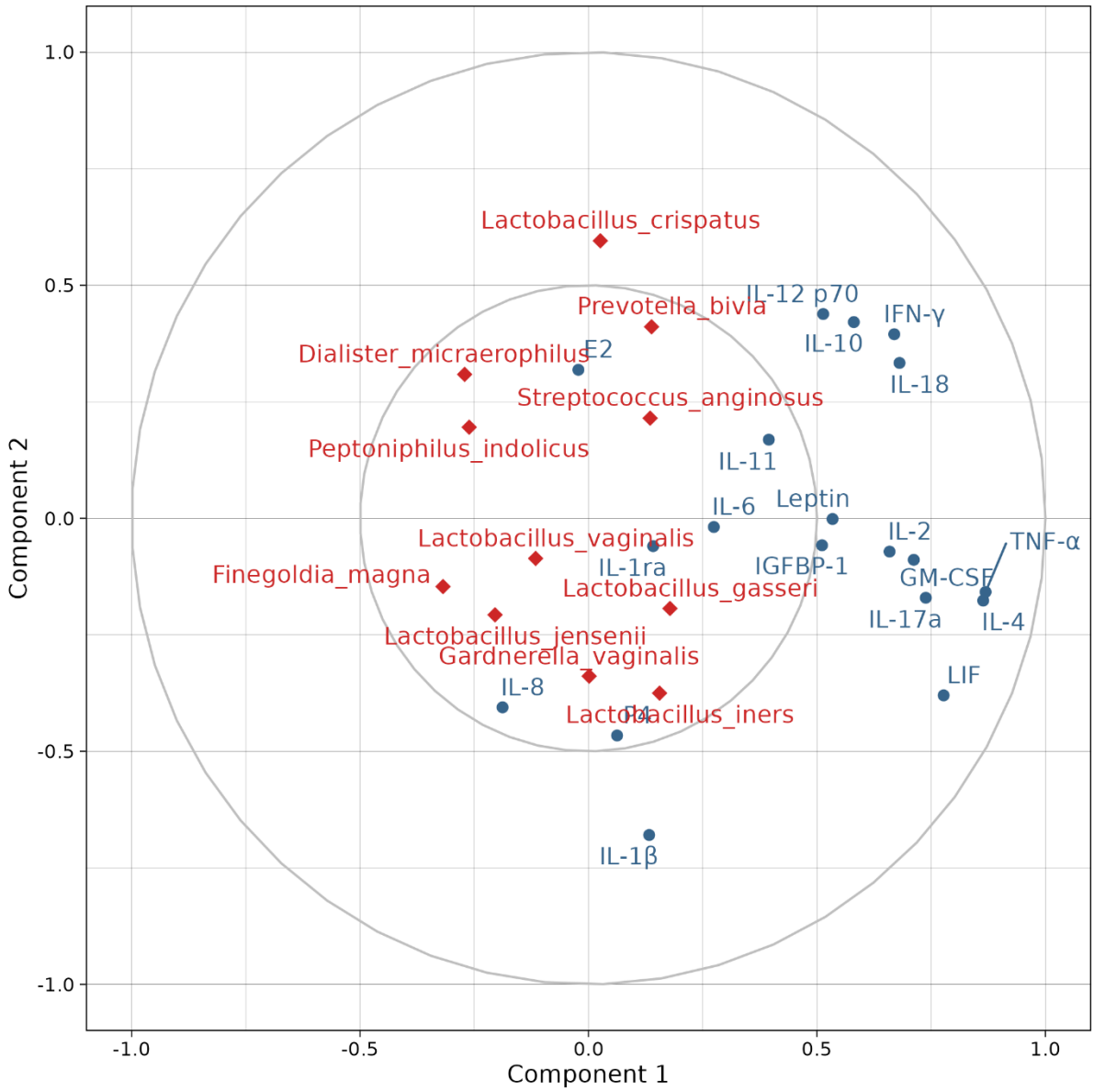


Figure 3.54: CCA variance plot for samples collected on the day of egg collection. CCAs for the first 2 principal dimensions of the relationship between microbiota, immune analytes, and serum hormones. Bacteria are indicated in red. Immune analytes and serum hormones are indicated in blue (n=28).

The only significant (negative) correlation observed with respect to adjusted p-values was between *L. crispatus* and IL-1β (p=0.003, q=0.04) (Figures 3.55 and 3.56).

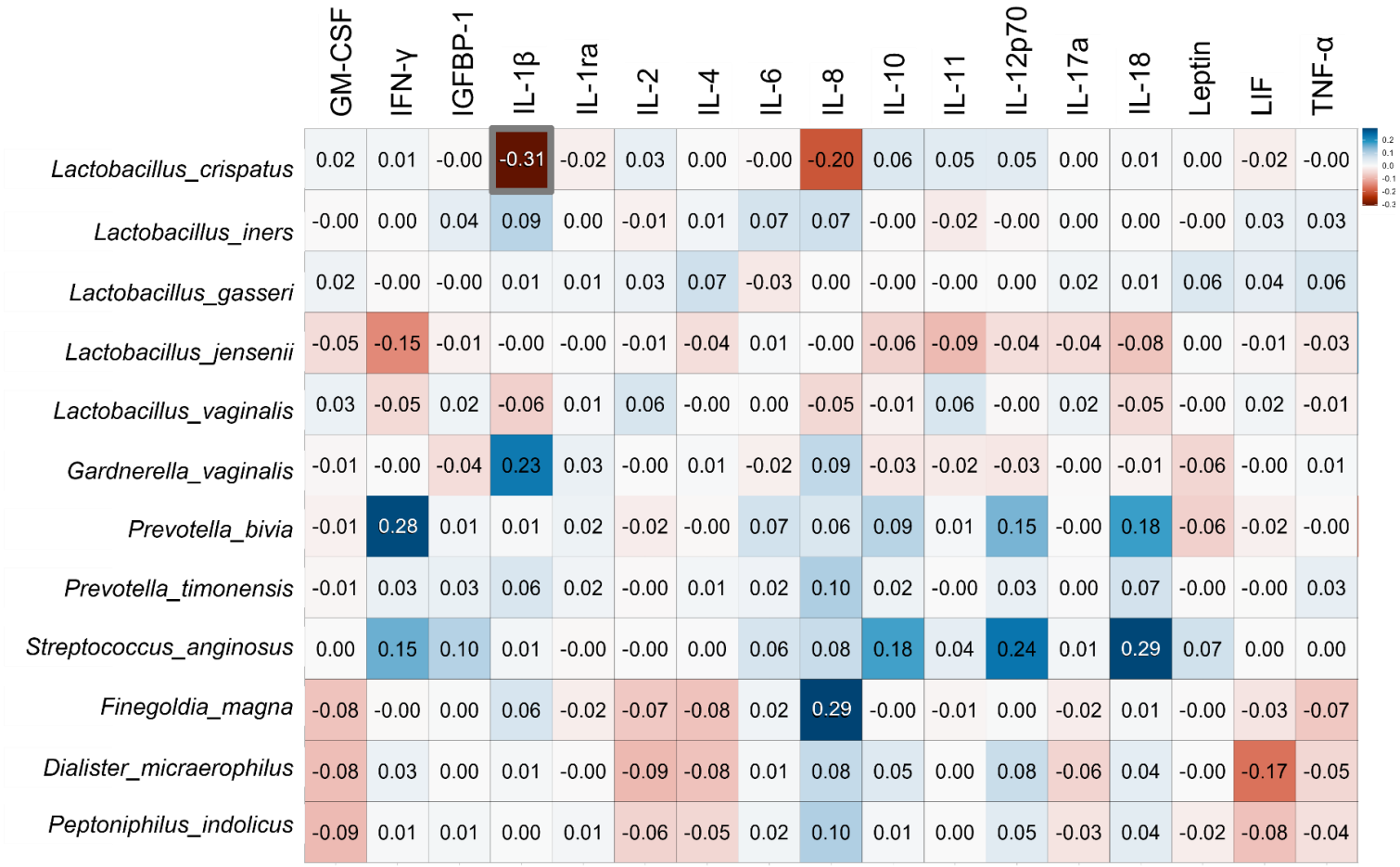


Figure 3.55: Linear regression R2 values for highly abundant taxa and immune analytes for samples collected on the day of egg collection. Several positive and inverse associations were observed. The blue shades represent positive associations and red shades inverse associations. thick cell-borders indicate a significant q-value. Thick cell-borders indicate a significant q-value (n=28).

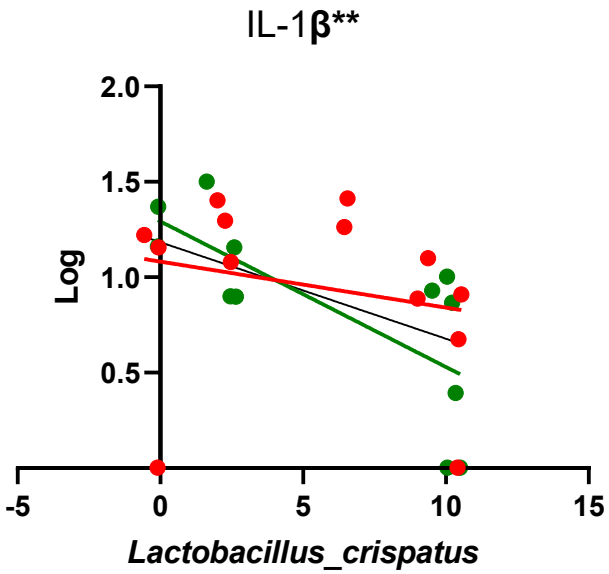


Figure 3.56: Linear regression of *L. crispatus* and IL-1β for samples collected on the day of egg collection. CLR transformed relative abundance of *L. crispatus* inversely correlates with IL-1β ($p=0.003$, $q=0.04$, $R^2=0.30$, $n=25$). (●) Red dots and line indicate unsuccessful outcomes, (●) green dots and line indicate successful outcomes.

3.8.4.5 Embryo transfer

Several immune analytes were clustered and closely associated including TNF-α, IL-12p70, IL-17a, IGFBP-1, GM-CSF, IL-10, IL-4, Leptin, IL-18, IL-2, IL-6, and LIF. *Lactobacillus* species were closely associated with this cluster of cytokines. *L. crispatus* and *G. vaginalis* negatively and positively correlate with IL-1β (Figure 3.57).

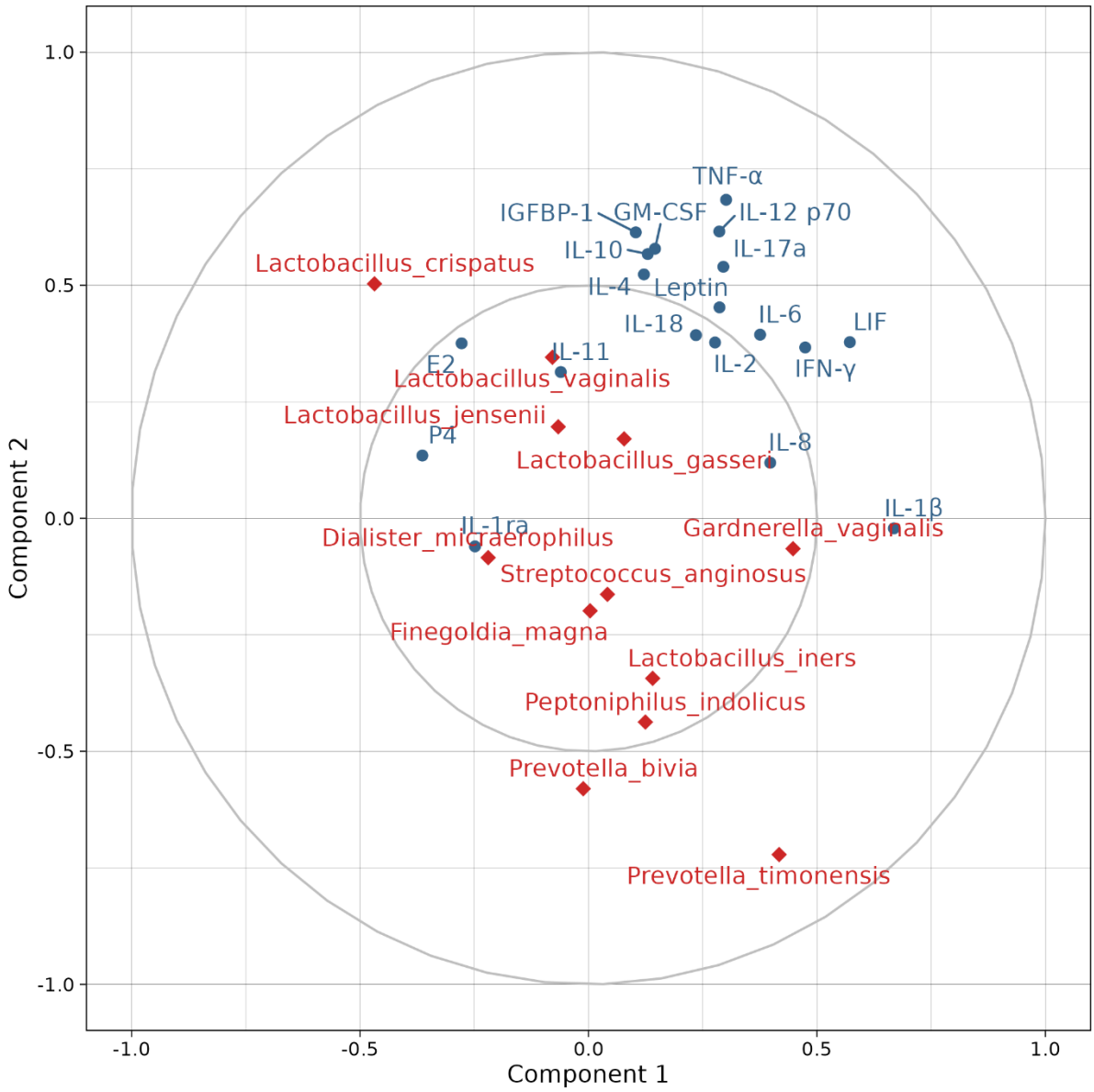


Figure 3.57: CCA variance plot for samples collected on the day of embryo transfer. CCAs for the first 2 principal dimensions of the relationship between microbiota, immune analytes, and serum hormones. Bacteria are indicated in red. Immune analytes and serum hormones are indicated in blue (n=27).

There were no significant relationships observed between any of the highly abundant taxa and immune analytes with respect to adjusted p-values (3.58).

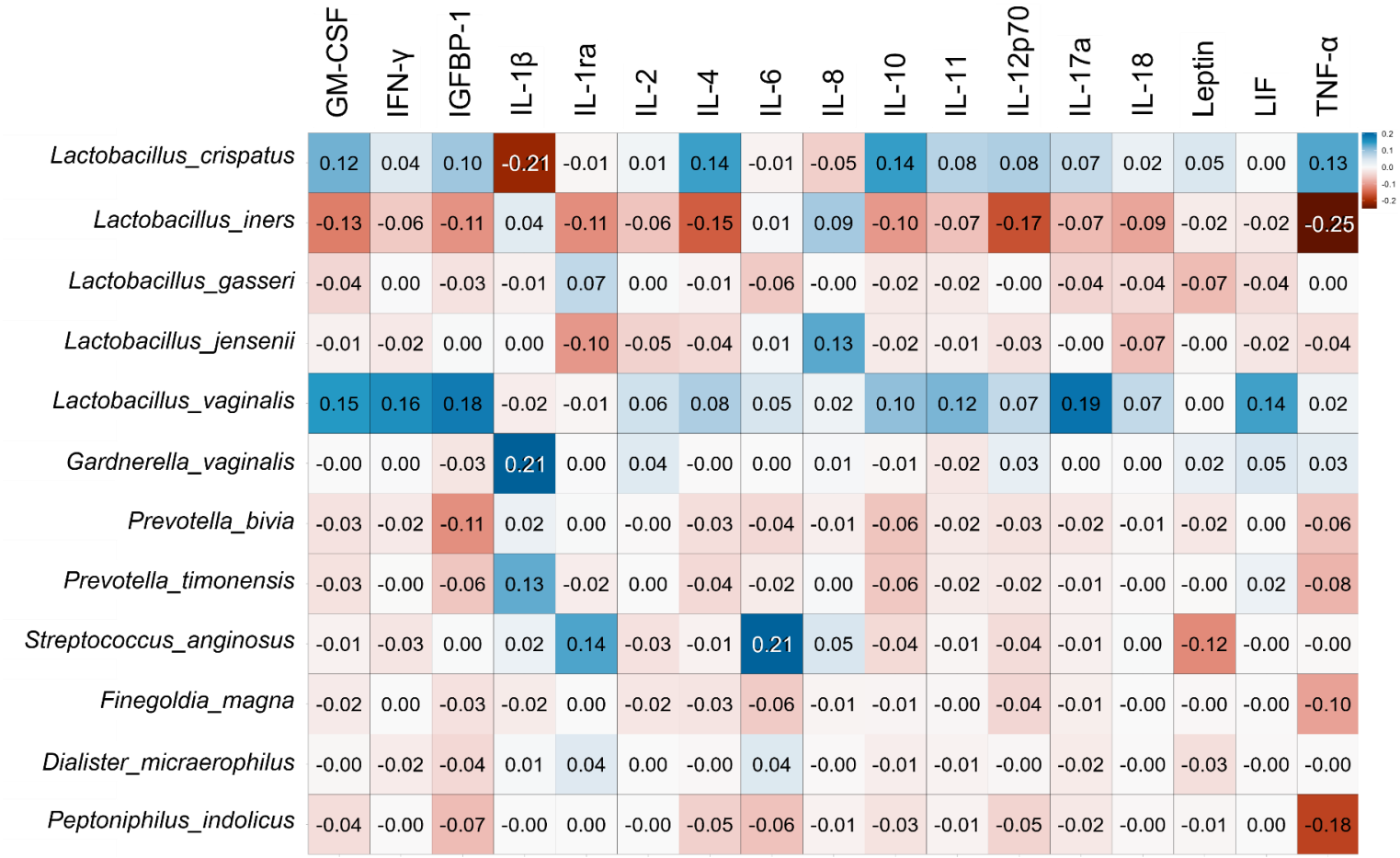


Figure 3.58: Linear regression R2 for highly prevalent taxa and immune analytes for samples collected on the day of embryo transfer. There were no significant associations based on adjusted p-values (n=27).

3.8.5 Within patient changes in vaginal microbiota across clinical sampling timepoints

Within patient changes in relative abundance of highly abundant taxa were next assessed across paired samples collected at subsequent clinical visits. The transitions between consecutive stages of sample collection were done for patients with data available at sequential key timepoints throughout fresh IVF cycles.

3.8.5.1 Coordination appt to pituitary suppression

Within patient changes for vaginal taxa were assessed in the transition from samples collected at coordination appointment and throughout pituitary suppression. *P. timonensis* abundance was reduced from the hormonally unregulated stage to the low estrogenic state (Figure 3.59). No other significant changes were observed for other taxa during this transition.

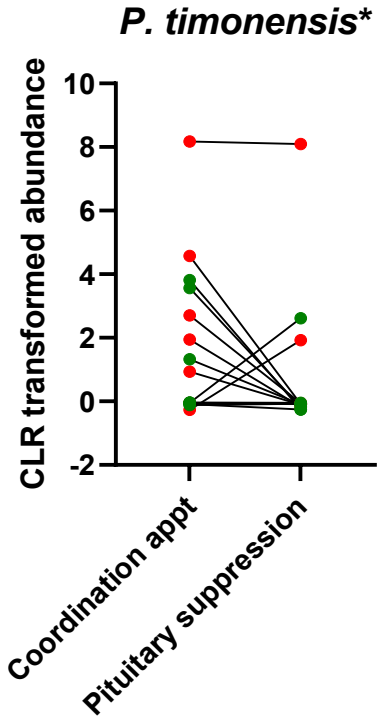


Figure 3.59: Within patient abundance change of *P. timonensis* for samples collected at coordination appointment and throughout pituitary suppression. CLR transformed abundance of *P. timonensis* was reduced from coordination appointment to pituitary suppression. Pairwise Wilcoxon signed rank test (p=0.04, n=15). (●) Red dots indicate unsuccessful outcomes, (●) green dots indicate successful outcomes.

3.8.5.2 Pituitary suppression to ovarian stimulation

Abundance of *P. timonensis*, *F. magna* and *P. indolicus* increased from pituitary suppression to ovarian stimulation (Figure 3.60).

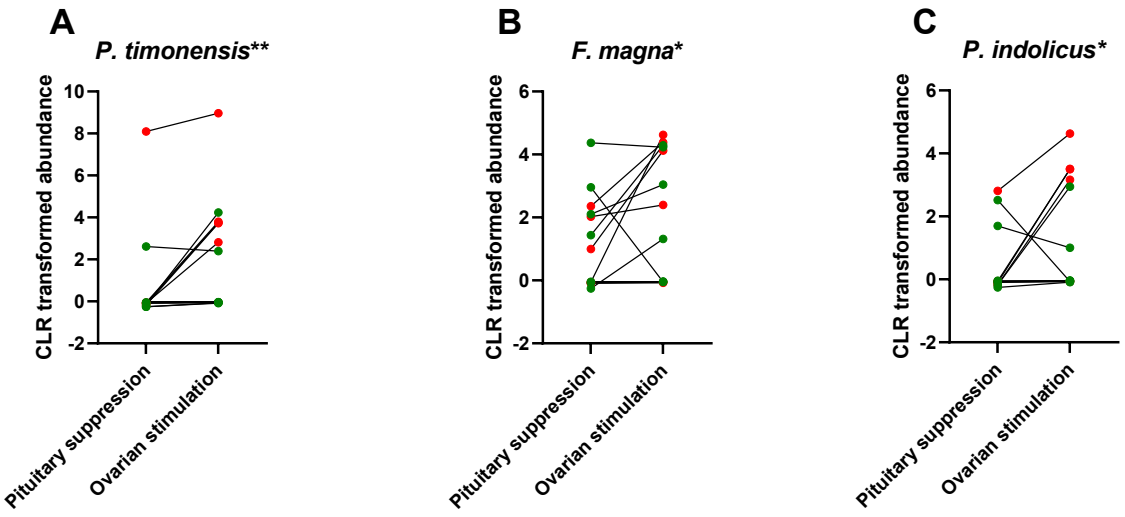


Figure 3.60: Within patient relative abundance changes of vaginal taxa throughout pituitary suppression to ovarian stimulation. CLR transformed abundance of A) *P. timonensis* (p=0.006), B) *F. magna* (p=0.04), and C) *P. indolicus* (p=0.04) increased from pituitary suppression to ovarian stimulation. Pairwise Wilcoxon signed rank tests (n=13). (●) Red dots indicate unsuccessful outcomes, (●) green dots indicate successful outcomes.

3.8.5.3 Ovarian stimulation to egg collection

There were no significant changes observed in relative abundance of the highly abundant taxa in transition from ovarian stimulation to the day of egg collection. This analysis included 22 cycles for which samples was available throughout ovarian stimulation and on the day of egg collection.

3.8.5.4 Egg collection to embryo transfer

Abundance of *F. magna* decreased from egg collection to embryo transfer (Figure 3.61).

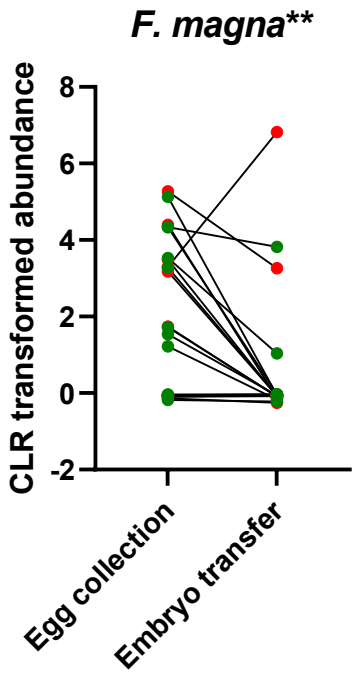


Figure 3.61: Within patient relative abundance changes of vaginal taxa from egg collection to embryo transfer. CLR transformed abundance of *F. magna* (p=0.002) decreased from egg collection to embryo transfer. Pairwise Wilcoxon signed rank tests (n=24). (●) Red dots indicate unsuccessful outcomes, (●) green dots indicate successful outcomes.

3.9 Vaginal bacteria random forest modelling for predicting IVF success rates

The analysis in previous sections of this chapter alluded to the E2 dependant relationships between immune analytes and vaginal bacteria. The significance of some of these interactions also related to successful clinical outcomes. To assess the biomarker feasibility of these interactions, random forest modelling was used for samples collected on the day of embryo transfer. Data modelling was done for CST classifications and specific ASVs (CLR transformed) as well as their interactions with host hormones and immune analytes. ROC curves were very close to the line representing random chances indicating that they do not have strong specificity and sensitivity. This suggested that the ability of vaginal microbiota in predicting IVF success rates was not strong on the day of embryo transfer.

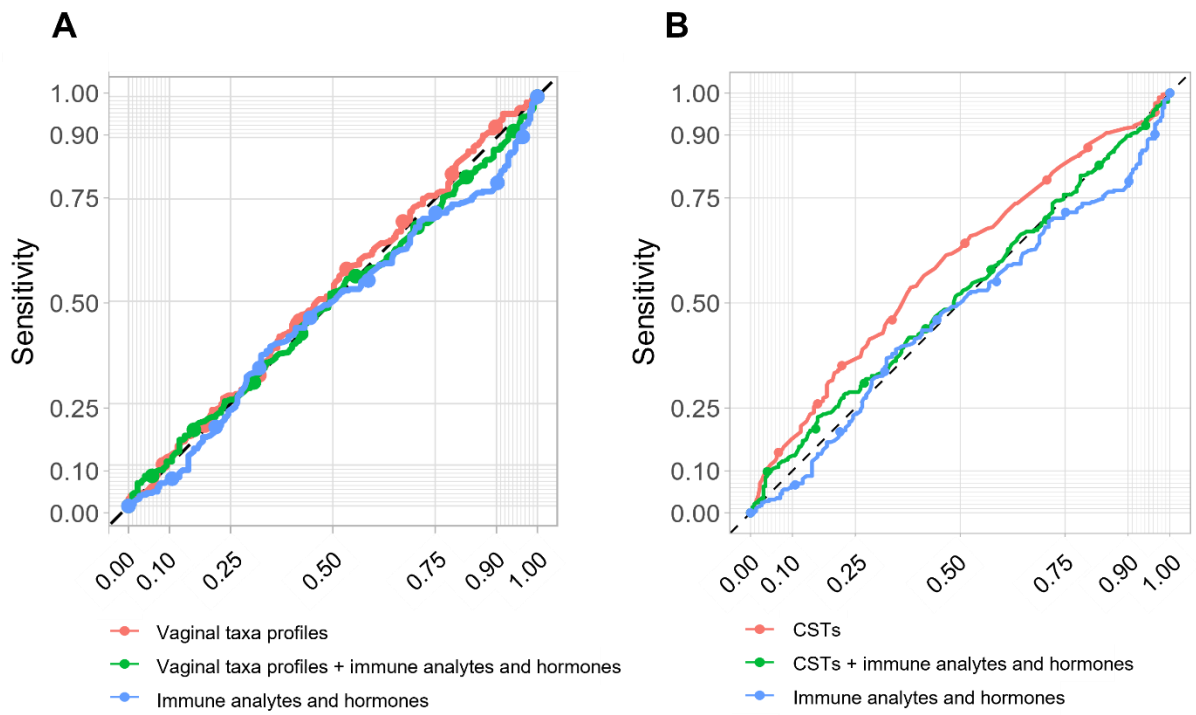


Figure 3.62: Capacity of vaginal microbiota, immune analytes and hormones to predict IVF clinical success rates tested using random forest classifiers. A) Three random forest models were built based on vaginal taxa profiles only (AUC: 0.48 ± 0.17), vaginal taxa profiles plus host immunity and hormones (AUC: 0.49 ± 0.13), and host immunity and hormones only (AUC: 0.48 ± 0.15). Area under the curve values suggested poor capacity to predict IVF clinical success rates. B) Random forest modelling based on CST profiles (AUC: 0.44 ± 0.14) and CST, hormones, and immune response profiles (AUC: 0.53 ± 0.13). No strong predictive model based on CSTs and host immunity and response was observed.

Table 3.12: Performance metrics for the random forest predictions models.

Metrics	Vaginal taxa	Vaginal taxa + hormones + immune profiles	CST profiles	CST+ hormones+ immune profiles	Hormones+ immune profiles
AUC (±SD)	0.48 (0.17)	0.49 (0.13)	0.44 (0.14)	0.53 (0.13)	0.48 (0.15)
F1 (±SD)	0.42 (0.15)	0.42 (0.15)	0.38 (0.13)	0.41 (0.14)	0.43 (0.16)
Sensitivity (±SD)	0.39 (0.22)	0.41 (0.20)	0.28 (0.20)	0.39 (0.18)	0.41 (0.23)
Specificity (±SD)	0.58 (0.21)	0.58 (0.22)	0.61 (0.24)	0.62 (0.19)	0.56 (0.21)
Balanced accuracy (±SD)	0.49 (0.13)	0.50 (0.12)	0.44 (0.14)	0.50 (0.11)	0.49 (0.13)

3.9.1 Prediction of IVF success using ReceptIVFity™-type vaginal microbiome parameters

A recent study from Koedooder and colleagues reported that at the time of the first clinical visit, the ratio of *L. crispatus* to *L. iners* at 60% relative abundance is a marker of successful clinical outcomes (196). Therefore, a similar approach to predict IVF outcome was performed using relative abundance data for the samples collected at coordination appointment. No relationships with IVF clinical outcomes were identified using this approach (p=0.99, Fisher's exact test).

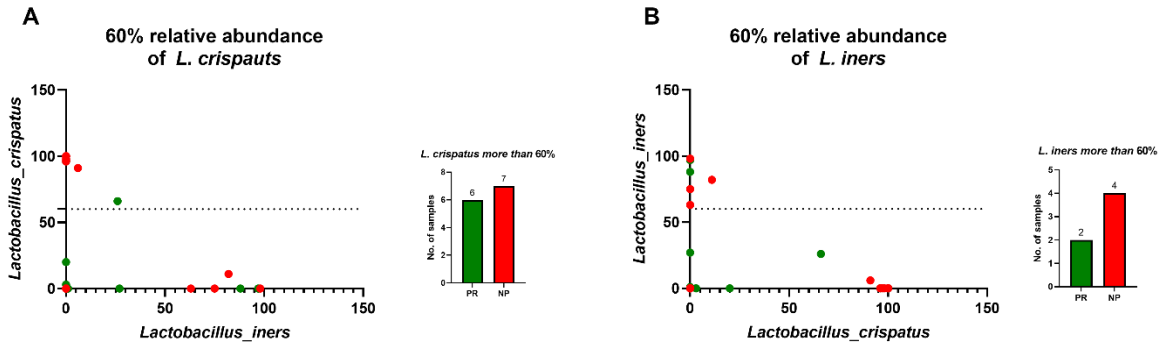


Figure 3.63: Clinical success predictability model based on the ReceptIVFity study. A) 60% relative abundance of *L. crispatus*, B) 60% relative abundance of *L. iners*.

3.10 Discussion

One of the first objectives of the research described in this chapter was to investigate and characterise the potential interplay between hormones, microbiota and immune response in women undergoing IVF treatment and ultimately to determine if these factors are important modulators of clinical outcome. Initially it was planned that samples collected from patients undergoing either fresh or frozen IVF cycles would be combined and analysed collectively, given that there exist commonly defined clinical stages between the two (i.e., coordination appointment, pituitary suppression, and embryo transfer). However, analysis of hormonal levels collected from fresh and frozen cycles showed major differences in the concentrations of E2 at these clinical stages (Figure 3.3). In natural cycles, E2 concentrations reach between 300-400 pg/mL prior to ovulation. In women undergoing IVF treatment, successful embryo implantation has been reported over a wide range of E2 concentrations (10 to 1000 pg/mL) (511, 512). Concentrations of E2 in excess of 2300 pg/mL have been associated with reduced implantation rates (46) although there are some reports of successful clinical outcomes in women with E2 levels >3000 pg/mL on the day of ET (513). While these differences may reflect the underlying aetiologies driving impaired fertility in these women, it is also possible that differences in hormonal levels between the cohorts was due to differences in the treatment protocols used. The two major suppression/stimulation protocols used here were the Long Day 21 (LD21) cycle gonadotropin-releasing hormone agonist (luteal phase support) and GnRH antagonist. The choice of protocol was determined by the clinical team and was dependent on several factors including patient history and demographics. For example, in patients with maternal age of <35 years old and within their first 3 IVF attempts, a midluteal GnRHa protocol has been shown to produce superior clinical pregnancy rates (41.2%) than GnRH antagonist protocol (25.3%) (514). In patients with a history of repeated IVF failures, the GnRHa protocol has been reported to result in a higher rate of successful outcomes (20.8%) compared with GnRH antagonist (14.5%) (515), and is associated with higher endometrial thickness and receptivity (516). However, several studies have also reported no significant differences in pregnancy outcomes between GnRHa and GnRH antagonist protocols (517-519). Consistent with these latter findings, we did not observe any statistically significant differences in clinical pregnancy rates based on treatment protocols in this cohort (GnRHa 11 pregnancies (60%) verses GnRH antagonist 5 cycles (45%)) (Table 3.2).

Of the women undergoing a frozen cycle in the ART1 cohort, 6/7 were treated with the LD21 protocol whereas 20/32 women received the LD21 protocol during fresh cycle treatment. However, it is important to note that unlike women undergoing fresh cycle treatment, women sampled during a frozen cycle do not undergo ovarian stimulation or egg collection prior to

embryo transfer. Because of these major differences in hormonal levels and treatment procedures, subsequent analyses designed to investigate microbiota-host interactions in the context of differing hormonal environments were limited to those women undergoing fresh cycles.

Vaginal microbiota are strongly linked to the local immune response in various contexts of reproductive health (520). The expression of vaginal immune analytes on the day of ET was associated with successful embryo implantation in our study cohort. Therefore, it was hypothesised that specific vaginal microbiota may be key modulators of the levels of these immune markers. To explore this, analyses were performed on the most abundant vaginal species (25% prevalence, Figure 3.22) as well as CST classifications of the vaginal microbiota (133, 142). CST classification of the vaginal microbiota have been widely used to identify links between sub-optimal vaginal microbiota and increased risks of sexually transmitted diseases, preterm birth, and clinical IVF outcomes (204, 521-523). CST I (*L. crispatus* dominated) is widely considered to represent the optimal vaginal environment for reproductive health and function (524, 525). In contrast, CST IV profiles are enriched for BV associated bacteria including *G. vaginalis* and *Candidatus* Lachnocurva vaginae (previously known as BVAB1) and are associated with adverse reproductive outcomes (142, 526). In this cohort, no differences were observed in the proportions of CSTs with respect to clinical outcome following IVF treatment (Tables 3.9 and 3.10). However, a trend increase in the proportion of CST I in samples with successful clinical outcomes was observed at all sample timepoints (Table 3.9). Similarly, successful clinical outcomes were associated with Lacto-dominant samples at the time of embryo transfer (86% v 57%) (Table 3.10). This is consistent with earlier findings indicating that dominance of the vagina by *Lactobacillus* species, particularly *L. crispatus,* is associated with higher rates of successful clinical outcomes (196, 217, 498, 499, 527). It is possible that prevalence of CST I was not significantly associated with successful pregnancy in our study cohort due to the restricted sample size. However, several other studies have failed to identify a relationship between vaginal microbiota and clinical outcomes of IVF (213, 528). For example, Vergaro et al. reported that BV associated compositions do not affect live birth rates at the time of ET (220) and Mangot-Bertrand et al. found that embryo implantation rates of women with BV at the time of egg collection were not statistically significant (218). However, these studies are all limited to relatively small patient populations and there remains a clear need to undertake larger scale investigations of the vaginal microbiota in the context of IVF treatment success.

One of the proposed mechanisms supporting improved reproductive health outcomes in women with *Lactobacillus* species dominance of the vagina involves increased stability of the microbiome, which helps to repel colonisation by pathogens. This appears to be particularly

important during pregnancy and is associated with healthy term births. For example Romero et al., found that *Lactobacillus* species were the dominant species throughout normal pregnancies and *L. vaginalis*, *L. crispatus*, *L. gasseri* and *L. jensenii* associated with high levels of stability (146). Similarly, MacIntyre et al. reported that *L. crispatus* was associated with low α-diversity and richness and greater stability during pregnancy (145) and women with reduced stability have higher rates of preterm birth (483). However, no difference in microbiota stability across cycles was observed between successful and unsuccessful IVF outcomes in this patient cohort (Figure 3.26).

Previous studies have indicated a link between vaginal E2 levels and increased dominance by *Lactobacillus* species (529, 530). This is thought to be mediated via E2 mediated deposition of glycogen into vaginal epithelial cells which can be used as a preferential food source by *Lactobacillus* species (501, 502). In the current study the prevalence of *Lactobacillus* associated CSTs did not significantly increase following ovarian stimulation which may indicate that supraphysiological levels of E2 do not further potentiate a *Lactobacillus* dominated vaginal microbiome (Figure 3.24). It may also be possible that the timespan between samples collected at coordination appointment and pituitary suppression were not long enough for the glycogen depositions to be depleted in absence of E2. Recently, Carosso et al. (239) reported that ovarian stimulation and P4-support throughout the IVF cycle significantly changed the vaginal microbiota by reduction of *Lactobacillus* and increasing *Atopobium* and *Prevotella*. However, similar results were not observed here and others have also reported no change on the vaginal microbiome in women receiving vaginal progesterone supplementation during pregnancy (204).

The dynamics of hormones, immune analytes and bacteria were modelled using CCA to illustrate shared correlations between bacteria and the host (Figures 3.35, 3.43, 3.48, 3.50, 3.54 and 3.57). Data were then analysed to identify specific linear relationships between cervico-vaginal bacteria compositions and immune analytes (Figures 3.36, 3.44, 3.49, 3.51, 3.55 and 3.58). In cross-sectional data modelling, an inverse correlation between *L. crispatus* and IL-1β was consistently observed. *L. crispatus* dominance of the vaginal niche has been associated with low vaginal inflammation in many studies (359, 360, 531, 532). However interestingly, the anticorrelation between *L. crispatus* and IL-1β was not observed in the low estrogenic state of pituitary suppression (Figure 3.49). IL-1β is a proinflammatory cytokine involved in strong and rapid immune responses and its transcription is generally inhibited by E2 via the action of estrogen receptors (533). In presence of pathogens however, a dose dependant response of E2 stimulates monocyte secretion of IL-1β. Further, pattern recognition receptors expressed on the surface of vaginal epithelial cells such as TLR2, 3, 5, and 6 drive upregulation of inflammatory analytes such as IL-1β, IL-6 and IL-8 under the influence of E2

(533). The E2 concentrations during pituitary suppression resembled that of post-menopausal women (<20 pg/mL) (Figure 3.2). In addition to lack of immune modulation, the low concentration of E2 disrupt modulation of nitric oxide activity, antioxidative effects and plasma membrane actions that can lead to altered immune cell functions (534, 535). The altered role of immune analytes in response to bacteria at low estrogenic states was further highlighted by the relationship pattern exhibited between *G. vaginalis* and IL-1β. *G. vaginalis* positively correlated with IL-1β cross-sectionally except for the time of pituitary suppression (Figure 3.49).

The CCA modelling at the hormonally unregulated time of coordination appointment, also identified a close association between P4 and Leptin (Figure 3.43). P4 has been previously shown to regulate Leptin during the menstrual cycle particularly during the luteal phase of the cycle (536, 537). P4 was also associated with IL-2 and IL-10, which are anti-inflammatory cytokines. *F. magna*, *S. anginosus* and *L. iners* were closely associated with IGFBP-1, IL-6, and IL-8. IL-6 is pro-inflammatory cytokine and IL-8 is a neutrophil chemoattractant and links between these immune analytes and pathogenic vaginal bacteria such as *F. magna* have previously been reported (538). *P. bivia* and *G. vaginalis* were closely associated with IL-1ra, IL-18 and LIF. The close association between *P. bivia* and *G. vaginalis* is understood to play a key role in onset of BV as *P. bivia* supports establishment and maintenance of *G. vaginalis* biofilms (539). *P. bivia* is an anaerobe associated with production of epithelial cytokines (540, 541). *P. bivia* produce lipopolysaccharides and ammonia that can create a toxic vaginal environment capable of damaging the host (542, 543).

At ovarian stimulation, immune analytes were not closely associated with *Lactobacillus* species (Figure 3.50). Instead, *S. anginosus* and *D. micraerophilus* were found to associate with several inflammatory markers such as IGFBP-1, IL-6, IL-12p70, and IL-18. The role of *Dialister* species in infections has been outlined in the literature (544), however, the clinical significance in relation to vaginal inflammation has not been fully described. The observations of the current study suggest that *D. micraerophilus* induces strong inflammation particularly during artificial hormonal manipulations. *S. anginosus* has emerged as a pathogen causing aerobic vaginitis (AV), a type of vaginal infection caused by aerobic bacteria (545). *S. anginosus* can cause lysis of the vaginal epithelia cells. Overall, these findings indicate that vaginal inflammation in response to vaginal pathogen colonisation is at least partly mediated by E2.

At embryo transfer, sex hormones were closely associated with all *Lactobacillus* species apart from *L. iners* (Figure 3.57). *L. iners* is associated with transition of the vaginal microbiome towards a dysbiotic state and consistent with this often presented in women with BV (546).

Furthermore, there are reports that suggest dominance by *L. iners* is a risk factor for preterm birth (204). In the current dataset, *L. iners* was closely correlated with BV associated bacteria at ET, however, this did not appear to relate to clinical pregnancy rates, despite *L. iners* being associated with pro-inflammatory cytokines at the time of embryo transfer.

Another noteworthy observation at the time of embryo transfer was low relative abundance of *F. magna*, and *P. timonensis* (Figure 3.25). Longitudinal observations suggested that *F. magna*, and *P. timonensis* were also susceptible to changes in successive stages of sample collection. *P. timonensis* abundance also reduced in transition from coordination appointment to pituitary suppression. Subsequently, the transition from pituitary suppression to ovarian stimulation coincided with increased abundance of both *F. magna*, and *P. timonensis*. Abundance of *F. magna* was then significantly reduced from egg collection to embryo transfer. The published literature suggests that *P. timonensis* is an inducer of IL-1β (547), this trend was observed in the current dataset on the day of ET (significant p-value but not q-value) (Figure 3.58). Similarly, *F. magna* induced inflammation particularly IL-8 (significant p-value but not q-value). In addition to BV, *F. magna* has been isolated in soft tissue abscesses, acute wound infections and endocarditis (548). *F. magna* are also known to trigger release of neutrophil extracellular traps and induce oxidative burst and is associated with upregulation of key immune components such as IL-8 (549).

Increased vaginal bacterial load has been reported to be an important factor related to risk of early spontaneous preterm birth and preterm prelabour rupture of membranes (550). CST III and IV associated samples have higher bacterial loads than CST I, II and V (550). However, in this cohort, no relationship was observed between bacterial load and CSTs, immune mediators nor clinical outcomes (Figure 3.27). Moreover, the combined capacity of these factors to predict IVF success at the time of embryo transfer was relatively poor, although this may reflect the small sample size of the patient cohort examined (Figure 3.62).

It is well established that sex hormones directly and indirectly mediate immune cell function in the lower reproductive tract via several complex mechanisms. E2 and P4 mediate transcription of target genes in several innate and adaptive immune cells in the lower reproductive tract including epithelial and stromal cells, macrophages, dendritic cells, and natural killer cells by coupling to their membrane or intracellular nuclear receptors, which function as ligand-activated transcription factors. The complexity of hormonal mediation of immune response throughout the reproductive tract is highlighted by differences in the recruitment and function of immune cells to the lower and upper reproductive tracts during different stages of the menstrual cycle (533). To begin to investigate the potential interaction between hormonal levels during IVF treatment and host immune response in the lower reproductive tract, pro-

and anti-inflammatory cytokines were assayed in CVF samples. Target immune mediators were selected based on the role they play in vaginal and endometrial processes in healthy reproductive environments in peri-conceptional period and regulation of early pregnancy (533, 551) and included pro- and anti-inflammatory cytokines and chemokines as well as growth factors (552). Integration of immune analytes with E2 levels using all samples available (n=128) indicated that E2 has a generally anti-inflammatory effect during IVF with an inverse relationship identified between several immune mediators including IGFBP-1, IL-1ra, IL-6, IL-8, IL-18, LIF and TNF-α (Table 3.4). This is broadly consistent with previous reports on women undergoing controlled ovarian stimulation which was associated with suppressed immune responses (553). Cross-sectional regression analysis of E2 and immune analytes at different stages of sampling provided similar findings at the time of coordination appointment where E2 was found to inversely correlate with IGFBP-1, IL-1β, IL-6, IL-8, and LIF (Figures 3.8 and 3.9). As expected, pituitary suppression and decreased E2 led to a loss of these relationships.

Interestingly, not all E2-immune mediator relationships were restored during the transition from pituitary suppression to ovarian stimulation where E2 levels were increased on average 246-fold. Instead, these supraphysiological concentrations of E2 were associated with reduced levels of IFN-γ and IL-1β (Figure 3.9). At this stage, P4 levels remained relatively low, and no associations were identified between P4 and any immune analytes. In the uterus, P4 reduces IFN-γ levels by regulating the cytotoxicity of uNK cells (554). uNK cells are the most abundant lymphocyte in the uterus and support the spiral arteriole modification and successful pregnancy by secreting a wide array of analytes including IFN-γ (555). Recruitment, differentiation, and function of uNK cells is mediated via activating gene expression of immunomodulatory or angiogenic proteins (556). Indirect regulation of uNK cells occurs through stromal cells and T lymphocytes that act as intermediary cells transducing the effects of P4 (556). In response to P4, these cells produce Hoxa-10, and Th-2 cytokines (557, 558).

The importance of P4 in regulation of immunity during IVF was highlighted during the transition from ovarian stimulation to the time of egg collection and embryo transfer where levels of P4 increased on average by 14-fold and 13-fold respectively (Table 3.1). During this time, when E2 levels remained consistent, increased concentration of IL-1β, IL-1ra, and IL-8 were observed (Figure 3.16). Increased concentrations of IL-1β and IL-8 in the endometrium have previously been reported to play an important role in preparation of the endometrium for acceptance of the embryo (559). IL-1β and IL-8 also play an important role in implantation (560) whereby IL-1β stimulates endothelial LIF and Leptin production during the window of implantation and IL-8 is a regulator of trophoblast invasion through increased metalloproteinase 9 (MMP9) activity (561). IL-1β and IL-8 are locally secreted by stromal cells, macrophages, uNK cells, and uterine endothelial cells (370) but *in vivo* studies also indicate

that IL-1β is also expressed by the human conceptus (560). Consistent with an important role in endometrial preparation and IVF success, IL-1β and IL-8 were found to be significantly higher in CVF samples of patients with successful clinical pregnancy outcomes on the day of embryo transfer (Table 3.5). Moreover, concentrations of IGFBP-1 were also significantly higher in the vagina of patients with successful clinical outcomes on the day of embryo transfer (Table 3.5). In the uterus, IGFBP-1 is produced by stromal cells during decidualisation and is stimulated by P4 and cAMP (562). It has also been reported that IL-1β can modulate stimulation of IGFBP-1 (563). Collectively, these findings indicates that immune markers associated with IVF success are detectable in the vagina, which is a more practical and non-invasive sampling site compared to the endometrium.

The relationship between increased inflammation and successful embryo transfer has long been recognised. Endometrial scratching a procedure where the lining of the endometrium is scratched using a sterile plastic tube to trigger an inflammatory repair which purportedly increases the receptivity to embryo implantation is still practiced by many clinics worldwide (564). However, a recent Cochrane review reported that clinical pregnancy and live birth rates were not improved following a scratching procedure based on moderate quality of evidence (565). The review also considered miscarriages as a measure of safety associated with endometrial scratching but did not find any association between scratching and miscarriage rates. However, the procedure is likely to cause discomfort in women as well as a small amount of bleeding. Based on these evidence, endometrial scratching is not considered to be a part of routine IVF treatment and the HFEA considers it an amber-rated ‘add-on’ in treatment cycles.

Integration of immune mediator levels and hormonal concentrations from the total dataset also found significant differences between the regression slopes for IL-1ra with both E2 and P4 with respect to clinical outcomes. Higher concentrations of serum hormones were associated with reduced IL-1ra concentrations in samples collected from patients with successful outcomes. The IL-1 system is a major part of the innate immune response of endometrial stromal cells and is considered an important paracrine factor assisting in embryo implantation (566). In mice, studies have shown that the pregnancy rates of animals treated with an IL-1 receptor antagonist are significantly lower than controls (13% v 60%) (567). IL-1ra competitively binds to the IL-1 receptor and inhibits IL-1 bioactivity (568). Furthermore, stromal cell expression of IL-1β and IL-1ra at appropriate ratios is thought to contribute to maternal-embryo interactions involved in successful implantation (569).

3.10.1 Limitations

There are several limitations of the research reported in this chapter. As mentioned, statistical power was restricted due to a relatively small sample size. It should be noted that some serial samples from patients could not collected during last-minute changes of appointment times which limited the ability to undertake longitudinal modelling for all patients. However, it was still possible to observe several significant and unique relationships in the data. Further, the high dimensionality of the data collected for each patient sample is a major strength of this work and allowed for detailed integration of different datasets and a more wholistic assessment of microbiota-host response in the context of different hormonal conditions during IVF treatment.

Another possible limitation relates to the method used for characterisation of the vaginal microbiota. Metataxonomic analyses used the V1-V2 hypervariable regions of the 16S rRNA gene which are particularly effective for resolving *Lactobacilli*, *Pseudomonas*, and *Megasphaera* species but the primer efficiency is less effective against *Gardnerella*, *Bifidobacterium bifidum* and *C. trachomatis* (570). However it is important to note that there is no single hypervariable region that can distinguish all bacterial strains in a given sample (571).

3.10.2 Summary of main findings

In summary, the data presented in this chapter highlight important relationships between hormones, immune analytes, and cervico-vaginal bacteria at 5 major stages of fresh IVF cycles. Hormonal manipulation during IVF appears to modulate host-immune response to vaginal microbiota and likely, microbiota-host interactions at other sites relevant to IVF success (e.g. endometrium). These changes may have clinical significances for patients undergoing fresh IVF cycles.

4 CHAPTER IV: The cervicovaginal microbiota in women undergoing frozen IVF cycle treatment

4.0 INTRODUCTION

Frozen IVF cycles were developed to utilise surplus embryos from previous IVF cycles. Particularly since the development of vitrification for cryopreservation, the survival rates of oocytes, cleavage and blastocyst embryos has improved significantly (572). The success rates between fresh and frozen IVF cycles are comparable and according to some reports better rates are observed for frozen cycles (573). An advantage of frozen IVF cycles is that they do not require a new ovarian stimulation protocol which heightens the risks associated with OHSS (574). Ovarian stimulation protocols are also associated with premature P4 elevation on the day of hCG administration, which is linked with decreased clinical pregnancy rates in fresh IVF cycles (575).

A meta-analysis comparing obstetric and perinatal outcomes between fresh and frozen IVF cycles reported that singleton babies from frozen IVF cycles were at lower risk of preterm delivery, low birth weight and small for gestational age compared with babies from fresh cycles (576). However, the same report suggested that babies from frozen IVF cycles were at greater risk of hypertensive disorders of pregnancy, large for gestational age and high birth weight. There were no differences in risks associated with congenital anomalies and perinatal mortalities between fresh and frozen IVF cycles.

Given that the 2 fundamental factors for a successful pregnancy is embryo quality and a receptive endometrium, another advantage of frozen IVF cycles is the ability to perform PGT-A which allows choosing of euploid embryos (Section 1.2.3, page 8) (577). The risk of failed implantation is associated with advanced maternal age, which is linked to the higher rates of aneuploidy in embryos (71). Studies indicate that PGT-A is beneficial in improving implantation and live birth rates per embryo transfer (71).

Currently, studies linking the vaginal microbiota to IVF success have typically not considered whether microbiota can be considered an independent factor in shaping the outcome of fresh and frozen cycles. Based on data presented in Chapter 3, differences in hormonal manipulations of patients could lead to changes in microbiota compositions that may be relevant for influencing chances of IVF success. It was hypothesised that vaginal bacteria play an important role in shaping clinical outcomes of frozen IVF cycles. To test this hypothesis,

the vaginal microbiota was characterised in patients undergoing frozen IVF cycles and the composition compared between successful and unsuccessful outcomes.

4.1 Results: Patient recruitment and sample collection

A total of 97 cycles were included from women recruited to the ART2 study. Of these, 2 patients withdrew consent, 10 cycles were cancelled and 1 cycle was postponed leaving a final total of 84 cycles included in the analyses. Additionally, 7 frozen IVF cycles recruited from the ART1 study were included for the work described in this chapter.

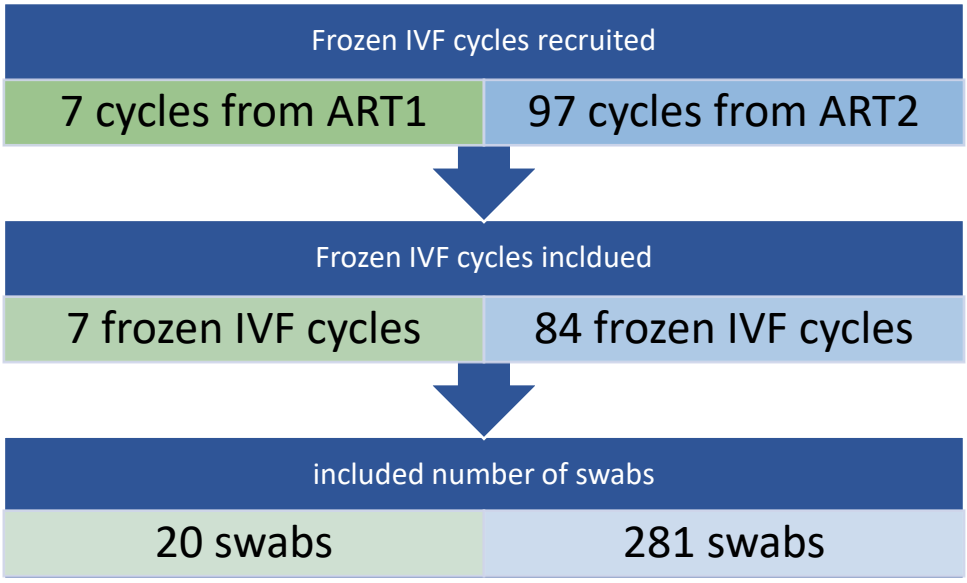


Figure 4.1: Summary of frozen cycles recruited and sampled in ART1 and ART2 studies.

4.2 Patient demographics for frozen IVF cycles

Of the 91 frozen IVF cycles included in this study, 55 cycles resulted in successful pregnancy (60%), 47 (52%) were live births (including 3 twin births) and 8 (8%) were miscarriages. Of the remaining cycles, 34 (38%) did not have a successful embryo implantation and 2 cycles (2%) had a biochemical pregnancy.

A combination of Cetrotide (GnRH antagonist) (n=34, 37%), and mid-luteal protocol (n=47, 52%) were used for pituitary suppression as well as 10 (11%) natural cycles. Of the 91 cycles included in the final study population, 34 underwent PGT-A or PGD.

Patient demographic and clinical outcome data is presented in Table 4.1.

Table 4.1: Patient demographics and clinical outcomes for women undergoing frozen IVF cycles. For statistical comparison of categorical variables, Fisher's exact test was used. For statistical comparison of BMI, unpaired T-test was used. Note: *<30 age category was excluded from contingency analysis due to low number of cycles available.

Factors	**Pregnant** (n=55)	**Not pregnant** (n=36)	**p-value**
Ethnicity			
Caucasian (n=80, 88%)	49 (61%)	31 (39%)	0.74
Asian/Black (n=11, 12%)	6 (55%)	5 (45%)	
Age			
<30 (n=2, 2%)*	1 (50%)	1 (50%)	0.26
30-36 (n=31, 34%)	22 (71%)	9 (29%)	
>36 (n=58, 64%)	32 (55%)	26 (45%)	
Suppression protocol			
cetrotide (GnRH antagonist) (n=34, 37%)	20 (59%)	14 (41%)	0.30
mid-luteal protocol (GnRHa) (n=47, 52%)	31 (66%)	16 (34%)	
Natural cycle (n=10, 11%)	4 (40%)	6 (60%)	
testing			
PGD/PGT-A (n=34, 37%)	19 (56%)	15 (44%)	0.51
No preimplantation testing (n=57, 63%)	36 (63%)	21 (37%)	
BMI (±SD)	22.8±3.8 (n=36)	22.9±3.8 (n=27)	0.99

4.3 Characterisation and comparison of vaginal microbiota in frozen IVF cycles

Apart from being collected form a different clinic, sample collection for ART2 coincided with the onset of the COVID-19 pandemic in London.

4.3.1 CST classification of cervico-vaginal bacteria in frozen IVF cycles

Classification of vaginal microbiota profiles using the VALENCIA algorithm indicated that the most prevalent CST in the total sample cohort was CST I (88/296, 30%) followed by CST IV (75/296, 25%), CST III (67/296, 22%), CST II (38/296, 13%) and CST V (28/296, 10%). The mean richness and diversity of these significantly differed (Kruskal-Wallis tests, $p<0.0001$) with CST IV profiles having significantly higher richness than CSTs I, III and V (Dunn's multiple comparison $p<0.0001$ and $p=0.006$ respectively). CST I had lower diversity than CSTs II and V (Dunn's multiple comparison $p=0.0008$ and $p<0.0001$ respectively) (Figure 4.2).

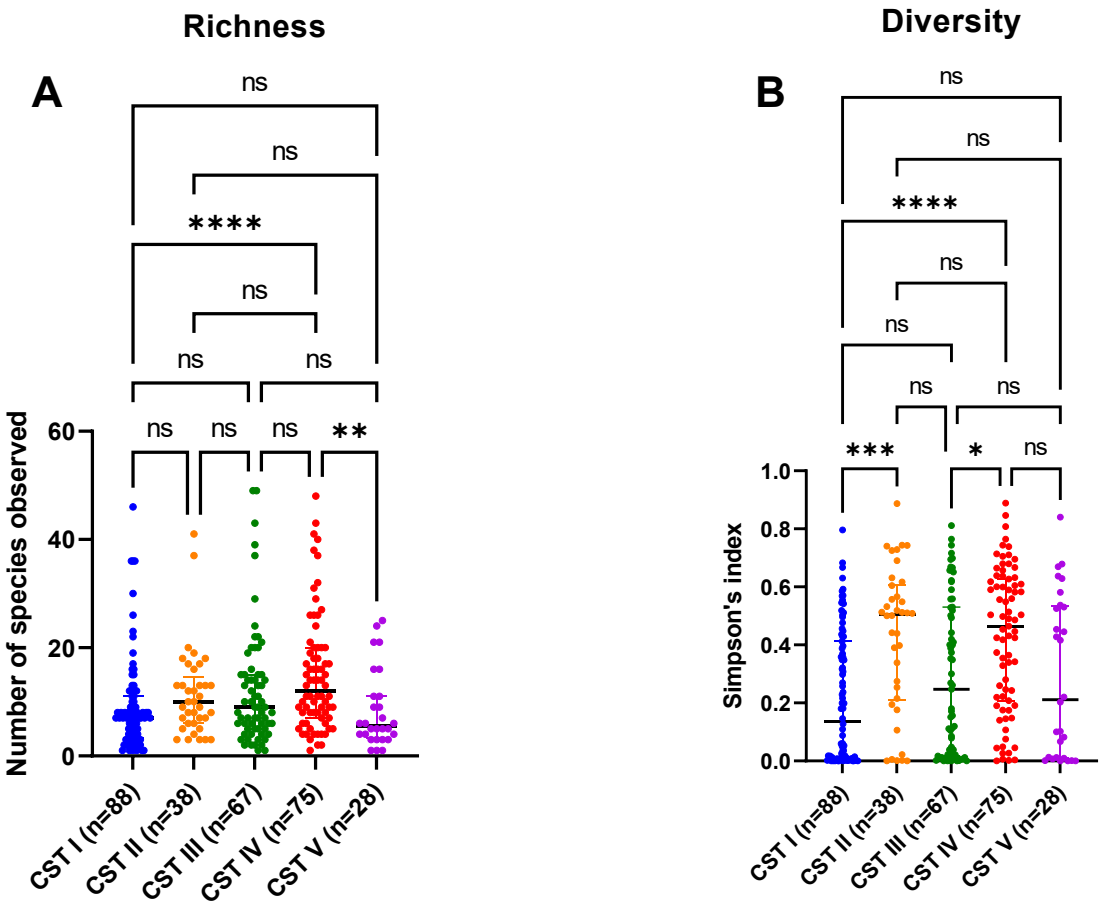


Figure 4.2: Comparison of mean richness and diversity of vaginal CST groups identified in frozen IVF cycles. A) Mean species richness of CST IV profiles was significantly higher than CSTs I and V (Dunn's multiple comparison p<0.0001 and p=0.006 respectively). B) Mean diversity of CST I profiles was significantly lower than CSTs II and IV (Dunn's multiple comparison p=0.0008 and p<0.0001 respectively). CST III diversity was also significantly lower than CST IV (Dunn's multiple comparison p=0.01).

The prevalence of these CSTs were significantly different across clinical stages for women undergoing frozen IVF treatments (Figure 4.3, X^2 p<0.0001) with the proportions of CST III and CST IV decreasing from coordination appointment to the day of embryo transfer. In contrast, the proportion of CST II and CST V profiles increased from coordination appointment across the remaining timepoints. Consistent with analysis strategy used in Chapter 3, the prevalence of i. CST I vs all other CSTs combined and ii. Lacto-dominated CSTs vs CST IV was also examined. No difference in the prevalence of CST I vs other CSTs was identified throughout the frozen treatment cycles (X^2 p=0.46). However, the prevalence of Lacto-dominated CSTs increased from coordination appointment through pituitary suppression and samples collected on the day of embryo transfer compared to CST IV profiles (X^2 p=0.02).

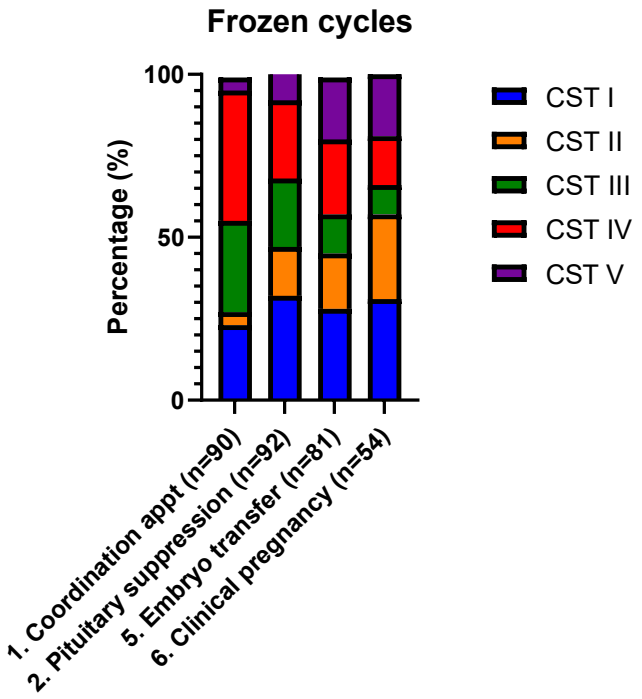


Figure 4.3: CST representations at various stages of sample collection for frozen IVF cycles. Prevalence of CSTs III and IV decreased from coordination appointment to latter stages of sample collection. Prevalence of CSTs II and V increased from coordination appointment to samples collected throughout pituitary suppression and on the day of embryo transfer.

The next analyses aimed to compare the prevalence of CSTs across equivalent sample collection timepoints i) coordination appointment, ii) pituitary suppression and iii) embryo transfer between patients in the fresh and frozen cohorts. Due to small sample sizes, only the comparison between the prevalence of CSTs I and IV could be performed however no significant difference was detected (X^2 p=0.27 and p=0.21 respectively, Figure 4.4).

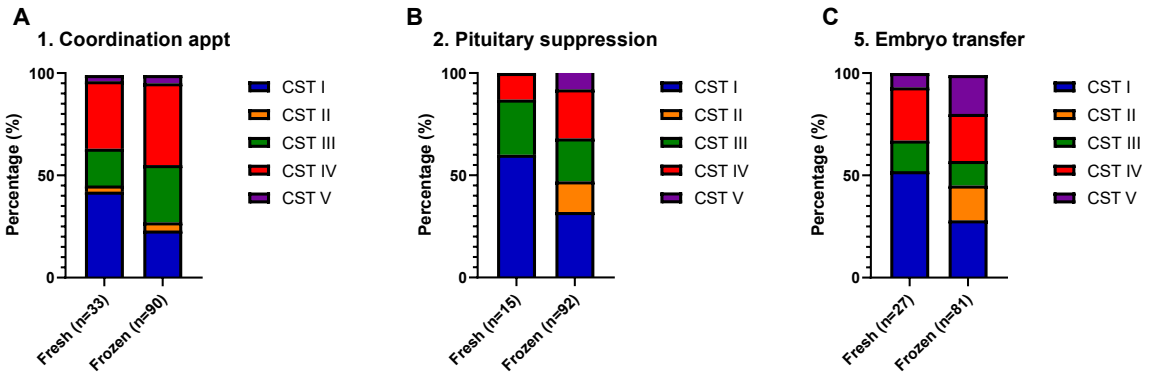


Figure 4.4: Comparison of CSTs at equivalent stages of sample collection between fresh and frozen IVF cycles. A) Coordination appointment, B) Pituitary suppression, and C) Embryo transfer. At coordination, 42% of samples were classified as CST I for fresh IVF cycles, compared to 23% of samples at the same stage for frozen IVF cycles. Throughout pituitary suppression and on the day of embryo transfer, CST I is more prevalent in fresh cycles. The prevalence of CST IV decreases from the first sample collection point for both fresh and frozen cycles. Despite these trends, no significant difference in prevalence of the CSTs I or IV were detected between fresh and frozen cycles.

To determine whether any specific taxa were significantly changing across each of the sample collection stages irrespective of clinical outcomes, a linear mixed effects model was used (Table 4.2). The model included stages 1 to 5 of sample collection irrespective of treatment outcomes. Stage 6 was plotted on Figure 4.5 for the sake of comparison but was excluded from the modelling. Significant changes were observed for *L. jensenii, L. gasseri, P. bivia, P. timonensis, L. vaginalis, F. magna,* and *P. indolicus* (p and $q<0.05$ for all, ANOVA linear mixed effects modelling).

Table 4.2: Longitudinal changes across stages for highly abundant taxa. p-values for changes for taxa. ANOVA linear mixed effects modelling of highly abundant taxa based on cross-sectional data collection timepoints. *L. jensenii, L. gasseri, P. bivia, P. timonensis, L, vaginalis, F. magna* and *P. indolicus* significantly changed throughout IVF cycles. Adjusted p-values (q-values) were calculated using the Benjamini-Hochberg procedure.

Bacterial	p-value	q-value
L. iners	0.12	0.16
L. crispatus	0.84	0.92
G. vaginalis	0.93	0.93
L. jensenii	**0.0003**	**0.007**
L. gasseri	**0.0003**	**0.007**
S. anginosus	0.25	0.31
P. bivia	**0.0003**	**0.001**
P. timonensis	**0.0008**	**0.002**
L. vaginalis	**0.01**	**0.02**
F. magna	**<0.0001**	**<0.0001**
P. indolicus	**<0.0001**	**0.0002**
D. micraerophilus	0.08	0.12

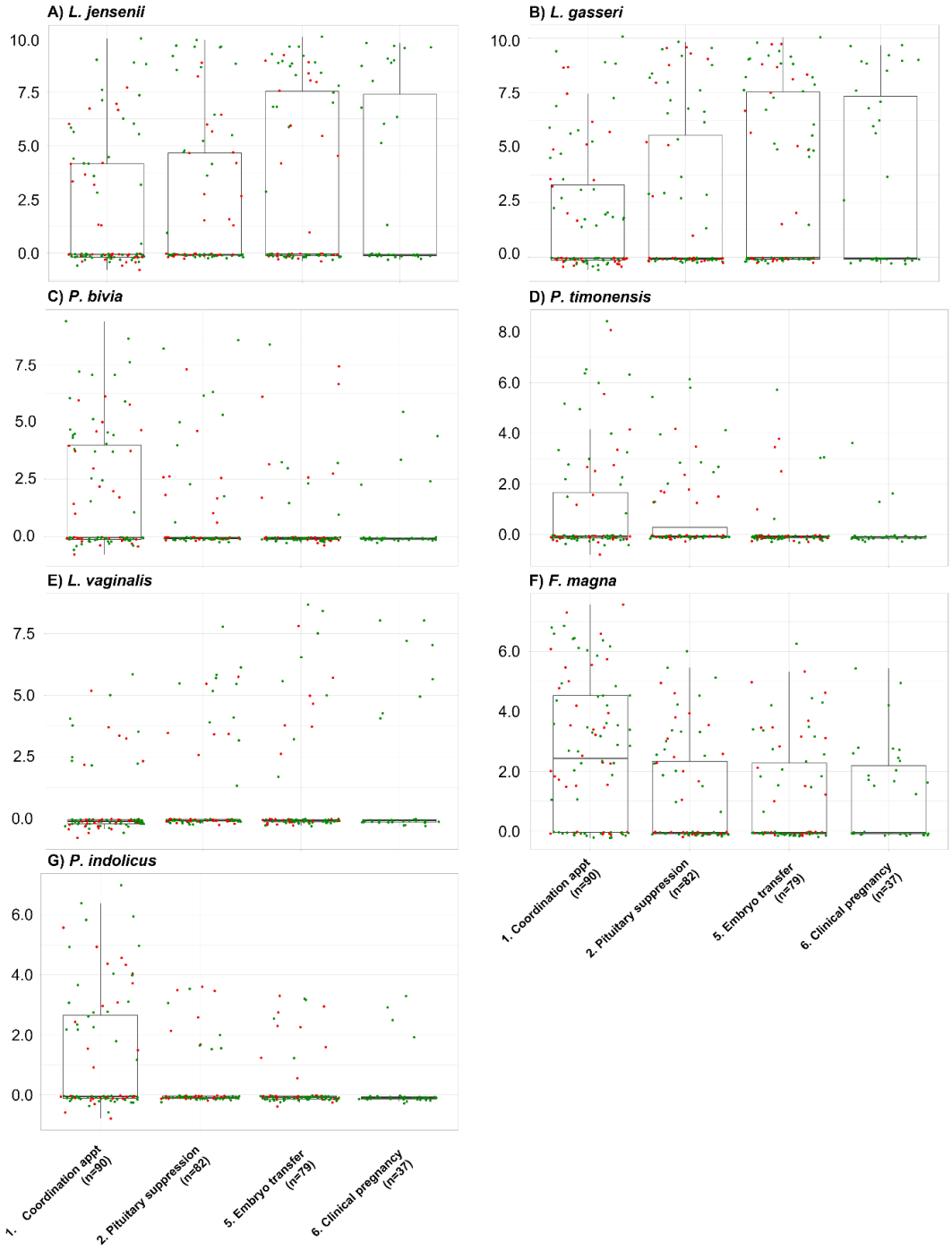


Figure 4.5: Longitudinal abundance changes of bacterial species during frozen IVF treatment cycles. A) *L. jensenii* (p=0.003, q=0.007), B) *L. gasseri* (p=0.003, q=0.007), C) *P. bivia* (p=0.0003, q=0.001), D) *P. timonensis* (p=0.0006, q=0.002), E) *L. vaginalis* (p=0.01, q=0.02), F) *F. magna* (p<0.0001, q<0.0001) and G) *P. indolicus* (p<0.0001, q<0.0001) changed significantly throughout sample collection timepoints. Data presented on a natural Log scale. Green dots indicate successful clinical outcomes and red dots indicate unsuccessful clinical outcomes.

The next set of analyses assessed whether the prevalence of CSTs related to clinical outcomes at each of the sample collection timepoints throughout frozen IVF cycles. First, data were assessed based on prevalence of CST I compared to the combination of the other 4 CSTs (Table 4.3). At pituitary suppression, significantly higher prevalence of CST I profiles were observed in women who subsequently did not become pregnant (17% CST I, 83% other CSTs, Fisher's exact test p=0.01). While a similar trend was observed at coordination appointment and on the day of embryo transfer, this did not reach statistical significance (Fisher's exact p>0.05).

Table 4.3: Cross-sectional CST representations according to outcome for frozen IVF cycles: CST I vs other CSTs. Prevalence of CST I was significantly lower than other CSTs throughout pituitary suppression in cycles with successful clinical outcomes. At coordination appointment and samples collected on the day of embryo transfer, there were no significant associations between prevalence of CST I and clinical outcomes (Fisher's exact). No differences in treatment outcomes at any stages of sample collection were detected when comparing Lacto-dominant vs CST IV profiles.

1. Coordination appointment	**CST I**	**Other CSTs**	**p-value**
Pregnant (n=54)	11 (20%)	43 (80%)	0.13
Not pregnant (n=33)	12 (36%)	21 (64%)	
2. Pituitary suppression			
Pregnant (n=52)	9 (17%)	43 (83%)	0.01*
Not pregnant (n=33)	14 (42%)	19 (58%)	
5. Embryo transfer			
Pregnant (n=53)	13 (25%)	40 (75%)	0.21
Not pregnant (n=29)	11 (38%)	18 (62%)	

Next, data were assessed based on prevalence of CST Lacto-dominant compared to the CST IV (Table 4.4). There were no significant associations with treatment outcomes at any stages of sample collection using Fisher's exact tests.

Table 4.4: Cross-sectional CSTs representations according to outcome for frozen IVF cycles: CST Lacto-dominant vs CST IV. There were no significant associations between prevalence of CST Lacto-dominant with clinical outcomes at any stages of sample collection throughout frozen IVF cycles (Fisher's exact tests).

1. Coordination appointment	**CST Lacto-dominant**	**CST IV**	**p-value**
Pregnant (n=54)	30 (55%)	24 (45%)	0.11
Not pregnant (n=33)	24 (73%)	9 (27%)	
2. Pituitary suppression			
Pregnant (n=52)	33 (63%)	19 (37%)	0.15
Not pregnant (n=33)	26 (79%)	7 (21%)	
5. Embryo transfer			
Pregnant (n=53)	36 (68%)	17 (32%)	0.31
Not pregnant (n=29)	23 (79%)	6 (21%)	

4.4 Stability of vaginal microbiome throughout frozen IVF cycles

The microbial stability for each patient across frozen IVF cycles was next compared between clinical outcomes groups. This was performed using a similar strategy to that described in Chapter 3 for fresh IVF cycles, where a stable vaginal microbiome was defined as classification of the same CST for all samples available per patient (Figures 4.6). Samples collected in pregnancy were excluded for this analysis. Patients 5 ART1 (pregnant) and patient 55 (not pregnant) were excluded due to only having 1 sample available for analysis.

Samples with live births and miscarriages were considered to have had successful IVF outcomes. The difference in CST stability rates according to clinical pregnancy was not significant (p=0.52, Fisher's exact test). Of the 55 cycles resulting in clinical pregnancy, 30 (54%) had stable vaginal microbiomes across the treatment cycles. There were 36 cycles that did not achieve clinical pregnancies of which 20 (55%) had stable vaginal microbiomes. The proportion of stable vaginal microbiomes was also comparable between live births and miscarriages as outcomes; for live births (41 cycles), 24 cycles had stable CSTs (59%) compared to 4 out of 8 (50%) for miscarriages (p=0.83, Fisher's exact test).

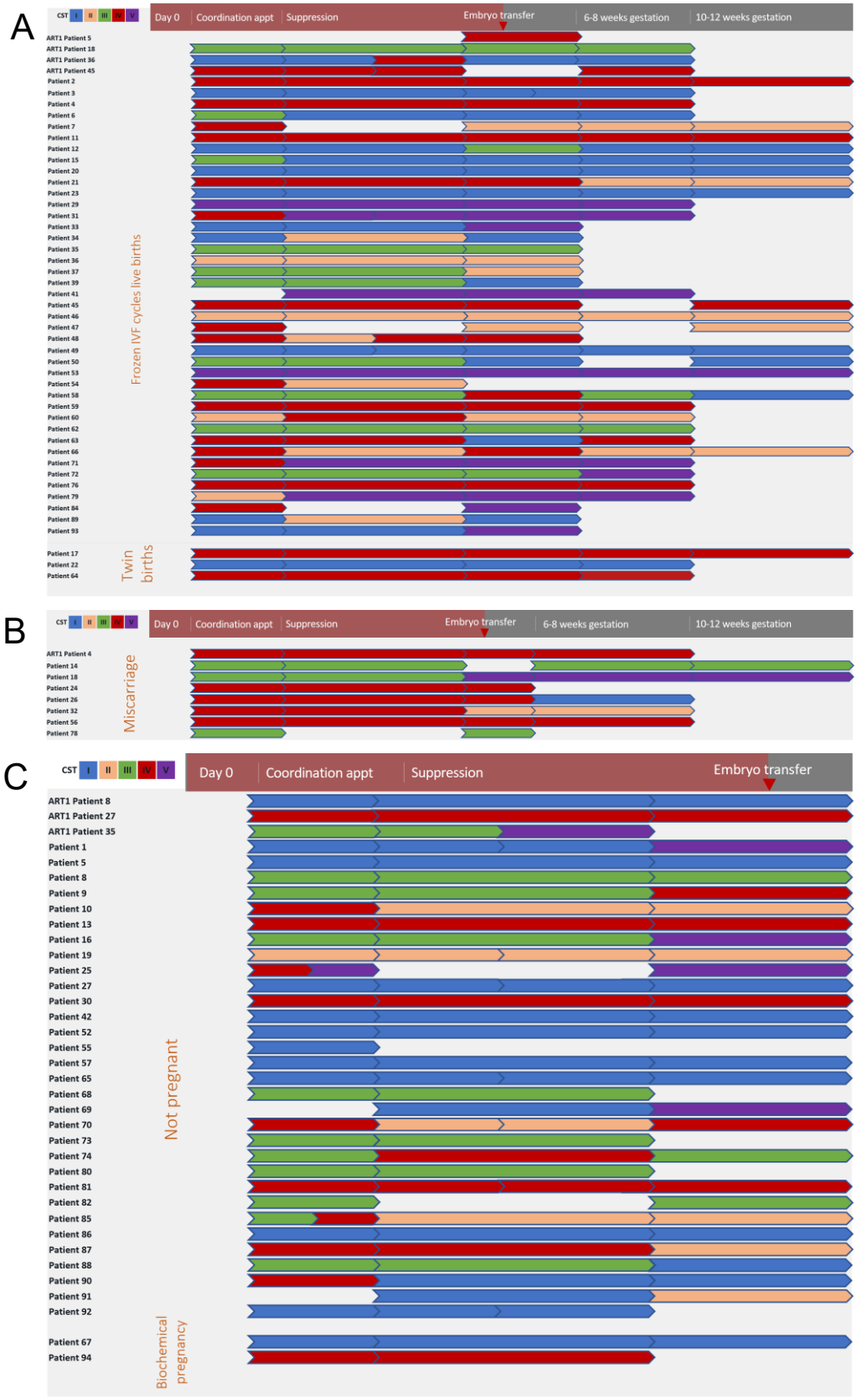


Figure 4.6: Microbiota stability across frozen IVF cycles. Patients are stratified based on outcome: A) clinical pregnancy, B) clinical pregnancy followed by miscarriage or C) unsuccessful embryo implantation.

4.5 Vaginal bacterial load at embryo transfer for frozen IVF cycles

Having examined microbiota composition, the following set of analyses aimed to determine whether bacterial load within samples was associated with clinical outcomes. Bacterial load was first analysed based on CST classifications of samples where no significant differences were observed (Kruskal-Wallis test p=0.60) (Figure 4.7).

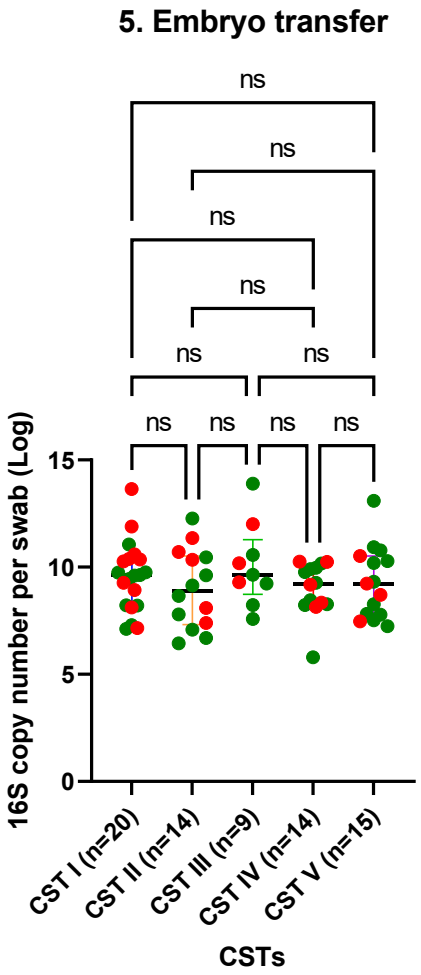


Figure 4.7: CSTs and bacterial load for samples collected on the day of embryo transfer. No significant differences in bacterial load between CSTs as observed (p=0.60). Dunn's multiple comparisons indicated on the plot (p>0.05). (●) Red dots and indicate unsuccessful outcomes, (●) green dots indicate successful outcomes.

Similarly, no significant differences in bacterial load between samples collected from women who had either a successful or unsuccessful clinical outcomes were observed using the Mann-Whitney test (p=0.12) (Figure 4.8).

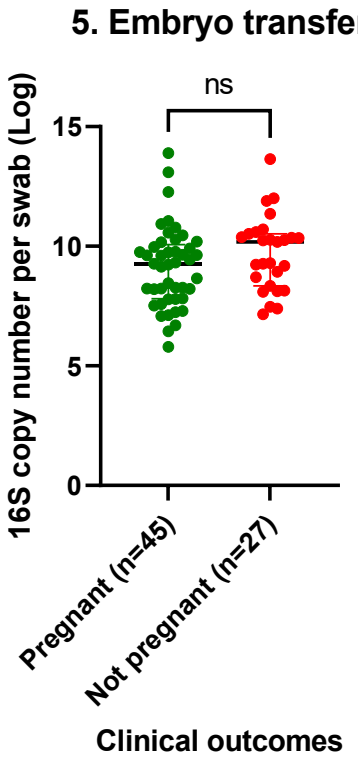


Figure 4.8: Clinical outcomes and bacterial load for samples collected on the day of embryo transfer. No significant difference between groups was observed (p=0.12, Mann-Whitney test).

Comparison of bacterial load between fresh and frozen IVF cohorts on the day of embryo transfer showed significantly higher load in fresh compared to frozen cycles (Mann-Whitney test p=0.0002) (Figure 4.9).

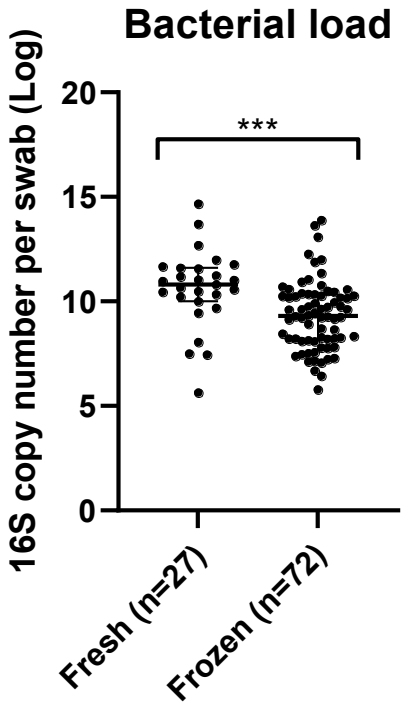


Figure 4.9: Fresh and frozen bacterial load for samples collected on the day of embryo transfer. Bacterial load for patients undergoing fresh IVF cycles were significantly higher than frozen cycles. Mann-Whitney test (p=0.0002).

4.6 The relationship between highly abundant vaginal taxa and clinical treatment outcomes

The relationship between highly abundant taxa and clinical treatment outcomes were analysed cross-sectionally. Relative abundance of *L. crispatus* was significantly higher for patients with unsuccessful clinical outcomes at coordination appointment, pituitary suppression and on the day of embryo transfer (Mann-Whitney tests, p=0.02, p=0.006, and p=0.007 respectively) (Figure 4.10).

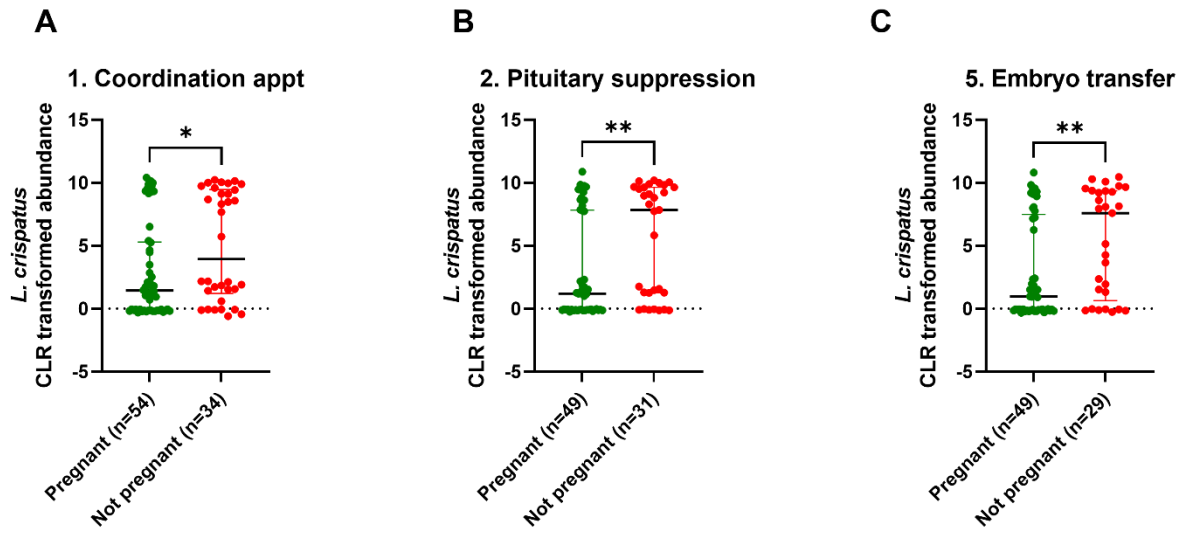


Figure 4.10: Comparison of relative abundance of *L. crispatus* based on clinical outcomes. CLR transformed relative abundance of *L. crispatus* was significantly higher for patients with unsuccessful treatment outcomes at A) Coordination appointment (p=0.02), B) pituitary suppression (p=0.006), and C) embryo transfer (p=0.007). Mann-Whitney tests.

The association of *L. crispatus* with unsuccessful cycles is not in line with the published literature. Given that CLR transformations are based on division by hyper geometric means, the high/low data points on the CLR transformed scale may be affected by the presence of other taxa which may distort the observed significances. To elucidate whether this is the case, the species diversity for CST I were compared cross-sectionally according to clinical outcomes (Figure 4.11).

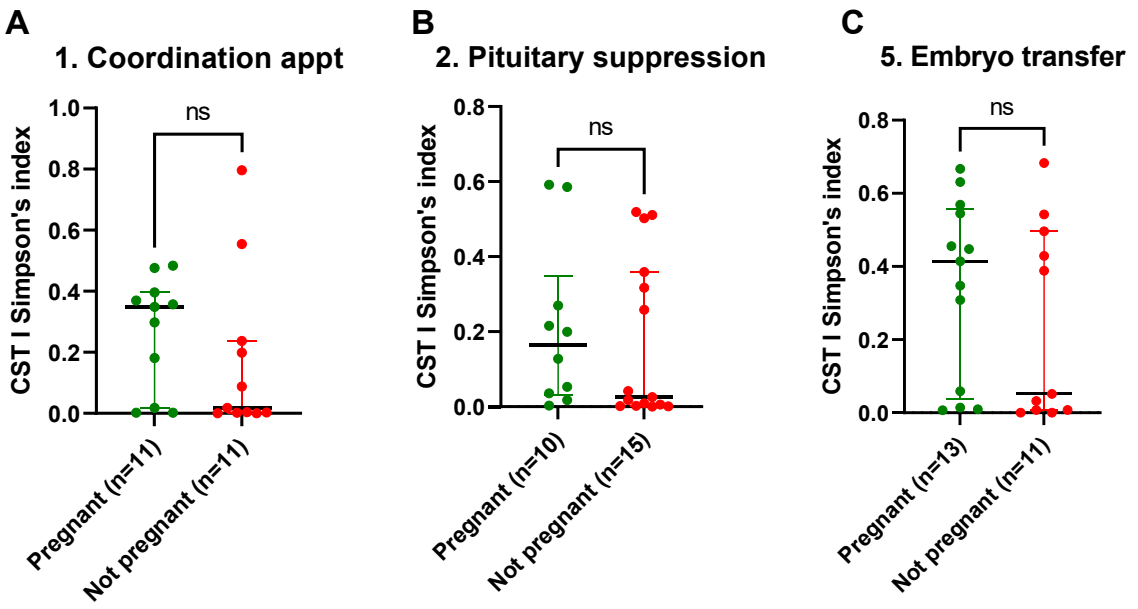


Figure 4.11: Comparison of species diversity for CST I based on clinical outcomes. There were no significant differences in species diversity using Simpson's index at any stage of sample collection. A) Coordination appointment (p=0.24), B) Pituitary suppression (p=0.31), and C) Embryo transfer (p=0.27). Mann-Whitney tests.

In addition to *L. crispatus*, the relative abundance of *P. indolicus* was higher in patients with unsuccessful outcomes in samples collected on the day of embryo transfer based on clinical outcomes (p=0.01) (Figure 4.12).

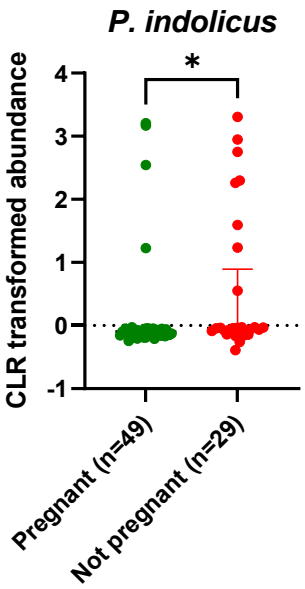


Figure 4.12: Comparison of relative abundance of *P. indolicus* based on clinical outcomes for samples collected on the day of embryo transfer. CLR transformed relative abundance of *P. indolicus* was significantly higher for patients with unsuccessful clinical outcomes in samples collected on the day of embryo transfer (Mann Whitney test p=0.01).

4.7 Longitudinal assessment of vaginal taxa

Analysis of changes in vaginal taxa relative abundance between consecutive stages of sample collection was performed for patients with data available at sequential key time points throughout frozen IVF cycles.

4.7.1 Coordination appointment to pituitary suppression

There were 77 longitudinal samples collected on coordination appointment and throughout pituitary suppression. This included 7 natural cycles which were excluded from within patient analysis on relative abundance of bacteria as these cycles did not consist of a pituitary downregulation protocol. The relative abundance of *L. jensenii* ($p=0.008$) and *L. vaginalis* ($p=0.0003$) significantly increased and the relative abundance of *F. magna* ($p<0.0001$) and *P. indolicus* ($p=0.02$) significantly decreased using Wilcoxon matched pairs signed rank tests (Figure 4.13).

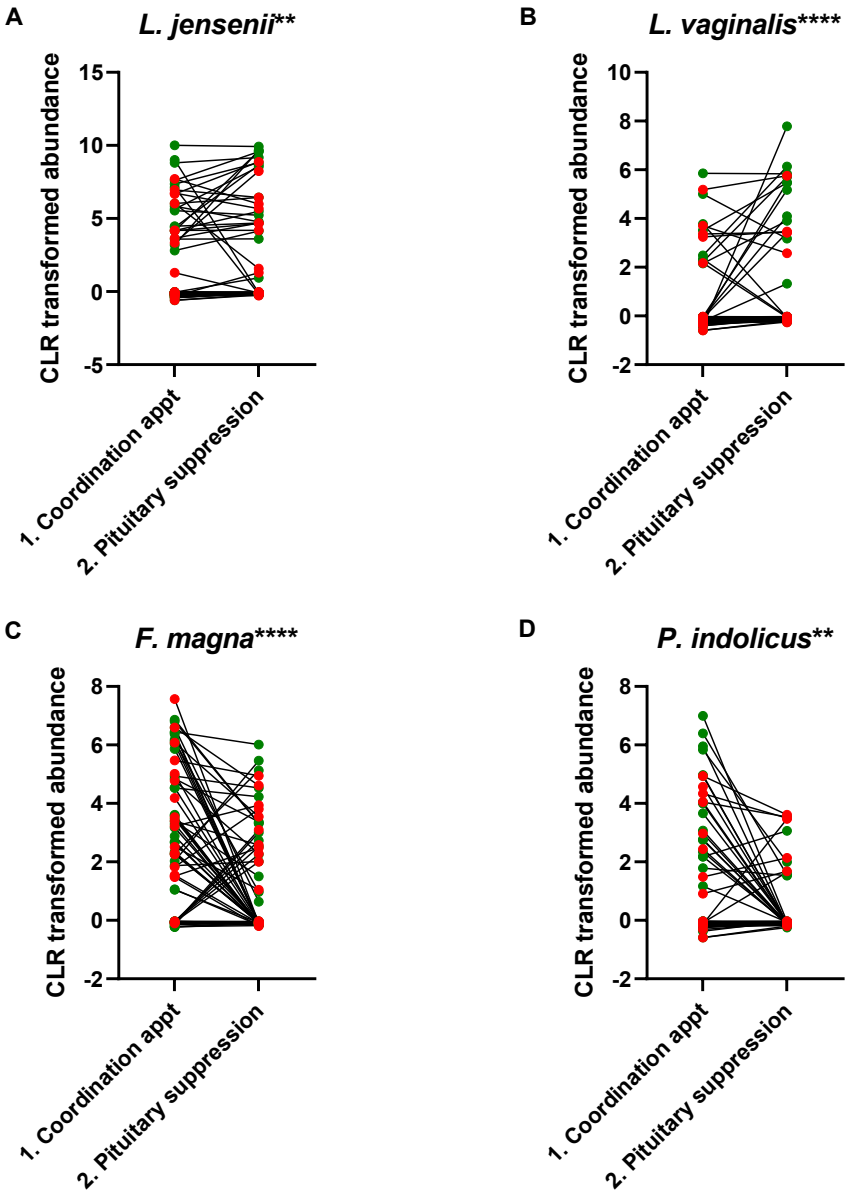


Figure 4.13: Within patient relative abundance changes of vaginal taxa for samples collected on coordination appointment and throughout pituitary suppression. CLR transformed abundance of A) *L. jensenii* (p=0.008) and B) *L. vaginalis* (p=0.0003) increased during this transition. Abundance of C) *F. magna* (p<0.0001) and D) *P. indolicus* (p=0.02) decreased from coordination appointment to pituitary suppression. Wilcoxon matched pairs signed rank tests (n=70). (●) Red dots indicate unsuccessful outcomes, (●) green dots indicate successful outcomes.

4.7.2 Pituitary suppression to embryo transfer

There were 30 cycles with samples collected throughout pituitary suppression and on the day of embryo transfer. Relative abundance of *L. iners* and *P. timonensis* were significantly reduced from pituitary suppression to embryo transfer using Wilcoxon matched pairs signed rank tests (Figure 4.14).

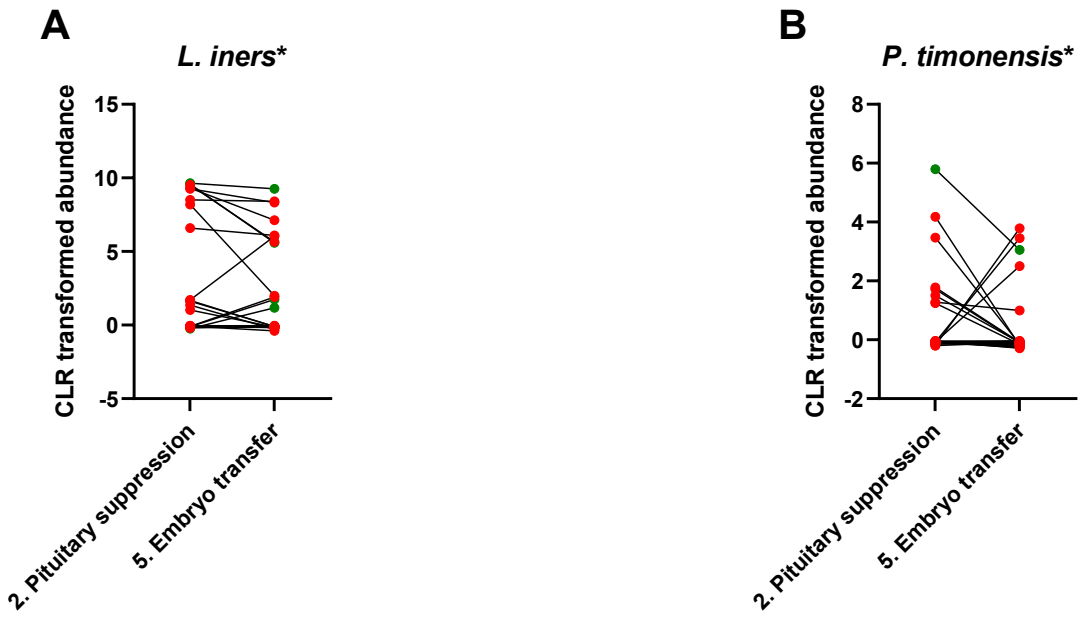


Figure 4.14: Within patient relative abundance changes of vaginal taxa throughout pituitary suppression to embryo transfer. CLR transformed abundance of A) *L. iners* and B) *P. timonensis* significantly increased in transition from pituitary suppression to embryo transfer (p=0.04 and p=0.03 respectively). Wilcoxon matched pairs signed rank tests (n=30). (●) Red dots indicate unsuccessful outcomes, (●) green dots indicate successful outcomes.

4.8 Vaginal bacteria of IVF cycles with preimplantation genetic testing and diagnosis (PGT-A and PGD)

PGT was done for 34 cycles in the frozen IVF cycles cohort. Based on the hypothesis that transfer of euploid embryos minimises the embryological factors associated with failure of implantation, bacteria compositions were analysed cross-sectionally for these 34 cycles. Based on clinical pregnancy rates, there were no significant differences between abundance of bacteria for samples collected at coordination appointment. Abundance of *L. crispatus* was significantly different based on treatment outcomes for samples collected throughout pituitary suppression and on the day of embryo transfer (p=0.008, and p=0.005 respectively. Mann-Whitney tests) (Figure 4.15). This broadly reflected the assessment done using all available data at every key stage of sample collection throughout frozen IVF cycles.

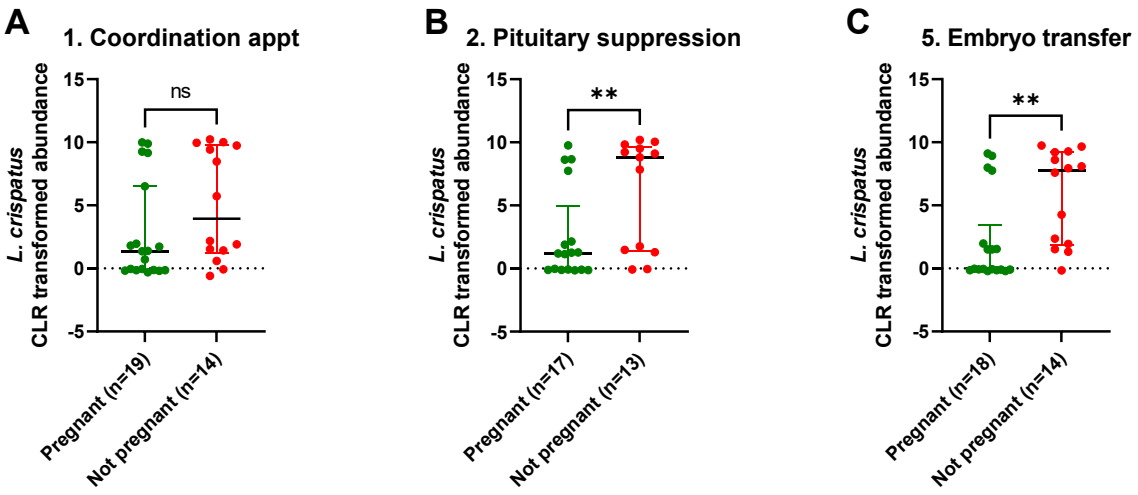


Figure 4.15: Comparison of relative abundance of *L. crispatus* for cycles with PGT based on clinical outcomes. CLR transformed relative abundance of *L. crispatus* was not significantly different based on clinical outcomes for patients who underwent PGT analysis at A) Coordination appointment (Mann-Whitney test, p=0.07). The relative abundance of *L. crispatus* was significantly higher in patients with unsuccessful clinical outcomes in the sub-cohort of patients with PGT analysis at B) Pituitary suppression, and C) Embryo transfer (Mann-Whitney tests, p=0.008 and p=0.005 respectively).

4.9 Vaginal bacteria random forest modelling for predicting IVF success rates

To assess the biomarker capability of vaginal microbiota of women undergoing frozen IVF cycles, random forest modelling was used for samples collected on the day of embryo transfer.

In a similar approach to Chapter 3 fresh IVF cycles, using random forest modelling the biomarker capability of vaginal taxa profiles and CST classifications were assessed. The ROC curves were close to the line representing random chance indicating that they do not have strong predictive characteristics (Figure 4.16).

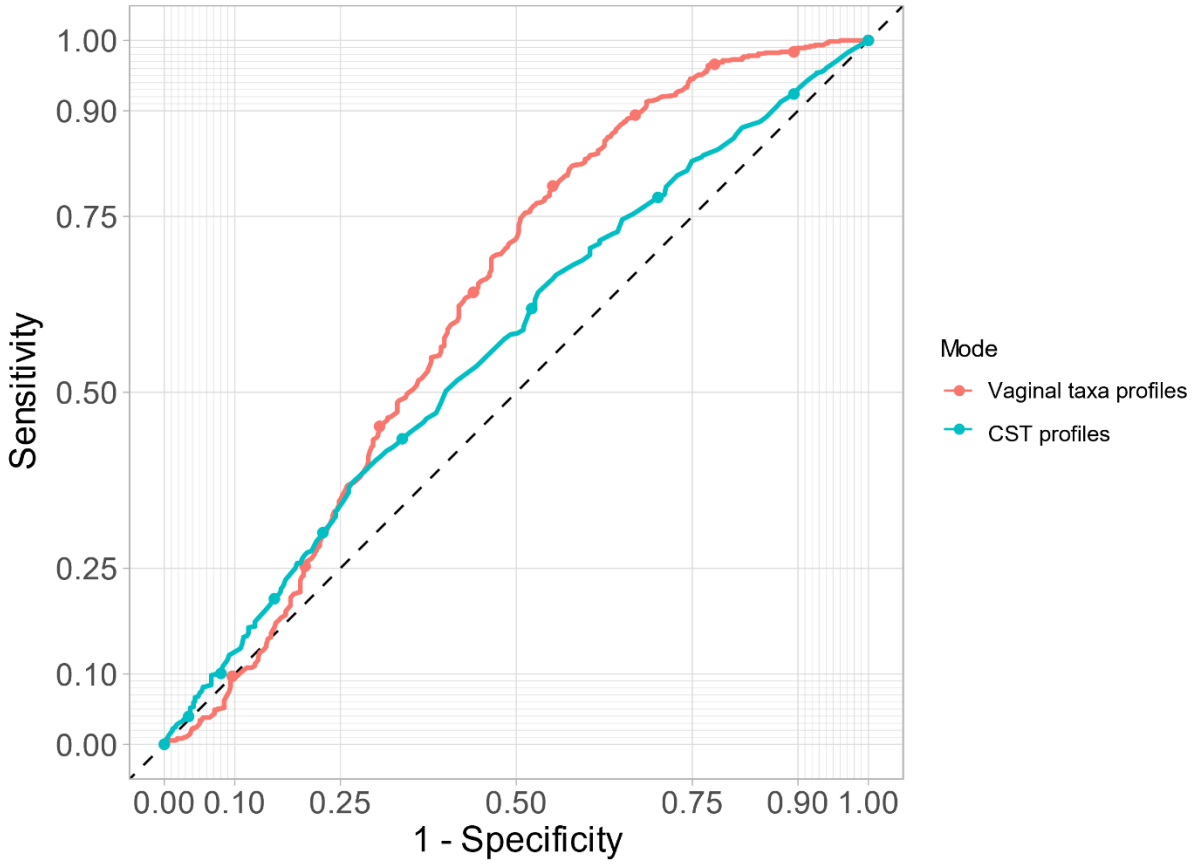


Figure 4.16: Random Forest modelling ROC curves. The biomarker capabilities of vaginal microbiota were assessed in predicting IVF clinical success rates. Random forest models were built based on vaginal taxa profiles (AUC: 0.64 ± 0.10) and CST profiles (AUC: 0.44 ± 0.08). The area under the curve for these profiles suggested low biomarker values in predicting IVF clinical success rates.

Table 4.5: Notable metrics for random forest modelling.

Metrics	Vaginal microbiota profiles	CST profiles
AUC (±SD)	0.64 (0.10)	0.44 (0.08)
F1 (±SD)	0.46 (0.12)	0.18 (0.05)
Sensitivity (±SD)	0.39 (0.13)	0.01 (0.04)
Specificity (±SD)	0.82 (0.10)	0.98 (0.05)
Balanced accuracy (±SD)	0.60 (0.07)	0.50 (0.02)

4.9.1 Prediction of IVF success using vaginal microbiome parameters akin to the ReceptIVFity™ study

In a similar approach to Koedooder and colleagues (196) and in line with analysis in Chapter 3 (Figure 3.63), this section of the study assessed the ratio of *L. crispatus* to *L. iners* and *vice versa* at 60% relative abundance as a marker of successful clinical outcomes (Figure 4.17).

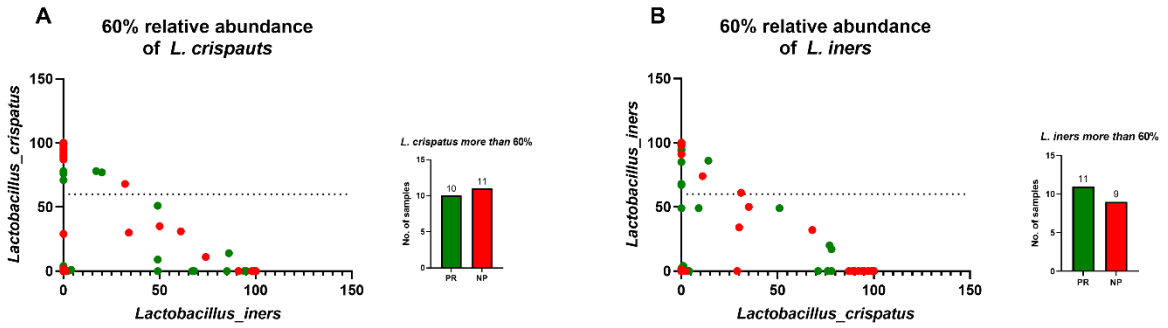


Figure 4.17: Clinical success predictability model based on the ReceptIVFity study. A) 60% relative abundance of *L. crispatus*, B) 60% relative abundance of *L. iners*.

No relationships with IVF clinical outcomes were identified using ratio of *L. crispatus* to *L. iners* or *vice versa* at 60% relative abundance threshold in this patient cohort (p=0.34, Fisher's exact test). Furthermore, combining fresh and frozen cohorts to assess the clinical success predictability in ratio of *L. crispatus* to *L. iners* and *vice versa* also did not find significant differences in clinical outcomes (p=0.99 Fisher's exact tests).

4.10 Discussion

This chapter aimed to characterise vaginal bacterial composition of women undergoing frozen IVF cycles and determine if this relates to clinical outcomes. The second objective was to compare these results with those of women undergoing fresh IVF cycles as described in Chapter 3 of this thesis. There are several key differences between fresh and frozen IVF cohorts, most notably the absence of an ovarian stimulation protocol which is associated with supraphysiological concentration of hormones. Frozen IVF cycles also can take advantage of preimplantation embryo testing for selection of euploid embryos. PGD is used for patients with known risks of a wide range of single gene disorders such as thalassaemia, sickle cell anaemia, cystic fibrosis, Huntington's disease as well as inherited cancer predisposition (578). PGT-A is used for patients at risk of having aneuploid embryos particularly for patients with advanced maternal age (579).

In contrast to what was observed in the fresh cycles, CST I was more prevalent in cycles with unsuccessful pregnancy outcomes at every stage of sample collection in the frozen cycle cohort (Table 4.3). This association reached statistical significance at pituitary suppression where CST I samples made up 17% of cycles with successful clinical pregnancies and 42% of cycles with unsuccessful clinical pregnancies. Most studies in the literature suggest that *Lactobacillus* species are the optimal compositions for successful embryo implantation (196, 217, 499, 527). Furthermore, *L. crispatus* has specifically been associated with successful pregnancy in some studies (498, 499). However, there are a growing number of reports that suggest this may not always be the case. Hao et al. reported that abundance of *Lactobacillus* species was higher in patients that did not achieve clinical pregnancy compared with the pregnant patients in a fresh IVF cohort (222). Similarly, Koedooder et al., suggested high relative abundance of *L. crispatus* is associated with low treatment success rates (196). In their study, Koedooder and colleagues analysed samples collected from 192 women undergoing fresh embryo transfer by IVF/IVF-ICSI. Samples were divided into groups of 'favourable microbiome profiles' and 'unfavourable microbiome profiles'. These groups were determined based on representation of each CST in samples that reached successful pregnancy. Low relative abundance of *Lactobacillus* (<20%), high relative abundance of *L. jensenii* (>35%), and high relative abundance of *G. vaginalis* and *Proteobacteria* (>28%) were associated with pregnancy failure. Favourable microbiota profiles with an average or high chance of pregnancy were defined based on relative abundance of *L. crispatus*. Samples with >60% relative abundance of *L. crispatus* only had a 24% chance of achieving successful pregnancy in contrast to women with >60% relative abundance of *L. iners* who had a 50% chance of becoming pregnant. High chance of pregnancy (53%) was associated with <60%

relative abundance of *L. crispatus*. Although these findings are partly consistent with the data presented in this chapter, a similar analysis using relative abundance data from our frozen patient cohort failed to identify any capacity to predict outcome of IVF treatment (Figure 4.17). There are several key differences between Koedooder's report and the current study. Apart from being performed on patients undergoing fresh cycle treatments in their study, samples were collected about 2 months prior to start of the IVF cycles. The authors argue that although the vaginal microbiome is prone to occasional short-term changes, most communities are generally stable over several months. This view contrasts with evidence in the literature. The dynamics and stability of vaginal microbiota were recently investigated in a study by Gajer and colleagues where they characterised the vaginal bacteria composition daily in 32 healthy, non-pregnant women over a 16 week period (580). The findings indicated that composition of the vaginal microbiota is susceptible to change based on hormonal cycles, bacterial community composition and sexual activity (580). More recently, diet and exercise have also been implicated in stability of the vaginal microbiota (151). As reported in this thesis, suppression/stimulation protocols during IVF cycles that lead to major fluctuations in serum hormone levels associated with changes in the vaginal microbiota. Thus, it seems unlikely that microbial signatures captured 2 months prior to the start of an IVF cycle, are reflective of those at the time of embryo transfer.

Comparison of bacterial load between fresh and frozen cohorts suggested significantly higher load in fresh cycles (Figure 4.9). Patient recruitment and sample collections were done at different IVF clinics for fresh and frozen IVF cohorts, however, this was done using a common SOP which was distributed amongst clinical teams at both locations. However, it remains possible that different sample collection techniques contributed to the observed difference in bacterial load. Regardless, bacterial load was not significantly associated with CST profiles, or clinical pregnancy rates, when assessed at the time of embryo transfer in either fresh or frozen cycles (Figures 4.7 and 4.8). Similarly, other parameters of microbial ecology such as species richness and diversity were found to differ between the fresh and frozen cohorts, yet this was not related to clinical pregnancy outcomes. This is in contrast to Hyman et al., who found that diversity of vaginal bacterial compositions on the day of embryo transfer were correlated with clinical outcomes (217).

Temporal analysis of microbiota compositions for all 91 frozen cycles showed that the prevalence of vaginal CSTs at each sampling timepoint differed (Figure 4.3). While prevalence of CST I did not significantly change across time, there was an increase in CST II and CST V type profiles from the first sample collection point to embryo transfer. At the same time, there was a decrease in CSTs III and IV profiles. In comparison with these findings, women undergoing fresh cycles in the ART1 study had relatively higher prevalence of suboptimal CST

III and IV communities, which persisted at the same rate throughout treatment, and a lower clinical success rate of IVF. Based on the reported relationships between CSTs and host reproductive health, it is reasonable to assume that a shift toward more optimal *Lactobacillus* dominated CSTs would associate with improved reproductive health as seen in the frozen cycles. Both *L. gasseri* and *L. jensenii* (CSTs II and V respectively) are considered commensal species that protect the host against infections such as Chlamydia via a number of mechanisms including the production of D-lactic acid (581). D-lactic acid is produced exclusively by *L. crispatus*, *L. gasseri* and *L. jensenii* in the vagina which inhibits MMP-8 (Matrix Metalloproteinase 8) cleavage and activation via the enzyme EMMPRIN (vaginal Extracellular Matrix Metalloproteinase Inducer), which is secreted by the epithelial cells (582). In contrast, *L. iners* lacks the gene encoding D-lactate dehydrogenase, which means it can only produce L-lactic acid, which does not offer the same level of resistance to pathogens such as *C. trachomatis* (583). Moreover, CST IV communities have previously been linked with reduced clinical pregnancy rates in women undergoing IVF (216, 500) and a history of infertility has been associated with enrichments for *Gardnerella* and *Ureaplasma*, both of which are prominent members of CST IV (191).

While these findings require validation in larger cohorts, they support the notion that the improved IVF success rates observed in frozen cycles may in part be explained by overall higher prevalence of “optimal” microbiota compositions. However, there are several other factors that could explain this observation. Compared to fresh cycles, a higher proportion of women receiving frozen cycles had PGT-A, which would improve their overall chance of IVF success. A limitation of PGT is mosaicism which is identified as more than one distinct cell line within an embryo. Mosaicism occurs due to mitotic errors after fertilisation after the first three cleavage divisions and are frequent in embryos (584, 585). Incidence rate of mosaicism in trophectoderm biopsies is reported to occur between 4% and 32% (585, 586). Modern technologies such as NGS are capable of detecting mosaicism between 20% to 80% (587). Eliminating chromosomal abnormalities of embryos is relevant to microbiota-host interactions as outlined by Grewal et al. (588), where vaginal dysbiosis was correlated specifically with miscarriages of euploid pregnancies. The cohort of frozen IVF cycles studied in this chapter included 34 cycles that underwent PGT. However, in these women, clinical pregnancy rates and the vaginal bacterial compositions were similar as those who did not undergo PGT.

It is also notable that there were several differences in the composition of the vaginal microbiota between women in the fresh and frozen cycle cohorts (Figure 4.4). At coordination appointment, 42% of samples were classified as CST I for fresh IVF cycles, compared to 23% of women at the same stage for frozen IVF cycles. It is possible that this difference is due to the timing of sample collection between the two cohorts. There was no pre-determined timing

for sample collection for women undergoing fresh IVF cycles, meaning they were at various stages of their monthly cycle. The hormonal profiles recorded for these patients suggest that up to half of these women were in the follicular phase and others in the luteal phase. Sample collection at coordination appointment in frozen cycles was consistently performed on day 2-3 of their cycle. The bleeding event shortly before sample collection could account for lower prevalence of CST I in frozen cycles compared with fresh. Prevalence of CST III was higher at this stage for the frozen cycles. This is in line with the reported literature suggesting that menstruation causes a reversible decrease in *L. crispatus* abundance and increase in *L. iners*, *G. vaginalis*, *P. bivia*, and *A. vaginae* abundance (150, 589).

In this cohort of women undergoing frozen IVF cycles, sample collection at the time of pituitary suppression was typically done at day 12 of the cycle during a transvaginal ultra-sonography of the endometrium. Several studies have reported that endometrium thickness is a suitable surrogate for E2 levels during IVF cycles (590-593) and it can be used as a biomarker for serum hyper- or hypo-estrogenism, which is indicative of successful pituitary suppression (594). This approach, in addition to reducing the number of blood tests required for IVF, allows for visualisation of pelvic pathology and identification of endometrial polyps, ovarian cysts and uterine fibroids which can reduce the success rates of IVF (595). However, as shown in Figure 3.3 of Chapter 3, the E2 concentrations of women recruited in the ART1 study who were undergoing a frozen cycle, were highly variable and overall, significantly higher than those undergoing a fresh cycle during pituitary suppression. Despite this, the patients in the ART2 cohort had high clinical pregnancy rates of around 60%. Clinical pregnancy rates for women aged 30-36 was 71% and women aged >36 was 55%. Considering 64% of all cycles included were made up of women of >36 years of age, the clinical pregnancy rates were superior to national average (32% live birth rates for women under 35 and <32% for older age groups) (596). Overall live birth rates were higher in frozen cycles in this study compared with fresh cycles (52% vs 45%).

The findings presented in this chapter add to the increasing number of studies that report contradictory relationships between vaginal microbiota composition and IVF success rates. It has been suggested that there exists a microbial continuum from the lower to the upper female reproductive tract (230). However, several recent studies indicated that the vaginal microbiota may not be a suitable proxy of the endometrial microbiota. For example, Moreno et al. reported distinct bacterial communities in the uterus compared to matched vaginal samples in up to 20% of patients (232). In their study, endometrial compositions with >90% dominance by *Lactobacillus* species were associated with significantly higher implantation rates, ongoing

pregnancy and live birth rates (232). A study by Diaz-Martinez et al. also reported differences in the microbial profiles of the vaginal and endometrium (242). However, like the vagina, whether the endometrial microbiota composition is predictive of IVF success still appears questionable with a recent review indicated 5/8 studies fail to identify a relationship between the two (597). Despite the clear need to undertake larger and more specific studies, there are already several commercial tests offered by some IVF clinics that provide assessment of the endometrial microbiota and purport to be able to use this information to improve success rates. Tests such as ALICE (Analysis of Infectious Chronic Endometritis), EMMA (Endometrial Microbiome Metagenomic Analysis), and ERA (Endometrial Receptivity Analysis) offered by Igenomix, claim to assess the receptivity of the endometrium and determine the microbial compositions as treatment add-ons to improve clinical outcomes (598).

A limitation of the work carried out in this chapter is the lack of information regarding host response. There are several studies showing that specific host response to vaginal bacteria can vary amongst patients and may play an important role in key events leading up to implantation (520). Further, our studies are limited to the analyses of the bacterial component of the microbiome. It is possible that fungal and viral components of the vaginal microbiome are important mediators of IVF success, and this warrants further investigation. An unforeseen issue with the frozen IVF cohort study was that the sample collections coincided with the onset of Covid-19 pandemic in London and subsequent suspension of IVF cycles in March/April 2020. The relevance of this is just beginning to emerge in scientific literature. The exact impact of the pandemic on influencing the cervico-vaginal microbiota and shaping the clinical outcomes is unclear but it is possible that it has contributed towards certain ambiguities in the analysis. Unfortunately, there is no record of whether patients had been exposed to the virus at any stage of sample collection during this study.

4.10.2 Summary of main findings

The success rates for the frozen cycles are high compared to most other studies and national averages. This could mean that the findings here may not be reflective of the broader cohort of patients undergoing IVF treatments. The relationship observed for this cohort suggested that cross-sectionally, there is a significant difference in microbial compositions based on clinical treatment outcomes. This was characterised by higher abundance of *L. crispatus* in patients with unsuccessful embryo implantation. Sub-analyses of cycles with euploid embryos mirrored the findings of all cycles included in this chapter. However, prevalence of CSTs and abundance of specific taxa were not associated with strong biomarker capabilities in predicting IVF success rates.

5 CHAPTER V. Rapid metabolic profiling of the cervico-vaginal niche for prediction of microbiota composition and IVF success

5.0 INTRODUCTION

Metabolomics involves the measurement and quantitation of metabolites and small molecules and assessment of their functions in health and disease states (471). Metabolites are produced via biochemical reactions within and between cells. Metabolite profiles therefore provides a snapshot of the physiological status of cell, tissue or system. There are several high throughput analytical techniques that can be used for obtaining metabolic profiles. These often require time-consuming and complex sample preparation steps. Further complexity is added through the use of chromatography to separate metabolites on the basis of their chemical properties before analysis using a mass spectrometer.

Metabolomics has been used to study several sample types in the context of IVF including embryo culture media and follicular fluid where attempts have been made to identify metabolic biomarkers for embryo fitness and IVF success. Follicular fluid can be collected at the time of egg collection and is often discarded. However, studies generally have not been successful in isolating biomarkers from the this sample type using targeted analysis of low molecular weight molecules (472). Studies on embryo culture media have indicated that there are metabolic differences depending on the potential of an embryo for implantation, however metabolic profiling of this type has not had an impact on clinical practices (599, 600). A recent study indicated recurrent implantation failure was associated with higher vaginal fluid levels of 2',3-cyclic UMP and inositol phosphate and lower glycerophospholipids and benzopyran compared with a control group (499).

Recently development ambient ionization techniques have addressed these issue removing the need for sample preparation and chromatographic separation of metabolites prior to MS analysis (601). One such technique is Desorption Electrospray Ionisation Mass Spectrometry (DESI-MS) which allows for direct on-sample analysis in real time (Section 1.5, page 54) (602, 603). Recently, the MacIntyre and Takats laboratory at Imperial College London developed Direct on-swab metabolic profiling by DESI-MS (480). The method works by directing a pneumatically assisted electrospray onto swab samples from a short distance. Molecules (i.e., metabolites, lipids, and small compounds) in the swab are dissolved and ionised and are taken up in secondary droplets that form during the analytical process. These are then directed via an inlet capillary into a mass spectrometer where a detailed chemical profile can be acquired in only a couple of minutes. Recently it was shown that this methods could enable the robust prediction of vaginal microbiota composition and host immune response in pregnancy (483).

DESI-MS can analyse an array of lipids, peptides, proteins, and their metabolites (604). Due to high sensitivity and specificity, DESI-MS has wide clinical applications including in various aspects of reproduction such as diagnosis of epithelial ovarian cancer (605). Furthermore, DESI-MS can effectively discriminate between purified bacterial samples with high taxonomic resolution directly from glass slide, agar plates or elusion swabs (606).

Biproducts of glycogen metabolism by *Lactobacillus* species include amines and bacteriocins and the relative contribution of lactic acid is varied which contributes to their metabolic output (607). Studies using LC-MS have identified specific metabolite markers associated with bacteria of the cervicovaginal mucus (475, 476). There are several metabolites associated with vaginal dysbiosis characterised by reduced lactic acid concentrations and increased levels of short-chain fatty acids such as acetate, propionate, isobutyrate, succinate, formate, and threitol (475, 476, 480, 608-610). The exact understanding of how these metabolites contribute to bacteria-host interactions is not fully explored. Additionally, the biochemical changes associated with vaginal bacterial compositions and their relationship with successful embryo implantation is limited to a handful of studies and merits further investigation.

Based on the hypothesis that the interplay between hormones, immune analytes and bacteria are reflected in the mucosal metabolome, the biomarker capabilities of the bacterial metabolite markers were assessed in the context of IVF treatments to address ambiguities in microbiota-host signalling. The aim of this chapter is to test the feasibility of using DESI-MS to predict the microbiota composition at key stages of sample collection including on the day of embryo transfer and to identify metabolic markers that are predictive of successful embryo implantation.

5.1 Results

5.1.1 Prediction of vaginal microbiota composition using DESI-MS profiles

This pilot study was performed using swabs collected from women undergoing fresh IVF cycle treatment samples at coordination appointment, pituitary suppression and on the day of embryo transfer. To begin with, the capacity of DESI-MS swab profiling to predict vaginal microbiota composition was assessed using all available samples. Resulting metabolic profiles were analysed using unsupervised PCA analysis to assess the metabolic variation across the data set. Assessment of the first and second principal components indicated that the majority of the variance the dataset was not related to microbiota composition. However, when the second and third principal components were plotted and samples were coloured on the basis of *Lactobacillus* dominance or depletion, there was clustering of *Lactobacillus*-depleted samples toward to the top righthand side of the plot (Figure 5.1). This indicated that some variance in the metabolic profile of the swabs was likely correlated with the microbiota composition.

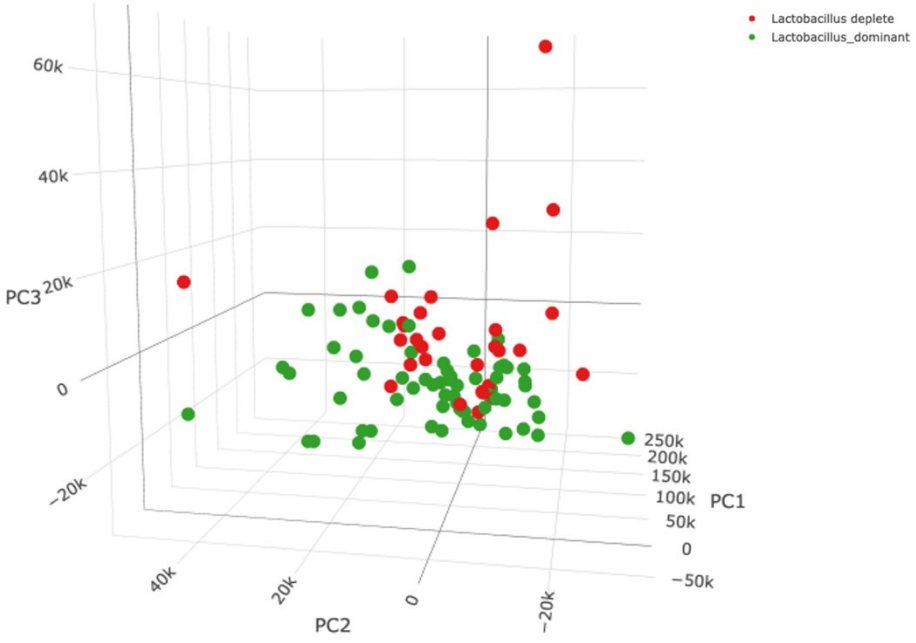


Figure 5.1: PCA analysis for metabolites. Three-dimensional unsupervised PCA analysis of cervico-vaginal metabolites. Samples were collected at coordination appointment, throughout pituitary suppression and on the day of embryo transfer. Green dots represent Lacto-dominant CSTs and red dots represent CST IV (n=94).

To further investigate how the metabolic profiles of the swabs reflect microbial compositions of the vagina, a supervised random forest classifier model was built using 2/3 of the available

data. The microbial composition of the remaining 1/3 of swab samples was predicted using this model and ROC curves were generated by Monte-Carlo cross validation using balanced sub-sampling. Six different models were built to determine if increasing numbers of features (5 to 100) would improve predictive performance. Overall, the models showed strong predictive capacity with mean predictive accuracies of between 71.8% to 75.3% (Figure 5.2)

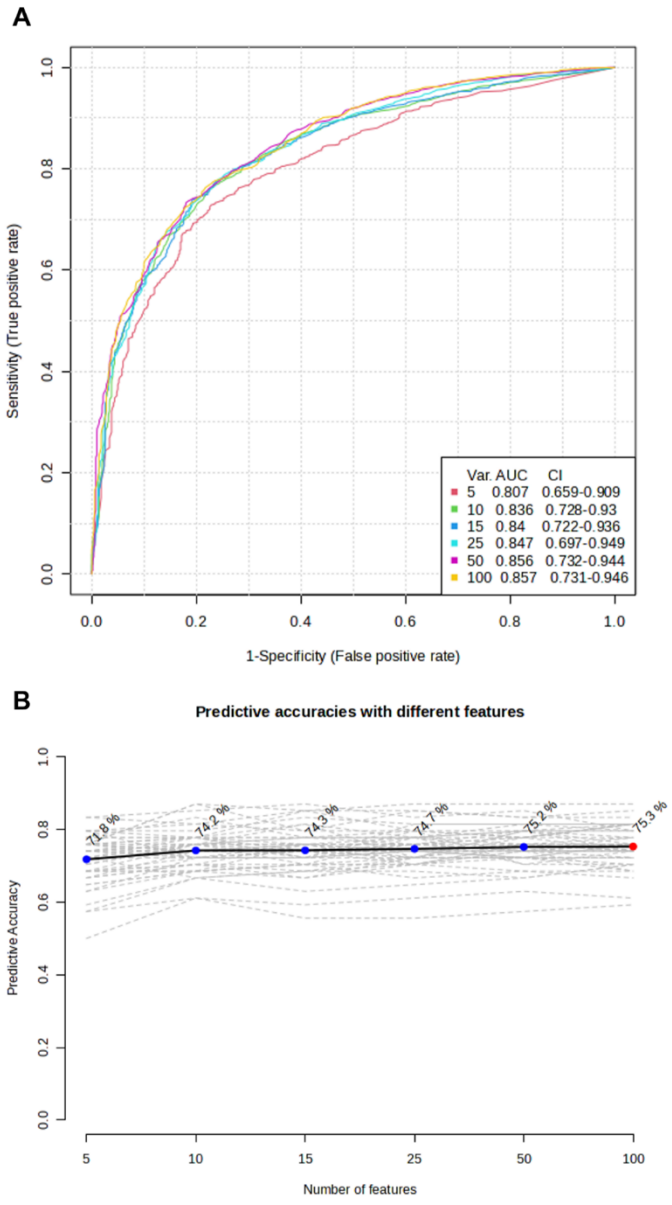


Figure 5.2: Random Forest models for prediction of vaginal microbiota composition using DESI-MS metabolic profiles. A) ROC curves for six different random forest models. Models were built using 5, 10, 15, 25, 50 and 100 features with AUCs demonstrated by different colours. The highest scoring random forest model used 100 features and had a cross validated AUC of 0.857 (CI: 0.731-0.946). B) Predictive accuracies using different number of features for each model.

The top 15 metabolites and their contribution to the discriminatory power of the random forest model designed to differentiate *Lactobacillus* dominated and depleted samples are presented in Figure 5.3. Metabolites were ranked based on selected frequency (%). The relative concentration of these metabolites in *Lactobacillus* dominated and depleted samples are presented in Figure 5.4. These include 5 features (*m/z* 217.1193593, 455.3278604, 148.9893034, 788.5433636 and 130.0876903) that were significantly higher in *Lactobacillus* dominated samples and one feature (*m/z* of 309.2794715) that was significantly higher in *Lactobacillus* depleted samples.

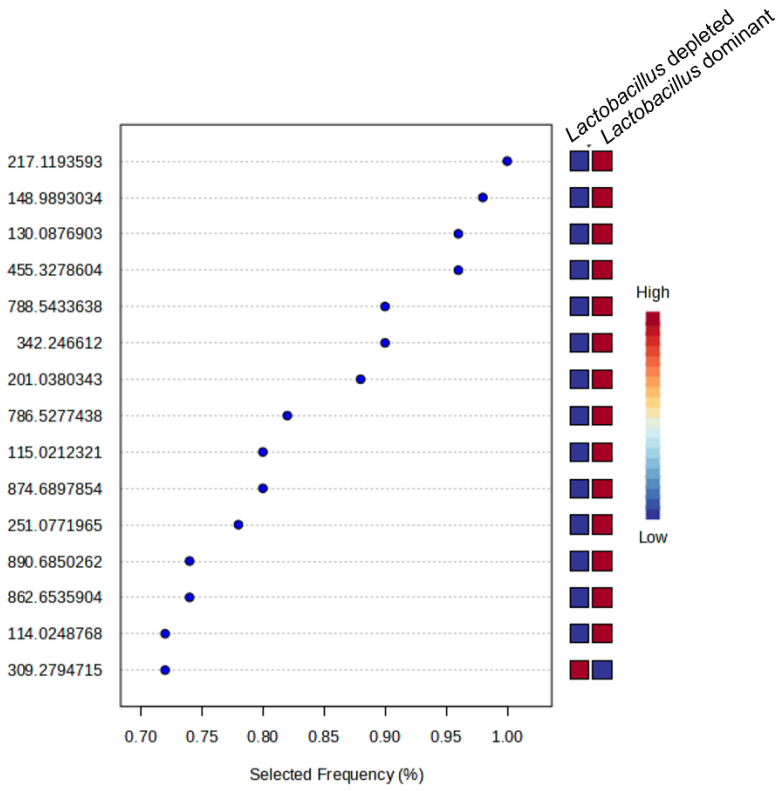


Figure 5.3: Metabolite feature importance for discriminating between *Lactobacillus* dominance and depletion. Top 15 most frequent features identified by random forest modelling. Coloured boxes indicate the intensity values of the corresponding *m/z* feature based on dominance or depletion of *Lactobacillus* (red: upregulation, blue: downregulation).

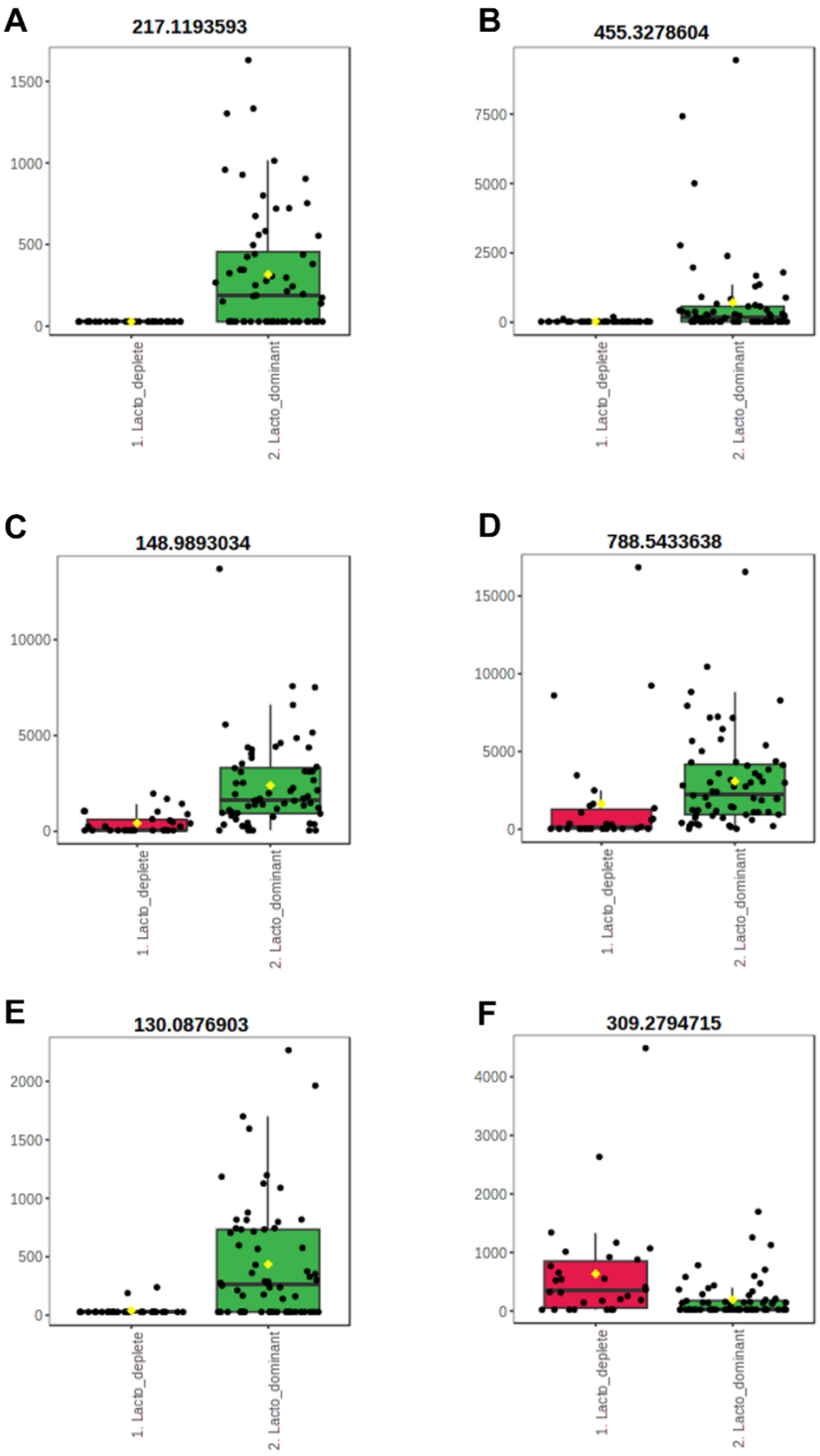


Figure 5.4: Representative features discriminating vaginal *Lactobacillus* dominance and depletion. Five metabolites were upregulated in samples categorised as *Lactobacillus* dominated including A) *m/z* 217.1193593, B) *m/z* 455.3278604, C) *m/z* 148.9893034, D) *m/z* 788.5433636 and E) *m/z* 130.0876903. F) A feature (*m/z* 309.2794715) upregulated in samples categorised as *Lactobacillus* depleted is also shown for comparison. (*Lactobacillus* depleted n=30, Lacto-dominant n=64).

5.1.2 Prediction of microbiota composition under differing hormonal conditions

Next, the capacity of DESI-MS to predict vaginal microbiota composition in women sampled at differing stages of hormonal manipulation was tested. Random forest modelling of the DESI-MS profiles indicated a strong ability to predict *Lactobacillus* dominance or depletion at each of the sampling stages (Figure 5.5). The metabolites most strongly contributing to the discriminating capacity of the model at coordination appointment included *m/z* 148.9893034 (higher in *Lactobacillus* dominated samples, n=39). At pituitary suppression, *m/z* 204.7614518 (upregulated in *Lactobacillus* dominated samples, n=22), and at embryo transfer *m/z* 217.1193593 (upregulated in *Lactobacillus* dominated samples, n=33) were the most strongly discriminating features. The number of samples available for analysis throughout pituitary suppression was smaller than the other stages of sample collection. There were only 6 Lacto deplete samples and 16 Lacto-dominant and subsequently wide confidence intervals observed at pituitary suppression were likely due to the comparatively low number of samples analysed at this time point (6 *Lactobacillus* depleted, 16 *Lactobacillus* dominated). For samples collected throughout pituitary suppression, the model built using 5 features had comparatively low predictive value, however, the model build using 100 features was associated with improved predictive ability and on par with data modelling for samples collected at coordination appointment and on the day of embryo transfer.

The top 15 most important metabolites discriminating between Lacto-dominant and depleted samples at each stage of sample collection are presented in Figure 5.6.

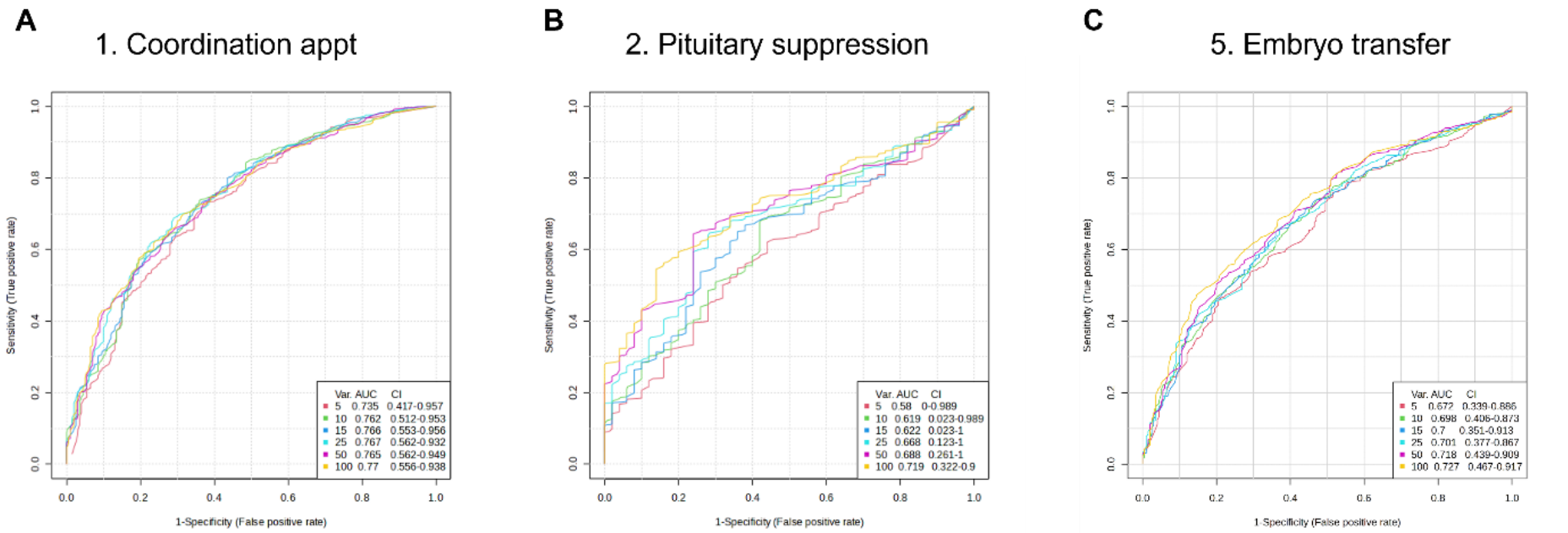


Figure 5.5: Random Forest modelling for microbiota composition prediction at different stages of sample collection. ROC curves for six different random forest models were built using 5, 10, 15, 25, 50 and 100 features demonstrated by different colours. AUC is indicated as a predictor of accuracy. A) Coordination appointment, the highest scoring random forest model was using 100 features AUC: 0.77 (CI:0.55-0.93) (n=39). B) Pituitary suppression, the highest scoring random forest model was using 100 features AUC: 0.71 (CI:0.32-0.9) (n=22). C) Embryo transfer, the highest scoring random forest model was using 100 features AUC: 0.72 (CI:0.46-0.91) (n=33).

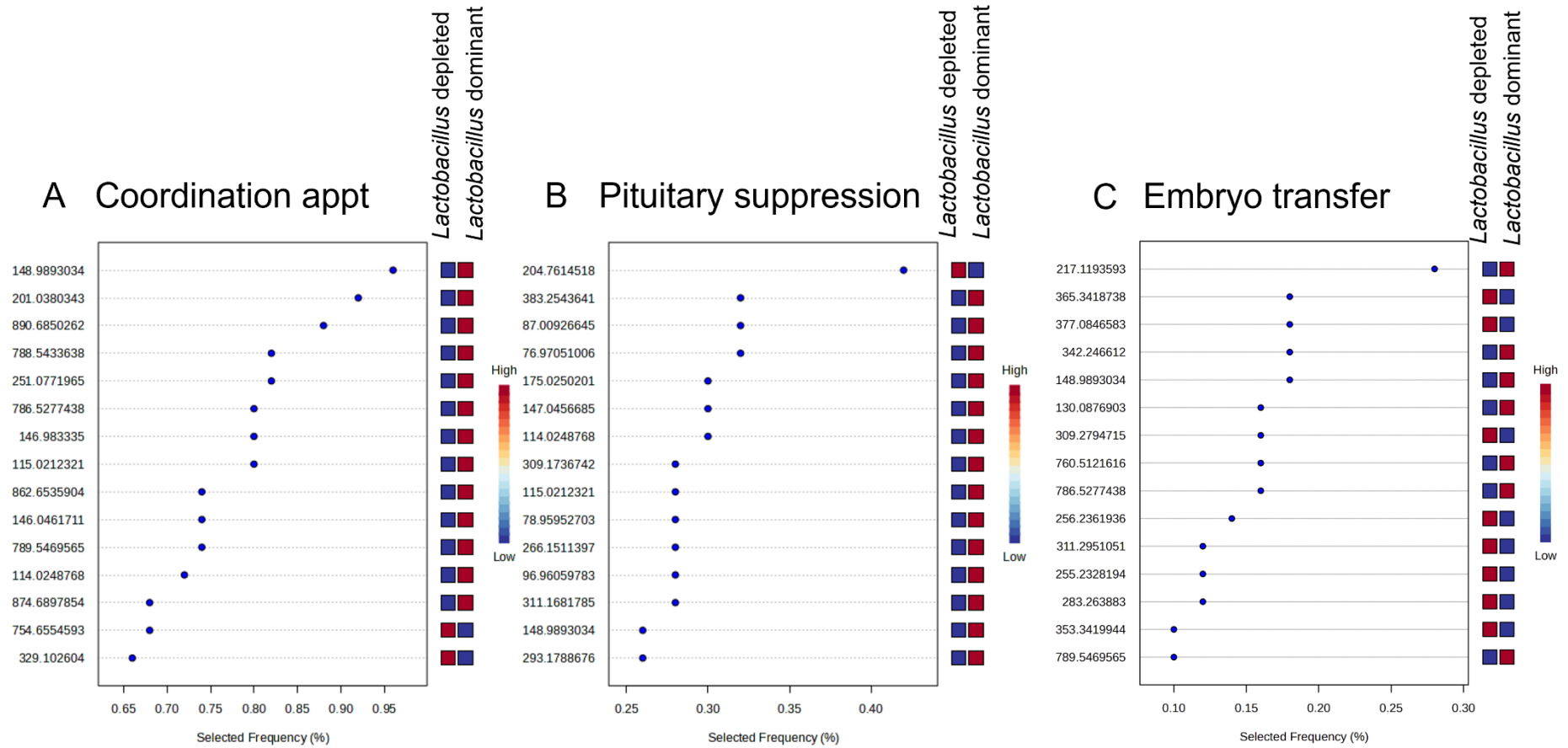


Figure 5.6: Top 15 important features discriminating between *Lactobacillus* dominant and depleted samples at different stages of sample collection. The most important features were based on selected frequency (%) in predicting vaginal bacteria composition. A) Coordination appointment, B) Pituitary suppression and C) Embryo transfer. Red indicates upregulation and blue indicates downregulation of metabolites.

Scatter plots of a representative discriminatory feature (*m/z* 148.9893034) facilitating prediction of *Lactobacillus* dominated samples at coordination appointment, pituitary suppression and on the day of embryo transfer are presented in Figure 5.7.

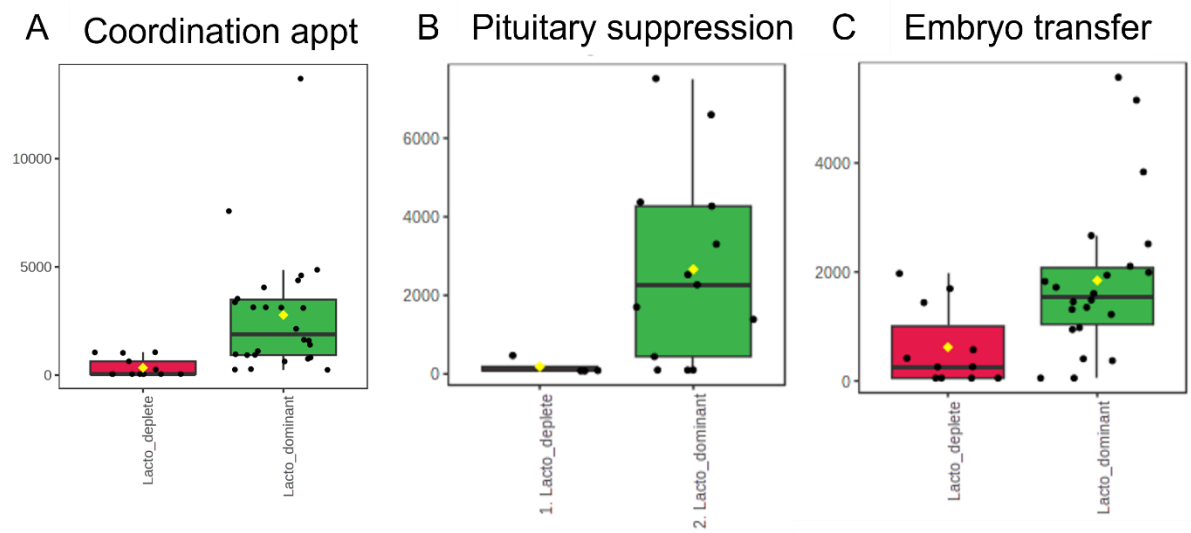


Figure 5.7: Feature *m/z* 148.9893034 discriminating between vaginal compositions at different stages of sample collection. Random Forest modelling for bacterial composition prediction at different stages of sample. Feature *m/z* 148.9893034 is upregulated in Lacto-dominant samples at A) Coordination appointment (n=39), B) Pituitary suppression (n=22), C) Embryo transfer (n=33).

Additionally, *m/z* 786.5277438 and *m/z* 789.5469565 were found to be upregulated in *Lactobacillus* dominated samples at coordination and on the day of embryo transfer (Figure 5.8).

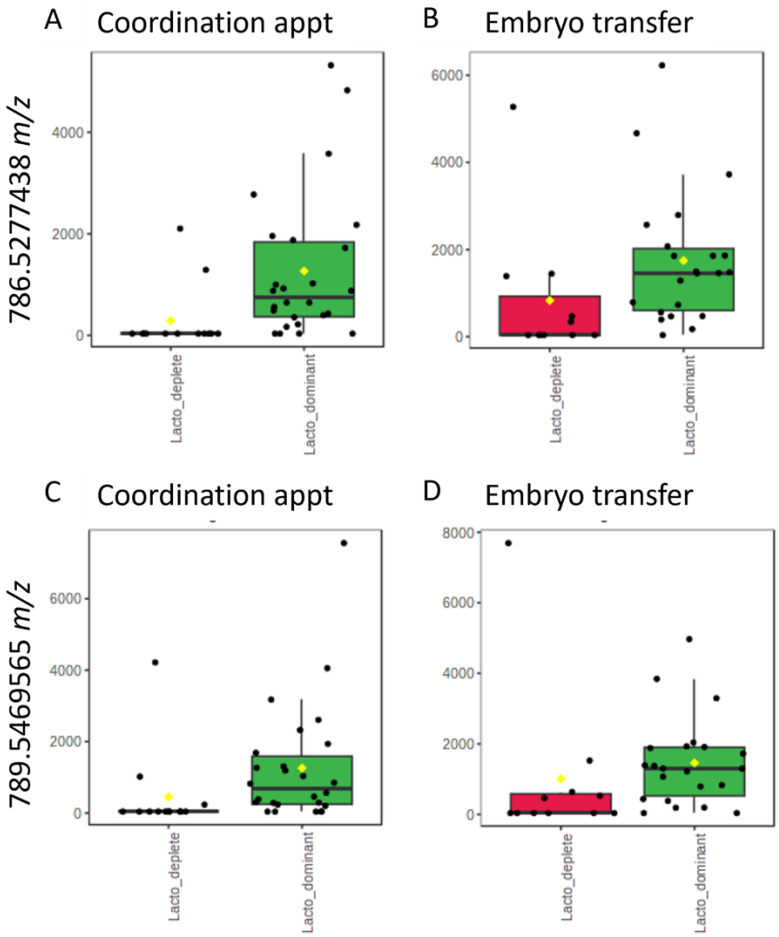


Figure 5.8: Features *m/z* 786.5277438 and *m/z* 789.5469565 discriminating between vaginal compositions at different stages of sample collection. Random Forest modelling for bacterial composition prediction at different stages of sample collection. Feature *m/z* 786.5277438 is upregulated in Lacto-dominant samples at A) Coordination appointment (n=39), and B) Embryo transfer (n=33). Feature *m/z* 789.5469565 is upregulated in Lacto-dominant samples at C) Coordination appointment (n=39), and D) Embryo transfer (n=33).

Next, the capacity of direct swab analysis by DESI-MS to predict clinical outcome using samples collected at each of the sampling time points including the coordination appointment, pituitary suppression and on the day of embryo transfer were tested (Figure 5.9). Strongest prediction of outcome was observed at pituitary suppression where the AUC was 85%. As noted earlier, wide confidence intervals are likely due to small sample sizes at this timepoint (Figure 5.9, Panel B). Poorer prediction was observed for samples collected at coordination appointment (ave AUC:0.61) and on the day of embryo transfer (ave AUC:0.43). The top 15 most important metabolites discriminating between successful IVF outcomes at each stage of sample collection are presented in Figure 5.10.

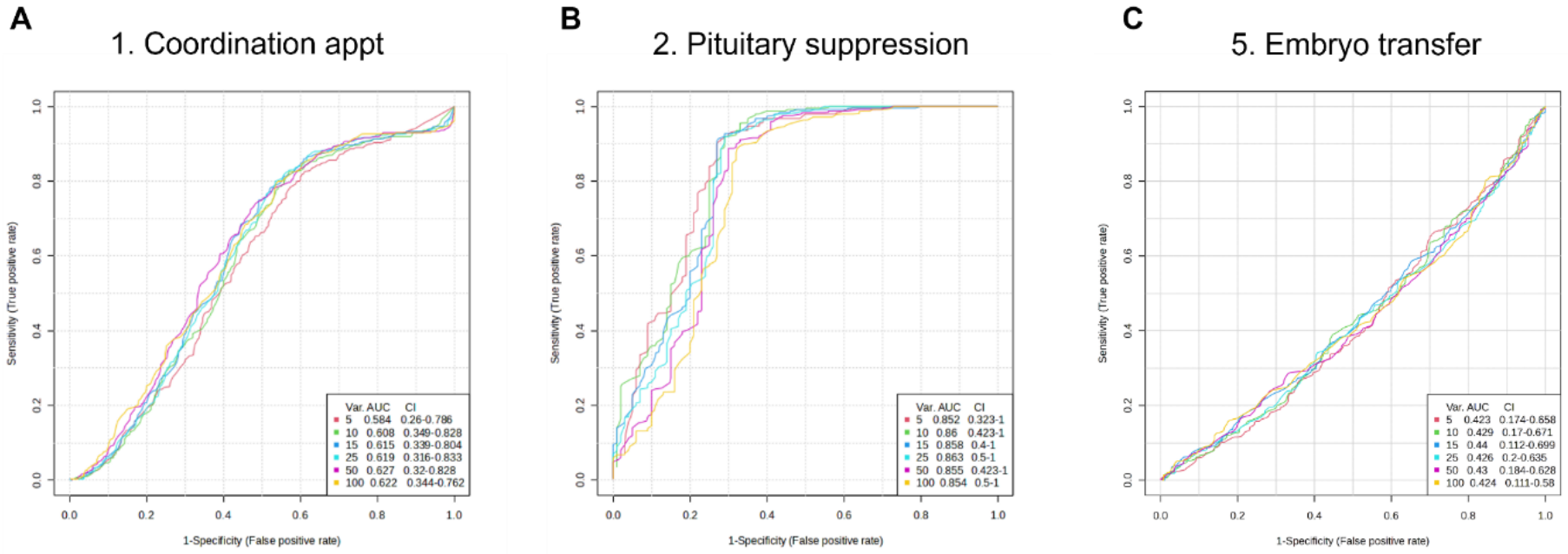


Figure 5.9: Random Forest modelling for treatment outcome prediction at different stages of sample collection. ROC curves for six different Random Forest models were built using 5, 10, 15, 25, 50 and 100 features demonstrated by different colours. AUC is indicated as a predictor of accuracy. A) Coordination appointment, the highest scoring random forest model was using 50 features AUC: 0.62 (CI:0.32-0.82) (n=39). B) Pituitary suppression, the highest scoring random forest model was using 25 features AUC: 0.86 (CI:0.5-1) (n=22). C) Embryo transfer, the highest scoring random forest model was using 15 features AUC: 0.44 (CI: 0.11-0.69) (n=33).

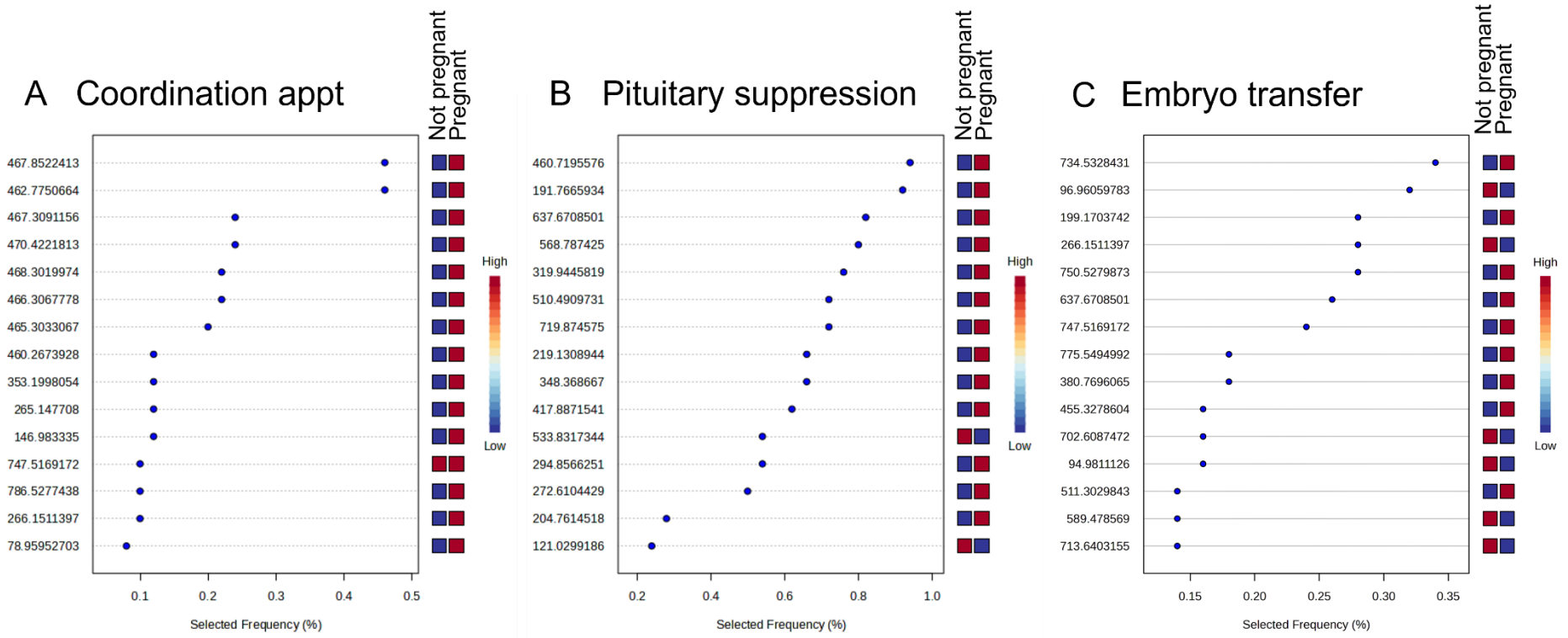


Figure 5.10: Top 15 important features discriminating between treatment outcomes at different stages of sample collection. The most important features were based on selected frequency (%) in predicting vaginal bacteria composition based on successful embryo implantation at different stages of sample collection. A) Coordination appointment, B) Pituitary suppression and C) Embryo transfer. Red indicates upregulation of metabolites and blue indicates downregulation.

Some metabolites were found to discriminate between successful and unsuccessful treatment outcomes at more than 1 stage of sample collection. For example, feature *m/z* 747.5169172 was higher in samples with successful clinical outcomes at coordination and on the day of embryo transfer (Figure 5.11).

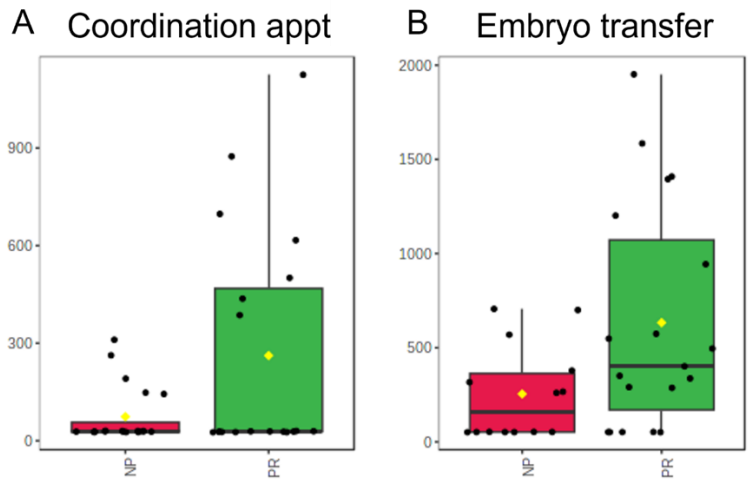


Figure 5.11: Feature *m/z* 747.5169172 discriminating between successful and unsuccessful pregnancy at different stages of sample collection. Feature *m/z* 747.5169172 is upregulated in samples with successful pregnancy at A) Coordination appointment (n=39), and B) Embryo transfer (n=33).

Feature *m/z* 266.1511397 was significantly higher in samples with successful outcomes at coordination appointment, however it was subsequently decreased in samples successful clinical outcomes on the day of embryo transfer (Figure 5.12).

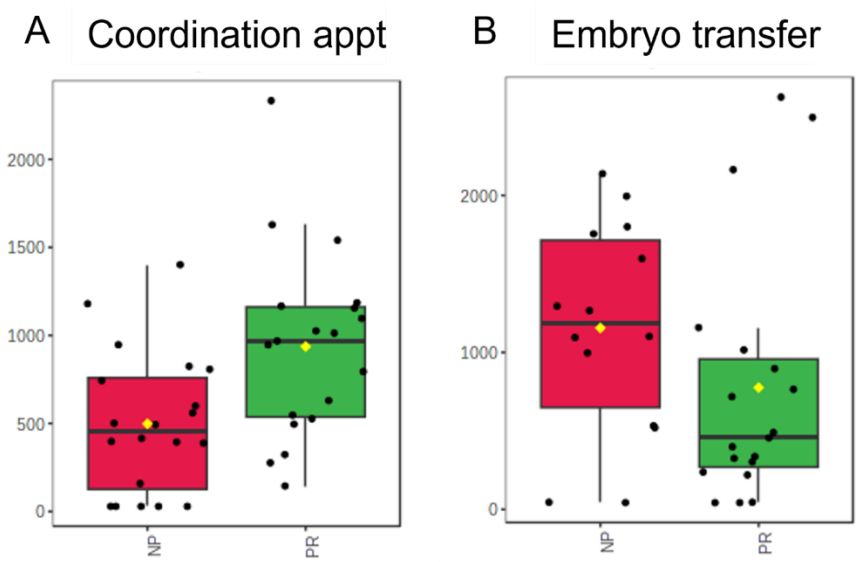


Figure 5.12: Feature *m/z* 266.1511397 discriminating between successful and unsuccessful pregnancy at different stages of sample collection. Feature *m/z* 266.1511397 is upregulated in samples with successful pregnancy at A) Coordination appointment (n=39). It is downregulated at B) Embryo transfer (n=33).

Samples from women experiencing successful clinical outcomes were also found to have significantly higher levels of *m/z* 637.6708501 at pituitary suppression and embryo transfer (Figure 5.15).

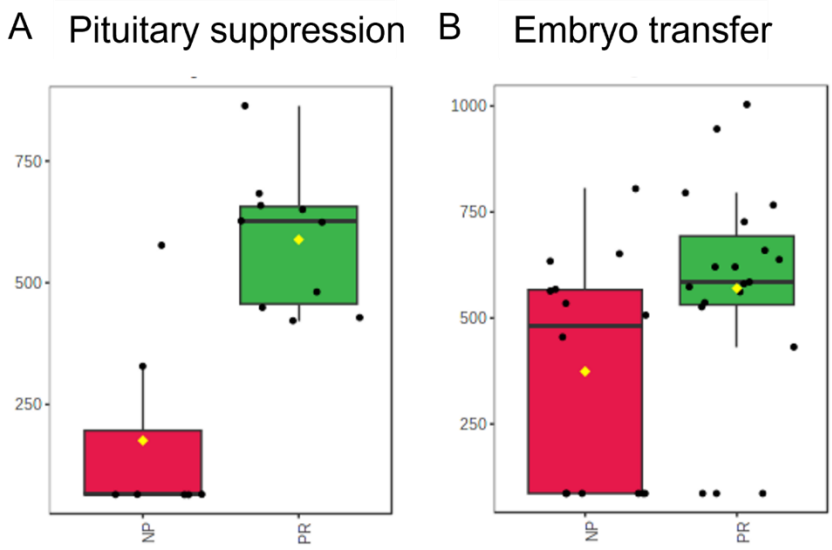


Figure 5.13: Feature *m/z* 637.6708501 discriminating between successful and unsuccessful pregnancy at different stages of sample collection. Feature *m/z* 637.6708501 is upregulated in samples with successful pregnancy at A) Pituitary suppression (n=22) and B) Embryo transfer (n=33).

5.1.3 Putative identification of discriminatory metabolites

Putative identification of metabolites permitting discrimination of *Lactobacillus* dominant and depleted compositions, or those significantly differing between women who had successful or unsuccessful treatment outcomes was undertaken by identifying accurate masses of metabolites to four decimal places. This procedure included pre-processing steps of lock mass correction, background subtraction, deionising and smoothing. The accurate masses were then inputted into databases LIPID MAPS (611) and Metlin (612) where the molecular formula of the compound was obtained. The molecular formula was then inputted in ChemCalc (613) where the monoisotopic mass was confirmed, and isotopic distribution was displayed (in centroid mode). The molecular formula and accurate masses were then used to search for biological candidates in the databases mentioned above, with the highest-ranked match based on delta value (<0.01) (Table 5.1).

Table 5.1: Important metabolites identified by Random Forest modelling. Metabolites that significantly discriminated between *Lactobacillus* dominant or depleted compositions or based on treatment outcomes.

***m/z* measured**	***m/z* theoretical**	**Ppm error**	**Metabolite annotation**	**Adduct**	**MS level of annotation**	**Predictive model feature identified in**
130.0876	130.0874	1.53	Leucine	[M-H]-	3	Upregulated in Lacto dominant using all available data.
148.9893	148.9914	-14.09	Thiomalic acid	[M-H]-	3	Upregulated in Lacto dominant using all available data. As well as at coordination appt, pituitary suppression and ET.
204.7614			Unknown		3	Upregulated for Lacto-dominant at pituitary suppression.
217.1193	217.1194	-0.46	Leucyl-Serine	[M-H]-	3	Upregulated for Lacto-dominant using all available samples and at ET.
266.1511	266.1550	-14.6	4-Piperidinemethanol a,a-diphenyl	[M-H]-	3	Upregulated for pregnant patients at coordination and upregulated for not pregnant samples at embryo transfer.
309.2794	309.2799	-1.38	Phytenic acid (C20:1)	[M-H]-	3	Upregulated for Lacto-depleted samples using all available data.
455.3278	455.3313	-7.55	Amino-sulfonyl hepten yl-amino oxo octadecanoic	[M-H]-	3	Upregulated for Lacto-dominant samples using all available data.
637.6708			Unknown		3	Upregulated for pregnant patients at pituitary suppression and embryo transfer.
747.5169	747.5182	-1.73	Phosphatidyl glycerol (PG) (34:1)	[M-H]-	3	Upregulated for pregnant patients using all available data. Upregulated for pregnant samples at coordination an embryo transfer.
786.5277	786.5291	-1.77	phosphatidyl serine (PS) (36:2)	[M-H]-	3	Upregulated in Lacto-dominant samples at coordination appointment and embryo transfer.
788.5433	788.5447	-1.77	phosphatidyl serine (PS) (36:1)	[M-H]-	3	Upregulated for Lacto-dominant samples using all available data.
789.5469	789.5475	-0.75	Isotope of phosphatidyl serine (PS) (36:1)	[M-H]-	3	Upregulated in Lacto-dominant samples at coordination and on the day of ET.

5.2 Discussion

This pilot study aimed to assess the biomarker characteristics of cervico-vaginal metabolites in predicting microbial composition and successful embryo implantation using a direct on-swab metabolic profiling method. The random forest modelling successfully identified metabolic signatures associated with bacterial compositions of the vagina for IVF patients (Figure 5.2). This finding supports studies of MacIntyre laboratory in association of metabolic signatures in identification of microbial compositions throughout pregnancy (483).

The results in Chapters 3 and 4, alluded to the role for microbiota composition in success of IVF treatments. Based on Random Forest modelling, there was no strong predictive model associated with outcome based on microbiota composition (Figure 5.9). Given that some studies have suggested strong microbial signatures in prediction of IVF outcomes (196, 614), in this chapter we aimed to assess whether metabolic signatures of the vaginal mucosa can predict microbial compositions and IVF treatment success rates. Using DESI-MS has several advantages over metataxonomic sequencing of vaginal bacteria. Metataxonomic studies require DNA extraction protocols and NGS which are lengthy, expensive, and labour intensive. Whereas DESI-MS is capable of cost-effective analysis and rapid data processing which makes it highly suitable for bedside patient care.

Results of studies on application of DESI-MS from our group have been very promising (480, 483). This pilot study is the first of its kind to use DESI-MS on samples collected from patients undergoing IVF treatments. Here we identified metabolic signatures associated with *Lactobacillus* dominance and depletion in vaginal samples. This suggests that internally cross validated Random Forest modelling methodology is robust and suitable for biomarker discovery and can potentially have relevant clinical importance (Figure 5.5). We included samples representing diverse hormonal states. There were shared signatures amongst isolated metabolites at different hormonal levels suggesting reproducibility of metabolic signatures in this study.

The biochemical vaginal milieu changes significantly at high and low estrogenic states (615). Some metabolites are produced directly by bacteria or produced by the host in response to certain bacteria (499). Putative identification of important features discriminating between *Lactobacillus* dominant and depleted compositions, identified Thiomalic acid to be upregulated in Lacto-dominant samples (Table 5.1). This metabolite was important in analysis using all available data as well as at specific stages of sample collection including samples collected on coordination appointment, throughout pituitary suppression and on the day of embryo transfer. Thiomalic acid has been previously identified to be upregulated in Lacto-dominant

samples in a study by Pruski et al. (483). Thiomalic acid is likely to be relevant in the biochemical processes associated with *Lactobacillus* species and are hitherto unidentified functional roles. Other important metabolites discriminating between Lacto-dominant and depleted samples included Leucine, Amino-sulfonyl hepten yl-amino oxo octadecanoic acid and phosphatidylserine (36:1) that were upregulated in Lacto-dominant samples using all available data (Table 5.1). It is difficult to interpret the relevance of these metabolites without evaluating the metabolic pathways and differences in metabolic activity.

Random forest modelling for vaginal microbiota prediction based on dominance by *Lactobacillus* species was generally strong and comparable at different stages. Data modelling for prediction of outcomes however suggested that random forest modelling on the day of embryo transfer did not have a strong predictive value (Figure 5.9). This was in line with analysis on bacterial composition and quantity on the day of embryo transfer reported in Chapter 3. For samples collected throughout pituitary suppression however, this modelling was stronger (Figure 5.9). This should however be interpreted with a degree of caution due to lower number of samples available for analysis at this stage (n=22). A metabolic signature identified for discriminating between successful and unsuccessful embryo implantations was phosphatidylglycerol (34:1). Phosphatidylglycerol is a lipid present in animals and plants, and it can be a major component of bacteria membranes and represent up to 25% of phospholipids in Gram-negative bacteria (616). Recent studies suggest that phosphatidylglycerol are recognised by T-cells and play an important role in innate immune response (617). Discovery of metabolites related to IVF treatment outcomes prior to embryo transfer has the potential to revolutionise IVF treatments. While additional experimentation is likely required to confirm the identifications of metabolites, putative identifications are likely to be functionally relevant in the vagina niche. The results of this pilot study are promising in ability of DESI-MS to identify metabolites discriminating between successful and unsuccessful cycles at earlier stages of IVF treatments.

A limiting factor of ionization sources is ion suppression due to matrix effect (481, 602, 618). Ion suppression effect is an important indicator of quantification ability of ionization source assessment (619). Presence of less volatile compounds can change the efficiency of droplet formation which subsequently can affect the quantity of charged ions reaching the detector (620). DESI-MS has better ion suppression effects compared with conventional ionization sources. DESI-MS analysis on complicated matrices such as urine and serum suggest that the quantitative performance of DESI-MS exhibits lower ion suppression effects due to the *in-situ* extraction process (621, 622). Benchmarking of the spectral quality is done manually in DESI-MS analyses. Therefore, the optimisation procedure is partially subjective. This limitation is associated with lack of reproducibility amongst DESI-MS studies (623). DESI-MS

instrumentation is not fully standardised with only a handful of protocols describing the operation optimisation and geometric parameters available.

Future work on this project would include building random forest models using all available data which would potentially make the confidence intervals narrower and improve the Random Forest models. Inclusion of samples collected throughout ovarian stimulation and on the day of egg collection would add 52 additional samples and inclusion of serum hormones and immune analytes presented in Chapter 3 of this thesis will produce more in-depth results. It may also be important to identify biomarkers that discriminate between CST I and CST III. Unlike other *Lactobacillus* species*, L. iners* has been frequently found in BV samples and implicated to play a role in preterm birth (204, 624). Furthermore, CCA analysis presented in Chapter 3 of this thesis suggested that *L. iners* relationship with immune analytes resembles those of CST IV more than other *Lactobacillus* species.

Studies on the microbiota of the upper reproductive tract, have identified endometrial microbiota including communities that are independent of vaginal communities (230, 232). The significance of endometrial microbiota in IVF outcomes is outlined by a growing body of evidence (237, 241). Endometrial sample analysis using DESI-MS could potentially further identify metabolic signatures associated with success of IVF treatments.

There are different ways to extract out different classes of metabolites. Presently, beam of methanol water was used to dissolve the metabolites into ionised secondary droplets which are then taken up into a MS (480). If we change the composition of the solvent into acetonitrile or other organic solvents, it will dissolve a different set of metabolites and lipids that can possibly identify other clinically relevant metabolites for this study.

DESI-MS is a novel technology which is fast evolving and using different solvents is one of many steps that can improve the usability of DESI-MS. The current methodology used shows great promise in prediction of microbiota composition and potentially clinical IVF outcomes and provides a great foundation for future studies on metabolome of IVF cycles.

6. CHAPTER VI: Assessment of seminal microbiota and their relationships with seminal quality and function parameters

6.0 INTRODUCTION

Sperm counts worldwide have reduced by more than 50% since the 1970s (625). Accordingly, poor semen quality is now observed in half of couples with infertility (626). Male infertility may arise from obesity, diabetes, varicocele, symptomatic genitourinary infection, or several genetic factors; however, up to 24% of cases remain unexplained (9). Recent studies have revealed that increased levels of sperm DNA fragmentation and semen reactive oxygen species (ROS) are associated with infertility, impaired preimplantation, embryo development, and recurrent miscarriage (269, 270, 627, 628). There is an urgent clinical need to understand how sperm DNA fragmentation and semen ROS arise to develop novel therapeutic targets for male infertility.

As discussed in section 1.3.2.3.1 of the introduction, seminal leukocytes are a major source of ROS. Leukocytospermia is associated with increased semen ROS, sperm DNA damage and impaired sperm motility (282). Furthermore, leukocytospermia is associated with bacterial infections (629), and antibiotic treatment may improve sperm parameters (630). Bacteriospermia identified using semen culture is associated with suboptimal seminal parameters including reduced sperm count (304, 321, 322), motility (321-323, 329, 332), abnormal morphology (304, 332) and increased sperm DNA fragmentation (304). Recently, NGS approaches have investigated the possibility that semen contains a microbiota (121, 346-349). However, these studies, mostly limited to small patient cohorts, have produced inconsistent results and have failed to identify a consistent microbial compositional structure related to semen fertility parameters. It remains unclear whether a genuine semen microbiota exists and if so whether it associates with clinical and molecular markers of male reproduction.

In this study it was hypothesised that semen microbiota composition and/or bacterial load associates with functional semen parameters, including ROS levels and DNA damage. To test this, relationships between metataxonomic profiles of bacteria, bacterial copy number and key parameters of function and quality in semen samples were explored.

6.1 Study population characteristics and demographics at study entry

Semen samples were collected from a total of 223 men including controls with proven paternity (n=63) and patients undergoing various fertility investigations (n=160). The latter included 58 men diagnosed with Male Factor Infertility (MFI), male partners of women with Recurrent Pregnancy Loss (RPL) (n=46), and male partners of couples diagnosed with Unexplained Infertility (UI). The overall mean age of the total cohort was 38.1 ± 6 (mean ± SD). The mean age for controls was 40.1 ± 8, and the mean age for patients undergoing various fertility investigations was 37 ± 4.8. Of these, 48 patients self-identified as Asian, 9 Black, 156 Caucasian, 3 Hispanic, 2 mixed-race and 5 'other'. To enable statistical comparison, patients were categorised as Caucasian (n=156) and non-Caucasian (n=67) (Table 6.1). Ethnicity representation amongst recruited cohorts were not significantly different (p=0.38, Chi-square test).

Table 6.1: Comparison of mean age and prevalence of ethnicities in male study recruitment cohorts. RPL: Recurrent Pregnancy Loss, MFI: male Factor Infertility, UI: Unexplained Infertility.

Study cohort	Age (mean ± SD)	Ethnicity
Controls (n=63)	40.1 ± 8.0	39/63 (62%) Caucasian
		24/63 (38%) non-Caucasian
RPL (n=46)	38.2 ± 5.0	35/46 (76%) Caucasian
		11/46 (24%) non-Caucasian
MFI (n=58)	36.3 ± 4.5	41/58 (70%) Caucasian
		17/58 (30%) non-Caucasian
UI (n=56)	37 ± 4.7	41/56 (73%) Caucasian
		15/56 (27%) non-Caucasian

6.2 Semen quality and functional parameters of the study population

Reference limits for microscopic semen qualities were based on the WHO laboratory manual 5th edition (248). A compound parameter termed "Semen quality" was also assessed whereby samples displaying one or a combination of low sperm concentration, motility and morphology were considered 'sub-optimal'. Thresholds for relevant microscopic factors are outlined below in Table 6.2. Of note, sexual abstinence according to the WHO laboratory manual is between 2 to 7 days (248). All but 4 samples included in this study were within this abstinence period.

Table 6.2: WHO defined lower limits of seminal parameters.

Parameter	Lower limit
Semen Volume (mL)	1.5
Sperm Concentration (Mil/mL)	15
Progressive Motility (%)	32
Sperm Morphology (%)	4
pH	≥7.2

To facilitate categorical statistical analyses, the first and third quartiles of age were calculated, and patients were categorised into: <34, 34-41, <41 years old. The remaining categorical classifications in Table 6.3 were based on clinically defined thresholds. To determine the DNA fragmentation index, the TUNEL assay was used on 183 of the samples. These samples included controls (n=63), RPLs (n=46), MFIs (n=43), and UIs (n=31). The threshold to distinguish between high and low DNA fragmentation was 20% with specificity of 89.4% and sensitivity of 96.9% (631). For the remaining 40 patients (MFIs, n=15 and UIs, n=25) the Comet assay was used. Thresholds for high and low DNA fragmentation categorisation were based on the average Comet scores. The fertile range was defined as score of <27% indicating a low risk of male infertility. The upper limit of optimal ROS was internally determined at 3.77 RLU/sec/10^6 sperm (95% CI) based on an established protocol (287).

Table 6.3: Patient demographics and notable parameters of seminal quality and function for controls and study subjects. The prevalence of sperm DNA fragmentation and ROS were higher in patients undergoing fertility investigations compared to controls. Prevalence of oligospermia was also significantly higher in study subjects. Fisher's exact tests for all except age. Chi-square test for age. (n=223).

Factor	Categories	Controls	Study subjects	p-value
DNA frag index	Low	45/114 (40%)	69/114 (60%)	**0.0002*** **
	High	12/ 82 (15%)	70/82 (85%)	
ROS	<3.77 RLU/s	53/143 (37%)	90/143 (63%)	**0.02***
	>3.77 RLU/s	5/33 (15%)	28/33 (85%)	
Semen volume	Optimal	55/208 (26%)	153/208 (84%)	**0.03***
	Sub-optimal	8/15 (53%)	7/15 (47%)	
Age	<34	11/49 (22%)	38/49 (88%)	**0.04***
	34-41	31/124 (25%)	93/124 (85%)	
	>41	21/50 (42%)	29/50 (58%)	
Ethnicity	Caucasian	39/156 (25%)	117/156 (75%)	0.10
	Non-Caucasian	24/67 (36%)	43/67 (64%)	
Concentration	>15 M/mL	58/182 (32%)	124/182 (68%)	**0.01***
	<15 M/mL	5/41 (21%)	36/41 (79%)	
Progressive motility	>32%	60/207 (29%)	147/207 (71%)	0.56
	<32%	3/16 (19%)	13/16 (81%)	
Sperm morphology	>4%	22/74 (30%)	52/74 (70%)	0.87
	<4%	41/144 (28%)	103/144 (72%)	
Semen quality	Optimal	24/78 (31%)	54/78 (69%)	0.53
	Sub-optimal	39/145 (27%)	106/145 (73%)	

The prevalence of high sperm DNA fragmentation was significantly higher in the study subjects undergoing various fertility investigations compared with controls. Study subjects made up 85% of samples categorised as having high sperm DNA fragmentation and compared with controls, accounted for 85% of samples with high ROS. Furthermore, oligospermic samples were mostly from study subjects 79% compared with 21% of controls.

6.3 Genera level classification of semen microbiota profiles

A total of 7,886 ASVs were identified in the semen dataset, 94 of which were identified as kit or environmental contaminants. Identification of contaminants was based upon frequency (82 ASVs) and prevalence (12 ASVs) of the ASVs as detected in kit and environmental control samples. After removing these, a total of 7,998,565 high quality sequencing reads were identified in the semen samples and included in subsequent analyses.

Given that there is a lack of a consensus on the compositional structure of seminal microbiota in the literature, the first goal of this study was to determine if any common or shared bacterial profiles could be observed within the study cohorts. Hierarchical clustering analysis (Ward's linkage) was performed, and Silhouette scores were calculated to determine the optimal number of clusters within the dataset. Using sequence data resolved to genera level, three major clusters were identified. These clusters were characterised by high abundance of 1. *Streptococcus*, 2. *Prevotella*, and 3. *Lactobacillus* and *Gardnerella* (Figure 6.1).

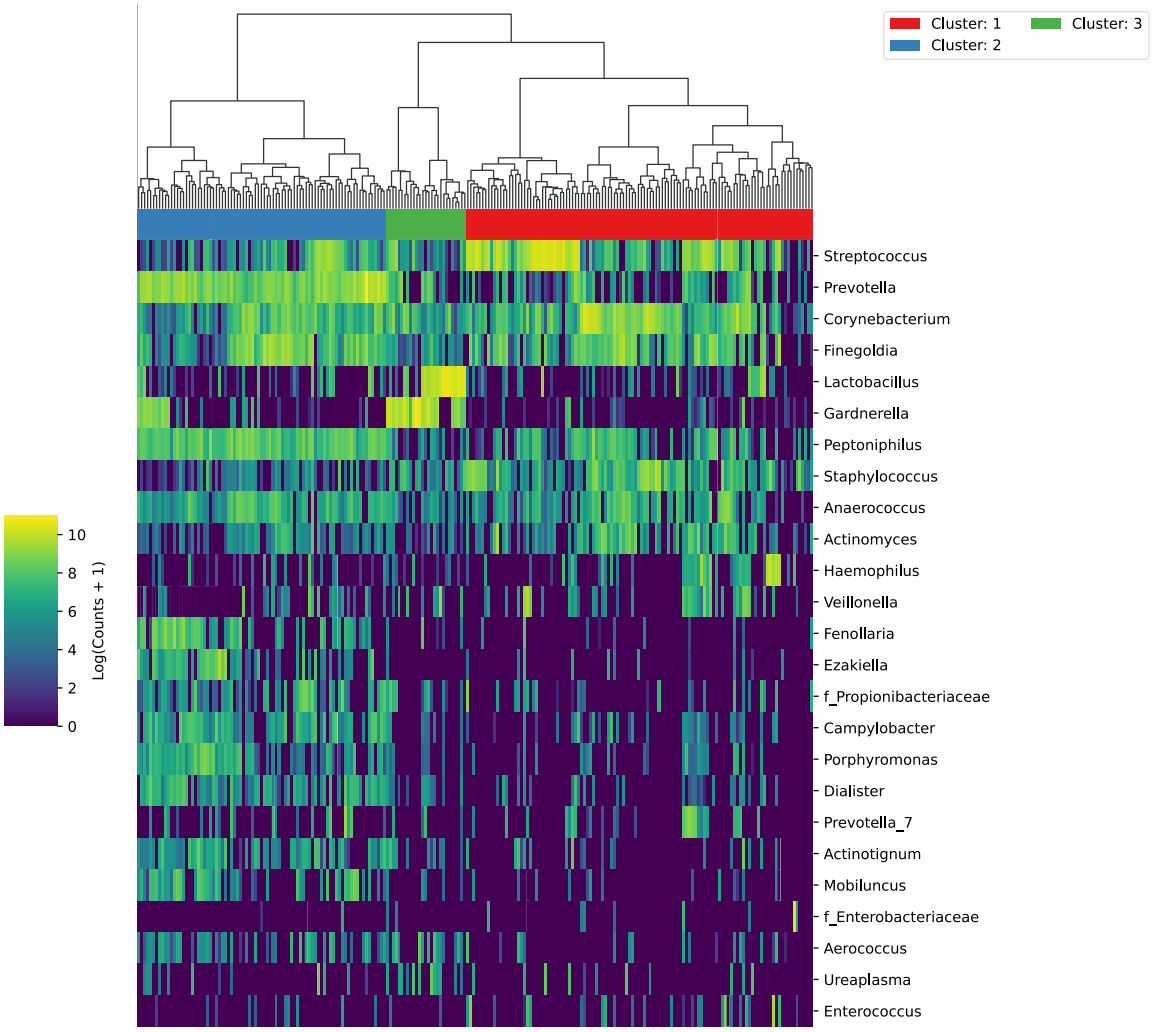


Figure 6.1: Heatmap of Log10 transformed read counts of top 25 most abundant genera identified in semen samples. Samples clustered into three major microbiota groups based mainly on dominance by *Streptococcus* (Group 1), *Prevotella* (Group 2), or *Lactobacillus* and *Gardnerella* (Group 3). (n=223, Ward's linkage).

Average Silhouette scores suggested that 3 clusters were the optimal number of clusters for genera level classification of seminal microbiota (Figure 6.2). The Silhouette scores, a metric used to calculate the goodness of fit for a clustering technique, indicated that cluster 3 type profiles had the most robust fit. Plotting of the top 6 most abundant genera in each of the clusters confirmed that these clusters were compositionally distinct from one another.

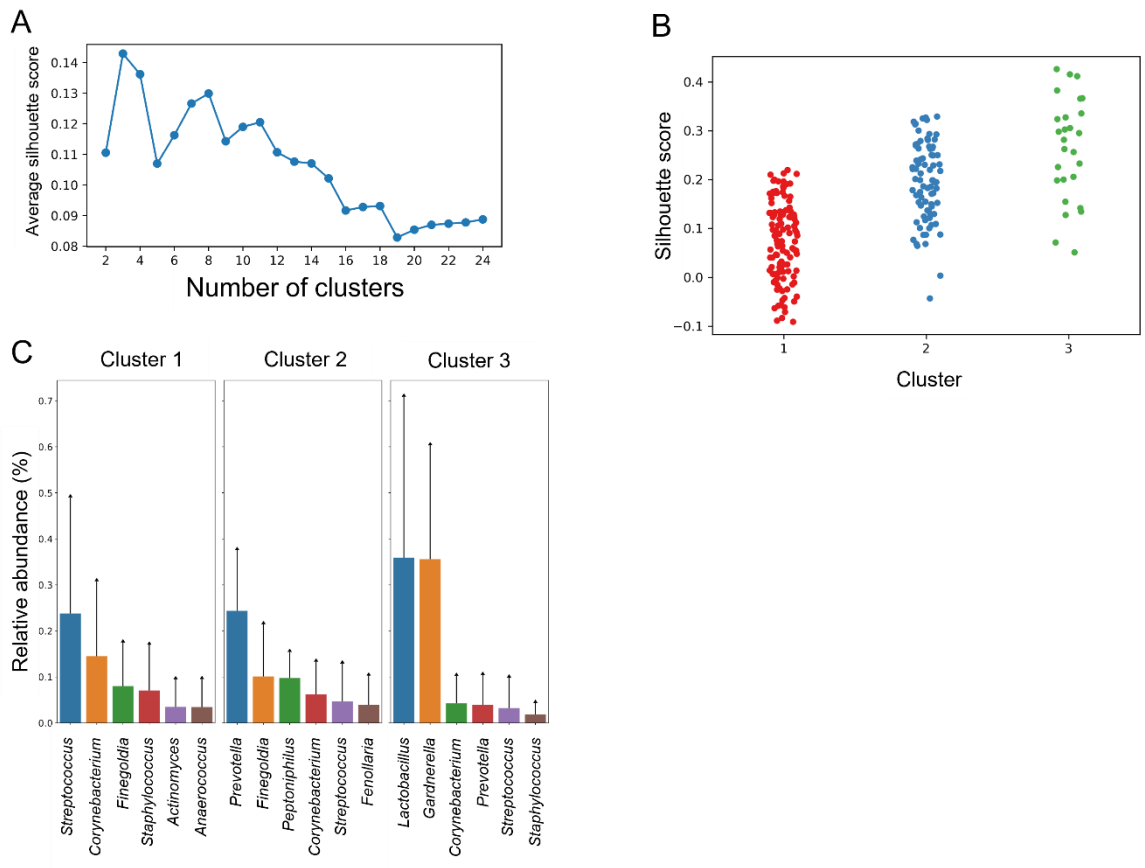


Figure 6.2: Genera level categorisation of seminal microbiota identified three major clusters. A). Average Silhouette scores for number of clusters, B) Silhouette scores of individual samples within each cluster, and C) Relative abundance of the top 6 most abundant genera within each cluster.

Bacterial richness and diversity were also found to be significantly different between the 3 clusters (Kruskal-Wallis tests, $p<0.0001$). Cluster 2 which was characterised by high relative abundance of *Prevotella,* had significantly higher richness than Clusters 1 and 3 with Cluster 1 having significantly higher richness than Cluster 3. Similar differences in diversity (assessed using Simpson's index) were observed between clusters with Cluster 2 having significantly higher diversity than Clusters 1 and 3. Cluster 1 had significantly higher diversity than Cluster 3.

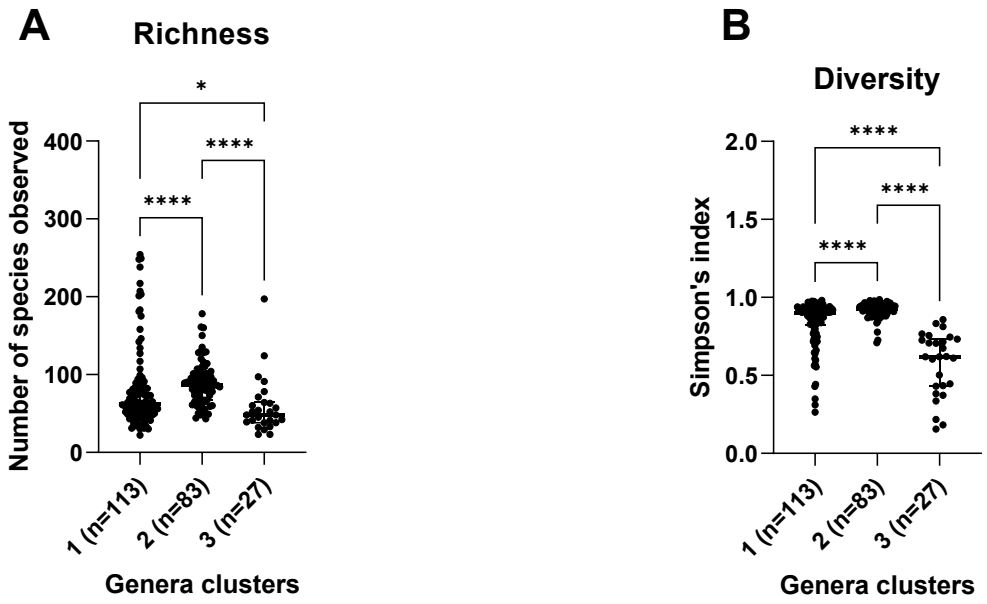


Figure 6.3: Ecological parameters of seminal microbiota clusters at genera level. A) Species richness ($p<0.0001$; Kruskal-Wallis test) and B) diversity ($p<0.0001$; Kruskal-Wallis test) significantly differed across clusters as assessed by comparing the number of species observed and the Simpson's diversity index, respectively. Dunn's multiple comparison test was used as a post-hoc test for between group comparisons (*$p<0.05$, ****$p<0.0001$).

Analysis of bacterial load by qPCR indicated that Cluster 2 samples had a significantly higher mean bacterial 16S rRNA copy number than Cluster 1 samples ($p<0.0001$, Kruskal-Wallis test) (Figure 6.4).

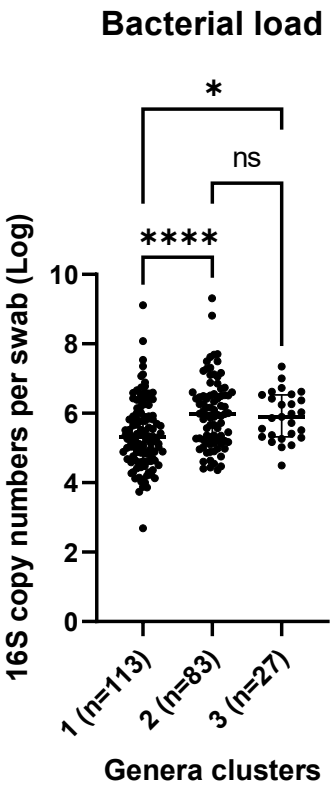


Figure 6.4: Bacterial load of seminal microbiota clusters at genera level. Clusters 2 and 3 have significantly higher bacterial loads compared to Cluster 1. Kruskal-Wallis test ($p<0.0001$). Dunn's multiple comparison test was used as a post-hoc test for between group comparisons (*$p<0.05$, ****$p<0.0001$).

6.4 Assessment of semen microbiota at species level resolution

A similar analysis strategy for identifying potential microbial profiles was performed for the semen samples using sequence data resolved to species level. This led to the identification of 15 bacterial clusters (Figure 6.5). These clusters were characterised by high abundance of 1. *Corynebacterium tuberculostearicum*, 2. *Prevotella timonensis*, 3. *Gardnerella vaginalis*, 4. *Lactobacillus iners*, 5. *Finegoldia magna*, 6. *Streptococcus anginosus*, 7. *Haemophilus parainfluenza*, 8. Unidentified Firmicutes, 9. *Corynebacterium tuberculostearicum*, 10. *Streptococcus*, 11. *Corynebacterium glucuronolyticum*, 12. *Streptococcus*, 13. *Streptococcus mitis*, 14. *Prevotella colorans*, and 15. *Streptococcus agalactiae*. The relative abundance of top 6 most abundant taxa each species level cluster is demonstrated in Figure 6.6.

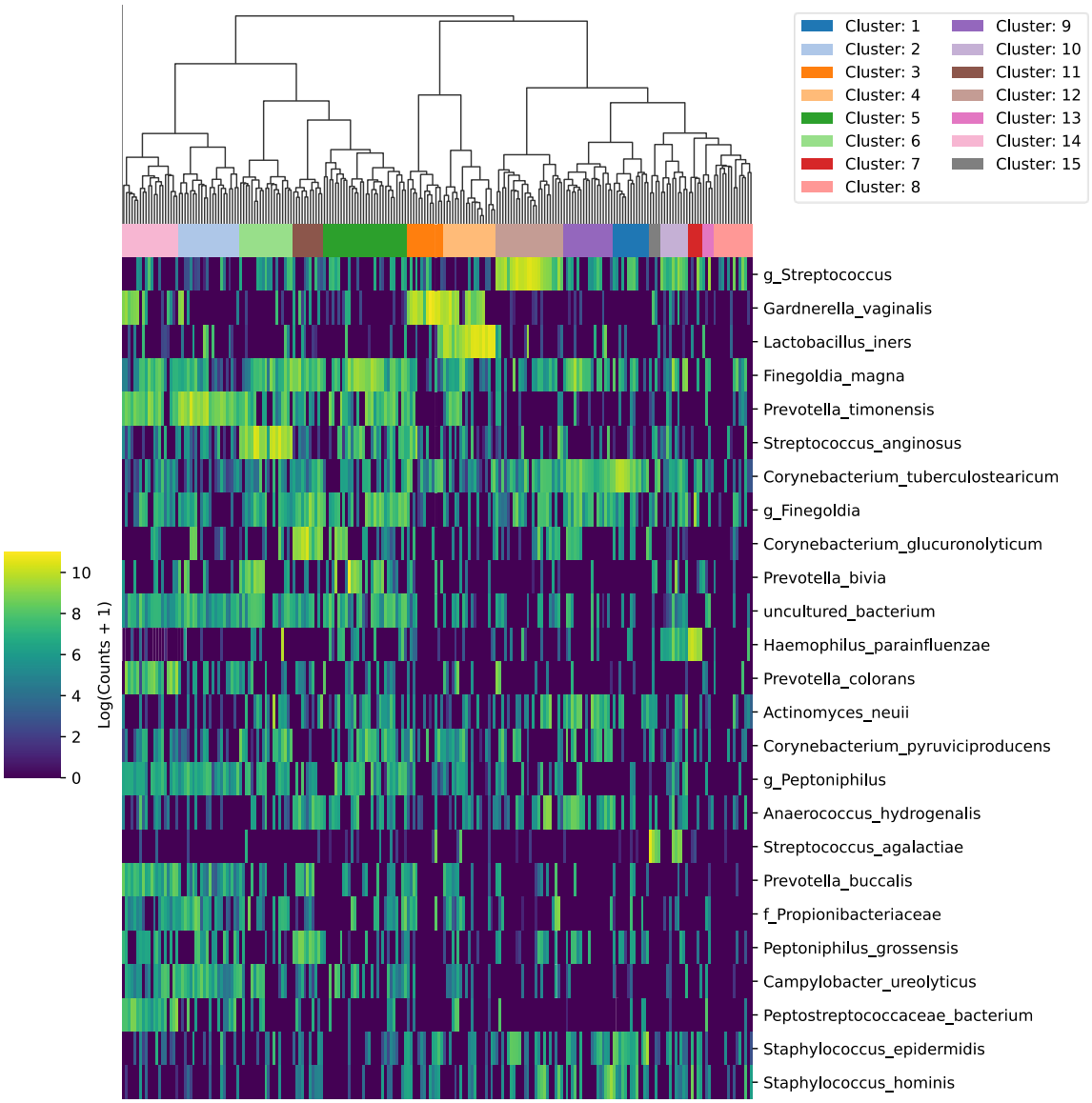


Figure 6.5: Heatmap of Log10 transformed read counts of top 25 most abundant species identified in semen samples. Samples clustered into fifteen microbial groups including *G. vaginalis, L. iners, F. magna,* and *P. timonensis*. (n=223, Ward's linkage).

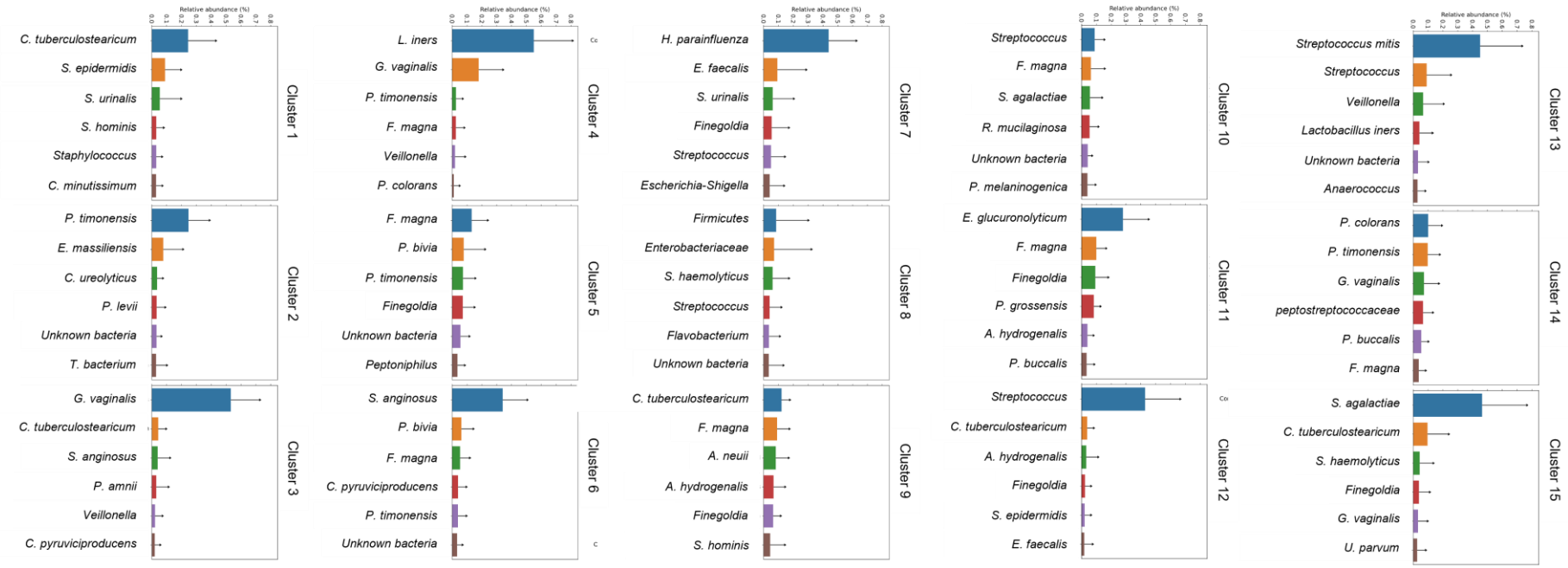


Figure 6.6: Relative abundance of the top 6 most abundant species in the identified in semen microbial clusters at species-level taxonomy.

While the average Silhouette scores indicated that 15 clusters were the optimal number of clusters for species level classification of seminal microbiota, plotting of the individual sample Silhouette scores within each cluster highlighted the overall poor fit (indicated by values around 0) of many of the samples to a specific cluster (Figure 6.7). Accordingly, it was determined that the profiles of bacterial clusters generated for semen samples using genera level sequence data were most robust, and therefore these were used for subsequent integration of bacterial profiles with sperm function and quality parameters.

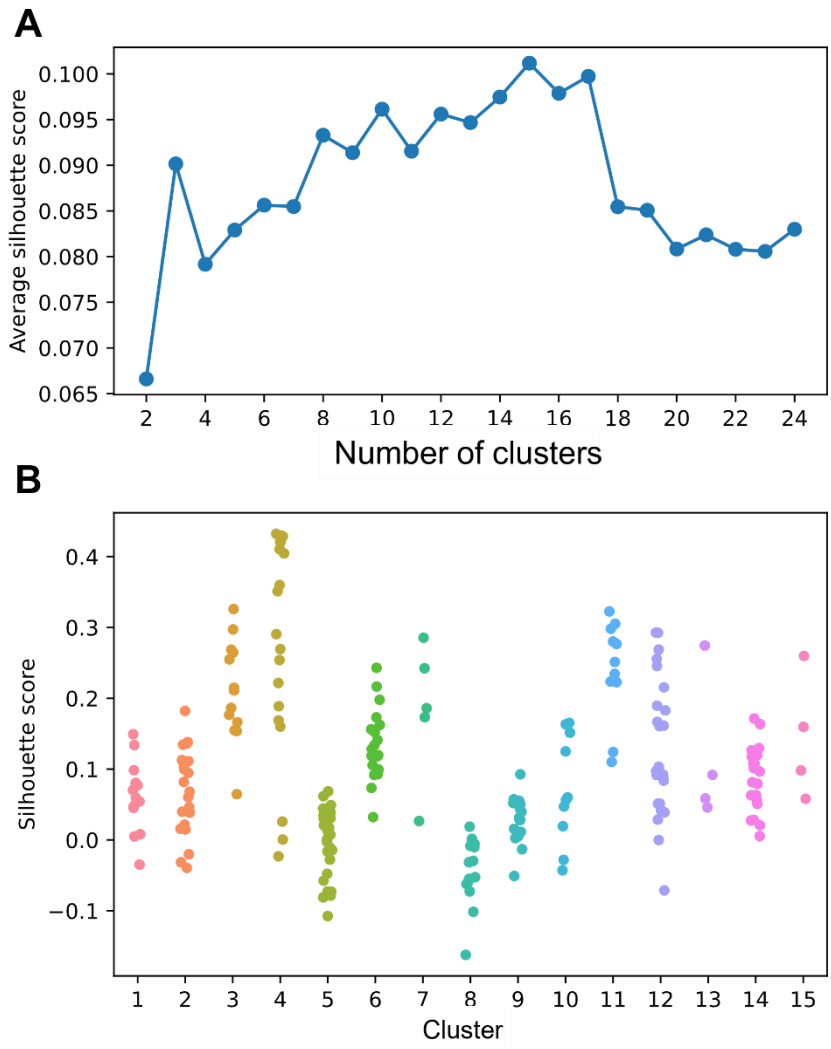


Figure 6.7: Species level categorisation of seminal microbiota. A). Average Silhouette scores for 15 clusters at species level B) Silhouette scores of individual samples in microbial groups.

6.5 Relationship between semen microbiota genera clusters and semen function and quality parameters

As presented in Table 6.4, there were no significant associations between observed key clinical and semen functional and quality parameters and the bacterial clusters (p>0.05, Chi-square test). This included DNA fragmentation, ROS and other functional assessments of semen quality such as concentration, progressive motility and morphology.

Table 6.4: Distribution of clinical factors, microscopic seminal parameters, confounding factors, and recruitment cohorts according to genera clusters. Chi-square tests.

Factors	Thresholds	Cluster 1	Cluster 2	Cluster 3	p-value
DNA frag index	Low	60 (53%)	39 (34%)	15 (13%)	0.47
	High	37 (45%)	35 (43%)	10 (12%)	
ROS	<3.77 RLU/s	74 (52%)	56 (39%)	13 (9%)	0.81
	>3.77 RLU/s	19 (58%)	11 (33%)	3 (9%)	
Semen volume	optimal	105 (50%)	80 (38%)	23 (12%)	0.12
	sub-optimal	8 (53%)	3 (20%)	4 (27%)	
Cohorts	Control	36 (57%)	22 (35%)	5 (8%)	0.76
	MFI	26 (45%)	25 (45%)	7 (10%)	
	RPL	23 (50%)	17 (37%)	6 (13%)	
	UI	28 (50%)	19 (34%)	9 (16%)	
Age	a. <34	30 (61%)	14 (29%)	5 (10%)	0.58
	b. 34-41	59 (48%)	49 (40%)	16 (12%)	
	c. >41	24 (48%)	20 (40%)	6 (12%)	
Ethnicity	Caucasian	82 (53%)	57 (37%)	17 (10%)	0.58
	non-Caucasian	31 (46%)	26 (39%)	10 (15%)	
Concentration	1. >15 M/ml	93 (51%)	67 (37%)	22 (12%)	0.96
	2. <15 M/ml	20 (49%)	16 (39%)	5 (12%)	
Progressive motility	1. >32%	105 (51%)	78 (38%)	24 (11%)	0.67
	2. <32%	8 (50%)	5 (31%)	3 (19%)	
Morphology	1. >4%	37 (50%)	24 (32%)	13 (18%)	0.19
	2. <4%	72 (50%)	58 (40%)	14 (10%)	
Semen quality	Optimal	41 (53%)	24 (31%)	13 (16%)	0.17
	sub-optimal	72 (50%)	59 (17%)	14 (33%)	

Similarly, no relationship was observed between bacterial richness and diversity and any of the key clinical and semen functional and quality parameters assessed (Table 6.5).

Table 6.5: Richness and diversity of seminal bacterial based on seminal quality and function parameters. Categorical classifications of seminal parameters were based on the clinically defined thresholds. Mann-Whitney tests for all except age. Kruskal-Wallis test was used for age.

Factors	Richness p-value	Diversity p-value
DNA frag index	0.68	0.89
ROS	0.25	0.23
Semen volume	0.54	0.85
Age	0.14	0.12
Ethnicity	0.31	0.24
Concentration	0.79	0.66
Progressive motility	0.38	0.54
Morphology	0.82	0.97
Semen quality	0.74	0.90

Bacterial load was not associated with any of the quality and function parameters of semen ($p>0.05$, Mann-Whitney tests) however, it was on average higher in patients >41 years of age compared with <34 years of age (Figure 6.8, $p=0.03$, Kruskal-Wallis test).

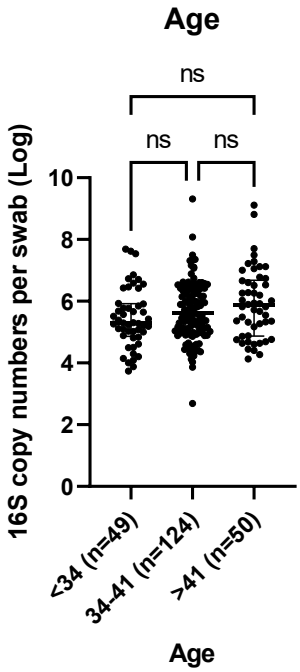


Figure 6.8: Bacterial load of seminal microbiota based on age. Patient age groups are not significantly different in terms of bacterial loads (p=0.09). Dunn's multiple comparison p-values demonstrated on the plot.

6.6 Non-parametric differential abundance analysis of semen microbiota

While no major relationships between identified bacterial clusters and clinical and semen parameters were observed, it remained possible that individual taxa associate with important parameters of semen quality and function. To investigate this, non-parametric linear regression was used to examine potential associations between genera relative abundance and sperm quality and function parameters. The seminal parameters were categorised based on previously described clinical thresholds and their relationship with specific bacteria at genera level were assessed using Welch's corrected T-test (Table 6.6). Several relationships were detected however only 2 withstood corrections for multiple testing. Increasing relative abundance of *Flavabacterium* was found to be positively associated with poorer sperm quality and sperm morphology. Relative abundance of *Finegoldia* and *Cutibacterium* were inversely associated with sperm DNA fragmentation, whereas *Porphyromonas* and *Varibaculum* were positively associated with sperm DNA fragmentation. *Corynebacterium* was inversely associated with ROS and positively with semen volume.

Table 6.6: Non-parametric differential abundance analysis for specific taxa at genera level. Positive t-values indicate a positive relationship, and negative t-values describe a negative relationship between relative abundance of taxa and seminal quality and function parameters. Significant relationships are indicated using p-values. q-values represent adjusted p-values for multiple comparisons.

Sperm quality and function parameters	Genera	Welch corrected t	p-value	q-value
Sperm DNA fragmentation	*Finegoldia*	-2.36	**0.01***	0.27
	Cutibacterium	-2.20	**0.02***	0.27
	Porphyromonas	2.16	**0.03***	0.27
	Varibaculum	2.11	**0.03***	0.27
ROS	*Lactobacillus*	2.18	**0.02***	0.66
	Corynebacterium	-2.04	**0.04***	0.66
Semen quality	*Flavobacterium*	3.39	**0.0008*****	**0.02***
	Prevotella	2.26	**0.02***	0.38
Sperm concentration	*Porphyromonas*	-2.08	**0.03***	0.61
Sperm morphology	*Flavobacterium*	3.64	**0.0003*****	**0.01***
	Prevotella	2.03	**0.04***	0.67
Semen volume	*Corynebacterium*	2.27	**0.02***	0.32
	Actinotigum	-2.20	**0.02***	0.32
	Varibaculum	-2.16	**0.03***	0.32

High relative abundance of *Lactobacillus* was associated with elevated ROS. Non-parametric differential abundance analysis using species level taxonomy showed that this association was largely driven by *L. iners* (p=0.02, Welch's test, Table 6.7). Finally, *Actinotigum* and *Varibaculum* were found to inversely associate with semen volume. Other relationships identified at species levels included an unidentified species of *Flavobacterium* and semen quality and sperm morphology which withstood the multiple comparison testing (p=0.0008, q=0.02 and p=0.0003, q=0.01 for semen quality and sperm morphology respectively).

Table 6.7: Non-parametric differential abundance analysis for specific taxa at species level. Positive t-values indicate a positive relationship, and a negative t-value describes a negative relationship between relative abundance of taxa and seminal quality and function parameters. Significant relationships are indicated using p-values. q-values represent adjusted p-values for multiple comparisons.

Clinical factor	Species	Welch corrected t	p-value	q-value
Sperm DNA fragmentation	*Peptostreptococcaceae bacterium*	2.18	**0.03***	0.91
ROS	*Lactobacillus iners*	2.24	**0.02***	0.94
	Unidentified *Anaerococcus*	-2.03	**0.04***	0.94
Semen quality	Unidentified *Flavobacterium*	3.76	**0.0002*****	**0.01***
	Corynebacterium tuberculostearicum	-2.06	**0.04***	0.82
Semen volume	*Corynebacterium tuberculostearicum*	2.64	**0.008**	0.24
	Unidentified *Varibaculum*	-2.48	**0.01**	0.24
	Staphylococcus epidermidis	2.35	**0.01**	0.24
	Unidentified *Peptoniphilus*	-2.32	**0.02**	0.24
	Dialister propionicifaciens	-2.24	**0.02**	0.24
	Prevotella colorans	-2.14	**0.03**	0.26
Cohorts	*Staphylococcus haemolyticus*	0.04	**0.02**	0.97

Given that *Flavobacterium* was found to associate with several parameters of poor semen quality, particularly morphology, further investigation of the relative abundance of this genus in patients with normal and abnormal semen parameters was performed. As outlined in figure 6.9, the relative abundance of *Flavobacterium* was significantly higher in semen samples classified as abnormal. Furthermore, the prevalence of *Flavobacterium* was higher in samples with abnormal semen quality and low percentage of morphologically normal sperm.

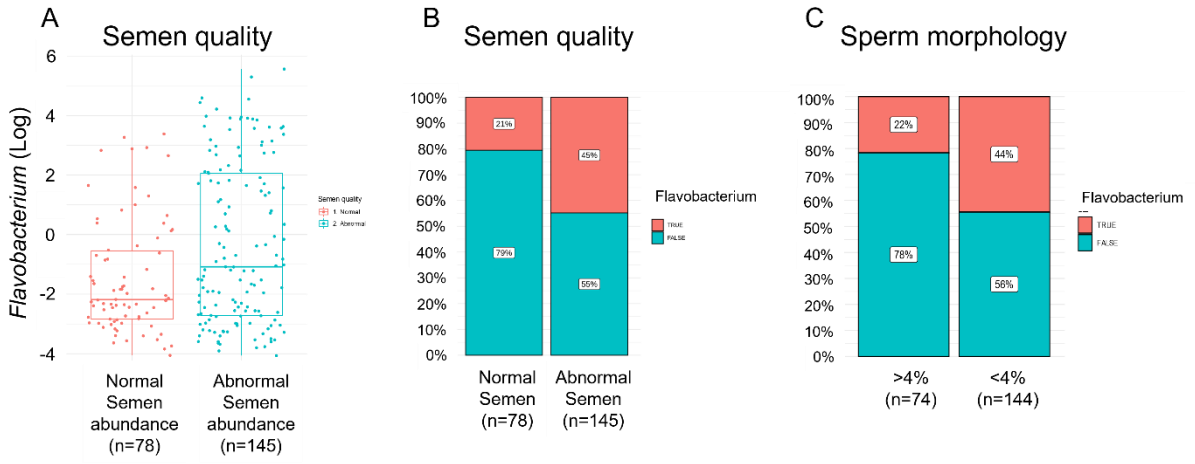


Figure 6.9: Relative abundance and prevalence matrices of *Flavobacterium* in relation to semen quality. A) Comparison of relative abundance of *Flavobacterium* in samples with normal and abnormal semen. Relative abundance of *Flavobacterium* is significantly higher in samples with abnormal semen (p=0.0002, q=0.01). B) *Flavobacterium* prevalence matrix according to semen quality. *Flavobacterium* is significantly more prevalence in abnormal semen quality samples (p=0.0003). C) *Flavobacterium* prevalence matrix according to sperm morphology. *Flavobacterium* is significantly more prevalence in samples with low percentage of morphologically normal sperm (p=0.0009).

6.7 Comparison of semen quality and function parameters in controls and cohorts of men undergoing fertility investigations

The next set of analyses sought to determine if potential relationships between semen quality and function and the microbiota could be more readily detected within specific patient cohorts under investigation. The rationale behind this was that MFI patients were most likely enriched for poor semen phenotypes compared to controls and other patient cohorts under investigation. As expected, compared to either controls of men of partners with RPL or diagnosed with UI, MFI samples had lower concentration, poorer progressive motility, and morphology as well as elevated ROS and DNA fragmentation (Figure 6.10).

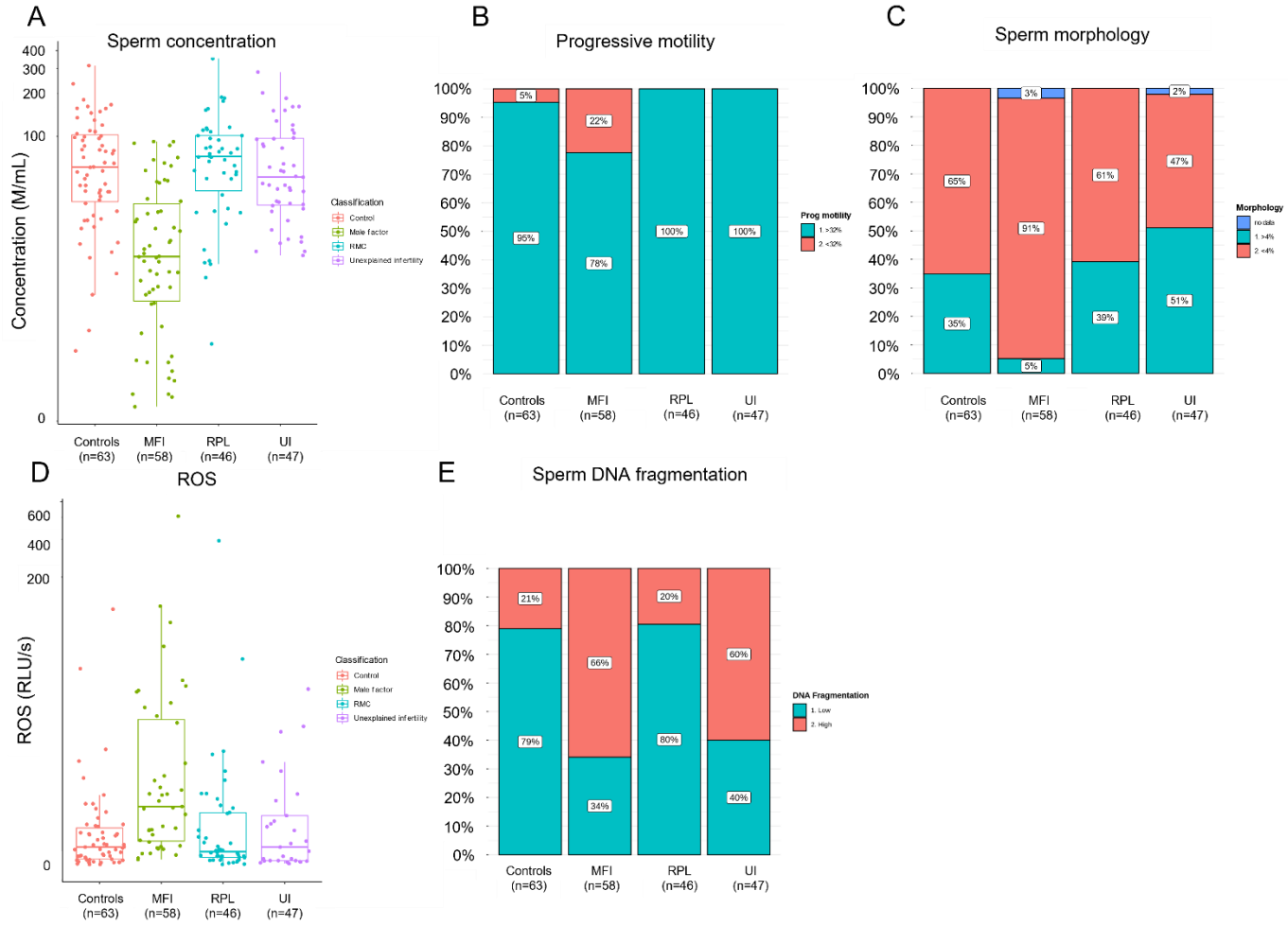


Figure 6.10: Seminal quality and function parameters according to recruited cohorts. Comparison of microscopic semen parameters A) concentration ($p<0.0001$) B) progressive motility ($p<0.0001$), C) morphology ($p<0.0001$) suggested poor semen quality for MFI patients. Comparison of clinical semen qualities D) ROS, E) sperm DNA fragmentation index.

6.8 Assessment of seminal function and quality parameters within controls and study subjects and their relationships with seminal microbiota

Comparison of the mean number of species observed as well as the mean Simpson's Index indicated that bacterial richness and diversity parameters across the control and male patient study cohorts was similar (Figure 6.11) (Kruskal-Wallis test, $p>0.05$). Within the controls and the three cohorts of patients undergoing fertility investigations, richness varied greatly and ranged between 23-254 for controls and 22-249 for patients undergoing fertility investigations. Similarly, Simpson's diversity index varied between 0.18-0.98 for controls and 0.15-0.80 for patients undergoing fertility investigations.

.

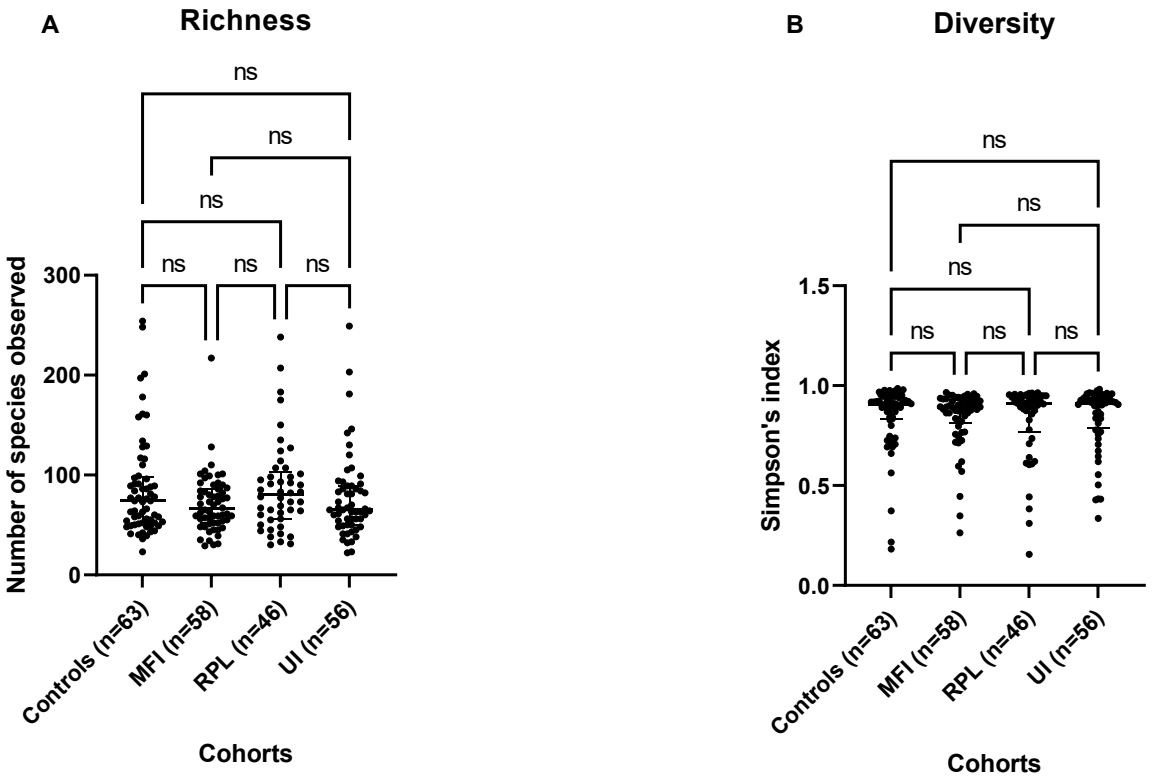


Figure 6.11: Ecological parameters of seminal microbiota for the recruited study cohorts. A) Species richness (p=0.30), and B) Simpson's diversity index (p=0.49) was not significantly different based on recruited study cohorts. Kruskal-Wallis tests with Dunn's multiple comparison p-values demonstrated on the plots.

The estimated bacterial load was also similar between the control and patient cohorts with approximately 24,638,496 (±162,087,490), 48,820,327 (±280,780,247), 3,372,590 (±6,608,918), and 4,242,510 (±16,766,685) 16S rRNA copies per 1 mL of semen detected in controls, men diagnosed with male factor infertility, male partners of women with recurrent pregnancy loss and male partners of couples diagnosed with unexplained infertility, respectively (Figure 6.12).

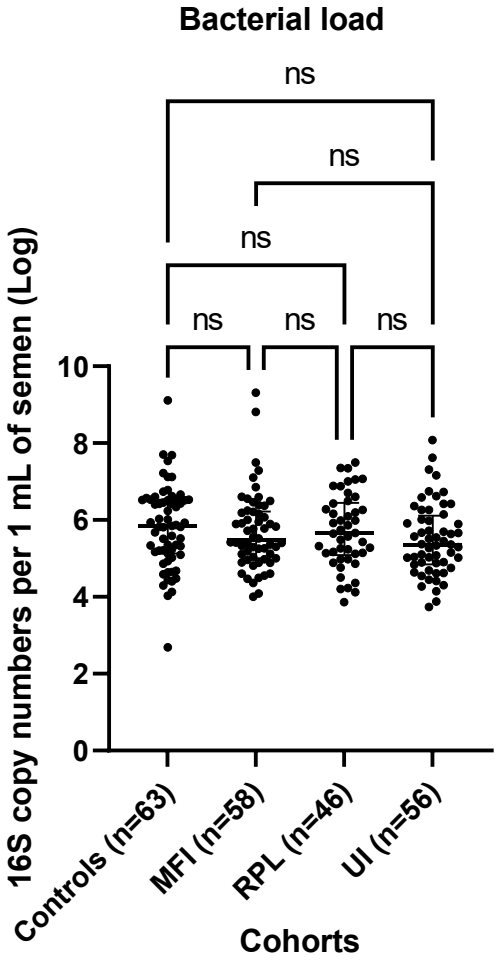


Figure 6.12: Bacterial load of seminal microbiota in recruited study cohorts. There were no significant differences in bacterial load based on recruited study cohorts using the number of 16S rRNA genes per 1 mL of semen. Kruskal-Wallis test (p=0.22). Dunn's multiple comparison p-values demonstrated on the plot.

To focus analyses toward the most extreme phenotypes of good and poor semen quality and function, a sub analysis of only controls and MFI patients was performed (Table 6.8). Non-parametric differential abundance analysis identified an inverse relationship between sperm DNA fragmentation and relative abundance of *Cutibacterium* and a positive relationship with *Porphyromonas* and *Varibaculum*. These results were highly consistent with analyses performed on all available samples (Table 6.6).

Table 6.8: Non-parametric differential abundance analysis for specific taxa at genera level for controls and MFIs only. Positive t-values indicate a positive relationship, and a negative t-value describes a negative relationship between relative abundance of taxa and seminal quality and function parameters. Significant relationships are indicated using p-values. q-values represent adjusted p-values for multiple comparisons.

Clinical factor	Genera	Welch corrected t	p-value	q-value
Sperm DNA fragmentation	*Cutibacterium*	-2.56	**0.01***	0.31
	Porphyromonas	2.34	**0.02***	0.31
	Varibaculum	1.96	0.051	0.53
ROS	*Finegoldia*	-1.99	**0.04***	0.77
Sperm concentration	*Finegoldia*	2.04	**0.04***	0.71
Sperm morphology	*Flavobacterium*	3.64	**0.0003*****	**0.01***
	Prevotella	2.03	**0.04***	0.67
Semen volume	*Facklamia*	2.99	**0.003****	0.10
	Actinotignum	-2.20	**0.02***	0.36
	Dialister	-1.99	**0.04***	0.36

Relative abundance of *Finegoldia* was inversely associated with ROS levels but were positively associated with sperm concentration. No relationship was observed between overall sperm quality and specific genera; however, poor sperm morphology was positively associated with *Flavobacterium* and *Prevotella*. Similar to the results observed when analyses were performed on all available samples, *Actinotigum* was again found to negatively associated with semen volume in the sub-analysis of controls and MFIs. Additionally, *Facklamia* (positive) and *Dialister* (inverse) relationships were observed with semen volume.

When a similar sub analysis was performed for controls and MFI patients using species level taxonomy data, several species were found to be associated with semen parameters (Table 6.9). At species level, there was an unidentified *Anarococcus* species that negatively correlated in both sets of analysis with high ROS. Furthermore, *Corynebacterium tuberculostearicum* positively correlated with semen volume in both analyses. An unidentified *Flavobacteirum* associated with semen quality in both sets of analysis. Additionally, the unidentified *Flavobacterium* in the sub-analysis also positively correlated with ROS.

Table 6.9: Non-parametric differential abundance analysis for specific taxa at species for controls and MFIs only. Positive t-values indicate a positive relationship, and a negative t-value describes a negative relationship between relative abundance of taxa and seminal quality and function parameters. Significant relationships are indicated using p-values. q-values represent adjusted p-values for multiple comparisons.

Clinical factor	Species	Welch corrected t	p-value	q-value
Sperm DNA fragmentation	*Staphylococcus hominis*	-2.32	**0.02***	0.68
ROS	Unidentified *Flavobacterium*	2.42	**0.01**	0.54
	Unidentified *Anaerococcus*	-2.12	**0.03**	0.54
	Schaalia radingae	-2.12	**0.03***	0.54
	Haemophilus parainfluenza	2.02	**0.04***	0.54
Semen quality	Unidentified *Flavobacterium*	2.36	**0.01***	0.91
Semen volume	*Dialister micraerophilus*	-2.66	**0.008****	0.41
	Corynebacterium tuberculostearicum	2.27	**0.02***	0.44
	Staphylococcus epidermidis	2.22	**0.02***	0.44
	Actinotignum schaalii	-2.00	**0.04***	0.45
Cohorts	*Staphylococcus haemolyticus*	0.04	**0.01***	0.68

6.9 Discussion

Several recent studies have indicated the existence of a semen microbiota; however, these studies have been limited to small samples sizes (n<100) and have failed to reach a consensus on the compositional structure of the microbiota, or its biological relevance, particularly in the context of sperm function and quality (Table 1.6). This chapter characterised the semen microbiota in a diverse cohort of men including controls who fathered a child within 12 months of sample production as well as male patients undergoing fertility investigations diagnosed with MFI or UI, and partners of women with RPL. The study also aimed to examine any potential relationships between the microbiota and semen quality and functional parameters.

The three major semen microbiota clusters detected in our study were characterised by high abundance of *Streptococcus*, *Prevotella*, and *Lactobacillus* and *Gardnerella* (Figure 6.1). These finding are generally consistent with the study of Baud et al. who also reported 3 main microbiota profiles but these were characterised by an enrichment of *Prevotella* or *Lactobacillus* species or high bacterial diversity (349). The *Prevotella* enriched group was associated with higher bacterial loads compared with the other two groups. This is similar to the results presented in this chapter, where the *Prevotella*-enriched Cluster 2 samples were found to have higher bacterial loads compared with Cluster 1 (*Streptococcus*) (Figure 6.4). Furthermore, *Prevotella* was associated with high richness and diversity than the other microbial clusters. *Prevotella* species have been identified in multiple body sites where they have variable influences on host health and disease states. In the vagina they are generally considered to be pathogenic whereas in the gut, some species of *Prevotella* have been linked to improved glucose metabolism, while others are associated with adverse conditions like hypertension and gut inflammation (632, 633). While the functional role of these major genera remains to be elucidated, several studies have identified *Lactobacillus* and *Prevotella* species in semen samples (634, 635). A link between high abundance of *Prevotella* and reduced sperm concentration and motility has been previous reported, whereas high relative abundance of *Lactobacillus* has been associated with optimal semen quality, particularly normal sperm morphology (349). *Prevotella* were found in 90% of testicular samples (299) and are implicated to contribute to spermatogenesis defects and infertility (350, 636). In our study, no significant association was observed between the semen microbiota clusters and parameters of semen quality and function (Table 6.4).

When non-parametric differential abundance analysis was performed on species level data in the context of semen parameters of quality and function, several relationships were observed. This included unidentified species of *Anaerococcus* (inversely correlated with ROS),

Flavobacterium (associated with abnormal semen), *Varibaculum* and *Peptoniphilus* (inversely correlated with semen volume), which were significantly associated with quality and function parameters of sperm (Table 6.7). Similar to these findings, high abundance of *Anaerococcus* has been previously associated with reduced sperm quality (346). Other studies have reported high abundance of *Neisseria*, *Klebsiella* and *Pseudomonas* and low abundance of *Lactobacillus* with suboptimal microscopic semen quality (348), but these findings were not replicated in our cohorts. In our patients, high abundance of *Flavobacterium* was associated with abnormal semen quality and more specifically sperm morphology (Figure 6.9). *Flavobacterium* are gram-negative physiologically diverse aerobes with some species described to be opportunistic or pathogenic depending on the anatomical location and biological context (637). *Flavobacterium* has also been identified in testicular biopsies of infertile men (299). In this study, the authors were careful to account for potential sources of contamination by including several kit and negative controls. After accounting for contamination, *Flavobacterium* was still identified as one of the major genera in additional to *Bacteroides*, *Akkermansia*, *Faecalibacterium* and *Alistipes*. Recently, *Flavobacterium*, *Moraxella*, and *Brevundimonas* were identified to negatively correlate with sperm DNA fragmentation (638).

A unique aspect of our study was the integration of the microbiota data with paired measurements of sperm DNA damage and semen ROS level. Our analyses identified a positive associated between *L. iners* and increased ROS (Table 6.7). The literature suggests that *L. iners* plays an important role in reproduction such as increasing the risks of preterm births and miscarriages (204, 639). Additionally, one study reported that male partners of women with recurrent miscarriages have increased levels of semen ROS and sperm DNA fragmentation (270). There is no consensus regarding the role of *Lactobacillus* species in seminal quality. Some studies have reported that low abundance of *Lactobacillus* in semen is associated with reduced sperm motility or increased viscosity (347-349, 640), whilst others have found associations between *Lactobacillus* with asthenospermia and azoospermia (346, 350). Garcia-Segura et al., reported a potentially protective role for *Lactobacillus* against sperm DNA fragmentation. They found that high abundance of *Lactobacillus* species inversely correlate with sperm DNA fragmentation (638). The mechanisms by which *Lactobacillus* could protect sperm against DNA fragmentation is not explored, however, it is possible that the mechanism involves production of short-chain fatty acids produced by Lactobacilli that prevent sperm lipid peroxidation by ROS (641).

The strategy used to characterise the semen microbiota was high throughput sequencing of the V1-V2 hypervariable regions of the bacterial 16S rRNA genes. The methodology used was consistent with that performed for the analysis of vaginal samples described in Chapters 3-5.

This allowed for the implementation of well-established protocols and data processing strategies that had been previously optimised ensuring the generation of data that would be comparable across body niches and sample types. Consistent with the rationale for the vaginal samples, a mixed forward primer designed to target the V1-V2 hypervariable regions of the 16S rRNA gene was chosen due to its capacity to provide good resolution of major reproductive tract species, particularly *Lactobacillus* species. Recent studies of the putative semen microbiota have identified several species commonly observed in the vagina including *Lactobacillus*, *Gardnerella* and *Prevotella* species (347, 349) thus it was considered important to sequence a variable region of the 16S rRNA gene that permits detection and coverage of these species. However, it is important to recognise that these primers may not amplify equally well all bacterial species that could be potential present in semen due to differences in annealing efficiency and specificity. As a result, the relative abundances of some species within the samples may be underestimated (642) (643). This is a widely recognised limitation of short-read amplicon sequencing approaches and future studies could address this by implementing more expensive and time-consuming long read sequencing technologies or shotgun sequencing approaches.

While acknowledging the limitations of metataxonomics based profiling, this approach still permitted the generation of high-quality sequencing data that could be analysed as several different taxonomic levels. When data was mapped at genera level, semen samples were able to be categorised into 3 major microbial clusters. Unlike other studies in the literature, we used an objective statistical approach (i.e., Silhouette methods) to determine the optimal number of microbial clusters our data supported (Figure 6.2). Interestingly, when this approach was applied using species level data, poor goodness of fit was observed within the resulting clusters (Figure 6.7). This result contrasts with that found for vaginal samples where statistically robust and reproducible clusters based on species level metataxonomic profiles have been reported in several studies (142, 483). This result may also reflect differences in the way in which vaginal bacteria have co-evolved with the host to the point where mutualistic relationships between specific species and the host are demonstrable. Major differences in the bacterial load observed in these two sample types provides further evidence that a vaginal microbiota has coevolved with the host to promote optimal health. As reported in earlier chapters and by others, the vagina has substantially higher bacterial load compared to semen which in most cases is immunologically well tolerated by the host. Collectively these results point towards the likelihood that microbiota detected in semen are the result of transient colonisation events. Alternatively, the microbiota content in semen may reflect contamination of the sample during the collection procedure. Consistent with this, several semen samples were found to contain species known to be commensal to the skin including *Streptococcus*,

Corynebacterium and *Staphylococcus* (644). To control and test for this, future studies could include a swab of the penile skin prior to collection of semen and ideally perform sampling over several timepoints. The potential that semen samples are prone to contamination can also be highlighted by other studies in the literature. A study by Hou et al., reported 6 potential semen microbiota groups based on compositional similarities and rank abundance of detected taxa (346). However, one group, which accounted for almost 20% of the cohort, was dominated by *Ralstonia*, which is commonly associated with contamination of medical devices, water and DNA extraction kit components (645). Unfortunately, this study did not include any negative controls which would have allowed them to determine if *Ralstonia* or other detected taxa were derived from sources of environmental contamination. In contrast, in the current study, we included several air and kit contaminant negative controls that allowed for careful assessment of potential sources of environmental contamination.

In summary semen has a microbiota characterised by 3 major composition clusters. Semen bacteria consisted of bacterial genera frequently isolated from the vagina and some resembling skin microbiota. This study is the largest to date on seminal microbiota using metataxonomic characterisation of seminal bacteria. The highly abundant seminal bacteria in this study were in concert with the published literature, however, there were several novel findings. In this study we found that the bacterial load is related to composition. Samples with high abundance of *Prevotella, Lactoabcillus* and *Gardnerella* were associated with higher bacterial load compared with samples characterised by high abundance of *Streptococcus.* The prevalence of these clusters however was not associated with semen quality parameters, however, relative abundance of specific taxa are related to specific parameters of semen parameters including a previously unreported inverse correlation between *Flavobacterium* and sperm morphology. Although the data indicate that semen microbiota likely represent transient colonisation, the presence of specific taxa may influence semen parameters relevant to the likelihood of reproductive success.

7 CHAPTER VII

7.0 Overall conclusions

Global fertility rates are in decline. There are multiple factors underlying this trend. In the developed world, many women choose to start their families later in life which coincides with a reduction in their natural fecundity. Modern lifestyles including exposure to pesticides and air pollution, unbalanced diet, smoking, and excessive alcohol consumption can reduce gamete and embryo qualities which further contribute to increased rates of infertility (246, 247, 646, 647). IVF is now widely used to treat a range of infertility factors associated with both male and females (12). IVF protocols are evolving and the development of super-ovulatory protocols have improved pregnancy rates and reduced cycle cancelations (13). However, infertility remains unexplained in a quarter of cases. There is an urgent need to increase understanding of the mechanisms of unexplained infertility (9). Our understanding of the bacteria of the reproductive tract and their associations with maintenance of health has gained traction with emergence of metataxonomic technologies in mainstream research (Tables 1.3, 1.4 and 1.6). Vaginal, endometrial, and seminal microbiota have all been implicated in successful and unsuccessful embryo implantation and have been proposed to be relevant clinical factors potentially contributing to unexplained infertility cases. Bacterial vaginosis associated bacterial species are generally linked with adverse reproductive outcomes (121, 241, 499); whilst *Lactobacillus* species (especially *Lactobacillus crispatus*) are linked to a healthy vaginal ecosystem and successful pregnancy outcomes (237, 352, 499).

Inclusion of fresh and frozen IVF cycles in this thesis aimed to address different study questions. In Chapter 3, investigations assessed the interplay between hormones, immune analytes and composition of vaginal bacteria and addressed their relationships with clinical IVF outcomes whereas in Chapter 5, the capacity of vaginal metabolic profiles to predict composition of vaginal microbiota and successful pregnancy in IVF cycles was assessed. The data presented supports the role of hormonal regulation of microbiota composition and immune response and the relevance of these interactions to IVF success rates. For samples collected on the day of embryo transfer, successful embryo implantation was associated with increased concentrations of pro-inflammatory cytokines (Table 3.5). Some IVF centres offer endometrial scratching as a treatment add-on based on the hypothesis that a repair mechanism by immune analytes in the endometrium increases endometrial receptivity (564). Although endometrial scratching is not considered as part of routine IVF treatments offered to patients, our data supports the hypothesis that inflammation is associated with increased rates of embryo implantation on the day of embryo transfer. Data modelling suggested that immune

response to bacteria compositions is hormone dependant and during the suppression of serum hormones, these interactions are altered. In agreement with the published literature, *G. vaginalis* positively and *L. crispatus* negatively correlated with IL-1β at each stage of sample collection except for samples collected throughout pituitary suppression (Figures 3.35, 3.43, 3.48, 3.50, 3.54 and 3.57). The implication of different immune response at a low estrogenic state in fresh IVF cycles requires further investigation and the clinical implications remain to be elucidated.

In depth and objective analyses of vaginal bacteria presented in Chapters 3 and 4 found no direct links between vaginal bacterial community compositions and successful treatment outcomes (Figure 3.62 and 4.16). To assess whether metabolic signatures could be reflective of successful embryo implantation, we undertook the first study to use DESI-MS on a cohort of patients undergoing IVF treatments. The analysis validated the ability of DESI-MS to predict vaginal compositions in patients undergoing IVF with similar accuracy to other studies undertaken in pregnancy (482, 483). Thiomalic acid was upregulated in *Lactobacillus* dominant samples at every sample collection timepoint throughout IVF cycles (Figure 5.3). Upregulation of thiomalic acid in samples with high abundance of *Lactobacillus* was also previously observed by Pruski et al. (483). Further investigation on the clinical relevance of thiomalic acid and how it shapes vaginal and endometrial function is warranted. Shared metabolic signatures associated with successful embryo implantation were also identified at different hormonal milieu. This included putative identification of phosphatidylglycerol. This pilot study provides a platform for future studies assessing the clinical application of metabolic signatures in predicting IVF success.

An interesting observation distinguishing between the bacterial compositions of fresh and frozen IVF cohorts were the differences in stability of specific taxa (Figures 3.26 and 4.6). Cross-sectional abundance analysis for highly abundant taxa in fresh IVF cycles found that only *F. magna* and *P. timonensis* were susceptible to change in successive stages of sample collection (Figure 3.6). Using the same linear mixed effects modelling on frozen IVF cycles, we found that in addition to *F. magna* and *P. timonensis*, other bacteria species such as *L. jensenii, L. gasseri, P. bivia, L, vaginalis,* and *P. indolicus* significantly changed throughout IVF cycles (Figure 4.5). This suggests that vaginal bacteria in frozen IVF cycles are more susceptible to change, although these changes did not relate to clinical pregnancy outcomes for either frozen or fresh cycle cohorts.

To assess the role of reproductive microbiota in male infertility, we characterised the semen microbiota in a diverse cohort of men including controls of proven paternity to examine potential relationships between microbiota and semen quality and parameters. Our analysis

found several clinically relevant bacterial species including *Lactobacillus*, *Gardnerella* and *Prevotella* in semen (Figure 6.1). Our data suggests that the seminal microbiome is mostly due to transient colonisation, however some bacteria appear to have significant relationships with seminal quality and function parameters and thus contribute to reproductive success. Seminal microbiota are likely sourced from male reproductive tract organs such as the testes, and skin contaminations (299, 644). In this study, *Flavobacterium* was identified as having a significant association with sperm quality and, more specifically, sperm morphology (Figure 6.9). The presence of *Flavobacterium* has been demonstrated in testicular biopsies of infertile men (299), as well as in the vagina (217) and endometrium (237). *Flavobacterium* is known to insert oxidative pressure on carbohydrates (648). Our Data supports the concept that *Flavobacterium* may have adverse functions through activation of oxidative stress since we found that an unidentified species of *Flavobacterium* positively correlated with seminal ROS.

In this thesis, one of the main aims was to assess whether vaginal bacteria composition and load can act as biomarkers in predicting success of IVF treatments. To achieve this, samples were collected at key timepoints throughout IVF treatment cycles characterised by natural hormonal regulation, systemic pituitary suppression and supraphysiological concentrations of serum hormones. Characterisation of vaginal microbiota composition into CSTs was undertaken using a nearest centroid classifier method with high degree of inter-study reproducibility (142). Within-patient assessment of vaginal CSTs suggested that 47% of fresh and 55% of frozen IVF cycles have stable vaginal bacterial compositions (Figures 3.26 and 4.6). This finding is in agreement with that of Gajer et al., which suggested in the short term, some vaginal communities undergo compositional changes whilst others maintain stability (580). The composition and stability of vaginal microbiota communities was not associated with clinical IVF outcomes in either fresh or frozen IVF cohorts. Similarly bacterial load of samples collected on the day of embryo transfer for both fresh and frozen IVF cycles were not associated with successful pregnancy.

Initial analysis of serum hormone concentrations in fresh and frozen IVF cycles suggested that hormone levels in fresh cycles reach supraphysiological concentrations which are significantly higher than those of the frozen cycles (Figure 3.3). Given the active role of serum hormones in regulation of immunological and reproductive processes, it is important to treat fresh and frozen modes of IVF treatment as independent procedures for future analyses. Pituitary suppression and ovarian stimulation protocols are chosen by clinicians based on patient history and demographics. The aim is to treat the patient using the most suitable protocols to find the right balance between patient health and maximising the chance of successful treatment outcomes. Very high concentrations of E2 could contribute to the aetiologies associated with OHSS and reduced implantation rates but as shown in this thesis, also modify

microbiota-host interactions which in some patients may impact their reproductive potential (46, 649).

This work began with the hypothesis that hormonal manipulation during IVF treatments modify vaginal microbiota-host immune response, which are collectively important for subsequent success of IVF. The first part of this hypothesis has been proven in that we found significant effects of the endocrine environment at different stages of the IVF treatment protocol upon the vaginal microbiota, and host response to it. Contrary to what has been previously published, we found that the structure of the vaginal microbiota at any stage of the IVF treatment protocol was not a strong biomarker of IVF success, and surprisingly found that unsuccessful, frozen IVF cycles were associated with enrichment for *L. crispatus.* Although the structure of the vaginal microbiota alone was not a good predictor of IVF success, more broad assessment of the metabolism of the vagina by DESI-MS appeared to have potential in discriminating outcomes for IVF treatment and is an area that would merit further exploration. We also found that DESI-MS has high accuracy in predicting the structure of the vaginal microbiota in women undergoing IVF, which supports the concept that this technology will in the future be useful for assessing vaginal microbiota structure in a range of different clinical settings, both within and without pregnancy. Our second hypothesis was that semen harbours a microbiome that modulates parameters of sperm quality and function. This hypothesis was proven, in that, we demonstrate that there is a semen microbiome, and that several genera were found to significantly relate to seminal parameters.

References

1. Simón C, & Rubio, C. (Eds.). Handbook of Genetic Diagnostic Technologies in Reproductive Medicine: Improving Patient Success Rates and Infant Health (2nd ed.)2022.
2. Vollset SE, Goren E, Yuan C-W, Cao J, Smith AE, Hsiao T, et al. Fertility, mortality, migration, and population scenarios for 195 countries and territories from 2017 to 2100: a forecasting analysis for the Global Burden of Disease Study. The Lancet. 2020;396(10258):1285-306.
3. Martin LJ. Delaying, debating and declining motherhood. Culture, Health & Sexuality. 2021;23(8):1034-49.
4. Naeye RL. Maternal age, obstetric complications, and the outcome of pregnancy. Obstetrics and gynecology. 1983;61(2):210-6.
5. United Nations DoE, Social Affairs PD. World Fertility Report 2015: Highlights. United Nations New York; 2017.
6. Fertility problems: Briefing paper [Internet]. NICE. 2014 [cited 30/11/2019]. Available from: https://www.nice.org.uk/guidance/qs73/documents/fertility-problems-briefing-paper2.
7. Thonneau P, Marchand S, Tallec A, Ferial ML, Ducot B, Lansac J, et al. Incidence and main causes of infertility in a resident population (1,850,000) of three French regions (1988-1989). Human reproduction (Oxford, England). 1991;6(6):811.
8. Sharlip ID, Jarow JP, Belker AM, Lipshultz LI, Sigman M, Thomas AJ, et al. Best practice policies for male infertility. Fertility and Sterility. 2002;77(5):873-82.
9. Fertility facts and figures 2008 [Internet]. 2010 [cited 02/08/2017]. Available from: http://hfeaarchive.uksouth.cloudapp.azure.com/www.hfea.gov.uk/docs/2010-12-08_Fertility_Facts_and_Figures_2008_Publication_PDF.pdf.
10. Assisted Reproductive Technology [Internet]. CDC. 2019 [cited 15/04/2022]. Available from: https://www.cdc.gov/art/whatis.html.
11. Steptoe PC, Edwards RG. BIRTH AFTER THE REIMPLANTATION OF A HUMAN EMBRYO. The Lancet. 1978;312(8085):366.
12. Brinsden PR, Brinsden PR. Thirty years of IVF: the legacy of Patrick Steptoe and Robert Edwards. Hum Fertil (Camb). 2009;12(3):137-43.
13. Ng C, Trew G. Endocrinological insights into different in vitro fertilization treatment aspects. Expert Rev Endocrinol Metab. 2012;7(4):419-32.
14. Fertility treatments 2014-2016 Trends and figures [Internet]. www.hfea.gov.uk. 2018 [cited 09/05/2018]. Available from: https://www.hfea.gov.uk/media/2563/hfea-fertility-trends-and-figures-2017-v2.pdf.
15. Belchetz PE, Plant TM, Nakai Y, Keogh EJ, Knobil E. Hypophysial responses to continuous and intermittent delivery of hypopthalamic gonadotropin-releasing hormone. Science. 1978;202(4368):631-3.
16. Fritz MS, Leon. Clinical Gynecologic Endocrinology and Infertility. 8th ed: Lippincott, Williams & Wilkins; 2011.
17. Savoy-Moore RT, Swartz KH. Several GnRH stimulation frequencies differentially release FSH and LH from isolated, perfused rat anterior pituitary cells. Adv Exp Med Biol. 1987;219:641-5.
18. Wildt L, Hausler A, Marshall G, Hutchison JS, Plant TM, Belchetz PE, et al. Frequency and amplitude of gonadotropin-releasing hormone stimulation and gonadotropin secretion in the rhesus monkey. Endocrinology. 1981;109(2):376-85.
19. Thompson IR, Kaiser UB. GnRH pulse frequency-dependent differential regulation of LH and FSH gene expression. Mol Cell Endocrinol. 2014;385(1-2):28-35.
20. J G Pierce a, Parsons TF. Glycoprotein Hormones: Structure and Function. Annual Review of Biochemistry. 1981;50(1):465-95.
21. Jiang X, Liu H, Chen X, Chen PH, Fischer D, Sriraman V, et al. Structure of follicle-stimulating hormone in complex with the entire ectodomain of its receptor. Proc Natl Acad Sci U S A. 2012;109(31):12491-6.

22. Kakar SS, Musgrove LC, Devor DC, Sellers JC, Neill JD. Cloning, sequencing, and expression of human gonadotropin releasing hormone (GnRH) receptor. Biochemical and Biophysical Research Communications. 1992;189(1):289-95.
23. Davidson JS, Wakefield IK, Millar RP. Absence of rapid desensitization of the mouse gonadotropin-releasing hormone receptor. Biochem J. 1994;300 (Pt 2):299-302.
24. Willars GB, Heding A, Vrecl M, Sellar R, Blomenrohr M, Nahorski SR, et al. Lack of a C-terminal tail in the mammalian gonadotropin-releasing hormone receptor confers resistance to agonist-dependent phosphorylation and rapid desensitization. J Biol Chem. 1999;274(42):30146-53.
25. Burger LL, Haisenleder DJ, Dalkin AC, Marshall JC. Regulation of gonadotropin subunit gene transcription.33(3):559.
26. Evans JJ, Anderson GM. Balancing ovulation and anovulation: integration of the reproductive and energy balance axes by neuropeptides. Human reproduction update. 2012;18(3):313-32.
27. Inoue T, Miki Y, Abe K, Hatori M, Hosaka M, Kariya Y, et al. Sex steroid synthesis in human skin in situ: the roles of aromatase and steroidogenic acute regulatory protein in the homeostasis of human skin. Mol Cell Endocrinol. 2012;362(1-2):19-28.
28. Cui J, Shen Y, Li R. Estrogen synthesis and signaling pathways during aging: from periphery to brain. Trends Mol Med. 2013;19(3):197-209.
29. Hillier SG, Whitelaw PF, Smyth CD. Follicular oestrogen synthesis: the 'two-cell, two-gonadotrophin' model revisited. Mol Cell Endocrinol. 1994;100(1-2):51-4.
30. Biason-Lauber A, Boscaro M, Mantero F, Balercia G. Defects of steroidogenesis. J Endocrinol Invest. 2010;33(10):756-66.
31. Reed BG, Carr BR. The Normal Menstrual Cycle and the Control of Ovulation. In: Feingold KR, Anawalt B, Boyce A, Chrousos G, de Herder WW, Dhatariya K, et al., editors. Endotext. South Dartmouth (MA): MDText.com, Inc.

Copyright © 2000-2023, MDText.com, Inc.; 2000.

32. Goletiani NV, Keith DR, Gorsky SJ. Progesterone: review of safety for clinical studies. Exp Clin Psychopharmacol. 2007;15(5):427-44.
33. hysiology, Progesterone [Internet]. 2022. Available from: https://www.ncbi.nlm.nih.gov/books/NBK558960/.
34. Stouffer RL, Hennebold JD. Chapter 23 - Structure, Function, and Regulation of the Corpus Luteum. In: Plant TM, Zeleznik AJ, editors. Knobil and Neill's Physiology of Reproduction (Fourth Edition). San Diego: Academic Press; 2015. p. 1023-76.
35. Arab H, Alharbi AJ, Oraif A, Sagr E, Al Madani H, Abduljabbar H, et al. The Role Of Progestogens In Threatened And Idiopathic Recurrent Miscarriage. Int J Womens Health. 2019;11:589-96.
36. Alper MM, Fauser BC. Ovarian stimulation protocols for IVF: is more better than less? Reproductive BioMedicine Online. 2017;34(4):345-53.
37. Lunenfeld B. Historical perspectives in gonadotrophin therapy. Human reproduction update. 2004;10(6):453-67.
38. Medicine PCotASfR. Gonadotropin preparations: past, present, and future perspectives. Fertility and Sterility. 2008;90(5):S13-S20.
39. Macklon NS, Stouffer RL, Giudice LC, Fauser BC. The science behind 25 years of ovarian stimulation for in vitro fertilization. Endocrine reviews. 2006;27(2):170-207.
40. Leão RBF, Esteves SC. Gonadotropin therapy in assisted reproduction: an evolutionary perspective from biologics to biotech. Clinics. 2014;69:279-93.
41. M Fatemi H, Blockeel C, Devroey P. Ovarian stimulation: today and tomorrow. Current pharmaceutical biotechnology. 2012;13(3):392-7.
42. Ortmann O, Weiss JM, Diedrich K. Gonadotrophin-releasing hormone (GnRH) and GnRH agonists: mechanisms of action. Reprod Biomed Online. 2002;5 Suppl 1:1-7.
43. Abbara A, Clarke SA, Dhillo WS. Novel Concepts for Inducing Final Oocyte Maturation in In Vitro Fertilization Treatment. Endocrine reviews. 2018;39(5):593-628.

44. Siristatidis CS, Gibreel A, Basios G, Maheshwari A, Bhattacharya S. Gonadotrophin-releasing hormone agonist protocols for pituitary suppression in assisted reproduction. Cochrane Database Syst Rev. 2015(11):Cd006919.
45. Cakmak H, Rosen MP. Chapter 8 - Current Clinical Approaches to Protecting the Ovary: GnRH Analogues. In: Anderson RA, Spears N, editors. Cancer Treatment and the Ovary. Boston: Academic Press; 2015. p. 109-32.
46. Forman RG, Frydman R, Egan D, Ross C, Barlow DH. Severe ovarian hyperstimulation syndrome using agonists of gonadotropin-releasing hormone for in vitro fertilization: a European series and a proposal for prevention**Presented in part at the 6th World Congress on In Vitro Fertilization, Jerusalem, Israel, April 2 to 7, 1989. Fertility and Sterility. 1990;53(3):502-9.
47. Palermo G, Sills ES. Intracytoplasmic Sperm Injection: Indications, Techniques and Applications2018.
48. Dyer S, Chambers GM, de Mouzon J, Nygren KG, Zegers-Hochschild F, Mansour R, et al. International Committee for Monitoring Assisted Reproductive Technologies world report: Assisted Reproductive Technology 2008, 2009 and 2010. Human reproduction (Oxford, England). 2016;31(7):1588-609.
49. Neal SA, Morin SJ, Franasiak JM, Goodman LR, Juneau CR, Forman EJ, et al. Preimplantation genetic testing for aneuploidy is cost-effective, shortens treatment time, and reduces the risk of failed embryo transfer and clinical miscarriage. Fertility and Sterility. 2018;110(5):896-904.
50. Hassold T, Hunt P. To err (meiotically) is human: the genesis of human aneuploidy. Nature Reviews Genetics. 2001;2(4):280-91.
51. Penrose LS. The relative effects of paternal and maternal age in mongolism. Journal of Genetics. 1933;27(2):219-24.
52. Mikwar M, MacFarlane AJ, Marchetti F. Mechanisms of oocyte aneuploidy associated with advanced maternal age. Mutation Research/Reviews in Mutation Research. 2020;785:108320.
53. Harper J. Preimplantation Genetic Diagnosis. 2 ed. Cambridge: Cambridge University Press; 2009.
54. National Summary Report for 2015 [Internet]. 2015 [cited 16/04/2022]. Available from: https://www.sartcorsonline.com/rptCSR_PublicMultYear.aspx?#patient-cumulative.
55. Zhang WY, von Versen-Höynck F, Kapphahn KI, Fleischmann RR, Zhao Q, Baker VL. Maternal and neonatal outcomes associated with trophectoderm biopsy. Fertil Steril. 2019;112(2):283-90.e2.
56. Siermann M, Claesen Z, Pasquier L, Raivio T, Tšuiko O, Vermeesch JR, et al. A systematic review of the views of healthcare professionals on the scope of preimplantation genetic testing. J Community Genet. 2022;13(1):1-11.
57. Gardner RL, Edwards RG. Control of the Sex Ratio at Full Term in the Rabbit by transferring Sexed Blastocysts. Nature. 1968;218(5139):346-8.
58. Handyside AH, Kontogianni EH, Hardy K, Winston RML. Pregnancies from biopsied human preimplantation embryos sexed by Y-specific DNA amplification. Nature. 1990;344(6268):768-70.
59. Munné S, Lee A, Rosenwaks Z, Grifo J, Cohen J. Diagnosis of major chromosome aneuploidies in human preimplantation embryos. Human reproduction (Oxford, England). 1993;8(12):2185-91.
60. Harper JC, Wilton L, Traeger-Synodinos J, Goossens V, Moutou C, SenGupta SB, et al. The ESHRE PGD Consortium: 10 years of data collection. Human reproduction update. 2012;18(3):234-47.
61. Munné S, Wells D. Detection of mosaicism at blastocyst stage with the use of high-resolution next-generation sequencing. Fertil Steril. 2017;107(5):1085-91.
62. Munné S, Weier HUG, Grifo J, Cohen J. Chromosome Mosaicism in Human Embryos. Biology of Reproduction. 1994;51(3):373-9.

63. Baart EB, Martini E, van den Berg I, Macklon NS, Galjaard R-JH, Fauser BCJM, et al. Preimplantation genetic screening reveals a high incidence of aneuploidy and mosaicism in embryos from young women undergoing IVF. Human Reproduction. 2005;21(1):223-33.
64. Wells D, Delhanty JD. Comprehensive chromosomal analysis of human preimplantation embryos using whole genome amplification and single cell comparative genomic hybridization. Molecular human reproduction. 2000;6(11):1055-62.
65. Zheng H, Jin H, Liu L, Liu J, Wang W-H. Application of next-generation sequencing for 24-chromosome aneuploidy screening of human preimplantation embryos. Mol Cytogenet. 2015;8:38-.
66. Sullivan-Pyke C, Dokras A. Preimplantation genetic screening and preimplantation genetic diagnosis. Obstetrics and Gynecology Clinics. 2018;45(1):113-25.
67. Montag M, van der Ven K, Rösing B, van der Ven H. Polar body biopsy: a viable alternative to preimplantation genetic diagnosis and screening. Reprod Biomed Online. 2009;18 Suppl 1:6-11.
68. Scott KL, Hong KH, Scott RT. Selecting the optimal time to perform biopsy for preimplantation genetic testing. Fertility and Sterility. 2013;100(3):608-14.
69. De Vos A, Staessen C, De Rycke M, Verpoest W, Haentjens P, Devroey P, et al. Impact of cleavage-stage embryo biopsy in view of PGD on human blastocyst implantation: a prospective cohort of single embryo transfers. Human Reproduction. 2009;24(12):2988-96.
70. Scott RT, Upham KM, Forman EJ, Zhao T, Treff NR. Cleavage-stage biopsy significantly impairs human embryonic implantation potential while blastocyst biopsy does not: a randomized and paired clinical trial. Fertility and Sterility. 2013;100(3):624-30.
71. Lee HL, McCulloh DH, Hodes-Wertz B, Adler A, McCaffrey C, Grifo JA. In vitro fertilization with preimplantation genetic screening improves implantation and live birth in women age 40 through 43. J Assist Reprod Genet. 2015;32(3):435-44.
72. Huang L, Bogale B, Tang Y, Lu S, Xie XS, Racowsky C. Noninvasive preimplantation genetic testing for aneuploidy in spent medium may be more reliable than trophectoderm biopsy. Proceedings of the National Academy of Sciences. 2019;116(28):14105-12.
73. Wu H-J, Wu E. The role of gut microbiota in immune homeostasis and autoimmunity. Gut Microbes. 2012;3(1):4-14.
74. Cummings JH, Macfarlane GT. Role of intestinal bacteria in nutrient metabolism. Clinical Nutrition. 1997;16(1):3-11.
75. Dethlefsen L, McFall-Ngai M, Relman DA. An ecological and evolutionary perspective on human–microbe mutualism and disease. Nature. 2007;449:811.
76. Hooper LV, Gordon JI. Commensal Host-Bacterial Relationships in the Gut. Science. 2001;292(5519):1115-8.
77. Lederberg J, McCray AT. `Ome Sweet `Omics--A Genealogical Treasury of Words. The Scientist. 2001 2001/04/02/:8.
78. Marchesi JR, Ravel J. The vocabulary of microbiome research: a proposal. Microbiome. 2015;3:31.
79. Venter JC, Adams MD, Myers EW, Li PW, Mural RJ, Sutton GG, et al. The Sequence of the Human Genome. Science. 2001;291(5507):1304-51.
80. Sirota I, Zarek SM, Segars JH. Potential Influence of the Microbiome on Infertility and Assisted Reproductive Technology. Semin Reprod Med. 2014;32(01):035-42.
81. The NIHHMPWG, Peterson J, Garges S, Giovanni M, McInnes P, Wang L, et al. The NIH Human Microbiome Project. Genome Research. 2009;19(12):2317-23.
82. Turnbaugh PJ, Ley RE, Hamady M, Fraser-Liggett CM, Knight R, Gordon JI. The Human Microbiome Project. Nature. 2007;449(7164):804-10.
83. Wassenaar TM, Panigrahi P. Is a foetus developing in a sterile environment? Letters in Applied Microbiology. 2014;59(6):572-9.
84. Aagaard K, Ma J, Antony KM, Ganu R, Petrosino J, Versalovic J. The placenta harbors a unique microbiome. Sci Transl Med. 2014;6(237):237ra65.
85. DiGiulio DB, Romero R, Amogan HP, Kusanovic JP, Bik EM, Gotsch F, et al. Microbial Prevalence, Diversity and Abundance in Amniotic Fluid During Preterm Labor: A Molecular and Culture-Based Investigation. PloS one. 2008;3(8):e3056.

86. Funkhouser LJ, Bordenstein SR. Mom Knows Best: The Universality of Maternal Microbial Transmission. 2013;11(8):e1001631.
87. DiGiulio DB. Diversity of microbes in amniotic fluid. Seminars in Fetal and Neonatal Medicine. 2012;17(1):2-11.
88. Dominguez-Bello MG, Costello EK, Contreras M, Magris M, Hidalgo G, Fierer N, et al. Delivery mode shapes the acquisition and structure of the initial microbiota across multiple body habitats in newborns. Proceedings of the National Academy of Sciences. 2010;107(26):11971-5.
89. Penders J, Thijs C, Vink C, Stelma FF, Snijders B, Kummeling I, et al. Factors influencing the composition of the intestinal microbiota in early infancy. Pediatrics. 2006;118(2):511.
90. Adlerberth I, Wold A. Establishment of the gut microbiota in Western infants. Oxford, UK2009. p. 229-38.
91. Madan JC, Farzan SF, Hibberd PL, Karagas MR. Normal neonatal microbiome variation in relation to environmental factors, infection and allergy. Current opinion in pediatrics. 2012;24(6):753.
92. Gerber GK. The dynamic microbiome. FEBS Letters. 2014;588(22):4131-9.
93. Yatsunenko T, Rey FE, Manary MJ, Trehan I, Dominguez-Bello MG, Contreras M, et al. Human gut microbiome viewed across age and geography. Nature. 2012;486:222.
94. Claesson MJ, Cusack S, Sullivan O, Greene-Diniz R, De Weerd H, Flannery E, et al. Composition, variability, and temporal stability of the intestinal microbiota of the elderly. Proceedings of the National Academy of Sciences of the United States of America. 2011;108:4586-91.
95. Zapata HJ, Quagliarello VJ. The Microbiota and Microbiome in Aging: Potential Implications in Health and Age-Related Diseases. Journal of the American Geriatrics Society. 2015;63(4):776-81.
96. Biagi E, Candela M, Fairweather-Tait S, Franceschi C, Brigidi P. Ageing of the human metaorganism: the microbial counterpart. The Official Journal of the American Aging Association. 2012;34(1):247-67.
97. Yoshikawa TT. Epidemiology and unique aspects of aging and infectious diseases. Clinical Infectious Diseases. 2000;30(6):931-3.
98. Narayan H, McGarry J. What Determines The Age At The Menopause? BMJ: British Medical Journal. 1991;302(6791):1540-.
99. Oliveira NSd, Lima ABFd, Brito JCRd, Sarmento ACA, Gonçalves AKS, Eleutério J. Postmenopausal Vaginal Microbiome and Microbiota. Frontiers in Reproductive Health. 2022;3.
100. Kim JM, Park YJ. Probiotics in the Prevention and Treatment of Postmenopausal Vaginal Infections: Review Article. J Menopausal Med. 2017;23(3):139-45.
101. Brotman RM, Shardell MD, Gajer P, Fadrosh D, Chang K, Silver MI, et al. Association between the vaginal microbiota, menopause status, and signs of vulvovaginal atrophy. Menopause. 2014;21(5):450-8.
102. Raz R, Stamm WE. A Controlled Trial of Intravaginal Estriol in Postmenopausal Women with Recurrent Urinary Tract Infections. New England Journal of Medicine. 1993;329(11):753-6.
103. Weinstock GM. Genomic approaches to studying the human microbiota. Nature. 2012;489(7415):250-6.
104. VerBerkmoes NC, Denef VJ, Hettich RL, Banfield JF. Systems biology: Functional analysis of natural microbial consortia using community proteomics. Nat Rev Microbiol. 2009;7(3):196-205.
105. Dickson RP, Erb-Downward JR, Prescott HC, Martinez FJ, Curtis JL, Lama VN, et al. Analysis of Culture-Dependent versus Culture-Independent Techniques for Identification of Bacteria in Clinically Obtained Bronchoalveolar Lavage Fluid. Journal of Clinical Microbiology. 2014;52(10):3605-13.

106. Jesumirhewe C, Ogunlowo PO, Olley M, Springer B, Allerberger F, Ruppitsch W. Accuracy of conventional identification methods used for Enterobacteriaceae isolates in three Nigerian hospitals. PeerJ. 2016;4:e2511.
107. García-Velasco JA, Menabrito M, Catalán IB. What fertility specialists should know about the vaginal microbiome: a review. Reproductive BioMedicine Online. 2017;35(1):103-12.
108. Wu R, Taylor E. Nucleotide sequence analysis of DNA: II. Complete nucleotide sequence of the cohesive ends of bacteriophage λ DNA. Journal of Molecular Biology. 1971;57(3):491-511.
109. Sanger F, Nicklen S, Coulson AR. DNA sequencing with chain-terminating inhibitors. Proceedings of the National Academy of Sciences of the United States of America. 1977;74(12):5463-7.
110. Kircher M, Kelso J. High-throughput DNA sequencing - concepts and limitations. BioEssays. 2010;32(6):524-36.
111. Raza K, Ahmad S. RECENT ADVANCEMENT IN NEXT-GENERATION SEQUENCING TECHNIQUES AND ITS COMPUTATIONAL ANALYSIS. arXiv preprint arXiv:160605254. 2016.
112. Cao Y, Fanning S, Proos S, Jordan K, Srikumar S. A Review on the Applications of Next Generation Sequencing Technologies as Applied to Food-Related Microbiome Studies. Frontiers in Microbiology. 2017;8(1829).
113. Chakravorty S, Helb D, Burday M, Connell N, Alland D. A detailed analysis of 16S ribosomal RNA gene segments for the diagnosis of pathogenic bacteria. J Microbiol Methods. 2007;69(2):330-9.
114. Van de Peer Y, Chapelle S, De Wachter R. A quantitative map of nucleotide substitution rates in bacterial rRNA. Nucleic Acids Res. 1996;24(17):3381-91.
115. Bayar E, Bennett PR, Chan D, Sykes L, MacIntyre DA. The pregnancy microbiome and preterm birth. Semin Immunopathol. 2020;42(4):487-99.
116. Amsel R, Totten PA, Spiegel CA, Chen KC, Eschenbach D, Holmes KK. Nonspecific vaginitis. Diagnostic criteria and microbial and epidemiologic associations. Am J Med. 1983;74(1):14-22.
117. Nugent RP, Krohn MA, Hillier SL. Reliability of diagnosing bacterial vaginosis is improved by a standardized method of gram stain interpretation. J Clin Microbiol. 1991;29(2):297-301.
118. Srinivasan S, Morgan MT, Liu C, Matsen FA, Hoffman NG, Fiedler TL, et al. More than meets the eye: associations of vaginal bacteria with gram stain morphotypes using molecular phylogenetic analysis. PLoS One. 2013;8(10):e78633.
119. Holm JB, France MT, Ma B, McComb E, Robinson CK, Mehta A, et al. Comparative Metagenome-Assembled Genome Analysis of "Candidatus Lachnocurva vaginae", Formerly Known as Bacterial Vaginosis-Associated Bacterium-1 (BVAB1). Front Cell Infect Microbiol. 2020;10:117.
120. Burton JP, Reid G. Evaluation of the bacterial vaginal flora of 20 postmenopausal women by direct (Nugent score) and molecular (polymerase chain reaction and denaturing gradient gel electrophoresis) techniques. J Infect Dis. 2002;186(12):1770-80.
121. Lundy SD, Sangwan N, Parekh NV, Selvam MKP, Gupta S, McCaffrey P, et al. Functional and Taxonomic Dysbiosis of the Gut, Urine, and Semen Microbiomes in Male Infertility. Eur Urol. 2021;79(6):826-36.
122. Kermes K, Punab M, Lõivukene K, Mändar R. Anaerobic seminal fluid micro-flora in chronic prostatitis/chronic pelvic pain syndrome patients. Anaerobe. 2003;9(3):117-23.
123. Javurek AB, Spollen WG, Ali AMM, Johnson SA, Lubahn DB, Bivens NJ, et al. Discovery of a novel seminal fluid microbiome and influence of estrogen receptor alpha genetic status. Scientific reports. 2016;6(1):1-14.
124. Cavarretta I, Ferrarese R, Cazzaniga W, Saita D, Lucianò R, Ceresola ER, et al. The microbiome of the prostate tumor microenvironment. European urology. 2017;72(4):625-31.

125. Alfano M, Ferrarese R, Locatelli I, Ventimiglia E, Ippolito S, Gallina P, et al. Testicular microbiome in azoospermic men—first evidence of the impact of an altered microenvironment. Human Reproduction. 2018;33(7):1212-7.
126. Lash AF, Kaplan B. A Study of Döderlein's Vaginal Bacillus. The Journal of Infectious Diseases. 1926;38(4):333-40.
127. Cruickshank R. Doderlein's Vaginal Bacillus: A Contribution to the Study of the Lacto-Bacilli. J Hyg (Lond). 1931;31(3):375-81.
128. Martin HL, Richardson BA, Nyange PM, Lavreys L, Hillier SL, Chohan B, et al. Vaginal lactobacilli, microbial flora, and risk of human immunodeficiency virus type 1 and sexually transmitted disease acquisition. J Infect Dis. 1999;180(6):1863-8.
129. Sewankambo N, Gray RH, Wawer MJ, Paxton L, McNaim D, Wabwire-Mangen F, et al. HIV-1 infection associated with abnormal vaginal flora morphology and bacterial vaginosis. Lancet. 1997;350(9077):546-50.
130. Hay PE, Lamont RF, Taylor-Robinson D, Morgan DJ, Ison C, Pearson J. Abnormal bacterial colonisation of the genital tract and subsequent preterm delivery and late miscarriage. BMJ. 1994;308(6924):295-8.
131. Leitich H, Bodner-Adler B, Brunbauer M, Kaider A, Egarter C, Husslein P. Bacterial vaginosis as a risk factor for preterm delivery: a meta-analysis. Am J Obstet Gynecol. 2003;189(1):139-47.
132. Martius J, Krohn MA, Hillier SL, Stamm WE, Holmes KK, Eschenbach DA. Relationships of vaginal Lactobacillus species, cervical Chlamydia trachomatis, and bacterial vaginosis to preterm birth. Obstet Gynecol. 1988;71(1):89-95.
133. Ravel J, Gajer P, Abdo Z, Schneider GM, Koenig SSK, McCulle SL, et al. Vaginal microbiome of reproductive-age women. Proceedings of the National Academy of Sciences. 2011;108(Supplement 1):4680-7.
134. Borgdorff H, van der Veer C, van Houdt R, Alberts CJ, de Vries HJ, Bruisten SM, et al. The association between ethnicity and vaginal microbiota composition in Amsterdam, the Netherlands. PLoS One. 2017;12(7):e0181135.
135. Callahan BJ, DiGiulio DB, Goltsman DSA, Sun CL, Costello EK, Jeganathan P, et al. Replication and refinement of a vaginal microbial signature of preterm birth in two racially distinct cohorts of US women. Proc Natl Acad Sci U S A. 2017;114(37):9966-71.
136. Fettweis JM, Brooks JP, Serrano MG, Sheth NU, Girerd PH, Edwards DJ, et al. Differences in vaginal microbiome in African American women versus women of European ancestry. Microbiology (Reading). 2014;160(Pt 10):2272-82.
137. Serrano MG, Parikh HI, Brooks JP, Edwards DJ, Arodz TJ, Edupuganti L, et al. Racioethnic diversity in the dynamics of the vaginal microbiome during pregnancy. Nat Med. 2019;25(6):1001-11.
138. Gajer P, Brotman RM, Bai G, Sakamoto J, Schutte UM, Zhong X, et al. Temporal dynamics of the human vaginal microbiota. Sci Transl Med. 2012;4(132):132ra52.
139. Martin DH, Marrazzo JM. The Vaginal Microbiome: Current Understanding and Future Directions. J Infect Dis. 2016;214 Suppl 1:S36-41.
140. Brown RG, Al-Memar M, Marchesi JR, Lee YS, Smith A, Chan D, et al. Establishment of vaginal microbiota composition in early pregnancy and its association with subsequent preterm prelabor rupture of the fetal membranes. Transl Res. 2019;207:30-43.
141. Brown SE, Schwartz JA, Robinson CK, O'Hanlon DE, Bradford LL, He X, et al. The Vaginal Microbiota and Behavioral Factors Associated With Genital Candida albicans Detection in Reproductive-Age Women. Sex Transm Dis. 2019;46(11):753-8.
142. France MT, Ma B, Gajer P, Brown S, Humphrys MS, Holm JB, et al. VALENCIA: a nearest centroid classification method for vaginal microbial communities based on composition. Microbiome. 2020;8(1):166.
143. Dominguez-Bello MG, Costello EK, Contreras M, Magris M, Hidalgo G, Fierer N, et al. Delivery mode shapes the acquisition and structure of the initial microbiota across multiple body habitats in newborns. Proc Natl Acad Sci U S A. 2010;107(26):11971-5.

144. Hickey RJ, Zhou X, Settles ML, Erb J, Malone K, Hansmann MA, et al. Vaginal microbiota of adolescent girls prior to the onset of menarche resemble those of reproductive-age women. MBio. 2015;6(2).
145. MacIntyre DA, Chandiramani M, Lee YS, Kindinger L, Smith A, Angelopoulos N, et al. The vaginal microbiome during pregnancy and the postpartum period in a European population. Scientific reports. 2015;5:8988.
146. Romero R, Hassan SS, Gajer P, Tarca AL, Fadrosh DW, Nikita L, et al. The composition and stability of the vaginal microbiota of normal pregnant women is different from that of non-pregnant women. Microbiome. 2014;2(1):4.
147. Nott PN, Franklin M, Armitage C, Gelder MG. Hormonal changes and mood in the puerperium. Br J Psychiatry. 1976;128:379-83.
148. DiGiulio DB, Callahan BJ, McMurdie PJ, Costello EK, Lyell DJ, Robaczewska A, et al. Temporal and spatial variation of the human microbiota during pregnancy. Proc Natl Acad Sci U S A. 2015;112(35):11060-5.
149. Eschenbach DA, Thwin SS, Patton DL, Hooton TM, Stapleton AE, Agnew K, et al. Influence of the normal menstrual cycle on vaginal tissue, discharge, and microflora. Clin Infect Dis. 2000;30(6):901-7.
150. Srinivasan S, Liu C, Mitchell CM, Fiedler TL, Thomas KK, Agnew KJ, et al. Temporal variability of human vaginal bacteria and relationship with bacterial vaginosis. PLoS One. 2010;5(4):e10197.
151. Song SD, Acharya KD, Zhu JE, Deveney CM, Walther-Antonio MRS, Tetel MJ, et al. Daily Vaginal Microbiota Fluctuations Associated with Natural Hormonal Cycle, Contraceptives, Diet, and Exercise. mSphere. 2020;5(4).
152. Bradshaw CS, Vodstrcil LA, Hocking JS, Law M, Pirotta M, Garland SM, et al. Recurrence of bacterial vaginosis is significantly associated with posttreatment sexual activities and hormonal contraceptive use. Clin Infect Dis. 2013;56(6):777-86.
153. Crucitti T, Hardy L, van de Wijgert J, Agaba S, Buyze J, Kestelyn E, et al. Contraceptive rings promote vaginal lactobacilli in a high bacterial vaginosis prevalence population: A randomised, open-label longitudinal study in Rwandan women. PLoS One. 2018;13(7):e0201003.
154. van de Wijgert JH, Verwijs MC, Turner AN, Morrison CS. Hormonal contraception decreases bacterial vaginosis but oral contraception may increase candidiasis: implications for HIV transmission. AIDS. 2013;27(13):2141-53.
155. Ahrens P, Andersen LO, Lilje B, Johannesen TB, Dahl EG, Baig S, et al. Changes in the vaginal microbiota following antibiotic treatment for Mycoplasma genitalium, Chlamydia trachomatis and bacterial vaginosis. PLoS One. 2020;15(7):e0236036.
156. Brown RG, Marchesi JR, Lee YS, Smith A, Lehne B, Kindinger LM, et al. Vaginal dysbiosis increases risk of preterm fetal membrane rupture, neonatal sepsis and is exacerbated by erythromycin. BMC Medicine. 2018;16(1):9.
157. Mayer BT, Srinivasan S, Fiedler TL, Marrazzo JM, Fredricks DN, Schiffer JT. Rapid and Profound Shifts in the Vaginal Microbiota Following Antibiotic Treatment for Bacterial Vaginosis. J Infect Dis. 2015;212(5):793-802.
158. Stokholm J, Schjorring S, Eskildsen CE, Pedersen L, Bischoff AL, Folsgaard N, et al. Antibiotic use during pregnancy alters the commensal vaginal microbiota. Clin Microbiol Infect. 2014;20(7):629-35.
159. Eschenbach DA, Patton DL, Hooton TM, Meier AS, Stapleton A, Aura J, et al. Effects of vaginal intercourse with and without a condom on vaginal flora and vaginal epithelium. J Infect Dis. 2001;183(6):913-8.
160. Plummer EL, Vodstrcil LA, Fairley CK, Tabrizi SN, Garland SM, Law MG, et al. Sexual practices have a significant impact on the vaginal microbiota of women who have sex with women. Sci Rep. 2019;9(1):19749.
161. Anderson DJ, Marathe J, Pudney J. The structure of the human vaginal stratum corneum and its role in immune defense. Am J Reprod Immunol. 2014;71(6):618-23.
162. Eckhart L, Lippens S, Tschachler E, Declercq W. Cell death by cornification. Biochim Biophys Acta. 2013;1833(12):3471-80.

163. Muenzner P, Bachmann V, Zimmermann W, Hentschel J, Hauck CR. Human-restricted bacterial pathogens block shedding of epithelial cells by stimulating integrin activation. Science. 2010;329(5996):1197-201.
164. Vornhagen J, Armistead B, Santana-Ufret V, Gendrin C, Merillat S, Coleman M, et al. Group B streptococcus exploits vaginal epithelial exfoliation for ascending infection. J Clin Invest. 2018;128(5):1985-99.
165. Averette HE, Weinstein GD, Frost P. Autoradiographic analysis of cell proliferation kinetics in human genital tissues. I. Normal cervix and vagina. Am J Obstet Gynecol. 1970;108(1):8-17.
166. Cole A. Innate Host Defense of Human Vaginal and Cervical Mucosae. Journal of Lower Genital Tract Disease. 2007;11(2):129-30.
167. Han L, Taub R, Jensen JT. Cervical mucus and contraception: what we know and what we don't. Contraception. 2017;96(5):310-21.
168. van Putten JPM, Strijbis K. Transmembrane Mucins: Signaling Receptors at the Intersection of Inflammation and Cancer. Journal of Innate Immunity. 2017;9(3):281-99.
169. Kumar N, Behera B, Sagiri SS, Pal K, Ray SS, Roy S. Bacterial vaginosis: Etiology and modalities of treatment-A brief note. J Pharm Bioallied Sci. 2011;3(4):496-503.
170. Becher N, Adams Waldorf K, Hein M, Uldbjerg N. The cervical mucus plug: structured review of the literature. Acta Obstet Gynecol Scand. 2009;88(5):502-13.
171. Cortés ME, Alfaro AA. The effects of hormonal contraceptives on glycemic regulation. Linacre Q. 2014;81(3):209-18.
172. Lai SK, Wang Y-Y, Wirtz D, Hanes J. Micro- and macrorheology of mucus. Adv Drug Deliv Rev. 2009;61(2):86-100.
173. Olmsted SS, Meyn LA, Rohan LC, Hillier SL. Glycosidase and proteinase activity of anaerobic gram-negative bacteria isolated from women with bacterial vaginosis. Sex Transm Dis. 2003;30(3):257-61.
174. Witkin SS, Mendes-Soares H, Linhares IM, Jayaram A, Ledger WJ, Forney LJ. Influence of vaginal bacteria and D- and L-lactic acid isomers on vaginal extracellular matrix metalloproteinase inducer: implications for protection against upper genital tract infections. mBio. 2013;4(4).
175. O'Hanlon DE, Moench TR, Cone RA. Vaginal pH and microbicidal lactic acid when lactobacilli dominate the microbiota. PLoS One. 2013;8(11):e80074.
176. Velraeds MM, van der Mei HC, Reid G, Busscher HJ. Inhibition of initial adhesion of uropathogenic Enterococcus faecalis by biosurfactants from Lactobacillus isolates. Appl Environ Microbiol. 1996;62(6):1958-63.
177. He Y, Niu X, Wang B, Na R, Xiao B, Yang H. Evaluation of the Inhibitory Effects of Lactobacillus gasseri and Lactobacillus crispatus on the Adhesion of Seven Common Lower Genital Tract Infection-Causing Pathogens to Vaginal Epithelial Cells. Front Med (Lausanne). 2020;7(284).
178. Macklaim JM, Gloor GB, Anukam KC, Cribby S, Reid G. At the crossroads of vaginal health and disease, the genome sequence of Lactobacillus iners AB-1. Proceedings of the National Academy of Sciences of the United States of America. 2011;108 Suppl 1(Suppl 1):4688-95.
179. Petrova MI, Reid G, Vaneechoutte M, Lebeer S. Lactobacillus iners: Friend or Foe? Trends in Microbiology. 2017;25(3):182-91.
180. Antonio MA, Rabe LK, Hillier SL. Colonization of the rectum by Lactobacillus species and decreased risk of bacterial vaginosis. J Infect Dis. 2005;192(3):394-8.
181. Eschenbach DA, Davick PR, Williams BL, Klebanoff SJ, Young-Smith K, Critchlow CM, et al. Prevalence of hydrogen peroxide-producing Lactobacillus species in normal women and women with bacterial vaginosis. J Clin Microbiol. 1989;27(2):251-6.
182. Ness RB, Hillier SL, Kip KE, Soper DE, Stamm CA, McGregor JA, et al. Bacterial vaginosis and risk of pelvic inflammatory disease. Obstet Gynecol. 2004;104(4):761-9.
183. Wang S, Wang Q, Yang E, Yan L, Li T, Zhuang H. Antimicrobial Compounds Produced by Vaginal Lactobacillus crispatus Are Able to Strongly Inhibit Candida albicans Growth,

Hyphal Formation and Regulate Virulence-related Gene Expressions. Front Microbiol. 2017;8:564.
184. Lewis FMT, Bernstein KT, Aral SO. Vaginal Microbiome and Its Relationship to Behavior, Sexual Health, and Sexually Transmitted Diseases. Obstet Gynecol. 2017;129(4):643-54.
185. van de Wijgert J. The vaginal microbiome and sexually transmitted infections are interlinked: Consequences for treatment and prevention. PLoS Med. 2017;14(12):e1002478.
186. Brotman RM. Vaginal microbiome and sexually transmitted infections: an epidemiologic perspective. J Clin Invest. 2011;121(12):4610-7.
187. Mitra A, MacIntyre DA, Marchesi JR, Lee YS, Bennett PR, Kyrgiou M. The vaginal microbiota, human papillomavirus infection and cervical intraepithelial neoplasia: what do we know and where are we going next? Microbiome. 2016;4(1):58.
188. Norenhag J, Du J, Olovsson M, Verstraelen H, Engstrand L, Brusselaers N. The vaginal microbiota, human papillomavirus and cervical dysplasia: a systematic review and network meta-analysis. BJOG : an international journal of obstetrics and gynaecology. 2020;127(2):171-80.
189. Mitra A, MacIntyre DA, Ntritsos G, Smith A, Tsilidis KK, Marchesi JR, et al. The vaginal microbiota associates with the regression of untreated cervical intraepithelial neoplasia 2 lesions. Nat Commun. 2020;11(1):1999.
190. Klatt NR, Cheu R, Birse K, Zevin AS, Perner M, Noel-Romas L, et al. Vaginal bacteria modify HIV tenofovir microbicide efficacy in African women. Science. 2017;356(6341):938-45.
191. Wee BA, Thomas M, Sweeney EL, Frentiu FD, Samios M, Ravel J, et al. A retrospective pilot study to determine whether the reproductive tract microbiota differs between women with a history of infertility and fertile women. Aust N Z J Obstet Gynaecol. 2018;58(3):341-8.
192. Zhao C, Wei Z, Yang J, Zhang J, Yu C, Yang A, et al. Characterization of the Vaginal Microbiome in Women with Infertility and Its Potential Correlation with Hormone Stimulation during In Vitro Fertilization Surgery. mSystems. 2020;5(4):e00450-20.
193. Kong Y, Liu Z, Shang Q, Gao Y, Li X, Zheng C, et al. The Disordered Vaginal Microbiota Is a Potential Indicator for a Higher Failure of in vitro Fertilization. Frontiers in Medicine. 2020;7(217).
194. Haahr T, Zacho J, Bräuner M, Shathmigha K, Skov Jensen J, Humaidan P. Reproductive outcome of patients undergoing in vitro fertilisation treatment and diagnosed with bacterial vaginosis or abnormal vaginal microbiota: a systematic PRISMA review and meta-analysis. BJOG : an international journal of obstetrics and gynaecology. 2019;126(2):200-7.
195. Haahr T, Humaidan P, Elbaek HO, Alsbjerg B, Laursen RJ, Rygaard K, et al. Vaginal Microbiota and In Vitro Fertilization Outcomes: Development of a Simple Diagnostic Tool to Predict Patients at Risk of a Poor Reproductive Outcome. The Journal of Infectious Diseases. 2018;219(11):1809-17.
196. Koedooder R, Singer M, Schoenmakers S, Savelkoul PHM, Morre SA, de Jonge JD, et al. The vaginal microbiome as a predictor for outcome of in vitro fertilization with or without intracytoplasmic sperm injection: a prospective study. Human reproduction (Oxford, England). 2019;34(6):1042-54.
197. Al-Memar M, Bobdiwala S, Fourie H, Mannino R, Lee YS, Smith A, et al. The association between vaginal bacterial composition and miscarriage: a nested case-control study. BJOG : an international journal of obstetrics and gynaecology. 2020;127(2):264-74.
198. Zhang F, Zhang T, Ma Y, Huang Z, He Y, Pan H, et al. Alteration of vaginal microbiota in patients with unexplained recurrent miscarriage. Exp Ther Med. 2019;17(5):3307-16.
199. Causes of child mortality [http://www.who.int/gho/child_health/mortality/causes/en/]. Accessed 7 July 2016.
200. Donders GG, Van Calsteren K, Bellen G, Reybrouck R, Van den Bosch T, Riphagen I, et al. Predictive value for preterm birth of abnormal vaginal flora, bacterial vaginosis and aerobic vaginitis during the first trimester of pregnancy. BJOG : an international journal of obstetrics and gynaecology. 2009;116(10):1315-24.

201. Flynn CA, Helwig AL, Meurer LN. Bacterial vaginosis in pregnancy and the risk of prematurity: a meta-analysis. The Journal of family practice. 1999;48(11):885-92.
202. McGregor JA, French JI, Seo K. Premature rupture of membranes and bacterial vaginosis. American journal of obstetrics and gynecology. 1993;169(2 Pt 2):463-6.
203. Bennett PR, Brown RG, MacIntyre DA. Vaginal Microbiome in Preterm Rupture of Membranes. Obstet Gynecol Clin North Am. 2020;47(4):503-21.
204. Kindinger LM, Bennett PR, Lee YS, Marchesi JR, Smith A, Cacciatore S, et al. The interaction between vaginal microbiota, cervical length, and vaginal progesterone treatment for preterm birth risk. Microbiome. 2017;5(1):6.
205. Stafford GP, Parker JL, Amabebe E, Kistler J, Reynolds S, Stern V, et al. Spontaneous Preterm Birth Is Associated with Differential Expression of Vaginal Metabolites by Lactobacilli-Dominated Microflora. Front Physiol. 2017;8:615.
206. Hocevar K, Maver A, Vidmar Simic M, Hodzic A, Haslberger A, Premru Sersen T, et al. Vaginal Microbiome Signature Is Associated With Spontaneous Preterm Delivery. Front Med (Lausanne). 2019;6:201.
207. Fettweis JM, Serrano MG, Brooks JP, Edwards DJ, Girerd PH, Parikh HI, et al. The vaginal microbiome and preterm birth. Nat Med. 2019;25(6):1012-21.
208. Freitas AC, Bocking A, Hill JE, Money DM, Group VR. Increased richness and diversity of the vaginal microbiota and spontaneous preterm birth. Microbiome. 2018;6(1):117.
209. Tabatabaei N, Eren AM, Barreiro LB, Yotova V, Dumaine A, Allard C, et al. Vaginal microbiome in early pregnancy and subsequent risk of spontaneous preterm birth: a case-control study. BJOG : an international journal of obstetrics and gynaecology. 2019;126(3):349-58.
210. Romero R, Hassan SS, Gajer P, Tarca AL, Fadrosh DW, Bieda J, et al. The vaginal microbiota of pregnant women who subsequently have spontaneous preterm labor and delivery and those with a normal delivery at term. Microbiome. 2014;2:18.
211. Stout MJ, Zhou Y, Wylie KM, Tarr PI, Macones GA, Tuuli MG. Early pregnancy vaginal microbiome trends and preterm birth. American journal of obstetrics and gynecology. 2017.
212. Nelson DB, Shin H, Wu J, Dominguez-Bello MG. The Gestational Vaginal Microbiome and Spontaneous Preterm Birth among Nulliparous African American Women. American journal of perinatology. 2016;33(9):887-93.
213. Ralph SG, Rutherford AJ, Wilson JD. Influence of bacterial vaginosis on conception and miscarriage in the first trimester: cohort study. Bmj. 1999;319(7204):220-3.
214. Liversedge NH, Turner A, Horner PJ, Keay SD, Jenkins JM, Hull MG. The influence of bacterial vaginosis on in-vitro fertilization and embryo implantation during assisted reproduction treatment. Hum Reprod. 1999;14(9):2411-5.
215. Eckert LO, Moore DE, Patton DL, Agnew KJ, Eschenbach DA. Relationship of vaginal bacteria and inflammation with conception and early pregnancy loss following in-vitro fertilization. Infect Dis Obstet Gynecol. 2003;11(1):11-7.
216. Selman H, Mariani M, Barnocchi N, Mencacci A, Bistoni F, Arena S, et al. Examination of bacterial contamination at the time of embryo transfer, and its impact on the IVF/pregnancy outcome. J Assist Reprod Genet. 2007;24(9):395-9.
217. Hyman RW, Herndon CN, Jiang H, Palm C, Fukushima M, Bernstein D, et al. The dynamics of the vaginal microbiome during infertility therapy with in vitro fertilization-embryo transfer. Journal of Assisted Reproduction and Genetics. 2012;29(2):105-15.
218. Mangot-Bertrand J, Fenollar F, Bretelle F, Gamerre M, Raoult D, Courbiere B. Molecular diagnosis of bacterial vaginosis: impact on IVF outcome. European Journal of Clinical Microbiology & Infectious Diseases. 2013;32(4):535-41.
219. Haahr T, Jensen JS, Thomsen L, Duus L, Rygaard K, Humaidan P. Abnormal vaginal microbiota may be associated with poor reproductive outcomes: a prospective study in IVF patients. Hum Reprod. 2016;31(4):795-803.
220. Vergaro P, Tiscornia G, Barragan M, Garcia D, Rodriguez A, Santalo J, et al. Vaginal microbiota profile at the time of embryo transfer does not affect live birth rate in IVF cycles with donated oocytes. Reprod Biomed Online. 2018.

221. Fu M, Zhang X, Liang Y, Lin S, Qian W, Fan S. Alterations in Vaginal Microbiota and Associated Metabolome in Women with Recurrent Implantation Failure. mBio. 2020;11(3):e03242-19.
222. Hao X, Li P, Wu S, Tan J. Association of the Cervical Microbiota With Pregnancy Outcome in a Subfertile Population Undergoing In Vitro Fertilization: A Case-Control Study. Front Cell Infect Microbiol. 2021;11:654202.
223. Sharma H, Tal R, Clark NA, Segars JH. Microbiota and pelvic inflammatory disease. Semin Reprod Med. 2014;32(1):43-9.
224. Brunham RC, Gottlieb SL, Paavonen J. Pelvic inflammatory disease. N Engl J Med. 2015;372(21):2039-48.
225. Tai F-W, Chang CY-Y, Chiang J-H, Lin W-C, Wan L. Association of Pelvic Inflammatory Disease with Risk of Endometriosis: A Nationwide Cohort Study Involving 141,460 Individuals. J Clin Med. 2018;7(11):379.
226. Khan KN, Fujishita A, Masumoto H, Muto H, Kitajima M, Masuzaki H, et al. Molecular detection of intrauterine microbial colonization in women with endometriosis. Eur J Obstet Gynecol Reprod Biol. 2016;199:69-75.
227. Møller BR, Kristiansen FV, Thorsen P, Frost L, Mogensen SC. Sterility of the uterine cavity. Acta Obstetricia et Gynecologica Scandinavica. 1995;74(3):216-9.
228. Giudice LC. Challenging dogma: the endometrium has a microbiome with functional consequences! 2016. p. 682-3.
229. Franasiak JM, Scott RT. Reproductive tract microbiome in assisted reproductive technologies. Fertility and Sterility. 2015;104(6):1364-71.
230. Chen C, Song X, Wei W, Zhong H, Dai J, Lan Z, et al. The microbiota continuum along the female reproductive tract and its relation to uterine-related diseases. Nature Communications. 2017;8(1):875.
231. Mitchell CM, Haick A, Nkwopara E, Garcia R, Rendi M, Agnew K, et al. Colonization of the upper genital tract by vaginal bacterial species in nonpregnant women. American Journal of Obstetrics and Gynecology. 2015;212(5):611.e1-.e9.
232. Moreno I, Codoñer FM, Vilella F, Valbuena D, Martinez-Blanch JF, Jimenez-Almazán J, et al. Evidence that the endometrial microbiota has an effect on implantation success or failure. American Journal of Obstetrics and Gynecology. 2016;215(6):684-703.
233. Zervomanolakis I, Ott HW, Hadziomerovic D, Mattle V, Seeber BE, Virgolini I, et al. Physiology of upward transport in the human female genital tract. Ann N Y Acad Sci. 2007;1101:1-20.
234. Moreno I, Franasiak JM. Endometrial microbiota—new player in town. Fertility and Sterility. 2017;108(1):32-9.
235. Walther-Antonio MR, Chen J, Multinu F, Hokenstad A, Distad TJ, Cheek EH, et al. Potential contribution of the uterine microbiome in the development of endometrial cancer. Genome Med. 2016;8(1):122.
236. Moreno I, Codoñer FM, Vilella F, Valbuena D, Martinez-Blanch JF, Jimenez-Almazán J, et al. Evidence that the endometrial microbiota has an effect on implantation success or failure. Am J Obstet Gynecol. 2016;215(6):684-703.
237. Franasiak JM, Werner MD, Juneau CR, Tao X, Landis J, Zhan Y, et al. Endometrial microbiome at the time of embryo transfer: next-generation sequencing of the 16S ribosomal subunit. Journal of Assisted Reproduction and Genetics. 2016;33(1):129-36.
238. Kyono K, Hashimoto T, Kikuchi S, Nagai Y, Sakuraba Y. A pilot study and case reports on endometrial microbiota and pregnancy outcome: An analysis using 16S rRNA gene sequencing among IVF patients, and trial therapeutic intervention for dysbiotic endometrium. Reprod Med Biol. 2019;18(1):72-82.
239. Carosso A, Revelli A, Gennarelli G, Canosa S, Cosma S, Borella F, et al. Controlled ovarian stimulation and progesterone supplementation affect vaginal and endometrial microbiota in IVF cycles: a pilot study. J Assist Reprod Genet. 2020;37(9):2315-26.
240. Riganelli L, Iebba V, Piccioni M, Illuminati I, Bonfiglio G, Neroni B, et al. Structural Variations of Vaginal and Endometrial Microbiota: Hints on Female Infertility. Front Cell Infect Microbiol. 2020;10:350.

241. Chen W, Wei K, He X, Wei J, Yang L, Li L, et al. Identification of Uterine Microbiota in Infertile Women Receiving in vitro Fertilization With and Without Chronic Endometritis. Front Cell Dev Biol. 2021;9:693267.
242. Diaz-Martínez MdC, Bernabeu A, Lledó B, Carratalá-Munuera C, Quesada JA, Lozano FM, et al. Impact of the Vaginal and Endometrial Microbiome Pattern on Assisted Reproduction Outcomes. J Clin Med. 2021;10(18):4063.
243. Ichiyama T, Kuroda K, Nagai Y, Urushiyama D, Ohno M, Yamaguchi T, et al. Analysis of vaginal and endometrial microbiota communities in infertile women with a history of repeated implantation failure. Reprod Med Biol. 2021;20(3):334-44.
244. Moreno I, Garcia-Grau I, Perez-Villaroya D, Gonzalez-Monfort M, Bahçeci M, Barrionuevo MJ, et al. Endometrial microbiota composition is associated with reproductive outcome in infertile patients. Microbiome. 2022;10(1):1.
245. Swain N. MG, Samanta L., Intasqui P. . Proteomics and Male Infertility. In: Proteomics in Human Reproduction: Springer, Cham; 2016.
246. Ricci E, Al Beitawi S, Cipriani S, Candiani M, Chiaffarino F, Viganò P, et al. Semen quality and alcohol intake: a systematic review and meta-analysis. Reproductive BioMedicine Online. 2017;34(1):38-47.
247. Vine MF, Tse C-KJ, Hu P-C, Young Truong K. Cigarette smoking and semen quality. Fertility and Sterility. 1996;65(4):835-42.
248. World Health O. WHO laboratory manual for the examination and processing of human semen. 5th ed ed. Geneva: World Health Organization; 2010.
249. Oko R, Maravei D. Distribution and possible role of perinuclear theca proteins during bovine spermiogenesis. Microsc Res Tech. 1995;32(6):520-32.
250. Tulsiani DRP, Abou-Haila A, Loeser CR, Pereira BMJ. The Biological and Functional Significance of the Sperm Acrosome and Acrosomal Enzymes in Mammalian Fertilization. Experimental cell research. 1998;240(2):151-64.
251. Abou-Haila A, Tulsiani DR. Mammalian sperm acrosome: formation, contents, and function. Arch Biochem Biophys. 2000;379(2):173-82.
252. Malo AF, Gomendio M, Garde J, Lang-Lenton B, Soler AJ, Roldan ER. Sperm design and sperm function. Biology letters. 2006;2(2):246-9.
253. Turner RM. Tales From the Tail: What Do We Really Know About Sperm Motility? Journal of Andrology. 2003;24(6):790-803.
254. Owen DH, Katz DF. A review of the physical and chemical properties of human semen and the formulation of a semen simulant. J Androl. 2005;26(4):459-69.
255. Emami N, Scorilas A, Soosaipillai A, Earle T, Mullen B, Diamandis EP. Association between kallikrein-related peptidases (KLKs) and macroscopic indicators of semen analysis: their relation to sperm motility. Biol Chem. 2009;390(9):921-9.
256. Sobrero AJ, MacLeod J. The Immediate Postcoital Test. Fertility and Sterility. 1962;13(2):184-9.
257. Holmes E, Björndahl L, Kvist U. Post-ejaculatory increase in human semen osmolality in vitro. Andrologia. 2019;51(7):e13311.
258. Organization WH. WHO laboratory manual for the examination and processing of human semen 2021. Available from: https://www.who.int/publications/i/item/9789240030787.
259. Johanisson E, Campana A, Luthi R, de Agostini A. Evaluation of `round cells' in semen analysis: a comparative study. Human reproduction update. 2000;6(4):404-12.
260. Wallach EE, Wolff H. The biologic significance of white blood cells in semen. Fertility and Sterility. 1995;63(6):1143-57.
261. Wolff H, Anderson DJ. Immunohistologic characterization and quantitation of leukocyte subpopulations in human semen. Fertil Steril. 1988;49(3):497-504.
262. Wolff H, Politch JA, Martinez A, Haimovici F, Hill JA, Anderson DJ. Leukocytospermia is associated with poor semen quality. Fertil Steril. 1990;53(3):528-36.
263. Eggert-Kruse W, Bellmann A, Rohr G, Tilgen W, Runnebaum B. Differentiation of round cells in semen by means of monoclonal antibodies and relationship with male fertility. Fertil Steril. 1992;58(5):1046-55.

264. Gonzales GF, Kortebani G, Mazzolli AB. Leukocytospermia and function of the seminal vesicles on seminal quality. Fertil Steril. 1992;57(5):1058-65.
265. el-Demiry MI, Young H, Elton RA, Hargreave TB, James K, Chisholm GD. Leucocytes in the ejaculate from fertile and infertile men. Br J Urol. 1986;58(6):715-20.
266. Kung AW, Ho PC, Wang C. Seminal leucocyte subpopulations and sperm function in fertile and infertile Chinese men. Int J Androl. 1993;16(3):189-94.
267. Aitken RJ, West K, Buckingham D. Leukocytic infiltration into the human ejaculate and its association with semen quality, oxidative stress, and sperm function. J Androl. 1994;15(4):343-52.
268. Tomlinson MJ, Barratt CL, Cooke ID. Prospective study of leukocytes and leukocyte subpopulations in semen suggests they are not a cause of male infertility. Fertil Steril. 1993;60(6):1069-75.
269. Benchaib M, Lornage J, Mazoyer C, Lejeune H, Salle B, François Guerin J. Sperm deoxyribonucleic acid fragmentation as a prognostic indicator of assisted reproductive technology outcome. Fertility and Sterility. 2007;87(1):93-100.
270. Jayasena CN, Radia UK, Figueiredo M, Revill LF, Dimakopoulou A, Osagie M, et al. Reduced Testicular Steroidogenesis and Increased Semen Oxidative Stress in Male Partners as Novel Markers of Recurrent Miscarriage. Clin Chem. 2019;65(1):161-9.
271. Panner Selvam MK, Agarwal A. A systematic review on sperm DNA fragmentation in male factor infertility: Laboratory assessment. Arab J Urol. 2018;16(1):65-76.
272. Poccia D. Remodeling of Nucleoproteins during Gametogenesis, Fertilization, and Early Development. In: Bourne GH, Jeon KW, Friedlander M, editors. International Review of Cytology. 105: Academic Press; 1986. p. 1-65.
273. Henkel RR, Franken DR. Sperm DNA Fragmentation: Origin and Impact on Human Reproduction. Journal of Reproductive and Stem Cell Biotechnology. 2011;2(2):88-108.
274. Marcon L, Boissonneault G. Transient DNA Strand Breaks during Mouse and Human Spermiogenesis: New Insights in Stage Specificity and Link to Chromatin Remodeling. Biology of Reproduction. 2004;70(4):910-8.
275. Aoki VW, Liu L, Carrell DT. Identification and evaluation of a novel sperm protamine abnormality in a population of infertile males. Human Reproduction. 2005;20(5):1298-306.
276. Agarwal A, Majzoub A, Baskaran S, Panner Selvam MK, Cho CL, Henkel R, et al. Sperm DNA Fragmentation: A New Guideline for Clinicians. World J Mens Health. 2020;38(4):412-71.
277. Ribas-Maynou J, Benet J. Single and Double Strand Sperm DNA Damage: Different Reproductive Effects on Male Fertility. Genes (Basel). 2019;10(2).
278. Sakkas D, Alvarez JG. Sperm DNA fragmentation: mechanisms of origin, impact on reproductive outcome, and analysis. Fertility and Sterility. 2010;93(4):1027-36.
279. Mahfouz R, Sharma R, Thiyagarajan A, Kale V, Gupta S, Sabanegh E, et al. Semen characteristics and sperm DNA fragmentation in infertile men with low and high levels of seminal reactive oxygen species. Fertil Steril. 2010;94(6):2141-6.
280. Rivlin J, Mendel J, Rubinstein S, Etkovitz N, Breitbart H. Role of hydrogen peroxide in sperm capacitation and acrosome reaction. Biol Reprod. 2004;70(2):518-22.
281. Miki H, Funato Y. Regulation of intracellular signalling through cysteine oxidation by reactive oxygen species. The Journal of Biochemistry. 2012;151(3):255-61.
282. Agarwal A, Gupta S, Sikka S. The role of free radicals and antioxidants in reproduction. Curr Opin Obstet Gynecol. 2006;18(3):325-32.
283. Sharma RK, Pasqualotto FF, Nelson DR, Thomas AJ, Jr., Agarwal A. The reactive oxygen species-total antioxidant capacity score is a new measure of oxidative stress to predict male infertility. Hum Reprod. 1999;14(11):2801-7.
284. Sanocka D, Kurpisz M. Reactive oxygen species and sperm cells. Reprod Biol Endocrinol. 2004;2:12-.
285. Agarwal A, Makker K, Sharma R. Clinical relevance of oxidative stress in male factor infertility: an update. American journal of reproductive immunology (New York, NY : 1989). 2008;59(1):2-11.

286. Ashok Agarwal MC, Hussein Adelrazik, Rakesh K. Sharma. Oxidative stress measurement in patients with male or female factor infertility. Transworld Research Network. 2008:195-218.
287. Homa ST, Vessey W, Perez-Miranda A, Riyait T, Agarwal A. Reactive Oxygen Species (ROS) in human semen: determination of a reference range. J Assist Reprod Genet. 2015;32(5):757-64.
288. Wang A, Fanning L, Anderson DJ, Loughlin KR. Generation of reactive oxygen species by leukocytes and sperm following exposure to urogenital tract infection. Archives of andrology. 1997;39(1):11-7.
289. Plante M, de Lamirande E, Gagnon C. Reactive oxygen species released by activated neutrophils, but not by deficient spermatozoa, are sufficient to affect normal sperm motility. Fertil Steril. 1994;62(2):387-93.
290. Ochsendorf FR. Infection and reactive oxygen species. Andrologia. 1998;30(S1):81-6.
291. Shi TY, Chen G, Huang X, Yuan Y, Wu X, Wu B, et al. Effects of reactive oxygen species from activated leucocytes on human sperm motility, viability and morphology. Andrologia. 2012;44 Suppl 1:696-703.
292. Morielli T, O'Flaherty C. Oxidative stress impairs function and increases redox protein modifications in human spermatozoa. Reproduction. 2015;149(1):113-23.
293. Ichikawa T, Oeda T, Ohmori H, Schill WB. Reactive oxygen species influence the acrosome reaction but not acrosin activity in human spermatozoa. Int J Androl. 1999;22(1):37-42.
294. Aitken RJ, Gordon E, Harkiss D, Twigg JP, Milne P, Jennings Z, et al. Relative impact of oxidative stress on the functional competence and genomic integrity of human spermatozoa. Biol Reprod. 1998;59(5):1037-46.
295. Kobatake E, Nakagawa H, Seki T, Miyazaki T. Protective effects and functional mechanisms of Lactobacillus gasseri SBT2055 against oxidative stress. PloS one. 2017;12(5):e0177106.
296. Landis GN, Tower J. Superoxide dismutase evolution and life span regulation. Mech Ageing Dev. 2005;126(3):365-79.
297. Altmäe S, Franasiak JM, Mändar R. The seminal microbiome in health and disease. Nature Reviews Urology. 2019;16(12):703-21.
298. Du Plessis SS, Gokul S, Agarwal A. Semen hyperviscosity: causes, consequences, and cures. Front Biosci (Elite Ed). 2013;5:224-31.
299. Molina NM, Plaza-Díaz J, Vilchez-Vargas R, Sola-Leyva A, Vargas E, Mendoza-Tesarik R, et al. Assessing the testicular sperm microbiome: a low-biomass site with abundant contamination. Reproductive BioMedicine Online. 2021;43(3):523-31.
300. Zozaya M, Ferris MJ, Siren JD, Lillis R, Myers L, Nsuami MJ, et al. Bacterial communities in penile skin, male urethra, and vaginas of heterosexual couples with and without bacterial vaginosis. Microbiome. 2016;4:16.
301. Mändar R, Punab M, Borovkova N, Lapp E, Kiiker R, Korrovits P, et al. Complementary seminovaginal microbiome in couples. Research in Microbiology. 2015;166(5):440-7.
302. Ma Z. Microbiome Transmission During Sexual Intercourse Appears Stochastic and Supports the Red Queen Hypothesis. Frontiers in Microbiology. 2022;12.
303. Monga M, Roberts JA. Spermagglutination by bacteria: receptor-specific interactions. J Androl. 1994;15(2):151-6.
304. Fraczek M, Hryhorowicz M, Gill K, Zarzycka M, Gaczarzewicz D, Jedrzejczak P, et al. The effect of bacteriospermia and leukocytospermia on conventional and nonconventional semen parameters in healthy young normozoospermic males. J Reprod Immunol. 2016;118:18-27.
305. Villegas J, Schulz M, Soto L, Sanchez R. Bacteria induce expression of apoptosis in human spermatozoa. Apoptosis. 2005;10(1):105-10.
306. Schuppe HC, Meinhardt A, Allam J, Bergmann M, Weidner W, Haidl G. Chronic orchitis: a neglected cause of male infertility? Andrologia. 2008;40(2):84-91.

307. Wang S, Zhang K, Yao Y, Li J, Deng S. Bacterial Infections Affect Male Fertility: A Focus on the Oxidative Stress-Autophagy Axis. Frontiers in Cell and Developmental Biology. 2021;9.
308. Wang H, Xu A, Gong L, Chen Z, Zhang B, Li X. The Microbiome, an Important Factor That Is Easily Overlooked in Male Infertility. Frontiers in Microbiology. 2022;13.
309. Wolff H, Panhans A, Stolz W, Meurer M. Adherence of Escherichia coli to sperm: a mannose mediated phenomenon leading to agglutination of sperm and E. coli. Fertil Steril. 1993;60(1):154-8.
310. Barbonetti A, Vassallo MR, Cinque B, Filipponi S, Mastromarino P, Cifone MG, et al. Soluble products of Escherichia coli induce mitochondrial dysfunction-related sperm membrane lipid peroxidation which is prevented by lactobacilli. PloS one. 2013;8(12):e83136.
311. Lang T, Dechant M, Sanchez V, Wistuba J, Boiani M, Pilatz A, et al. Structural and functional integrity of spermatozoa is compromised as a consequence of acute uropathogenic E. coli-associated epididymitis. Biology of reproduction. 2013;89(3):59, 1-10.
312. Bryan ER, Kollipara A, Trim LK, Armitage CW, Carey AJ, Mihalas B, et al. Hematogenous dissemination of Chlamydia muridarum from the urethra in macrophages causes testicular infection and sperm DNA damage†. Biology of Reproduction. 2019;101(4):748-59.
313. Satta A, Stivala A, Garozzo A, Morello A, Perdichizzi A, Vicari E, et al. Experimental Chlamydia trachomatis infection causes apoptosis in human sperm. Human Reproduction. 2006;21(1):134-7.
314. Khoder M, Osman M, Diene SM, Okdah L, Lalaoui R, Al Achkar M, et al. Evaluation of different testing tools for the identification of non-gonococcal Neisseria spp. isolated from Lebanese male semen: a strong and significant association with infertility. Journal of Medical Microbiology. 2019;68(7):1012-20.
315. Duru NK, Morshedi M, Oehninger S. Effects of hydrogen peroxide on DNA and plasma membrane integrity of human spermatozoa. Fertility and sterility. 2000;74(6):1200-7.
316. Singer M, Ouburg S. Effect of cytokine level variations in individuals on the progression and outcome of bacterial urogenital infections—a meta-analysis. FEMS Pathogens and Disease. 2016;74(2):ftv126.
317. Pellati D, Mylonakis I, Bertoloni G, Fiore C, Andrisani A, Ambrosini G, et al. Genital tract infections and infertility. European Journal of Obstetrics & Gynecology and Reproductive Biology. 2008;140(1):3-11.
318. Nunez-Calonge R, Caballero P, Redondo C, Baquero F, Martinez-Ferrer M, Meseguer M. Ureaplasma urealyticum reduces motility and induces membrane alterations in human spermatozoa. Human reproduction (Oxford, England). 1998;13(10):2756-61.
319. Farsimadan M, Motamedifar M. Bacterial infection of the male reproductive system causing infertility. Journal of Reproductive Immunology. 2020;142:103183.
320. Vilvanathan S, Kandasamy B, Jayachandran AL, Sathiyanarayanan S, Tanjore Singaravelu V, Krishnamurthy V, et al. Bacteriospermia and Its Impact on Basic Semen Parameters among Infertile Men. Interdiscip Perspect Infect Dis. 2016;2016:2614692.
321. Zeyad A, Hamad M, Amor H, Hammadeh ME. Relationships between bacteriospermia, DNA integrity, nuclear protamine alteration, sperm quality and ICSI outcome. Reprod Biol. 2018;18(1):115-21.
322. Zeyad A, Hamad MF, Hammadeh ME. The effects of bacterial infection on human sperm nuclear protamine P1/P2 ratio and DNA integrity. Andrologia. 2018;50(2).
323. Mashaly M, Masallat DT, Elkholy AA, Abdel-Hamid IA, Mostafa T. Seminal Corynebacterium strains in infertile men with and without leucocytospermia. Andrologia. 2016;48(3):355-9.
324. Ruggeri M, Cannas S, Cubeddu M, Molicotti P, Piras GL, Dessole S, et al. Bacterial agents as a cause of infertility in humans. New Microbiol. 2016;39(3):206-9.
325. Bussen S, Zimmermann M, Schleyer M, Steck T. Relationship of bacteriological characteristics to semen indices and its influence on fertilization and pregnancy rates after IVF. Acta Obstet Gynecol Scand. 1997;76(10):964-8.

326. Nasrallah YS, Anani M, Omar HH, Hashem AA. Microbiological profiles of semen culture in male infertility. Human Andrology. 2018;8(2):34-42.
327. Virecoulon F, Wallet F, Fruchart-Flamenbaum A, Rigot JM, Peers MC, Mitchell V, et al. Bacterial flora of the low male genital tract in patients consulting for infertility. Andrologia. 2005;37(5):160-5.
328. Gdoura R, Kchaou W, Znazen A, Chakroun N, Fourati M, Ammar-Keskes L, et al. Screening for bacterial pathogens in semen samples from infertile men with and without leukocytospermia. Andrologia. 2008;40(4):209-18.
329. Moretti E, Capitani S, Figura N, Pammolli A, Federico MG, Giannerini V, et al. The presence of bacteria species in semen and sperm quality. J Assist Reprod Genet. 2009;26(1):47-56.
330. Isaiah IN, Nche BT, Nwagu IG, Nnanna, II. Current studies on bacterospermia the leading cause of male infertility: a protégé and potential threat towards mans extinction. N Am J Med Sci. 2011;3(12):562-4.
331. Domes T, Lo KC, Grober ED, Mullen JB, Mazzulli T, Jarvi K. The incidence and effect of bacteriospermia and elevated seminal leukocytes on semen parameters. Fertil Steril. 2012;97(5):1050-5.
332. Ricci S, De Giorgi S, Lazzeri E, Luddi A, Rossi S, Piomboni P, et al. Impact of asymptomatic genital tract infections on in vitro Fertilization (IVF) outcome. PloS one. 2018;13(11):e0207684.
333. Sellami H, Znazen A, Sellami A, Mnif H, Louati N, Ben Zarrouk S, et al. Molecular detection of Chlamydia trachomatis and other sexually transmitted bacteria in semen of male partners of infertile couples in Tunisia: the effect on semen parameters and spermatozoa apoptosis markers. PloS one. 2014;9(7):e98903.
334. Kjærgaard N, Kristensen B, Hansen ES, Farholt S, Schønheyder HC, Uldbjerg N, et al. Microbiology of semen specimens from males attending a fertility clinic. APMIS. 1997;105.
335. Shalika S, Dugan K, Smith RD, Padilla SL. The effect of positive semen bacterial and Ureaplasma cultures on in-vitro fertilization success. Human reproduction (Oxford, England). 1996;11(12):2789-92.
336. Aghazarian A, Stancik I, Pflüger H, Lackner J. Influence of pathogens and moderate leukocytes on seminal interleukin (IL)-6, IL-8, and sperm parameters. Int Urol Nephrol. 2013;45(2):359-65.
337. Barghouthi SA. A universal method for the identification of bacteria based on general PCR primers. Indian J Microbiol. 2011;51(4):430-44.
338. López-Hurtado M, Velazco-Fernández M, Pedraza-Sánchez MJE, Flores-Salazar VR, Villagrana Zesati R, Guerra-Infante FM. Molecular detection of Chlamydia trachomatis and semen quality of sexual partners of infertile women. Andrologia. 2018;50(1).
339. Gdoura R, Keskes-Ammar L, Bouzid F, Eb F, Hammami A, Orfila J. Chlamydia trachomatis and male infertility in Tunisia. Eur J Contracept Reprod Health Care. 2001;6(2):102-7.
340. Hosseinzadeh S, Eley A, Pacey AA. Semen quality of men with asymptomatic chlamydial infection. J Androl. 2004;25(1):104-9.
341. Bezold G, Politch JA, Kiviat NB, Kuypers JM, Wolff H, Anderson DJ. Prevalence of sexually transmissible pathogens in semen from asymptomatic male infertility patients with and without leukocytospermia. Fertil Steril. 2007;87(5):1087-97.
342. Rybar R, Prinosilova P, Kopecka V, Hlavicova J, Veznik Z, Zajicova A, et al. The effect of bacterial contamination of semen on sperm chromatin integrity and standard semen parameters in men from infertile couples. Andrologia. 2012;44 Suppl 1:410-8.
343. Zeighami H, Peerayeh SN, Yazdi RS, Sorouri R. Prevalence of Ureaplasma urealyticum and Ureaplasma parvum in semen of infertile and healthy men. Int J STD AIDS. 2009;20(6):387-90.
344. Peerayeh SN, Yazdi RS, Zeighami H. Association of Ureaplasma urealyticum infection with varicocele-related infertility. J Infect Dev Ctries. 2008;2(2):116-9.

345. Mohseni Moghadam N, Kheirkhah B, Mirshekari TR, Fasihi Harandi M, Tafsiri E. Isolation and molecular identification of mycoplasma genitalium from the secretion of genital tract in infertile male and female. Iran J Reprod Med. 2014;12(9):601-8.
346. Hou D, Zhou X, Zhong X, Settles ML, Herring J, Wang L, et al. Microbiota of the seminal fluid from healthy and infertile men. Fertility and sterility. 2013;100(5):1261-9.
347. Weng S-L, Chiu C-M, Lin F-M, Huang W-C, Liang C, Yang T, et al. Bacterial Communities in Semen from Men of Infertile Couples: Metagenomic Sequencing Reveals Relationships of Seminal Microbiota to Semen Quality. PloS one. 2014;9(10):e110152.
348. Monteiro C, Marques PI, Cavadas B, Damião I, Almeida V, Barros N, et al. Characterization of microbiota in male infertility cases uncovers differences in seminal hyperviscosity and oligoasthenoteratozoospermia possibly correlated with increased prevalence of infectious bacteria. American journal of reproductive immunology (New York, NY : 1989). 2018;79(6):e12838.
349. Baud D, Pattaroni C, Vulliemoz N, Castella V, Marsland BJ, Stojanov M. Sperm Microbiota and Its Impact on Semen Parameters. Frontiers in Microbiology. 2019;10(234).
350. Yang H, Zhang J, Xue Z, Zhao C, Lei L, Wen Y, et al. Potential Pathogenic Bacteria in Seminal Microbiota of Patients with Different Types of Dysspermatism. Scientific reports. 2020;10(1):6876.
351. Okwelogu SI, Ikechebelu JI, Agbakoba NR, Anukam KC. Microbiome Compositions From Infertile Couples Seeking In Vitro Fertilization, Using 16S rRNA Gene Sequencing Methods: Any Correlation to Clinical Outcomes? Frontiers in Cellular and Infection Microbiology. 2021;11.
352. Yao Y, Qiu XJ, Wang DS, Luo JK, Tang T, Li YH, et al. Semen microbiota in normal and leukocytospermic males. Asian J Androl. 2022;24(4):398-405.
353. Sansonetti PJ. To be or not to be a pathogen: that is the mucosally relevant question. Mucosal Immunol. 2011;4(1):8-14.
354. Al-Nasiry S, Ambrosino E, Schlaepfer M, Morré SA, Wieten L, Voncken JW, et al. The Interplay Between Reproductive Tract Microbiota and Immunological System in Human Reproduction. Frontiers in Immunology. 2020;11(378).
355. Smith SB, Ravel J. The vaginal microbiota, host defence and reproductive physiology. The Journal of physiology. 2017;595(2):451-63.
356. Witkin SS, Linhares IM. Why do lactobacilli dominate the human vaginal microbiota? Bjog. 2017;124(4):606-11.
357. Hill GB. The microbiology of bacterial vaginosis. Am J Obstet Gynecol. 1993;169(2 Pt 2):450-4.
358. Eisen G, Sturm-Ramirez K, Kanki PJ, Gaye-Diallo A, Mboup S. High Levels of Tumor Necrosis Factor—α and Interleukin-1β in Bacterial Vaginosis May Increase Susceptibility to Human Immunodeficiency Virus. The Journal of Infectious Diseases. 2000;182(2):467-73.
359. Mattsby-Baltzer I, Platz-Christensen JJ, Hosseini N, Rosen P. IL-1beta, IL-6, TNFalpha, fetal fibronectin, and endotoxin in the lower genital tract of pregnant women with bacterial vaginosis. Acta Obstet Gynecol Scand. 1998;77(7):701-6.
360. Platz-Christensen JJ, Mattsby-Baltzer I, Thomsen P, Wiqvist N. Endotoxin and interleukin-1 alpha in the cervical mucus and vaginal fluid of pregnant women with bacterial vaginosis. Am J Obstet Gynecol. 1993;169(5):1161-6.
361. Wennerholm UB, Holm B, Mattsby-Baltzer I, Nielsen T, Platz-Christensen JJ, Sundell G, et al. Interleukin-1alpha, interleukin-6 and interleukin-8 in cervico/vaginal secretion for screening of preterm birth in twin gestation. Acta Obstet Gynecol Scand. 1998;77(5):508-14.
362. Lee SK, Kim CJ, Kim D-J, Kang J-H. Immune cells in the female reproductive tract. Immune Netw. 2015;15(1):16-26.
363. Paria B, Reese J, Das S, Dey S. Deciphering the cross-talk of implantation: Advances and challenges. Science (Washington). 2002;296(5576):2185-8.
364. Croy BA, van den Heuvel MJ, Borzychowski AM, Tayade C. Uterine natural killer cells: a specialized differentiation regulated by ovarian hormones. Immunological reviews. 2006;214:161-85.

365. Hanna J, Goldman-Wohl D, Hamani Y, Avraham I, Greenfield C, Natanson-Yaron S, et al. Decidual NK cells regulate key developmental processes at the human fetal-maternal interface. Nat Med. 2006;12(9):1065-74.
366. Das SK, Wang XN, Paria BC, Damm D, Abraham JA, Klagsbrun M, et al. Heparin-binding EGF-like growth factor gene is induced in the mouse uterus temporally by the blastocyst solely at the site of its apposition: a possible ligand for interaction with blastocyst EGF-receptor in implantation. Development (Cambridge, England). 1994;120(5):1071-83.
367. Castro-Rendon WA, Castro-Alvarez JF, Guzman-Martinez C, Bueno-Sanchez JC. Blastocyst-endometrium interaction: intertwining a cytokine network. Brazilian journal of medical and biological research = Revista brasileira de pesquisas medicas e biologicas. 2006;39(11):1373-85.
368. Okada S, Okada H, Sanezumi M, Nakajima T, Yasuda K, Kanzaki H. Expression of interleukin-15 in human endometrium and decidua. Mol Hum Reprod. 2000;6(1):75-80.
369. Dimitriadis E, Salamonsen LA, Robb L. Expression of interleukin-11 during the human menstrual cycle: coincidence with stromal cell decidualization and relationship to leukaemia inhibitory factor and prolactin. Mol Hum Reprod. 2000;6(10):907-14.
370. van Mourik MS, Macklon NS, Heijnen CJ. Embryonic implantation: cytokines, adhesion molecules, and immune cells in establishing an implantation environment. Journal of leukocyte biology. 2009;85(1):4-19.
371. Dunn CL, Kelly RW, Critchley HOD. Decidualization of the human endometrial stromal cell: an enigmatic transformation. Reproductive BioMedicine Online. 2003;7(2):151-61.
372. Kammerer U, von Wolff M, Markert UR. Immunology of human endometrium. Immunobiology. 2004;209(7):569-74.
373. Simon C, Martin JC, Pellicer A. Paracrine regulators of implantation. Bailliere's best practice & research Clinical obstetrics & gynaecology. 2000;14(5):815-26.
374. Wierman ME. Sex steroid effects at target tissues: mechanisms of action. Advances in physiology education. 2007;31(1):26-33.
375. Park H-J, Choi J-M. Sex-specific regulation of immune responses by PPARs. Experimental & molecular medicine. 2017;49(8):e364-e.
376. Marriott I, Bost KL, Huet-Hudson YM. Sexual dimorphism in expression of receptors for bacterial lipopolysaccharides in murine macrophages: a possible mechanism for gender-based differences in endotoxic shock susceptibility. Journal of reproductive immunology. 2006;71(1):12-27.
377. Taneja V. Sex Hormones Determine Immune Response. Frontiers in immunology. 2018;9:1931.
378. Givan AL, White HD, Stern JE, Colby E, Gosselin EJ, Guyre PM, et al. Flow cytometric analysis of leukocytes in the human female reproductive tract: comparison of fallopian tube, uterus, cervix, and vagina. American journal of reproductive immunology (New York, NY : 1989). 1997;38(5):350-9.
379. Smith JM, Wira CR, Fanger MW, Shen L. Human fallopian tube neutrophils–a distinct phenotype from blood neutrophils. American Journal of Reproductive Immunology. 2006;56(4):218-29.
380. Mselle TF, Meadows SK, Eriksson M, Smith JM, Shen L, Wira CR, et al. Unique characteristics of NK cells throughout the human female reproductive tract. Clinical immunology. 2007;124(1):69-76.
381. Kutteh WH, Prince SJ, Hammond KR, Kutteh CC, Mestecky J. Variations in immunoglobulins and IgA subclasses of human uterine cervical secretions around the time of ovulation. Clin Exp Immunol. 1996;104(3):538-42.
382. Kutteh WH, Moldoveanu Z, Mestecky J. Mucosal immunity in the female reproductive tract: correlation of immunoglobulins, cytokines, and reproductive hormones in human cervical mucus around the time of ovulation. AIDS Res Hum Retroviruses. 1998;14 Suppl 1:S51-5.
383. Huggins RG, Preti RG. VAGINAL ODORS AND SECRETIONS. Clinical Obstetrics and Gynecology. 1981;24(2):355-77.

384. Hafez ESE, Kenemans P. The vagina (normal). In: Hafez ESE, Kenemans P, editors. Atlas of Human Reproduction: By Scanning Electron Microscopy. Dordrecht: Springer Netherlands; 1982. p. 15-27.
385. Shaw JLV, Smith CR, Diamandis EP. Proteomic analysis of human cervico-vaginal fluid. Journal of proteome research. 2007;6(7):2859.
386. Enders AC, Schlafke S. A morphological analysis of the early implantation stages in the rat. American Journal of Anatomy. 1967;120(2):185-225.
387. Lopata A, Hay DL. The potential of early human embryos to form blastocysts, hatch from their zona and secrete HCG in culture. Human reproduction (Oxford, England). 1989;4(8 Suppl):87-94.
388. Ichikawa S, Shibata T, Takehara Y, Tamada H, Oda K, Murao S. Effects of proteinase inhibitors on preimplantation embryos in the rat. Journal of reproduction and fertility. 1985;73(2):385-90.
389. Gonzales DS, Jones JM, Pinyopummintr T, Carnevale EM, Ginther OJ, Shapiro SS, et al. Trophectoderm projections: a potential means for locomotion, attachment and implantation of bovine, equine and human blastocysts. Human reproduction (Oxford, England). 1996;11(12):2739-45.
390. Kirkegaard K, Hindkjaer JJ, Ingerslev HJ. Hatching of in vitro fertilized human embryos is influenced by fertilization method. Fertil Steril. 2013;100(5):1277-82.
391. Sathananthan H, Menezes J, Gunasheela S. Mechanics of human blastocyst hatching in vitro. Reprod Biomed Online. 2003;7(2):228-34.
392. Kim S-M, Kim J-S. A Review of Mechanisms of Implantation. Dev Reprod. 2017;21(4):351-9.
393. Jacobsen BM, Horwitz KB. Progesterone receptors, their isoforms and progesterone regulated transcription. Mol Cell Endocrinol. 2012;357(1-2):18-29.
394. Paterni I, Granchi C, Katzenellenbogen JA, Minutolo F. Estrogen receptors alpha (ERα) and beta (ERβ): subtype-selective ligands and clinical potential. Steroids. 2014;90:13-29.
395. Kelleher AM, Milano-Foster J, Behura SK, Spencer TE. Uterine glands coordinate on-time embryo implantation and impact endometrial decidualization for pregnancy success. Nature communications. 2018;9(1):2435.
396. Wetendorf M, DeMayo FJ. The progesterone receptor regulates implantation, decidualization, and glandular development via a complex paracrine signaling network. Mol Cell Endocrinol. 2012;357(1-2):108-18.
397. Wetendorf M, Wu S-P, Wang X, Creighton CJ, Wang T, Lanz RB, et al. Decreased epithelial progesterone receptor A at the window of receptivity is required for preparation of the endometrium for embryo attachment. Biology of reproduction. 2017;96(2):313-26.
398. Conneely O, Kettelberger D, Tsai M, Schrader W, O'Malley B. The chicken progesterone receptor A and B isoforms are products of an alternate translation initiation event. Journal of Biological Chemistry. 1989;264(24):14062-4.
399. Sartorius CA, Melville MY, Hovland AR, Tung L, Takimoto GS, Horwitz KB. A third transactivation function (AF3) of human progesterone receptors located in the unique N-terminal segment of the B-isoform. Molecular endocrinology. 1994;8(10):1347-60.
400. Labied S, Kajihara T, Madureira PA, Fusi L, Jones MC, Higham JM, et al. Progestins regulate the expression and activity of the forkhead transcription factor FOXO1 in differentiating human endometrium. Molecular endocrinology. 2006;20(1):35-44.
401. Li R, Wang X, Huang Z, Balaji J, Kim TH, Wang T, et al. The role of epithelial progesterone receptor isoforms in embryo implantation. iScience. 2021;24(12):103487.
402. Saini V, Arora S, Yadav A, Bhattacharjee J. Cytokines in recurrent pregnancy loss. Clinica Chimica Acta. 2011;412(9):702-8.
403. Medawar P. Some immunological and endocrinological problems raised by the evolution of viviparity in vertebrates. Symp Soc Exp Biol. 1952;7:320–38.
404. Wood GW, Hausmann E, Choudhuri R. Relative role of CSF-1, MCP-1/JE, and RANTES in macrophage recruitment during successful pregnancy. Mol Reprod Dev. 1997;46(1):62-9; discussion 9-70.

405. Bulmer JN, Pace D, Ritson A. Immunoregulatory cells in human decidua: morphology, immunohistochemistry and function. Reprod Nutr Dev. 1988;28(6b):1599-613.
406. Mor G, Romero R, Aldo PB, Abrahams VM. Is the trophoblast an immune regulator? The role of Toll-like receptors during pregnancy. Crit Rev Immunol. 2005;25(5):375-88.
407. Seshagiri PB, Vani V, Madhulika P. Cytokines and Blastocyst Hatching. American journal of reproductive immunology (New York, NY : 1989). 2016;75(3):208-17.
408. Arici A, Engin O, Attar E, Olive DL. Modulation of leukemia inhibitory factor gene expression and protein biosynthesis in human endometrium. The Journal of clinical endocrinology and metabolism. 1995;80(6):1908-15.
409. Garcia-Lloret MI, Morrish DW, Wegmann TG, Honore L, Turner AR, Guilbert LJ. Demonstration of functional cytokine-placental interactions: CSF-1 and GM-CSF stimulate human cytotrophoblast differentiation and peptide hormone secretion. Experimental cell research. 1994;214(1):46-54.
410. Huang JC, Liu DY, Yadollahi S, Wu KK, Dawood MY. Interleukin-1 beta induces cyclooxygenase-2 gene expression in cultured endometrial stromal cells. The Journal of clinical endocrinology and metabolism. 1998;83(2):538-41.
411. Simon C, Frances A, Piquette GN, el Danasouri I, Zurawski G, Dang W, et al. Embryonic implantation in mice is blocked by interleukin-1 receptor antagonist. Endocrinology. 1994;134(2):521-8.
412. Leach RE, Jessmon P, Coutifaris C, Kruger M, Myers ER, Ali-Fehmi R, et al. High throughput, cell type-specific analysis of key proteins in human endometrial biopsies of women from fertile and infertile couples. Human reproduction (Oxford, England). 2012;27(3):814-28.
413. Damario MA, Liu H-C, Mele CA, Horenstein MG, Rosenwaks Z. Immunohistochemical Analysis of Insulin-like Growth Factor–Binding Proteins -1, -2, and -3 in Implantation Sites of the Mouse. Journal of Assisted Reproduction and Genetics. 1998;15(8):513-20.
414. Robertson S, Seamark R. Granulocyte macrophage colony stimulating factor (GM-CSF) in the murine reproductive tract: stimulation by seminal factors. Reproduction, Fertility and Development. 1990;2(4):359-68.
415. Jabbour HN, Boddy SC. Prostaglandin E2 induces proliferation of glandular epithelial cells of the human endometrium via extracellular regulated kinase 1/2-mediated pathway. The Journal of clinical endocrinology and metabolism. 2003;88(9):4481-7.
416. von Wolff M, Classen-Linke I, Heid D, Krusche CA, Beier-Hellwig K, Karl C, et al. Tumour necrosis factor-alpha (TNF-alpha) in human endometrium and uterine secretion: an evaluation by immunohistochemistry, ELISA and semiquantitative RT-PCR. Mol Hum Reprod. 1999;5(2):146-52.
417. Cavagna M, Mantese JC. Biomarkers of endometrial receptivity--a review. Placenta. 2003;24 Suppl B:S39-47.
418. Colin LS, Petr K, Lisa JB, Harshida B, Inder G, Frank K, et al. Blastocyst implantation depends on maternal expression of leukaemia inhibitory factor. Nature. 1992;359(6390):76.
419. Chen JR, Cheng JG, Shatzer T, Sewell L, Hernandez L, Stewart CL. Leukemia inhibitory factor can substitute for nidatory estrogen and is essential to inducing a receptive uterus for implantation but is not essential for subsequent embryogenesis. Endocrinology. 2000;141(12):4365.
420. Nichols J, Davidson D, Taga T, Yoshida K, Chambers I, Smith A. Complementary tissue-specific expression of LIF and LIF-receptor mRNAs in early mouse embryogenesis. Mechanisms of Development. 1996;57(2):123-31.
421. Schafer-Somi S. Cytokines during early pregnancy of mammals: a review. Animal reproduction science. 2003;75(1-2):73-94.
422. Wegmann TG, Lin H, Guilbert L, Mosmann TR. Bidirectional cytokine interactions in the maternal-fetal relationship: is successful pregnancy a TH2 phenomenon? Immunology today. 1993;14(7):353-6.
423. Dealtry GB, O'Farrell MK, Fernandez N. The Th2 cytokine environment of the placenta. International archives of allergy and immunology. 2000;123(2):107-19.
424. Raghupathy R. Th1-type immunity is incompatible with successful pregnancy. Immunology today. 1997;18(10):478-82.

425. Bates MD, Quenby S, Takakuwa K, Johnson PM, Vince GS. Aberrant cytokine production by peripheral blood mononuclear cells in recurrent pregnancy loss? Human reproduction (Oxford, England). 2002;17(9):2439-44.
426. Chaouat G, Ledee-Bataille N, Zourbas S, Ostojic S, Dubanchet S, Martal J, et al. Cytokines, implantation and early abortion: re-examining the Th1/Th2 paradigm leads to question the single pathway, single therapy concept. American journal of reproductive immunology (New York, NY : 1989). 2003;50(3):177-86.
427. Strom TB, Roy-Chaudhury P, Manfro R, Xheng XX, Nickerson PW, Wood K, et al. The Th1/Th2 paradigm and the allograft response. Current Opinion in Immunology. 1996;8(5):688-93.
428. Agarwal R, Loganath A, Roy AC, Wong YC, Ng SC. Effect of T-helper 1 cytokines on secretion of T-helper 2 cytokines by term trophoblast cells in culture. Gynecological Endocrinology. 2000;14(5):305-10.
429. Ohbayashi N, Ikeda O, Taira N, Yamamoto Y, Muromoto R, Sekine Y, et al. LIF- and IL-6-Induced Acetylation of STAT3 at Lys-685 through PI3K/Akt Activation. Biological and Pharmaceutical Bulletin. 2007;30(10):1860-4.
430. Chatterjee P, Chiasson VL, Bounds KR, Mitchell BM. Regulation of the Anti-Inflammatory Cytokines Interleukin-4 and Interleukin-10 during Pregnancy. Frontiers in immunology. 2014;5:253.
431. Min B, Prout M, Hu-Li J, Zhu J, Jankovic D, Morgan ES, et al. Basophils Produce IL-4 and Accumulate in Tissues after Infection with a Th2-inducing Parasite. The Journal of Experimental Medicine. 2004;200(4):507-17.
432. Stanciu LA, Roberts K, Papadopoulos NG, Cho SH, Holgate ST, Coyle AJ, et al. IL-4 increases type 2, but not type 1, cytokine production in CD8+ T cells from mild atopic asthmatics. BioMed Central; 2016.
433. McKay LI, Cidlowski JA. Molecular Control of Immune/Inflammatory Responses: Interactions Between Nuclear Factor-κB and Steroid Receptor-Signaling Pathways. Endocr Rev. 1999;20(4):435-59.
434. Sen R, Baltimore D. Multiple nuclear factors interact with the immunoglobulin enhancer sequences. Cell. 1986;46(5):705-16.
435. Tak PP, Firestein GS. NF-kappaB: a key role in inflammatory diseases. The Journal of clinical investigation. 2001;107(1):7-11.
436. Lawrence T. The nuclear factor NF-kappaB pathway in inflammation. Cold Spring Harb Perspect Biol. 2009;1(6):a001651.
437. Oeckinghaus A, Ghosh S. The NF-kappaB family of transcription factors and its regulation. Cold Spring Harb Perspect Biol. 2009;1(4):a000034.
438. Caldenhoven E, Liden J, Wissink S, Van de Stolpe A, Raaijmakers J, Koenderman L, et al. Negative cross-talk between RelA and the glucocorticoid receptor: a possible mechanism for the antiinflammatory action of glucocorticoids. Mol Endocrinol. 1995;9(4):401-12.
439. Gilmore TD. NF-κB, KBF1, dorsal, and related matters. Cell. 1990;62(5):841-3.
440. Gilmore TD. Introduction to NF-κB: players, pathways, perspectives. Oncogene. 2006;25(51):6680-4.
441. Sun S-C, Chang J-H, Jin J. Regulation of nuclear factor-κB in autoimmunity. Trends Immunol. 2013;34(6):282-9.
442. Liu T, Zhang L, Joo D, Sun S-C. NF-κB signaling in inflammation. Signal Transduction and Targeted Therapy. 2017;2(1):17023.
443. Zhang H, Sun S-C. NF-κB in inflammation and renal diseases. Cell Biosci. 2015;5:63-.
444. Sun SC. The noncanonical NF-κB pathway. Immunological reviews. 2012;246(1):125-40.
445. Sun SC, Liu ZG. A special issue on NF-κB signaling and function. Cell Res. 2011;21(1):1-2.
446. Ade N, Antonios D, Kerdine-Romer S, Boisleve F, Rousset F, Pallardy M. NF-kappaB plays a major role in the maturation of human dendritic cells induced by NiSO(4) but not by DNCB. Toxicol Sci. 2007;99(2):488-501.

447. Wang N, Liang H, Zen K. Molecular mechanisms that influence the macrophage m1-m2 polarization balance. Frontiers in immunology. 2014;5:614.
448. Mussbacher M, Salzmann M, Brostjan C, Hoesel B, Schoergenhofer C, Datler H, et al. Cell Type-Specific Roles of NF-κB Linking Inflammation and Thrombosis. Frontiers in immunology. 2019;10:85-.
449. Micheau O, Lens S, Gaide O, Alevizopoulos K, Tschopp J. NF-kappaB signals induce the expression of c-FLIP. Mol Cell Biol. 2001;21(16):5299-305.
450. Urbanik T, Koehler BC, Wolpert L, Elßner C, Scherr A-L, Longerich T, et al. CYLD deletion triggers nuclear factor-κB-signaling and increases cell death resistance in murine hepatocytes. World J Gastroenterol. 2014;20(45):17049-64.
451. Joyce D, Albanese C, Steer J, Fu M, Bouzahzah B, Pestell RG. NF-kappaB and cell-cycle regulation: the cyclin connection. Cytokine Growth Factor Rev. 2001;12(1):73-90.
452. Park JM, Greten FR, Wong A, Westrick RJ, Arthur JSC, Otsu K, et al. Signaling Pathways and Genes that Inhibit Pathogen-Induced Macrophage Apoptosis— CREB and NF-κB as Key Regulators. Immunity. 2005;23(3):319-29.
453. Perrot-Applanat M, Vacher S, Toullec A, Pelaez I, Velasco G, Cormier F, et al. Similar NF-κB gene signatures in TNF-α treated human endothelial cells and breast tumor biopsies. PloS one. 2011;6(7):e21589-e.
454. Richmond A. Nf-kappa B, chemokine gene transcription and tumour growth. Nature reviews Immunology. 2002;2(9):664-74.
455. Lockyer JM, Colladay JS, Alperin-Lea WL, Hammond T, Buda AJ. Inhibition of Nuclear Factor-κB–Mediated Adhesion Molecule Expression in Human Endothelial Cells. Circulation Research. 1998;82(3):314-20.
456. Ni S, Li C, Xu N, Liu X, Wang W, Chen W, et al. Follistatin-like protein 1 induction of matrix metalloproteinase 1, 3 and 13 gene expression in rheumatoid arthritis synoviocytes requires MAPK, JAK/STAT3 and NF-κB pathways. Journal of Cellular Physiology. 2019;234(1):454-63.
457. McKay LI, Cidlowski JA. Cross-Talk between Nuclear Factor-κB and the Steroid Hormone Receptors: Mechanisms of Mutual Antagonism. Molecular Endocrinology. 1998;12(1):45-56.
458. Stein B, Baldwin AS, Jr., Ballard DW, Greene WC, Angel P, Herrlich P. Cross-coupling of the NF-kappa B p65 and Fos/Jun transcription factors produces potentiated biological function. Embo j. 1993;12(10):3879-91.
459. Harnish DC. Estrogen receptor ligands in the control of pathogenic inflammation. Curr Opin Investig Drugs. 2006;7(11):997-1001.
460. Sun WH, Keller ET, Stebler BS, Ershler WB. Estrogen Inhibits Phorbol Ester-Induced IκBα Transcription and Protein Degradation. Biochemical and Biophysical Research Communications. 1998;244(3):691-5.
461. Quaedackers ME, van den Brink CE, van der Saag PT, Tertoolen LGJ. Direct interaction between estrogen receptor α and NF-κB in the nucleus of living cells. Mol Cell Endocrinol. 2007;273(1):42-50.
462. Feldman I, Feldman GM, Mobarak C, Dunkelberg JC, Leslie KK. Identification of proteins within the nuclear factor-kappa B transcriptional complex including estrogen receptor-alpha. American journal of obstetrics and gynecology. 2007;196(4):394.e1-.e13.
463. Critchley HO, Henderson TA, Kelly RW, Scobie GS, Evans LR, Groome NP, et al. Wild-type estrogen receptor (ERbeta1) and the splice variant (ERbetacx/beta2) are both expressed within the human endometrium throughout the normal menstrual cycle. The Journal of clinical endocrinology and metabolism. 2002;87(11):5265-73.
464. Critchley HO, Saunders PT. Hormone receptor dynamics in a receptive human endometrium. Reprod Sci. 2009;16(2):191-9.
465. Laird SM, Tuckerman EM, Cork BA, Li TC. Expression of nuclear factor kappa B in human endometrium; role in the control of interleukin 6 and leukaemia inhibitory factor production. Mol Hum Reprod. 2000;6(1):34-40.
466. Page M, Tuckerman EM, Li TC, Laird SM. Expression of nuclear factor kappa B components in human endometrium. J Reprod Immunol. 2002;54(1-2):1-13.

467. Rahman MM, McFadden G. Modulation of NF-κB signalling by microbial pathogens. Nature Reviews Microbiology. 2011;9(4):291-306.
468. Oeckinghaus A, Hayden MS, Ghosh S. Crosstalk in NF-κB signaling pathways. Nature immunology. 2011;12(8):695-708.
469. Nicholson JK, Lindon JC, Holmes E. 'Metabonomics': understanding the metabolic responses of living systems to pathophysiological stimuli via multivariate statistical analysis of biological NMR spectroscopic data. Xenobiotica. 1999;29(11):1181-9.
470. Jess A, Hazel MD, David B, Jim KH, Jem JR, Stephen GO, et al. High-throughput classification of yeast mutants for functional genomics using metabolic footprinting. Nature Biotechnology. 2003;21(6):692.
471. Wang JH, Byun J, Pennathur S. Analytical Approaches to Metabolomics and Applications to Systems Biology. Seminars in Nephrology. 2010;30(5):500-11.
472. Revelli A, Piane LD, Casano S, Molinari E, Massobrio M, Rinaudo P. Follicular fluid content and oocyte quality: from single biochemical markers to metabolomics. Reproductive Biology and Endocrinology : RB&E. 2009;7:40-.
473. Botros L, Sakkas D, Seli E. Metabolomics and its application for non-invasive embryo assessment in IVF. Molecular Human Reproduction. 2008;14(12):679-90.
474. Dodge LE, Williams PL, Williams MA, Missmer SA, Souter I, Calafat AM, et al. Associations between paternal urinary phthalate metabolite concentrations and reproductive outcomes among couples seeking fertility treatment. Reproductive Toxicology. 2015;58:184-93.
475. McMillan A, Rulisa S, Sumarah M, Macklaim JM, Renaud J, Bisanz JE, et al. A multi-platform metabolomics approach identifies highly specific biomarkers of bacterial diversity in the vagina of pregnant and non-pregnant women. Sci Rep. 2015;5:14174.
476. Srinivasan S, Morgan MT, Fiedler TL, Djukovic D, Hoffman NG, Raftery D, et al. Metabolic signatures of bacterial vaginosis. mBio. 2015;6(2).
477. Amabebe E, Reynolds S, Stern VL, Parker JL, Stafford GP, Paley MN, et al. Identifying metabolite markers for preterm birth in cervicovaginal fluid by magnetic resonance spectroscopy. Metabolomics. 2016;12:67.
478. Ghartey J, Bastek JA, Brown AG, Anglim L, Elovitz MA. Women with preterm birth have a distinct cervicovaginal metabolome. American Journal of Obstetrics and Gynecology. 2015;212(6):776.e1-.e12.
479. Correia GDS, Marchesi JR, MacIntyre DA. Moving beyond DNA: towards functional analysis of the vaginal microbiome by non-sequencing-based methods. Current Opinion in Microbiology. 2023;73:102292.
480. Pruski P, MacIntyre DA, Lewis HV, Inglese P, Correia GDS, Hansel TT, et al. Medical Swab Analysis Using Desorption Electrospray Ionization Mass Spectrometry: A Noninvasive Approach for Mucosal Diagnostics. Analytical Chemistry. 2017;89(3):1540-50.
481. Takáts Z, Wiseman JM, Gologan B, Cooks RG. Mass spectrometry sampling under ambient conditions with desorption electrospray ionization. Science (New York, NY). 2004;306(5695):471.
482. Pruski P, Lewis HV, Lee YS, Marchesi JR, Bennett PR, Takats Z, et al. Assessment of microbiota:host interactions at the vaginal mucosa interface. Methods. 2018;149:74-84.
483. Pruski P, Correia GDS, Lewis HV, Capuccini K, Inglese P, Chan D, et al. Direct on-swab metabolic profiling of vaginal microbiome host interactions during pregnancy and preterm birth. Nature Communications. 2021;12(1):5967.
484. QIAamp DNA Mini and Blood Mini Handbook [Internet]. 2016. Available from: https://www.qiagen.com/jp/resources/download.aspx?id=62a200d6-faf4-469b-b50f-2b59cf738962&lang=en.
485. Liu CM, Aziz M, Kachur S, Hsueh P-R, Huang Y-T, Keim P, et al. BactQuant: An enhanced broad-coverage bacterial quantitative real-time PCR assay. BMC Microbiology. 2012;12(1):56.
486. Vessey W, Perez-Miranda A, Macfarquhar R, Agarwal A, Homa S. Reactive oxygen species in human semen: validation and qualification of a chemiluminescence assay. Fertil Steril. 2014;102(6):1576-83.e4.

487. Agarwal A, Allamaneni SS, Said TM. Chemiluminescence technique for measuring reactive oxygen species. Reproductive BioMedicine Online. 2004;9(4):466-8.
488. Hughes CM, Lewis SE, McKelvey-Martin VJ, Thompson W. A comparison of baseline and induced DNA damage in human spermatozoa from fertile and infertile men, using a modified comet assay. MHR: Basic science of reproductive medicine. 1996;2(8):613-9.
489. Donnelly ET, McClure N, Lewis SE. The effect of ascorbate and α-tocopherol supplementation in vitro on DNA integrity and hydrogen peroxide-induced DNA damage in human spermatozoa. Mutagenesis. 1999;14(5):505-12.
490. Chambers MC, Maclean B, Burke R, Amodei D, Ruderman DL, Neumann S, et al. A cross-platform toolkit for mass spectrometry and proteomics. Nat Biotechnol. 2012;30(10):918-20.
491. Kozich JJ, Westcott SL, Baxter NT, Highlander SK, Schloss PD. Development of a Dual-Index Sequencing Strategy and Curation Pipeline for Analyzing Amplicon Sequence Data on the MiSeq Illumina Sequencing Platform. Applied and Environmental Microbiology. 2013;79(17):5112-20.
492. Wang Q, Garrity GM, Tiedje JM, Cole JR. Naïve Bayesian Classifier for Rapid Assignment of rRNA Sequences into the New Bacterial Taxonomy. Applied and Environmental Microbiology. 2007;73(16):5261-7.
493. Team RC. R: A language and environment for statistical computing. R Foundation for Statistical Computing, Vienna, Austria. Available online at https://www.R-project.org/. 2018.
494. Simpson EH. Measurement of Diversity. Nature. 1949;163(4148):688-.
495. Andreu A, Stapleton AE, Fennell CL, Hillier SL, Stamm WE. Hemagglutination, Adherence, and Surface Properties of Vaginal Lactobacillus Species. The Journal of Infectious Diseases. 1995;171(5):1237-43.
496. Sobel JD, Schneider J, Kaye D, Levison ME. Adherence of bacteria to vaginal epithelial cells at various times in the menstrual cycle. Infect Immun. 1981;32(1):194-7.
497. Ojala T, Kankainen M, Castro J, Cerca N, Edelman S, Westerlund-Wikström B, et al. Comparative genomics of Lactobacillus crispatus suggests novel mechanisms for the competitive exclusion of Gardnerella vaginalis. BMC Genomics. 2014;15(1):1070.
498. Eckert LO, Moore DE, Patton DL, Agnew KJ, Eschenbach DA. Relationship of vaginal bacteria and inflammation with conception and early pregnancy loss following in-vitro fertilization. Infect Dis Obstet Gynecol. 2003;11(1):11-7.
499. Fu M, Zhang X, Liang Y, Lin S, Qian W, Fan S. Alterations in Vaginal Microbiota and Associated Metabolome in Women with Recurrent Implantation Failure. mBio. 2020;11(3).
500. Haahr T, Jensen JS, Thomsen L, Duus L, Rygaard K, Humaidan P. Abnormal vaginal microbiota may be associated with poor reproductive outcomes: a prospective study in IVF patients. Human reproduction (Oxford, England). 2016;31(4):795-803.
501. Witkin SS. The vaginal microbiome, vaginal anti-microbial defence mechanisms and the clinical challenge of reducing infection-related preterm birth. Bjog. 2015;122(2):213-8.
502. Spear GT, French AL, Gilbert D, Zariffard MR, Mirmonsef P, Sullivan TH, et al. Human alpha-amylase present in lower-genital-tract mucosal fluid processes glycogen to support vaginal colonization by Lactobacillus. J Infect Dis. 2014;210(7):1019-28.
503. Tachedjian G, Aldunate M, Bradshaw CS, Cone RA. The role of lactic acid production by probiotic Lactobacillus species in vaginal health. Research in Microbiology. 2017;168(9):782-92.
504. Ashkar AA, Croy BA, editors. Functions of uterine natural killer cells are mediated by interferon gamma production during murine pregnancy. Seminars in Immunology; 2001: Elsevier.
505. Tokmadzić VS, Tsuji Y, Bogović T, LAŠKARIN G, Cupurdija K, Š TRBO N, et al. IL-18 is Present at the Maternal–Fetal Interface and Enhances Cytotoxic Activity of Decidual Lymphocytes. American Journal of Reproductive Immunology. 2002;48(4):191-200.
506. Croy BA, Chantakru S, Esadeg S, Ashkar AA, Wei Q. Decidual natural killer cells: key regulators of placental development (a review). Journal of reproductive immunology. 2002;57(1-2):151-68.

507. Smoothed conditional means ggplot2 [Internet]. 2022. Available from: https://ggplot2.tidyverse.org/reference/geom_smooth.html.
508. University TXLaM. Microbiome Analyst: Comprehensive statistical, functional adn integrative analysis of microbiome data: Xia Lab; 2023 [Available from: https://www.microbiomeanalyst.ca/.
509. Fettweis JM, Serrano MG, Brooks JP, Edwards DJ, Girerd PH, Parikh HI, et al. The vaginal microbiome and preterm birth. Nature Medicine. 2019;25(6):1012-21.
510. Brooks JP, Buck GA, Chen G, Diao L, Edwards DJ, Fettweis JM, et al. Changes in vaginal community state types reflect major shifts in the microbiome. Microb Ecol Health Dis. 2017;28(1):1303265.
511. Remohi J, Ardiles G, Garcia-Velasco J, Gaitán P, Simón C, Pellicer A. Endometrial thickness and serum oestradiol concentrations as predictors of outcome in oocyte donation. Human reproduction (Oxford, England). 1997;12(10):2271-6.
512. Li Q, Ruan L, Zhu L, Yang Z, Zhu M, Luo Y. Elevated estradiol levels in frozen embryo transfer have different effects on pregnancy outcomes depending on the stage of transferred embryos. Scientific reports. 2022;12(1):5592.
513. Diluigi A, Engmann L, Benadiva C, Maier D, Varhola J, Nulsen J. Serum Estradiol Level on Day of Embryo Transfer Is Associated With Implantation and Pregnancy Rates. Fertility and sterility. 2005;84:S265-S.
514. Orvieto R, Rabinson J, Meltzer S, Homburg R, Anteby E, Zohav E. GnRH agonist versus GnRH antagonist in ovarian stimulation: is the emperor naked? Clinical and Experimental Obstetrics & Gynecology. 2006;33(4):197-9.
515. Orvieto R, Homburg R, Meltcer S, Rabinson J, Anteby EY, Scharf S. GnRH agonist versus GnRH antagonist in controlled ovarian hyperstimulation: their role in patients with an unfavorable prognosis a priori. Fertility and sterility. 2009;91(4):1378-80.
516. Orvieto R, Meltzer S, Rabinson J, Zohav E, Anteby EY, Nahum R. GnRH agonist versus GnRH antagonist in ovarian stimulation: the role of endometrial receptivity. Fertility and sterility. 2008;90(4):1294-6.
517. Bodri D, Sunkara SK, Coomarasamy A. Gonadotropin-releasing hormone agonists versus antagonists for controlled ovarian hyperstimulation in oocyte donors: a systematic review and meta-analysis. Fertility and sterility. 2011;95(1):164-9.
518. Kolibianakis EM, Collins J, Tarlatzis BC, Devroey P, Diedrich K, Griesinger G. Among patients treated for IVF with gonadotrophins and GnRH analogues, is the probability of live birth dependent on the type of analogue used? A systematic review and meta-analysis. Human reproduction update. 2006;12(6):651-71.
519. Barmat LI, Chantilis SJ, Hurst BS, Dickey RP. A randomized prospective trial comparing gonadotropin-releasing hormone (GnRH) antagonist/recombinant follicle-stimulating hormone (rFSH) versus GnRH-agonist/rFSH in women pretreated with oral contraceptives before in vitro fertilization. Fertility and Sterility. 2005;83(2):321-30.
520. Chan D, Bennett PR, Lee YS, Kundu S, Teoh TG, Adan M, et al. Microbial-driven preterm labour involves crosstalk between the innate and adaptive immune response. Nat Commun. 2022;13(1):975.
521. van Houdt R, Ma B, Bruisten SM, Speksnijder A, Ravel J, de Vries HJC. Lactobacillus iners-dominated vaginal microbiota is associated with increased susceptibility to Chlamydia trachomatis infection in Dutch women: a case-control study. Sex Transm Infect. 2018;94(2):117-23.
522. Tamarelle J, de Barbeyrac B, Le Hen I, Thiébaut A, Bébéar C, Ravel J, et al. Vaginal microbiota composition and association with prevalent Chlamydia trachomatis infection: a cross-sectional study of young women attending a STI clinic in France. Sex Transm Infect. 2018;94(8):616-8.
523. Lledo B, Fuentes A, Lozano FM, Cascales A, Morales R, Hortal M, et al. Identification of vaginal microbiome associated with IVF pregnancy. Scientific reports. 2022;12(1):6807.
524. Lepargneur J-P, editor Lactobacillus crispatus as biomarker of the healthy vaginal tract. Annales de Biologie Clinique; 2016.

525. Anton L, Sierra L-J, DeVine A, Barila G, Heiser L, Brown AG, et al. Common Cervicovaginal Microbial Supernatants Alter Cervical Epithelial Function: Mechanisms by Which Lactobacillus crispatus Contributes to Cervical Health. Frontiers in Microbiology. 2018;9.
526. Chopra C, Bhushan I, Mehta M, Koushal T, Gupta A, Sharma S, et al. Vaginal microbiome: considerations for reproductive health. Future Microbiology. 2022;17(18):1501-13.
527. Kong N, Liu J, Zhang C, Jiang Y, Zhu Y, Yan G, et al. The relationship between serum oestrogen levels and clinical outcomes of hormone replacement therapy-frozen embryo transfer: a retrospective clinical study. BMC Pregnancy Childbirth. 2022;22(1):265.
528. Liversedge NH, Turner A, Horner PJ, Keay SD, Jenkins JM, Hull MGR. The influence of bacterial vaginosis on in-vitro fertilization and embryo implantation during assisted reproduction treatment. Human Reproduction. 1999;14(9):2411-5.
529. Vitali D, Wessels JM, Kaushic C. Role of sex hormones and the vaginal microbiome in susceptibility and mucosal immunity to HIV-1 in the female genital tract. AIDS research and therapy. 2017;14(1):1-5.
530. Shen J, Song N, Williams C, Brown C, Yan Z, Xu C, et al. Effects of low dose estrogen therapy on the vaginal microbiomes of women with atrophic vaginitis. Sci Rep 6: 24380. 2016.
531. Hedge SR, Barrientes F, Desmond RA, Schwebke JR. Local and Systemic Cytokine Levels in Relation to Changes in Vaginal Flora. The Journal of Infectious Diseases. 2006;193(4):556-62.
532. Byrne EH, Doherty KE, Bowman BA, Yamamoto HS, Soumillon M, Padavattan N, et al. Cervicovaginal bacteria are a major modulator of host inflammatory responses in the female genital tract. Immunity. 2015;42(5):965-76.
533. Wira CR, Fahey JV, Rodriguez-Garcia M, Shen Z, Patel MV. Regulation of mucosal immunity in the female reproductive tract: the role of sex hormones in immune protection against sexually transmitted pathogens. American journal of reproductive immunology (New York, NY : 1989). 2014;72(2):236-58.
534. Cuzzocrea S, Santagati S, Sautebin L, Mazzon E, Calabrò G, Serraino I, et al. 17β-estradiol antiinflammatory activity in carrageenan-induced pleurisy. Endocrinology. 2000;141(4):1455-63.
535. Subbiah MR. Mechanisms of cardioprotection by estrogens. Proceedings of the Society for Experimental Biology and Medicine. 1998;217(1):23-9.
536. Hardie L, Trayhurn P, Abramovich D, Fowler P. Circulating leptin in women: a longitudinal study in the menstrual cycle and during pregnancy. Clinical Endocrinology. 1997;47(1):101-6.
537. Al-Harithy RN, Al-Doghaither H, Abualnaja K. Correlation of leptin and sex hormones with endocrine changes in healthy Saudi women of different body weights. Ann Saudi Med. 2006;26(2):110-5.
538. Zeeuwen PL, Ederveen TH, van der Krieken DA, Niehues H, Boekhorst J, Kezic S, et al. Gram-positive anaerobe cocci are underrepresented in the microbiome of filaggrin-deficient human skin. J Allergy Clin Immunol. 2017;139(4):1368-71.
539. Castro J, Rosca AS, Muzny CA, Cerca N. Atopobium vaginae and Prevotella bivia Are Able to Incorporate and Influence Gene Expression in a Pre-Formed Gardnerella vaginalis Biofilm. Pathogens. 2021;10(2):247.
540. Spiegel CA, Amsel R, Eschenbach D, Schoenknecht F, Holmes KK. Anaerobic bacteria in nonspecific vaginitis. New England Journal of Medicine. 1980;303(11):601-7.
541. Randis TM, Ratner AJ. Gardnerella and Prevotella: Co-conspirators in the Pathogenesis of Bacterial Vaginosis. J Infect Dis. 2019;220(7):1085-8.
542. Aroutcheva A, Ling Z, Faro S. Prevotella bivia as a source of lipopolysaccharide in the vagina. Anaerobe. 2008;14(5):256-60.
543. Pybus V, Onderdonk AB. Evidence for a commensal, symbiotic relationship between Gardnerella vaginalis and Prevotella bivia involving ammonia: potential significance for bacterial vaginosis. Journal of infectious diseases. 1997;175(2):406-13.

544. Cobo F, Rodríguez-Granger J, Sampedro A, Navarro-Marí JM. Bartholin's abscess due to Dialister micraerophilus in a woman presenting with repetitive bartholinitis episodes. Médecine et Maladies Infectieuses. 2018;48(3):225-6.
545. Tao Z, Zhang L, Zhang Q, Lv T, Chen R, Wang L, et al. The Pathogenesis Of Streptococcus anginosus In Aerobic Vaginitis. Infect Drug Resist. 2019;12:3745-54.
546. Zheng N, Guo R, Wang J, Zhou W, Ling Z. Contribution of Lactobacillus iners to Vaginal Health and Diseases: A Systematic Review. Front Cell Infect Microbiol. 2021;11:792787.
547. De Seta F, Campisciano G, Zanotta N, Ricci G, Comar M. The Vaginal Community State Types Microbiome-Immune Network as Key Factor for Bacterial Vaginosis and Aerobic Vaginitis. Front Microbiol. 2019;10:2451.
548. Murphy EC, Frick I-M. Gram-positive anaerobic cocci–commensals and opportunistic pathogens. FEMS microbiology reviews. 2013;37(4):520-53.
549. Neumann A, Björck L, Frick IM. Finegoldia magna, an Anaerobic Gram-Positive Bacterium of the Normal Human Microbiota, Induces Inflammation by Activating Neutrophils. Front Microbiol. 2020;11:65.
550. Goodfellow L, Verwijs MC, Care A, Sharp A, Ivandic J, Poljak B, et al. Vaginal bacterial load in the second trimester is associated with early preterm birth recurrence: a nested case-control study. Bjog. 2021;128(13):2061-72.
551. Fahey JV, Wright JA, Shen L, Smith JM, Ghosh M, Rossoll RM, et al. Estradiol selectively regulates innate immune function by polarized human uterine epithelial cells in culture. Mucosal Immunology. 2008;1(4):317-25.
552. Dragin N, Nancy P, Villegas J, Roussin R, Le Panse R, Berrih-Aknin S. Balance between Estrogens and Proinflammatory Cytokines Regulates Chemokine Production Involved in Thymic Germinal Center Formation. Scientific reports. 2017;7(1):7970.
553. Kovats S. Estrogen receptors regulate innate immune cells and signaling pathways. Cellular Immunology. 2015;294(2):63-9.
554. Alimohamadi S, Javadian P, Gharedaghi MH, Javadian N, Alinia H, Khazardoust S, et al. Progesterone and threatened abortion: a randomized clinical trial on endocervical cytokine concentrations. J Reprod Immunol. 2013;98(1-2):52-60.
555. Brusilovsky M, Radinsky O, Yossef R, Campbell KS, Porgador A. Carbohydrate-mediated modulation of NK cell receptor function: structural and functional influences of heparan sulfate moieties expressed on NK cell surface. Frontiers in Oncology. 2014;4:185.
556. Gong H, Chen Y, Xu J, Xie X, Yu D, Yang B, et al. The regulation of ovary and conceptus on the uterine natural killer cells during early pregnancy. Reproductive Biology and Endocrinology. 2017;15(1):73.
557. Bogdan A, Berta G, Szekeres-Bartho J. PIBF positive uterine NK cells in the mouse decidua. Journal of Reproductive Immunology. 2017;119:38-43.
558. Miyaura H, Iwata M. Direct and indirect inhibition of Th1 development by progesterone and glucocorticoids. The Journal of Immunology. 2002;168(3):1087-94.
559. Rossi M, Sharkey AM, Viganò P, Fiore G, Furlong R, Florio P, et al. Identification of genes regulated by interleukin-1beta in human endometrial stromal cells. Reproduction. 2005;130(5):721-9.
560. Inagaki N, Stern C, McBain J, Lopata A, Kornman L, Wilkinson D. Analysis of intra-uterine cytokine concentration and matrix-metalloproteinase activity in women with recurrent failed embryo transfer. Human reproduction (Oxford, England). 2003;18(3):608-15.
561. Jovanović M, Stefanoska I, Radojcić L, Vićovac L. Interleukin-8 (CXCL8) stimulates trophoblast cell migration and invasion by increasing levels of matrix metalloproteinase (MMP)2 and MMP9 and integrins alpha5 and beta1. Reproduction. 2010;139(4):789-98.
562. Lathi RB, Hess AP, Tulac S, Nayak NR, Conti M, Giudice LC. Dose-dependent insulin regulation of insulin-like growth factor binding protein-1 in human endometrial stromal cells is mediated by distinct signaling pathways. The Journal of clinical endocrinology and metabolism. 2005;90(3):1599-606.

563. Fowler D, Nicolaides K, Miell J. Insulin-like growth factor binding protein-1 (IGFBP-1): a multifunctional role in the human female reproductive tract. Human reproduction update. 2000;6(5):495-504.
564. Endometrial scratching [Internet]. 2023. Available from: https://www.hfea.gov.uk/treatments/treatment-add-ons/endometrial-scratching/#:~:text=During%20the%20procedure%20the%20lining,receptive%20to%20an%20embryo%20implanting.
565. Lensen SF, Armstrong S, Gibreel A, Nastri CO, Raine-Fenning N, Martins WP. Endometrial injury in women undergoing in vitro fertilisation (IVF). Cochrane Database of Systematic Reviews. 2021(6).
566. Simón C, Frances A, Piquette G, Hendrickson M, Milki A, Polan ML. Interleukin-1 system in the materno-trophoblast unit in human implantation: immunohistochemical evidence for autocrine/paracrine function. The Journal of Clinical Endocrinology & Metabolism. 1994;78(4):847-54.
567. Simón C, Valbuena D, Krüssel J, Bernal A, Murphy CR, Shaw T, et al. Interleukin-1 receptor antagonist prevents embryonic implantation by a direct effect on the endometrial epithelium. Fertility and Sterility. 1998;70(5):896-906.
568. Arend WP, Malyak M, Guthridge CJ, Gabay C. Interleukin-1 receptor antagonist: role in biology. Annual review of immunology. 1998;16(1):27-55.
569. Huang H-Y, Wen Y, Kruessel JS, Raga F, Soong Y-K, Polan ML. Interleukin (IL)-1β Regulation of IL-1β and IL-1 Receptor Antagonist Expression in Cultured Human Endometrial Stromal Cells1. The Journal of Clinical Endocrinology & Metabolism. 2001;86(3):1387-93.
570. Liu Z, DeSantis TZ, Andersen GL, Knight R. Accurate taxonomy assignments from 16S rRNA sequences produced by highly parallel pyrosequencers. Nucleic acids research. 2008;36(18):e120-e.
571. Motooka D, Fujimoto K, Tanaka R, Yaguchi T, Gotoh K, Maeda Y, et al. Fungal ITS1 deep-sequencing strategies to reconstruct the composition of a 26-species community and evaluation of the gut mycobiota of healthy Japanese individuals. Frontiers in microbiology. 2017;8:238.
572. Loutradi KE, Kolibianakis EM, Venetis CA, Papanikolaou EG, Pados G, Bontis I, et al. Cryopreservation of human embryos by vitrification or slow freezing: a systematic review and meta-analysis. Fertility and sterility. 2008;90(1):186-93.
573. Sciorio R, Esteves SC. Clinical utility of freeze-all approach in ART treatment: A mini-review. Cryobiology. 2020;92:9-14.
574. Devroey P, Polyzos NP, Blockeel C. An OHSS-Free Clinic by segmentation of IVF treatment. Human reproduction. 2011;26(10):2593-7.
575. Venetis CA, Kolibianakis EM, Bosdou JK, Tarlatzis BC. Progesterone elevation and probability of pregnancy after IVF: a systematic review and meta-analysis of over 60 000 cycles. Human reproduction update. 2013;19(5):433-57.
576. Maheshwari A, Pandey S, Amalraj Raja E, Shetty A, Hamilton M, Bhattacharya S. Is frozen embryo transfer better for mothers and babies? Can cumulative meta-analysis provide a definitive answer? Human reproduction update. 2017;24(1):35-58.
577. Lawrenz B, Coughlan C, Melado L, Fatemi HM. The ART of frozen embryo transfer: back to nature! Gynecological Endocrinology. 2020;36(6):479-83.
578. Simpson JL, Kuliev A, Rechitsky S. Overview of Preimplantation Genetic Diagnosis (PGD): Historical Perspective and Future Direction. In: Levy B, editor. Prenatal Diagnosis. New York, NY: Springer New York; 2019. p. 23-43.
579. Sacchi L, Albani E, Cesana A, Smeraldi A, Parini V, Fabiani M, et al. Preimplantation Genetic Testing for Aneuploidy Improves Clinical, Gestational, and Neonatal Outcomes in Advanced Maternal Age Patients Without Compromising Cumulative Live-Birth Rate. J Assist Reprod Genet. 2019;36(12):2493-504.
580. Gajer P, Brotman RM, Bai G, Sakamoto J, Schütte UME, Zhong X, et al. Temporal Dynamics of the Human Vaginal Microbiota. Science Translational Medicine. 2012;4(132):132ra52-ra52.

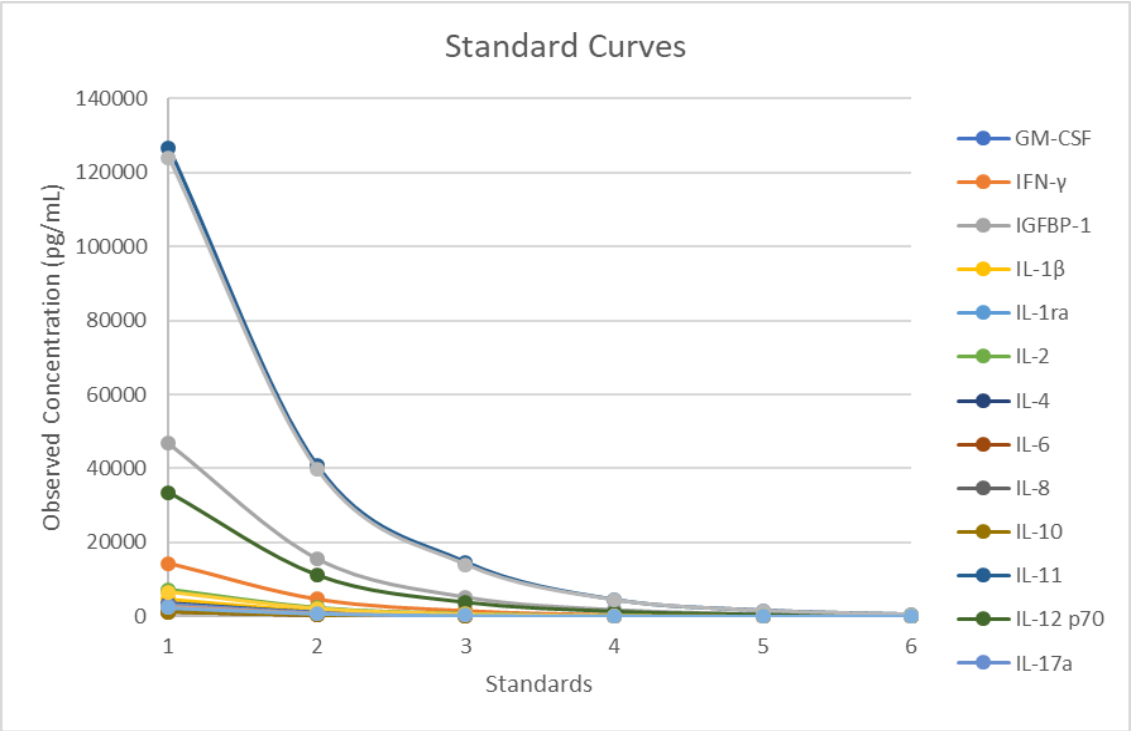
581. Gong Z, Luna Y, Yu P, Fan H. Lactobacilli Inactivate Chlamydia trachomatis through Lactic Acid but Not H2O2. PloS one. 2014;9(9):e107758.
582. Witkin SS, Mendes-Soares H, Linhares IM, Jayaram A, Ledger WJ, Forney LJ. Influence of vaginal bacteria and D-and L-lactic acid isomers on vaginal extracellular matrix metalloproteinase inducer: implications for protection against upper genital tract infections. mBio. 2013;4(4):e00460-13.
583. Edwards V, McComb E, Guttman H, Humphrys M, Forney L, Bavoil P, et al. P08. 06 lactic acid isomers differentially reduce chlamydia trachomatis infection in a ph dependent manner. BMJ Publishing Group Ltd; 2015.
584. Baart EB, Martini E, van den Berg I, Macklon N, Galjaard RH, Fauser B, et al. Preimplantation genetic screening reveals a high incidence of aneuploidy and mosaicism in embryos from young women undergoing IVF. Human reproduction. 2006;21(1):223-33.
585. Fragouli E, Alfarawati S, Daphnis DD, Goodall N-n, Mania A, Griffiths T, et al. Cytogenetic analysis of human blastocysts with the use of FISH, CGH and aCGH: scientific data and technical evaluation. Human Reproduction. 2011;26(2):480-90.
586. Vera-Rodriguez M, Rubio C. Assessing the true incidence of mosaicism in preimplantation embryos. Fertility and sterility. 2017;107(5):1107-12.
587. Kahraman S, Cetinkaya M, Yuksel B, Yesil M, Pirkevi Cetinkaya C. The birth of a baby with mosaicism resulting from a known mosaic embryo transfer: a case report. Human Reproduction. 2020;35(3):727-33.
588. Grewal K, Lee YS, Smith A, Brosens JJ, Bourne T, Al-Memar M, et al. Chromosomally normal miscarriage is associated with vaginal dysbiosis and local inflammation. BMC Medicine. 2022;20(1):38.
589. Lopes dos Santos Santiago G, Tency I, Verstraelen H, Verhelst R, Trog M, Temmerman M, et al. Longitudinal qPCR study of the dynamics of L. crispatus, L. iners, A. vaginae,(sialidase positive) G. vaginalis, and P. bivia in the vagina. 2012.
590. Fleischer AC, Kalemeris GC, Entman SS. Sonographic depiction of the endometrium during normal cycles. Ultrasound Med Biol. 1986;12(4):271-7.
591. Sakamoto C, Yoshimitsu K, Nakamura G, Ootsuka H, Yoshida K. Sonographic study of the endometrial responses to ovarian hormones in patients receiving ovarian stimulation. Int J Gynaecol Obstet. 1988;27(3):407-14.
592. Fleischer AC, Pittaway DE, Beard LA, Thieme GA, Bundy AL, James AE, Jr., et al. Sonographic depiction of endometrial changes occurring with ovulation induction. J Ultrasound Med. 1984;3(8):341-6.
593. Smith B, Porter R, Ahuja K, Craft I. Ultrasonic assessment of endometrial changes in stimulated cycles in an in vitro fertilization and embryo transfer program. J In Vitro Fert Embryo Transf. 1984;1(4):233-8.
594. Barash A, Weissman A, Manor M, Milman D, Ben-Arie A, Shoham Z. Prospective evaluation of endometrial thickness as a predictor of pituitary down-regulation after gonadotropin-releasing hormone analogue administration in an in vitro fertilization program. Fertil Steril. 1998;69(3):496-9.
595. Child TJ, Sylvestre C, Tan SL. Endometrial volume and thickness measurements predict pituitary suppression and non-suppression during IVF. Human Reproduction. 2002;17(12):3110-3.
596. IVF Overview [Internet]. 2023. Available from: https://www.nhs.uk/conditions/ivf/.
597. Toson B, Simon C, Moreno I. The Endometrial Microbiome and Its Impact on Human Conception. Int J Mol Sci. 2022;23(1).
598. EndomeTRIO: The endometrium matters [Internet]. 2023. Available from: https://www.igenomix.co.uk/genetic-solutions/endometrio-clinics/.
599. Hardarson T, Ahlström A, Rogberg L, Botros L, Hillensjö T, Westlander G, et al. Non-invasive metabolomic profiling of Day 2 and 5 embryo culture medium: a prospective randomized trial. Human Reproduction. 2011;27(1):89-96.
600. Vergouw CG, Botros LL, Roos P, Lens JW, Schats R, Hompes PGA, et al. Metabolomic profiling by near-infrared spectroscopy as a tool to assess embryo viability: a

novel, non-invasive method for embryo selection. Human Reproduction. 2008;23(7):1499-504.
601. Vega C, Spence C, Zhang C, Bills BJ, Manicke NE. Ionization Suppression and Recovery in Direct Biofluid Analysis Using Paper Spray Mass Spectrometry. J Am Soc Mass Spectrom. 2016;27(4):726-34.
602. Cody RB, Laramée JA, Durst HD. Versatile new ion source for the analysis of materials in open air under ambient conditions. Anal Chem. 2005;77(8):2297-302.
603. Takáts Z, Wiseman JM, Cooks RG. Ambient mass spectrometry using desorption electrospray ionization (DESI): instrumentation, mechanisms and applications in forensics, chemistry, and biology. J Mass Spectrom. 2005;40(10):1261-75.
604. Guenther S, Muirhead LJ, Speller AV, Golf O, Strittmatter N, Ramakrishnan R, et al. Spatially resolved metabolic phenotyping of breast cancer by desorption electrospray ionization mass spectrometry. Cancer Res. 2015;75(9):1828-37.
605. Dória ML, McKenzie JS, Mroz A, Phelps DL, Speller A, Rosini F, et al. Epithelial ovarian carcinoma diagnosis by desorption electrospray ionization mass spectrometry imaging. Scientific reports. 2016;6(1):39219.
606. Song Y, Talaty N, Tao WA, Pan Z, Cooks RG. Rapid ambient mass spectrometric profiling of intact, untreated bacteria using desorption electrospray ionization. Chem Commun (Camb). 2007(1):61-3.
607. Wang Y, Wu J, Lv M, Shao Z, Hungwe M, Wang J, et al. Metabolism Characteristics of Lactic Acid Bacteria and the Expanding Applications in Food Industry. Frontiers in Bioengineering and Biotechnology. 2021;9.
608. Yeoman CJ, Thomas SM, Miller ME, Ulanov AV, Torralba M, Lucas S, et al. A multi-omic systems-based approach reveals metabolic markers of bacterial vaginosis and insight into the disease. PloS one. 2013;8(2):e56111.
609. Preti G, Huggins GR. Cyclical changes in volatile acidic metabolites of human vaginal secretions and their relation to ovulation. Journal of Chemical Ecology. 1975;1(3):361-76.
610. Vitali B, Cruciani F, Picone G, Parolin C, Donders G, Laghi L. Vaginal microbiome and metabolome highlight specific signatures of bacterial vaginosis. European Journal of Clinical Microbiology & Infectious Diseases. 2015;34(12):2367-76.
611. Fahy E, Subramaniam S, Murphy RC, Nishijima M, Raetz CR, Shimizu T, et al. Update of the LIPID MAPS comprehensive classification system for lipids. J Lipid Res. 2009;50 Suppl(Suppl):S9-14.
612. Smith CA, O'Maille G, Want EJ, Qin C, Trauger SA, Brandon TR, et al. METLIN: a metabolite mass spectral database. Ther Drug Monit. 2005;27(6):747-51.
613. Patiny L, Borel A. ChemCalc: A Building Block for Tomorrow's Chemical Infrastructure. Journal of Chemical Information and Modeling. 2013;53(5):1223-8.
614. Vajpeyee M, Tiwari S, Yadav LB, Tank P. Assessment of bacterial diversity associated with assisted reproductive technologies through next-generation sequencing. Middle East Fertility Society Journal. 2022;27(1):28.
615. Srinivasan S, Hua X, Wu MC, Proll S, Valint DJ, Reed SD, et al. Impact of Topical Interventions on the Vaginal Microbiota and Metabolome in Postmenopausal Women: A Secondary Analysis of a Randomized Clinical Trial. JAMA Netw Open. 2022;5(3):e225032.
616. Dowhan W, Bogdanov M. Eugene P. Kennedy's Legacy: Defining Bacterial Phospholipid Pathways and Function. Frontiers in Molecular Biosciences. 2021;8.
617. Voelker DR, Numata M. Phospholipid regulation of innate immunity and respiratory viral infection. Journal of Biological Chemistry. 2019;294(12):4282-9.
618. Jackson AU, Talaty N, Cooks RG, Van Berkel GJ. Salt Tolerance of Desorption Electrospray Ionization (DESI). Journal of the American Society for Mass Spectrometry. 2007;18(12):2218-25.
619. Wang Z, Zhu H, Huang G. Ion suppression effect in desorption electrospray ionization and electrospray ionization mass spectrometry. Rapid Communications in Mass Spectrometry. 2017;31(23):1957-62.
620. Annesley TM. Ion Suppression in Mass Spectrometry. Clinical Chemistry. 2003;49(7):1041-4.

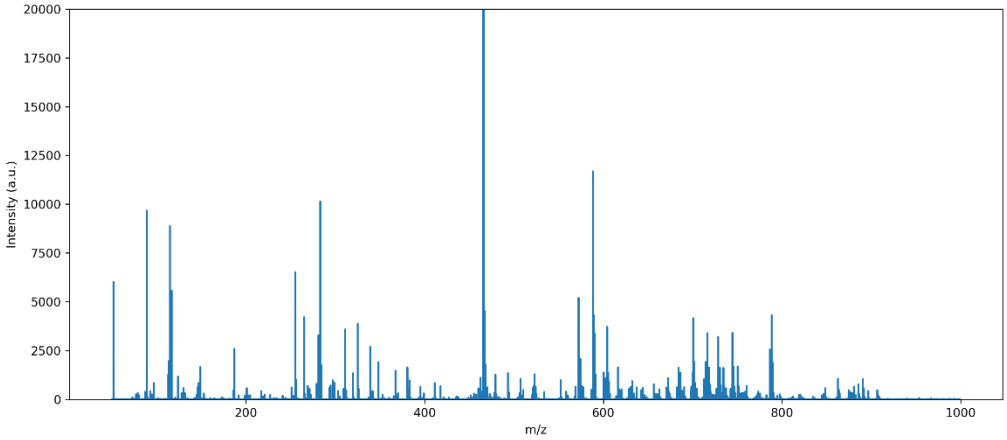
621. Towers MW, Karancsi T, Jones EA, Pringle SD, Claude E. Optimised Desorption Electrospray Ionisation Mass Spectrometry Imaging (DESI-MSI) for the Analysis of Proteins/Peptides Directly from Tissue Sections on a Travelling Wave Ion Mobility Q-ToF. Journal of the American Society for Mass Spectrometry. 2018;29(12):2456-66.
622. Shin YS, Drolet B, Mayer R, Dolence K, Basile F. Desorption electrospray ionization-mass spectrometry of proteins. Anal Chem. 2007;79(9):3514-8.
623. Abbassi-Ghadi N, Jones E, Veselkov K, Huang J, Kumar S, Strittmatter N, et al. Repeatability and reproducibility of desorption electrospray ionization-mass spectrometry (DESI-MS) for the imaging analysis of human cancer tissue: A gateway for clinical applications. Anal Methods. 2014;7.
624. Macklaim JM, Gloor GB, Anukam KC, Cribby S, Reid G. At the crossroads of vaginal health and disease, the genome sequence of Lactobacillus iners AB-1. Proc Natl Acad Sci U S A. 2011;108 Suppl 1(Suppl 1):4688-95.
625. Levine H, Jørgensen N, Martino-Andrade A, Mendiola J, Weksler-Derri D, Jolles M, et al. Temporal trends in sperm count: a systematic review and meta-regression analysis of samples collected globally in the 20th and 21st centuries. Human reproduction update. 2022.
626. Kumar N, Singh AK. Trends of male factor infertility, an important cause of infertility: A review of literature. J Hum Reprod Sci. 2015;8(4):191-6.
627. Aitken RJ, Bakos HW. Should we be measuring DNA damage in human spermatozoa? New light on an old question. Human reproduction (Oxford, England). 2021;36(5):1175-85.
628. Vorilhon S, Brugnon F, Kocer A, Dollet S, Bourgne C, Berger M, et al. Accuracy of human sperm DNA oxidation quantification and threshold determination using an 8-OHdG immuno-detection assay. Human reproduction (Oxford, England). 2018;33(4):553-62.
629. Eini F, Kutenaei MA, Zareei F, Dastjerdi ZS, Shirzeyli MH, Salehi E. Effect of bacterial infection on sperm quality and DNA fragmentation in subfertile men with Leukocytospermia. BMC Mol Cell Biol. 2021;22(1):42.
630. Jung JH, Kim MH, Kim J, Baik SK, Koh SB, Park HJ, et al. Treatment of Leukocytospermia in Male Infertility: A Systematic Review. World J Mens Health. 2016;34(3):165-72.
631. Sergerie M, Laforest G, Bujan L, Bissonnette F, Bleau G. Sperm DNA fragmentation: threshold value in male fertility. Human reproduction (Oxford, England). 2005;20(12):3446-51.
632. Kovatcheva-Datchary P, Nilsson A, Akrami R, Lee YS, De Vadder F, Arora T, et al. Dietary Fiber-Induced Improvement in Glucose Metabolism Is Associated with Increased Abundance of Prevotella. Cell Metab. 2015;22(6):971-82.
633. Li J, Zhao F, Wang Y, Chen J, Tao J, Tian G, et al. Gut microbiota dysbiosis contributes to the development of hypertension. Microbiome. 2017;5(1):14.
634. Bukharin OV, Kuz'min MD, Ivanov Iu B. [The role of the microbial factor in the pathogenesis of male infertility]. Zh Mikrobiol Epidemiol Immunobiol. 2000(2):106-10.
635. Ivanov IB, Kuzmin MD, Gritsenko VA. Microflora of the seminal fluid of healthy men and men suffering from chronic prostatitis syndrome. Int J Androl. 2009;32(5):462-7.
636. Ding N, Zhang X, Di Zhang X, Jing J, Liu SS, Mu YP, et al. Impairment of spermatogenesis and sperm motility by the high-fat diet-induced dysbiosis of gut microbes. Gut. 2020;69(9):1608-19.
637. Waśkiewicz A, Irzykowska L. Flavobacterium spp. – Characteristics, Occurrence, and Toxicity. In: Batt CA, Tortorello ML, editors. Encyclopedia of Food Microbiology (Second Edition). Oxford: Academic Press; 2014. p. 938-42.
638. Garcia-Segura S, del Rey J, Closa L, Garcia-Martínez I, Hobeich C, Castel AB, et al. Seminal Microbiota of Idiopathic Infertile Patients and Its Relationship With Sperm DNA Integrity. Frontiers in Cell and Developmental Biology. 2022;10.
639. Shahid M, Quinlivan JA, Peek M, Castaño-Rodríguez N, Mendz GL. Is there an association between the vaginal microbiome and first trimester miscarriage? A prospective observational study. Journal of Obstetrics and Gynaecology Research. 2022;48(1):119-28.
640. Mändar R. Microbiota of male genital tract: impact on the health of man and his partner. Pharmacol Res. 2013;69(1):32-41.

641. Markowiak-Kopeć P, Śliżewska K. The effect of probiotics on the production of short-chain fatty acids by human intestinal microbiome. Nutrients. 2020;12(4):1107.
642. Forney LJ, Zhou X, Brown CJ. Molecular microbial ecology: land of the one-eyed king. Current Opinion in Microbiology. 2004;7(3):210-20.
643. V. Wintzingerode F, Göbel UB, Stackebrandt E. Determination of microbial diversity in environmental samples: pitfalls of PCR-based rRNA analysis. FEMS Microbiology Reviews. 1997;21(3):213-29.
644. Byrd AL, Belkaid Y, Segre JA. The human skin microbiome. Nature Reviews Microbiology. 2018;16(3):143-55.
645. Nurjadi D, Boutin S, Schmidt K, Ahmels M, Hasche D. Identification and Elimination of the Clinically Relevant Multi-Resistant Environmental Bacteria Ralstonia insidiosa in Primary Cell Culture. Microorganisms. 2020;8(10).
646. Huang J, Okuka M, McLean M, Keefe DL, Liu L. Effects of cigarette smoke on fertilization and embryo development in vivo. Fertility and Sterility. 2009;92(4):1456-65.
647. Canipari R, De Santis L, Cecconi S. Female Fertility and Environmental Pollution. International Journal of Environmental Research and Public Health. 2020;17(23):8802.
648. Holmes B, Owen RJ, Steigerwalt AG, Brenner DJ. Flavobacterium gleum, a New Species Found in Human Clinical Specimens. International Journal of Systematic and Evolutionary Microbiology. 1984;34(1):21-5.
649. Nastri CO, Teixeira DM, Moroni RM, Leitão VMS, Martins WP. Ovarian hyperstimulation syndrome: pathophysiology, staging, prediction and prevention. Ultrasound in Obstetrics & Gynecology. 2015;45(4):377-93.
650. rrnDB [Internet]. University of Michigan. 2022 [cited 30/11/2022]. Available from: https://rrndb.umms.med.umich.edu/search/.

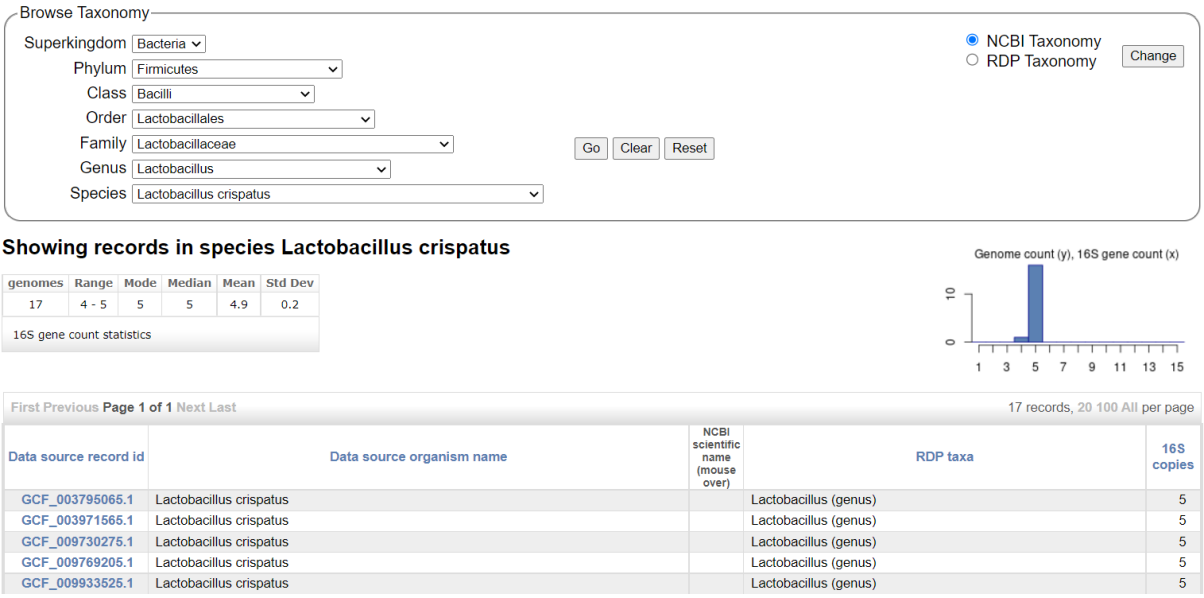
Appendix



Appendix Figure 1: Standard curves calculated using standard cocktails from the manufacturer following x3 serial dilutions. Mean values of 17 analytes in standards 1-6 across 5 analysed plates. Mean values of duplicate analyte concentrations were used to generate the standard curves. For all analytes, mean values were calculated for the standards across the plates. The range of detection for each analyte concentration were determined by generation of standard curves.



Appendix Figure 2: Representative DESI-MS spectral profile of a vagina swab sample.



Appendix Figure 3: Michigan database for 16S gene count statistics and 16S copies per species. The number of 16S copies associated with each species was determined using an online database (650). Where records were unable to provide 16S copy numbers for a particular species, the mean 16S copy number for the genus was used. This process was done for the top 100 most abundant species accounting for 95% of all sequences in the entire dataset. For the remaining 5% of sequences, the average number of 16S copy numbers for the top 100 species was used which was 4. Having accounted for percentage abundance of each species, calculating the quantity per 1 mL, and correcting for the number of 16S copies associated with each taxon, the total bacteria per 1mL of semen was calculated and used for analysis.

49 Spadina Ave. Suite 200
Toronto ON M5V 2J1 Canada
www.biorender.com

Confirmation of Publication and Licensing Rights

April 5th, 2023
Science Suite Inc.

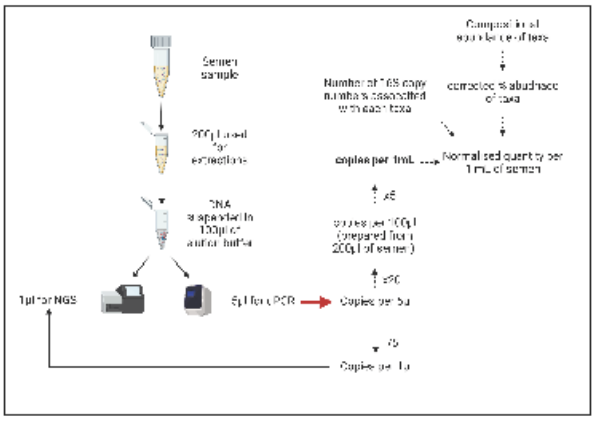
Subscription:	*Individual*
Agreement number:	*PM257M8ZST*
Journal name:	*Thesis*

To whom this may concern,

This document is to confirm that Shahriar Mowla has been granted a license to use the BioRender content, including icons, templates and other original artwork, appearing in the attached completed graphic pursuant to BioRender's Academic License Terms. This license permits BioRender content to be sublicensed for use in journal publications.

All rights and ownership of BioRender content are reserved by BioRender. All completed graphics must be accompanied by the following citation: "Created with BioRender.com".

BioRender content included in the completed graphic is not licensed for any commercial uses beyond publication in a journal. For any commercial use of this figure, users may, if allowed, recreate it in BioRender under an Industry BioRender Plan.



For any questions regarding this document, or other questions about publishing with BioRender refer to our BioRender Publication Guide, or contact BioRender Support at support@biorender.com.

49 Spadina Ave. Suite 200
Toronto ON M5V 2J1 Canada
www.biorender.com

Confirmation of Publication and Licensing Rights

April 5th, 2023
Science Suite Inc.

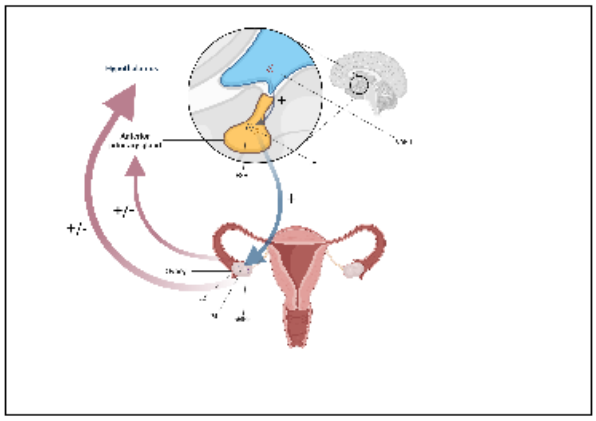
Subscription:	*Individual*
Agreement number:	*AJ257M9934*
Journal name:	*Thesis*

To whom this may concern,

This document is to confirm that Shahriar Mowla has been granted a license to use the BioRender content, including icons, templates and other original artwork, appearing in the attached completed graphic pursuant to BioRender's Academic License Terms. This license permits BioRender content to be sublicensed for use in journal publications.

All rights and ownership of BioRender content are reserved by BioRender. All completed graphics must be accompanied by the following citation: "Created with BioRender.com".

BioRender content included in the completed graphic is not licensed for any commercial uses beyond publication in a journal. For any commercial use of this figure, users may, if allowed, recreate it in BioRender under an Industry BioRender Plan.



For any questions regarding this document, or other questions about publishing with BioRender refer to our BioRender Publication Guide, or contact BioRender Support at support@biorender.com.

49 Spadina Ave. Suite 200
Toronto ON M5V 2J1 Canada
www.biorender.com

Confirmation of Publication and Licensing Rights

April 5th, 2023
Science Suite Inc.

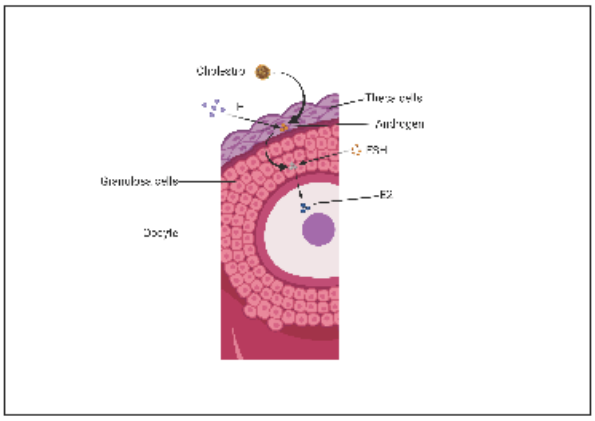
Subscription:	*Individual*
Agreement number:	*HL257M9BWA*
Journal name:	*thesis*

To whom this may concern,

This document is to confirm that Shahriar Mowla has been granted a license to use the BioRender content, including icons, templates and other original artwork, appearing in the attached completed graphic pursuant to BioRender's Academic License Terms. This license permits BioRender content to be sublicensed for use in journal publications.

All rights and ownership of BioRender content are reserved by BioRender. All completed graphics must be accompanied by the following citation: "Created with BioRender.com".

BioRender content included in the completed graphic is not licensed for any commercial uses beyond publication in a journal. For any commercial use of this figure, users may, if allowed, recreate it in BioRender under an Industry BioRender Plan.



For any questions regarding this document, or other questions about publishing with BioRender refer to our BioRender Publication Guide, or contact BioRender Support at support@biorender.com.

49 Spadina Ave. Suite 200
Toronto ON M5V 2J1 Canada
www.biorender.com

Confirmation of Publication and Licensing Rights

April 5th, 2023
Science Suite Inc.

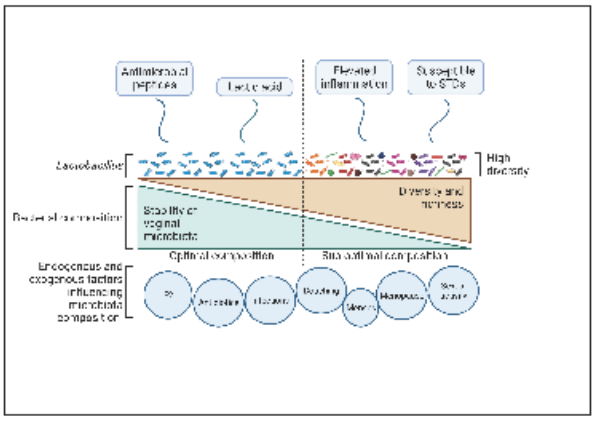
Subscription: *Individual*
Agreement number: *AE257MA2OD*
Journal name: *Thesis*

To whom this may concern,

This document is to confirm that Shahriar Mowla has been granted a license to use the BioRender content, including icons, templates and other original artwork, appearing in the attached completed graphic pursuant to BioRender's Academic License Terms. This license permits BioRender content to be sublicensed for use in journal publications.

All rights and ownership of BioRender content are reserved by BioRender. All completed graphics must be accompanied by the following citation: "Created with BioRender.com".

BioRender content included in the completed graphic is not licensed for any commercial uses beyond publication in a journal. For any commercial use of this figure, users may, if allowed, recreate it in BioRender under an Industry BioRender Plan.



For any questions regarding this document, or other questions about publishing with BioRender refer to our BioRender Publication Guide, or contact BioRender Support at support@biorender.com.